CROSS-DISCIPLINARY APPROACHES TO CHARACTERIZE GAIT AND POSTURE DISTURBANCES IN AGING AND RELATED DISEASES

EDITED BY: Simone Tassani, Egon Perilli and Martina Mancini
PUBLISHED IN: Frontiers in Bioengineering and Biotechnology

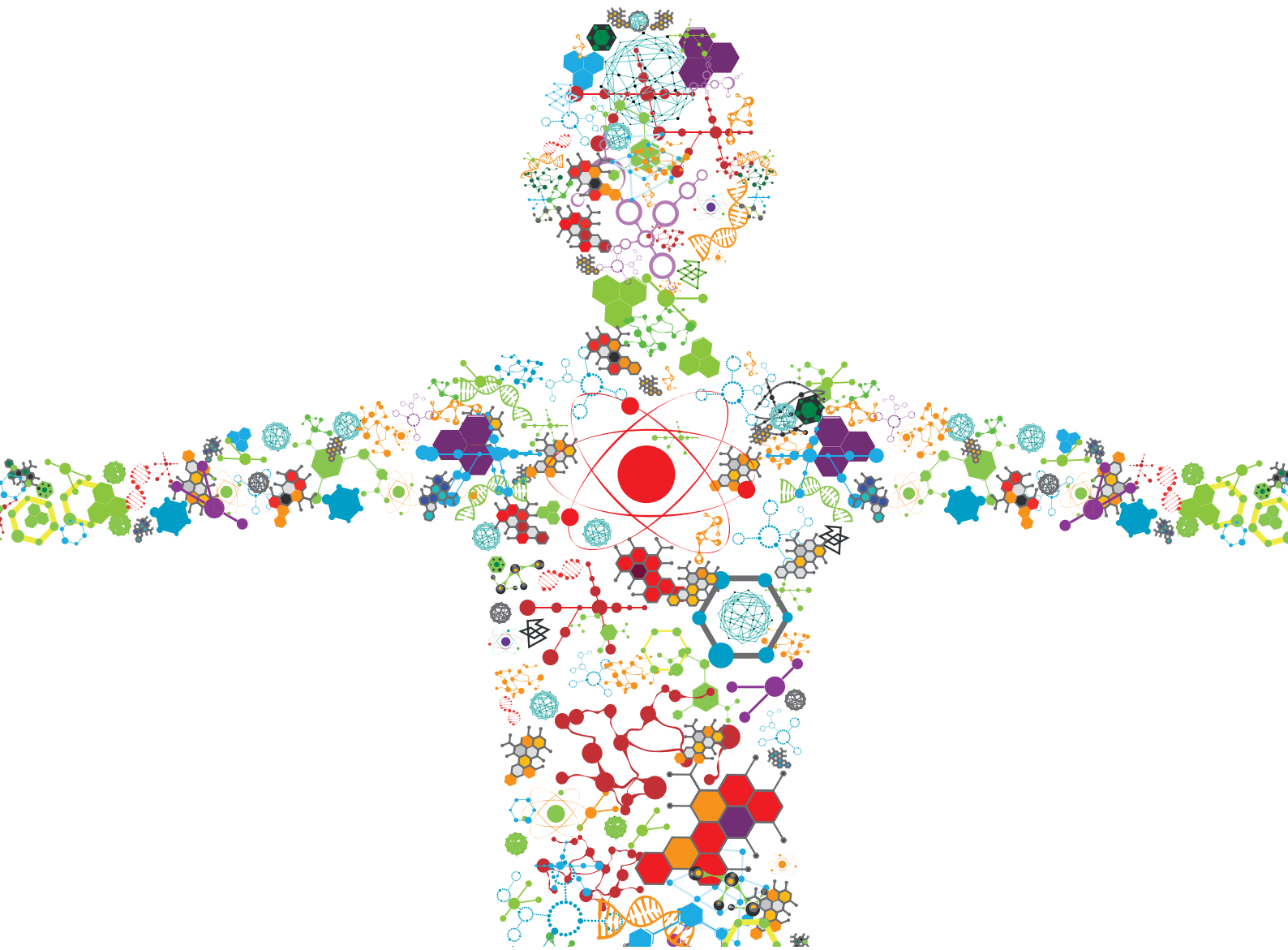

frontiers Research Topics

frontiers

ISSN 1664-8714
ISBN 978-2-88976-076-3
DOI 10.3389/978-2-88976-076-3

About Frontiers

Frontiers is more than just an open-access publisher of scholarly articles: it is a pioneering approach to the world of academia, radically improving the way scholarly research is managed. The grand vision of Frontiers is a world where all people have an equal opportunity to seek, share and generate knowledge. Frontiers provides immediate and permanent online open access to all its publications, but this alone is not enough to realize our grand goals.

Frontiers Journal Series

The Frontiers Journal Series is a multi-tier and interdisciplinary set of open-access, online journals, promising a paradigm shift from the current review, selection and dissemination processes in academic publishing. All Frontiers journals are driven by researchers for researchers; therefore, they constitute a service to the scholarly community. At the same time, the Frontiers Journal Series operates on a revolutionary invention, the tiered publishing system, initially addressing specific communities of scholars, and gradually climbing up to broader public understanding, thus serving the interests of the lay society, too.

Dedication to Quality

Each Frontiers article is a landmark of the highest quality, thanks to genuinely collaborative interactions between authors and review editors, who include some of the world's best academicians. Research must be certified by peers before entering a stream of knowledge that may eventually reach the public - and shape society; therefore, Frontiers only applies the most rigorous and unbiased reviews.
Frontiers revolutionizes research publishing by freely delivering the most outstanding research, evaluated with no bias from both the academic and social point of view. By applying the most advanced information technologies, Frontiers is catapulting scholarly publishing into a new generation.

What are Frontiers Research Topics?

Frontiers Research Topics are very popular trademarks of the Frontiers Journals Series: they are collections of at least ten articles, all centered on a particular subject. With their unique mix of varied contributions from Original Research to Review Articles, Frontiers Research Topics unify the most influential researchers, the latest key findings and historical advances in a hot research area! Find out more on how to host your own Frontiers Research Topic or contribute to one as an author by contacting the Frontiers Editorial Office: frontiersin.org/about/contact

CROSS-DISCIPLINARY APPROACHES TO CHARACTERIZE GAIT AND POSTURE DISTURBANCES IN AGING AND RELATED DISEASES

Topic Editors:
Simone Tassani, Pompeu Fabra University, Spain
Egon Perilli, Flinders University, Australia
Martina Mancini, Oregon Health and Science University, United States

Citation: Tassani, S., Perilli, E., Mancini, M., eds. (2022). Cross-Disciplinary Approaches to Characterize Gait and Posture Disturbances in Aging and Related Diseases. Lausanne: Frontiers Media SA. doi: 10.3389/978-2-88976-076-3

Table of Contents

frontiers | Frontiers in Bioengineering and Biotechnology

EDITORIAL
published: 12 April 2022
doi: 10.3389/fbioe.2022.888910

Editorial: Cross-Disciplinary Approaches to Characterize Gait and Posture Disturbances in Aging and Related Diseases

Simone Tassani[1]*, *Martina Mancini*[2], *Egon Perilli*[3] and *Juan Ramírez*[4]

[1]BCN MedTech, DTIC, Universitat Pompeu Fabra, Barcelona, Spain, [2]Department of Neurology, Oregon Health and Science University, Portland, OR, United States, [3]Medical Device Research Institute, College of Science and Engineering, Flinders University, Adelaide, SA, Australia, [4]Mechanical Engineering Department, Universidad Nacional de Colombia, Medellin, Colombia

Keywords: gait, multi-factorial analysis, repeatability, aging, imaging, musculo skeletal model, cognitive disorders, Parkinson

Editorial on the Research Topic

Cross-Disciplinary Approaches to Characterize Gait and Posture Disturbances in Aging and Related Diseases

Gait abnormalities can be caused by natural signs of aging and/or by specific diseases. Therefore, any study that aims to analyze gait in the elderly faces the problem of the interaction between, at least, these two factors. Even if gait analysis nowadays is a solid and well-known tool for research, the interpretation of the results is strongly linked to the interdependence among the different aspects that can affect the subjects in analysis. The most obvious solution to this problem is to focus on narrow studies centered on specific techniques or patients' conditions. Such studies are important, and in the past have led to several methodological advances. However, not considering age-related factors that are relevant for gait and posture analysis can generate misleading and contradictory results. Contemporary research often suffers from a lack of repeatability, inconsistency of results, and confounding of parameters. These problems can be related to the limited cross-disciplinary approaches applied. Specific studies can appear significant when performed individually, but they can lose significance when included in the wider research context in which they belong.

The current research topic presents a Research Topic of studies that tried to cross the borders of current musculoskeletal (MSK) science, setting interdisciplinary goals, merging multiple aspects, and therefore considering the effect that external factors can have over gait and its interpretation.

For instance, sight is known to affect posture, stability, and in general, movement in space, and for this reason, studying a combination of factors covering gait and the visual system can allow early detection of a range of various conditions.

In the work by Lirani-silva et al., as described in this very topic, eye-tracking systems were used during the gait of subjects with mild traumatic brain injury (mTBI). mTBI can result from several mechanisms and at any age; however, falling, which is a major problem in the elderly, clearly belongs to the possible causes leading to mTBI. The authors find a positive interaction between the condition of the patients and the saccade duration, showing how gait speed can be related to saccade time for people with mTBI. The interaction between the visual system and posture is also studied by Kahya et al. The authors present a relation between postural stability and pupillary response, as an index of cognitive workload during postural control in patients with Parkinson's disease (PD). PD patients showed a higher level of pupillary response, and therefore higher cognitive workload, together with a higher displacement of the center of pressure, related to reduced stability. The work presents a

OPEN ACCESS

Edited and reviewed by:
Markus O. Heller, University of Southampton, United Kingdom

***Correspondence:**
Simone Tassani
simone.tassani@upf.edu

Specialty section:
This article was submitted to Biomechanics, a section of the journal Frontiers in Bioengineering and Biotechnology

Received: *03 March 2022*
Accepted: *16 March 2022*
Published: *12 April 2022*

Citation:
Tassani S, Mancini M, Perilli E and Ramírez J (2022) Editorial: Cross-Disciplinary Approaches to Characterize Gait and Posture Disturbances in Aging and Related Diseases. Front. Bioeng. Biotechnol. 10:888910. doi: 10.3389/fbioe.2022.888910

potential tool to understand the neurophysiology underpinning falls and the risk of falls. Finally, the study by Ma et al. showed that patients with idiopathic rapid eye movement sleep behavior disorder, which are at high risk for conversion to PD, can be effectively monitored by measuring gait characteristics, such as range of motion and peak angular velocity of the trunk.

Taken together, the findings presented in this research topic suggest that different patterns of gait and posture can therefore be related to the development of different cognitive limitations and potentially be used for their early detection. In particular, the relation between different stages of Huntington's disease and gait presented here (Talman and Hiller) describing how gait abnormalities are multifactorial, relating to both motor manifestation and cognitive limitations.

Although the relationship between posture and cognitive condition seems strong, we must not fall into the temptation to believe that a single analysis looking at one single aspect of balance, can discriminate among all kinds of dementia. The study by Mc Ardle et al. showed how inertial sensors can be used to discriminate between Alzheimer's disease and Parkinson's disease dementia, but not between the mentioned diseases and dementia with Lewy bodies. Discrimination against control subjects was also possible only for patients with Parkinson's disease dementia, underlining the potential and limitations of inertial sensor-based posture analysis.

The relation between cognition and fall risk is a broad topic and can be approached from different sides (Zhang et al., 2019). The integrated use of different analysis techniques is interesting and finds an appropriate space in this research topic; the integration of diverse techniques is demonstrated to lead to more insightful results than those obtained by applying the same techniques individually. However, the need for integration also presents difficulties that are specific to the combination of different topics and must be properly studied as a research subject itself.

Imaging is one of the analysis techniques most often associated with movement analysis (Bürki et al., 2017; Maillet et al., 2012). Le Floch et al. present a correlation among cognitive impairments, history of falls, and brain areas identified using voxel-based morphometric analysis of magnetic resonance images (MRI). The authors find that older fallers have larger subvolumes in the bilateral striatum, suggesting an adaptive mechanism to falls in people with neurocognitive decline.

Given the great importance of imaging in the study of age-related diseases and its wide use in biomechanical modeling, also providing some space within this research topic for the study of the possible risks to which MRI operators are exposed to appeared to be important (Gurrera et al.). The study presents the integrated use of modeling of the magnetic field associated with the movement analysis of operators in the MRI environment. As a result the authors identify specific tasks that can be considered safe in such an MRI-related work environment.

MRI and other biomedical imaging techniques are often used for the development of biomechanical patient-specific models (Andreaus and Iacoviello, 2012). By combining imaging and modeling with gait analysis it is possible to further explore variables that can influence the analysis of human movement in the elderly. Here, De Pieri et al. studied hip contact forces (HCFs) in asymptomatic subjects to identify possible abnormalities that might lead to the development of osteoarthrosis (OA). The authors found that higher femoral antetorsion led to significantly higher anteromedial HCFs identifying a possible cause for future degeneration of the cartilage. The study is of particular interest because it stresses how the kinematic characteristics of gait might generate abnormal situations and possibly lead to the development of hip OA. Although morphometrical factors are often mentioned as a possible cause of cartilage degeneration, a study using MRI-based bone geometry coupled with subject-specific MSK modeling identified how the contribution of bone shape to model-derived joint kinematics lacked clinical relevance (De Roeck et al.), while underlining the dominant role of movement over the one of morphology variability. The loads produced by different gait patterns propagate to the tissue and cell level and can initiate, for instance, the degeneration of cartilage in OA subjects. A variety of analysis techniques can be organized in multiple subsequent levels using the output of one model as a boundary condition of the next one. This approach allows researchers to create a top-down multilevel model that can be used to explore the effect of macro-factors over the micro ones. Caravaggi et al. present an original methodology to study the effect of cyclic joint loading on cartilage metabolism, combining biomechanical data and medical imaging with molecular information. The protocol has the potential to be applied to explore molecular pathways in the development of OA. This information on pathways can also be crucial for the selection of OA therapies. Nowadays, the decision to select conservative treatments or surgery is mainly related to the beliefs of the medical doctor treating the patient. The result is that patients with a similar degree of OA can follow very different clinical treatment regimes. There is a need to develop new approaches and metrics that can help clinicians in the selection of the best therapy for a specific patient. As a step in this direction, Tassani et al. have presented a multifactorial approach that allowed the stratification of patients in several groups with comparable knee OA but different clinical characteristics. The work allowed the study of nonlinear interaction among multiple factors and showed how the functionality, in terms of step time, speed, and double stance, might be a better indicator than contact forces and moments, for the identification of the appropriate clinical treatment.

In the context of the integration of multiple models and factors, the study of uncertainty related to MSK models driven by gait analysis is one of the topics presented in this Research Topic (Curreli et al.). The authors present a crucial problem in the typical approach to couple MSK and finite element models (FEMs): The identification and quantification of the uncertainties related to the boundary conditions. Different complex and non-linear models coupled together can interact with each other to create a dynamic and non-linear system. Such models will present high variability of the output despite small variability of the input, thus limiting the repeatability of the results when interactions among factors are not considered. Curreli et al. apply variable inputs to MSK models to study the impact of total knee replacement showing how the different

kinematic definitions implemented in the models influence the motion and the load history of the artificial joint.

This Research Topic thus brings together 12 peer-reviewed papers addressing the two main factors that influence the analysis of human motion: the interaction of gait with cognitive conditions and the integration of multiple techniques for gait analysis. As illustrated convincingly in the research collected here, an understanding of the role that factors not directly related to the motor system can have on the final analysis of human motion is highly relevant for the interpretation of our results.

We hope that the reader will find in this Research Topic a useful reference for the state of the art in gait and posture disturbances in aging and age-related diseases.

AUTHOR CONTRIBUTIONS

ST has prepared the draft of the editorial while all the other have revised it critically. All the authors gave the final approval of the version to be submitted.

REFERENCES

Andreaus, U., and Iacoviello, D. (2012). *Biomedical Imaging and Computational Modeling in Biomechanics*. Springer Science \\& Business Media.

Bürki, C. N., Bridenbaugh, S. A., Reinhardt, J., Stippich, C., Kressig, R. W., and Blatow, M. (2017). Imaging Gait Analysis: An fMRI Dual Task Study. *Brain Behav.* 7 (8), e00724–13. doi:10.1002/brb3.724

Maillet, A., Pollak, P., and Debû, B. (2012). Imaging Gait Disorders in Parkinsonism: A Review. *J. Neurol. Neurosurg. Psychiatry* 83 (10), 986–993. doi:10.1136/jnnp-2012-302461

Zhang, W., Low, L.-F., Schwenk, M., Mills, N., Gwynn, J. D., and Clemson, L. (2019). Review of Gait, Cognition, and Fall Risks with Implications for Fall Prevention in Older Adults with Dementia. *Dement Geriatr. Cogn. Disord.* 48 (1–2), 17–29. doi:10.1159/000504340

Conflict of Interest: The authors declare that the research was conducted in the absence of any commercial or financial relationships that could be construed as a potential conflict of interest.

frontiers in Bioengineering and Biotechnology

ORIGINAL RESEARCH
published: 10 March 2021
doi: 10.3389/fbioe.2021.610426

Volumetric Brain Changes in Older Fallers: A Voxel-Based Morphometric Study

Maxime Le Floch[1,2], Pauline Ali[2,3], Marine Asfar[1,2], Dolores Sánchez-Rodríguez[4], Mickaël Dinomais[2,3] and Cédric Annweiler[1,2,5] on behalf of the SAM group*

[1] Department of Geriatric Medicine, Angers University Hospital, Angers University Memory Clinic, Research Center on Autonomy and Longevity, University of Angers, Angers, France, [2] School of Medicine, Faculty of Health, University of Angers, Angers, France, [3] Department of Physical and Rehabilitation Medicine, Laboratoire Angevin de Recherche en Ingénierie des Systèmes, Angers University Hospital, Université d'Angers, Angers, France, [4] Department of Public Health, University of Liège, Liège, Belgium, [5] Department of Medical Biophysics, Robarts Research Institute, Schulich School of Medicine & Dentistry, University of Western Ontario, London, ON, Canada

OPEN ACCESS

Edited by:
Simone Tassani,
Pompeu Fabra University, Spain

Reviewed by:
Oualid Benkarim,
McGill University, Canada
Maxime Montembeault,
University of California,
San Francisco, United States

***Correspondence:**
Cédric Annweiler
Cedric.Annweiler@chu-angers.fr;
ceannweiler@chu-angers.fr

Specialty section:
This article was submitted to Biomechanics, a section of the journal Frontiers in Bioengineering and Biotechnology

Received: 25 September 2020
Accepted: 15 February 2021
Published: 10 March 2021

Citation:
Le Floch M, Ali P, Asfar M, Sánchez-Rodríguez D, Dinomais M and Annweiler C (2021) Volumetric Brain Changes in Older Fallers: A Voxel-Based Morphometric Study. Front. Bioeng. Biotechnol. 9:610426. doi: 10.3389/fbioe.2021.610426

Background: Falls are frequent and severe in older adults, especially among those with cognitive impairments due to altered motor control. Which brain areas are affected among fallers remains yet not elucidated. The objective of this cross-sectional analysis was to determine whether the history of falls correlated with focal brain volume reductions in older adults.

Methods: Participants from the MERE study (n = 208; mean, 71.9 ± 5.9 years; 43% female; 38% cognitively healthy, 41% with mild cognitive impairment and 21% with dementia) were asked about their history of falls over the preceding year and received a 1.5-Tesla MRI scan of the brain. Cortical gray and white matter subvolumes were automatically segmented using Statistical Parametric Mapping. Age, gender, use of psychoactive drugs, cognitive status, and total intracranial volume were used as covariates.

Results: Fifty-eight participants (28%) reported history of falls. Fallers were older (P = 0.001), used more often psychoactive drugs (P = 0.008) and had more often dementia (P = 0.004) compared to non-fallers. After adjustment, we found correlations between the history of falls and brain subvolumes; fallers exhibiting larger gray matter subvolumes in striatum, principally in bilateral caudate nucleus, than non-fallers. By stratifying on cognitive status, these neuroanatomical correlates were retrieved only in participants with MCI or dementia. There were no correlations with the subvolumes of white matter.

Conclusion: Older fallers had larger subvolumes in bilateral striatum than non-fallers, principally within the caudate nucleus. This suggests a possible brain adaptative mechanism of falls in people with neurocognitive decline.

Keywords: accidental falls, older adults, brain, brain mapping, motor control

INTRODUCTION

Falls in older adults are not only frequent, with a prevalence reaching 35% after the age of 65 and 50% after 80, but also severe as they lead to adverse consequences including fractures, hospitalization, loss of independence, institutionalization and death; with significant health care costs (Katz and Shah, 2010). The challenge of the falls is that they can be prevented, at least in part, by identifying and correcting the risk factors for falls (Gillespie et al., 2012). Around 450 risk factors for falls are reported in the literature (Tinetti et al., 1988), including gait and balance disorders among the most important and frequent contributors (Rubenstein et al., 2001).

Human gait is an intentional motor behavior directed toward a goal that ensures the movement of the body in the horizontal plane through postural and balance constraints. Several factors influence motor function and gait performance, whether in the peripheral dimension of motor control (for example the declines in muscle strength, tone or osteoarticular functions) or in its central dimension (essentially the decline of brain health and function) (Allali et al., 2008). Specifically, the brain-level of motor control involves the integration of afferent information in the brain to generate a global motor control message and ultimately to produce complex motor responses that are adapted to multiple sensory inputs and environmental constraints (Annweiler et al., 2013). For this reason, older adults with prodromal or severe cognitive impairments exhibit significant gait disorders (Beauchet et al., 2015). Thus, the efficiency of gait control and the prevention of falls presuppose good health and function of the brain.

Only little is known about the brain changes met among older fallers, the most frequently reported changes being microvascular lesions such as leukoaraiosis (Callisaya et al., 2015). In previous studies, the brain was generally examined over a limited number of regions of interest defined *a priori*, such as the hippocampus and the somatosensory or premotor or prefrontal or parietal cortex, which increases the risk of ignoring unexpected focal changes (Beauchet et al., 2017). In addition, previous brain morphological analyzes have involved specific groups such as Parkinson's patients, identifying a reduction in gray matter volume (GM) in the right superior temporal gyrus and in the right inferior parietal lobule (Hsu et al., 2016), or within cognitively healthy individuals (CHI) with decreased GM volumes in the orbitofrontal cortex, anterior cingulum, insula, pallidum, and hippocampus (Maidan et al., 2020). To our knowledge, no whole-brain analysis in relation to falls has been conducted yet in individuals with mild cognitive impairment (MCI) or dementia.

We had the opportunity to examine the voxel-based morphometric (VBM) correlations of falls with the whole GM and white matter (WM) volumes in a large representative community survey of older adults with various cognitive statuses in the MERE cohort (Beauchet et al., 2013). We hypothesized that the brain of older fallers would be the seat of specific morphological changes, compared to non-fallers. The objectives of this cross-sectional analysis were (i) to determine whether the history of falls correlated with focal brain volume reductions in the MERE cohort, (ii) to specify the location of these morphological changes, and (iii) to determine if these changes depended on cognitive status.

MATERIALS AND METHODS

Participants

We studied participants followed in the Memory Clinic of the University Hospital of Angers, France, and recruited in the MERE study between November 2009 and 2015 (ClinicalTrials.gov number, NCT01315704). The MERE study is an observational prospective unicentric cohort study designed to examine gait and gait changes with time among older adults visiting the Memory Clinic of Angers University Hospital, France. The sampling and data collection procedures have been described elsewhere in detail (Annweiler et al., 2014a). The main exclusion criteria were age below 60 years, Mini-Mental State Examination (MMSE) score < 10, inability to walk independently, history of stroke, any acute medical illness in the preceding 3 months, current delirium, severe depression defined as 15-item Geriatric Depression Scale score > 10, poor vision, inability to understand or answer the study questionnaires, and refusal to participate in research. All participants included in the present analysis received a full medical examination and a magnetic resonance imaging (MRI) scan of the brain.

History of Falls

The participants were interviewed using a standardized questionnaire, gathering information on the history of falls over the preceding year. This face-to-face interview was based on standardized questions exploring the number, delay and location of falls (i.e., inside or outside the participant's house), the evoked causes and circumstances of falls (i.e., syncope or other acute medical event, body transfer from sitting position or walking or other physical activities such as cycling), and all physical traumatisms and inability to get up from the ground after a fall. A fall was defined as an event resulting in a person coming to rest unintentionally on the ground or another lower level, not as the result of a major intrinsic event or an overwhelming hazard. Fallers were defined as having experienced at least one fall in the preceding 12-month period.

MRI Procedures

MRI Acquisition

All images were acquired on the same 1.5 Tesla MRI scanner (Magnetom Avanto, Siemens Medical Solutions, Erlangen, Germany) at the University Hospital of Angers, France, using a standard MRI protocol (Dubois et al., 2009). A high-resolution 3D T1-weighted volume was obtained covering the whole brain (acquisition matrix $= 256 \times 256 \times 144$, FOV $= 240$mm, TE/TR/TI $= 4.07$ ms/2170 ms/1100 ms, flip angle $= 15°$, voxel size 1 mm $\times$ 1 mm $\times$ 1.3 mm).

Voxel-Based-Morphometry With DARTEL Analyses

All T1 images were converted from DICOM to NIFTI format using the MRIcron software[1]. Basic voxel-based morphometry (VBM) with DARTEL analysis[2] was conducted using standard functionalities (default options) available in the VBM8 toolbox[3] implemented in the SPM8 software[4]. VBM analysis was performed following standard procedures[5], as previously published (Dinomais et al., 2016). The default options of the VBM procedure provided in VBM8 were used. Native MR images were segmented into distinct tissue classes: GM, WM and cerebrospinal fluid (CSF), using a segmentation approach available in SPM8. The extended option "thorough cleanup," which is particularly useful for atrophic brain, was used during the first module "estimate and write." Customized DARTEL-templates were created using affine registered tissue segments (Ashburner, 2007). These customized DARTEL templates replaced the default DARTEL templates. Hence, GM and WM volumes were normalized using high dimensional spatial normalization to a customized DARTEL template. A modulation of the segmented and normalized GM (modulated GM) and WM (modulated WM) volumes were performed (Good et al., 2001). The final resolution of the modulated GM and WM images was 1.5 mm × 1.5 mm × 1.5 mm, but these were smoothed with a 4 mm FWHM (full-width-at-half-maximum) Gaussian Kernel to minimize individual gyral variations. All images were visually inspected to ensure that the steps described above were successful and that each modulated GM and WM map covered the whole brain.

Covariates

The following variables were used as potential confounders in the analyses: age, gender, use of psychoactive drugs, cognitive status, and total intracranial volume (TIV). Participants were asked to bring all their prescriptions and medications to the clinical center. Psychoactive drugs were defined as benzodiazepines, antidepressants and/or neuroleptics. The cognitive status was diagnosed during multidisciplinary meetings involving geriatricians, neurologists and neuropsychologists of Angers University Memory Center, France, and was based on a variety of standardized neuropsychological tests, physical examination findings, blood tests and MRI brain imaging (Annweiler et al., 2014b). Clinical suspicion of dementia was diagnosed using the Diagnostic and Statistical Manual of Mental Disorders, fourth edition, criteria (Guze, 1995). MCI was diagnosed according to consensual criteria (Albert et al., 2011). Non-demented participants without MCI and who had normal neuropsychological and functional performance were considered as CHI. Finally, the TIV was approximated for each participant by calculating the sum of GM, WM and CSF maps obtained during the pre-processing steps.

[1]https://people.cas.sc.edu/rorden/mricron/index.html

[2]http://www.neuro.uni-jena.de/vbm8/VBM8-Manual.pdf

[3]http://dbm.neuro.uni-jena.de/VBM8/

[4]http://www.fil.ion.ucl.ac.uk/spm

[5]http://www.fil.ion.ucl.ac.uk/~john/misc/VBMclass10.pdf

Ethics

Participants were included after having given their informed consent for research. The study was conducted in accordance with the ethical standards set forth in the Helsinki Declaration (1983). The study protocol was approved by the local Ethical Committee (2009/15).

Statistics

A descriptive analysis of the participants' characteristics was firstly performed using effectives and frequencies for qualitative variables, and means and standard deviations for continuous variables. Comparisons were performed according to the fallers and non-fallers groups using chi^2 test or Fisher exact test for qualitative variables, as appropriate, and Student *t*-test or Wilcoxon-Mann-Whitney test for quantitative variables according to the normal distribution assumption.

The smoothed, modulated, normalized imaging datasets were used for voxelwise statistical analysis using SPM8. A whole-brain random-effect full 2 (falls conditions) × 3 (cognitive status) ANOVA was conducted on the MRI data. This statistical analysis allows testing for potential differences between fallers and non-fallers brain volumes and the influence of the cognitive status. Thus, Statistical F-maps were created for each main effect and for each interaction, thus the GM variations across all conditions was determined using an F-contrast. Because F-maps do not contain information about the direction of the main effects, statistical t-contrasts were calculated to determine the direction of any significant main effects. All statistical parametric maps were interpreted after applying a false discovery rate (FDR) correction for multiple comparisons at the whole-brain level with a significance level p-Value (corrected) < 0.05. Minimum cluster size was set at 10 contiguous voxels. Anatomic toolbox 2.2c was used for anatomical localizations (Eickhoff et al., 2005). Age, gender, use of psychoactive drugs, cognitive status, and TIV were used as covariates of noninterest implement in our 2X3 full factorial design. Finally, the same analyses were conducted by stratifying on the cognitive status (i.e., within the CHI subgroup ($n = 79$), within the subgroup with MCI ($n = 86$), and finally within the subgroup with dementia ($n = 43$).

RESULTS

Clinical characteristics and brain subvolumes are presented in **Table 1**, and further neuropsychological data are provided in **Supplementary Appendix 1**. The prevalence of falls was 27.8%. Thirty-nine participants reported one fall over the preceding year, while 9 had 2 falls and 10 experienced 3 falls or more. Both groups (i.e., fallers and non-fallers) were similar in terms of total intracranial volume. Fallers were older ($P = 0.001$), more often female ($P = 0.014$), used more often psychoactive drugs ($P = 0.008$) and exhibited more frequent dementia ($P = 0.004$) (**Table 1**).

After adjusting for age, gender, use of psychoactive drugs, cognitive status and TIV, the VBM-DARTEL analysis by using anatomic toolbox 2.2c identified 17 clusters that positively correlated with falls, which are presented in **Table 2**; the most

TABLE 1 | Participants' characteristics ($n = 208$).

	Whole cohort ($n = 208$)	History of falls		*P*-value
		Yes ($n = 58$)	No ($n = 150$)	
Age, years (mean ± SD)	71.9 ± 5.9	74.5 ± 7.0	71 ± 5.0	0.001
Female gender	90 (43.2)	33 (56.9)	57 (38.0)	0.014
Use psychoactive drugs*	49 (23.6)	21 (36.2)	28 (18.7)	0.008
Total intracranial volume, cm^3 (mean ± SD)	1396.1 ± 127.3	1390.2 ± 140.8	1398.4 ± 122.1	0.676
Cognitive status				0.004
Dementia	43 (20.7)	20 (34.5)	23 (15.3)	
MCI	86 (41.3)	16 (27.6)	70 (46.7)	
Cognitively healthy	79 (38.0)	22 (37.9)	57 (38.0)	

*Data presented as n (%) where applicable; MCI: mild cognitive impairment; SD: standard deviation; *Use benzodiazepines and/or antidepressants and/or neuroleptics.*

significant clusters being located in the bilateral caudate nucleus, the bilateral amygdala, the bilateral putamen, the right insula and the left hippocampus. **Figure 1A** illustrates the main effect of falls and cognitive status on gray matter volumes while adjusting for potential confounders.

While stratifying on the cognitive status, the history of falls did not correlate with the subvolumes of GM in the CHI subgroup. The subgroup with MCI exhibited correlations with falls mainly in the bilateral caudate nucleus, the left amygdala and the left olfactory cortex after adjusting for potential confounders (**Figure 1B**) while, in the subgroup with dementia, fallers exhibited a greater GM subvolume principally in the bilateral caudate nucleus, the left middle cingulum and the bilateral insula (**Figure 1C**). More detailed results and corresponding *t*-tests according to anatomic toolbox 2.2c are shown in **Supplementary Appendices 2–6**.

Finally, the analysis revealed that falls did not correlate with the subvolumes of white matter across the whole brain.

DISCUSSION

We found, after adjusting for studied potential confounders, that older fallers had larger gray matter volume in striatum, principally in bilateral caudate nucleus, than non-fallers; a correlation retrieved in those with cognitive decline (either with MCI or dementia). In contrast, there was no between-group difference in white matter subvolumes.

Our study provides evidence of an association between falls and brain subvolumes, notably in the bilateral striatum (i.e., caudate nucleus, putamen). Although the contribution of the striatum to movements is increasingly recognized (Kreitzer and Malenka, 2008), the involvement in falls remains unclear so far. In fact, our results diverge from the hypothesis we originally formulated. We supposed *a priori* that smaller brain subvolumes would be found in fallers since it was previously reported that gait instability, which leads to greater fall risk, may be caused by brain morphological abnormalities such as white matter lesions or gray matter ischemic lesions (Callisaya et al., 2015; Taylor et al., 2018; Blumen et al., 2019). Also, gait disorders were previously associated with focal neuronal loss in brain areas involved in motor skills, visuospatial attention and executive functions (Allali et al., 2014). Briefly, the cerebral motor program is organized into five consecutive steps: sensory feedback, intention, planning, programming and execution (Beauchet et al., 2008), with the striatum being involved in all steps. More precisely, the caudate volume has been directly associated with executive functioning (Macfarlane et al., 2015), which plays a critical role in falls risks among older adults (Muir et al., 2013). Functional imaging data has largely corroborated the model of functional cortico-striatal connectivity (Postuma and Dagher, 2006). This key role of caudate nucleus is highlighted by the facts that Parkinsonian deficits and frontal gait are two main clinical presentations of higher-level gait disorders and are associated with dysfunction in both the basal ganglia and frontal regions (Helmich et al., 2010). Thus, finding morphological changes in caudate nucleus among fallers was not surprising. However, finding an increased subvolume of the caudate nucleus was not expected here, though not unprecedented. For instance, in one recent study, participants with neurosensitive pathology exhibited greater caudate subvolume in response to the lack of environmental information (Casseb et al., 2019). Another study reported that people with schizophrenia had caudate hypertrophy in response to the use of psychoactive drugs (Gur et al., 1998), and similar results were also found in animals models (Andersson et al., 2002).

Enlargement of key regions of the brain could represent an adaptative mechanism to maintain a physiological control of gait. Such brain plasticity corresponds to theories on age-related neurocognitive changes, which support the existence of adaptive strategies to maintain stable brain performance with advancing age (Cabeza et al., 2018). For instance, a recent study showed the effects of normal aging on the neural substrate of gait control using mental imagery during functional MRI of brain: hippocampal regions in older adults exhibited an increased activation compared to younger ones during a task requiring a precise control of gait (i.e., walking on surface consisting of cobbles stones) (Allali et al., 2014), which was interpretated as an adaptative mechanism to maintain a physiological control of gait. Besides normal aging, brain adaptative mechanisms have also been reported in response to functional decline in adults. For example, in functional MRI studies, a greater extent of hippocampal activation has been shown while performing an episodic memory task among patients with early stages of

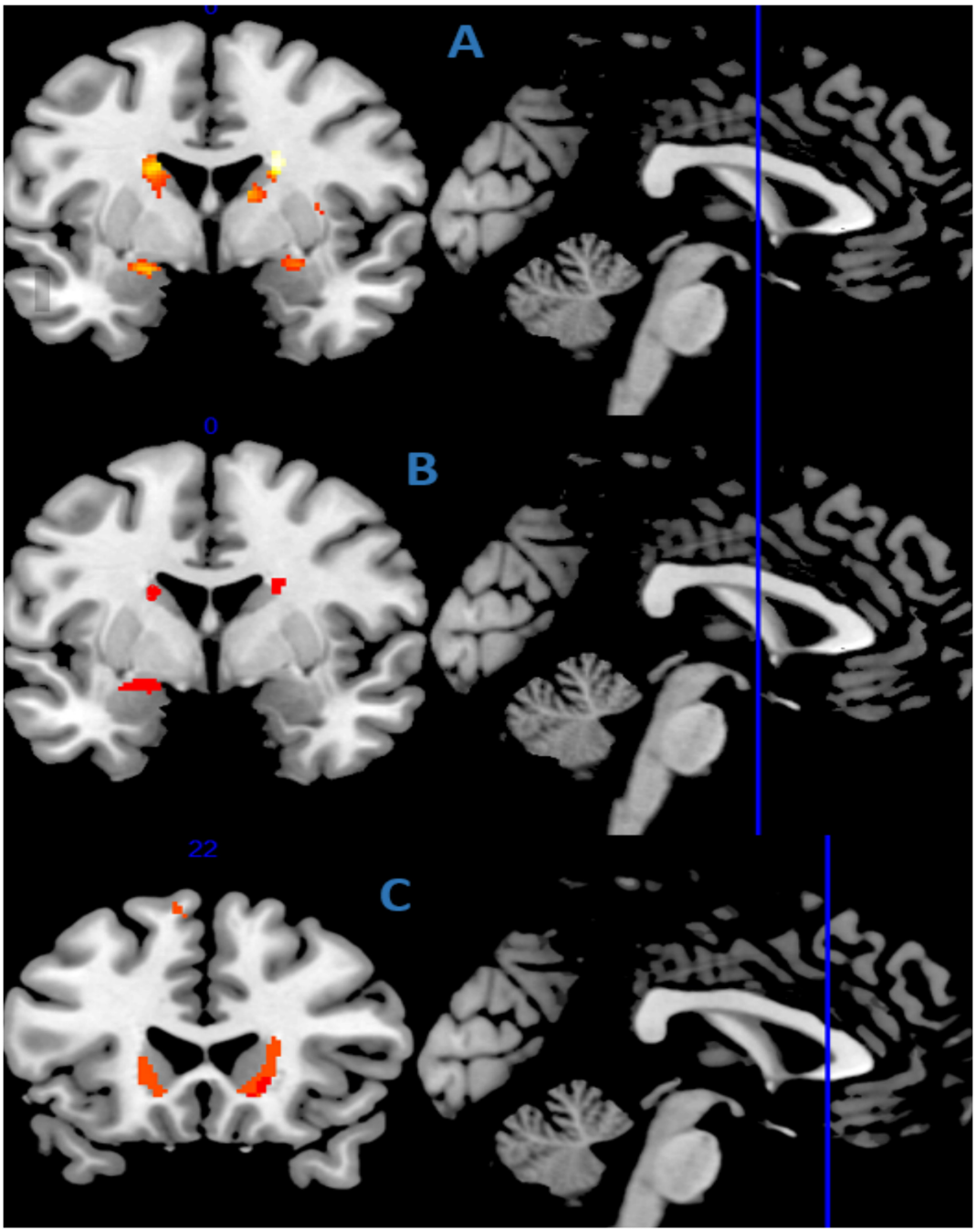

FIGURE 1 | Gray matter regions showing a positive correlation with falls **(A)** in the whole cohort, **(B)** in the subgroup with mild cognitive impairment ($n = 86$), and **(C)** in the subgroup with dementia ($n = 43$), after adjustment for potential confounders (age, gender, use psychoactive drugs, cognitive status, and TIV). The statistical map is co-registered and superimposed on 3D-T1 coronal, axial and sagittal slice (MNI T1 template available on MRICRON software). Results are shown with a significance of $P < 0.05$ and minimum cluster size of 10 continuous voxels.

dementia compared to CHI (Dickerson and Sperling, 2008; Smith et al., 2013). This is also consistent with the finding of an increase in caudate volume several years before the clinical onset of familial form of Alzheimer disease (Fortea et al., 2010). Similarly, hypertrophic olivary changes have been reported after axonal damage (Krings et al., 2003). The supplementary recruitment may reflect neurological strategies to cope with structural or functional anomalies (Whalley et al., 2004), even if this adaptation may ultimately be surpassed. Consistently, a J-shaped change in brain subvolumes has been reported while exploring the association between gait variability and brain morphology (Allali et al., 2014; Annweiler et al., 2014b). The

TABLE 2 | Detailed results of the VBM analysis after adjustment for potential confounders: correlation of gray matter volume with falls according to anatomic toolbox 2.2c.

	Brain region	*t*-score	MNI coordinates		
Cluster 1					
(638 voxels)	R Caudate Nucleus	30.36	21	−1	24
	R Caudate Nucleus	28.22	18	24	−5
	R Caudate Nucleus	25.52	20	14	19
	R Caudate Nucleus	21.15	20	−9	19
	R Caudate Nucleus	18.97	12	0	13
Cluster 2					
(513 voxels)	L Caudate Nucleus	27.99	−21	−12	25
	L Caudate Nucleus	24.45	−18	−4	24
	L Caudate Nucleus	19.60	−18	6	21
	L Caudate Nucleus	19.48	−20	11	24
	L Caudate Nucleus	19.39	−21	9	22
	L Caudate Nucleus	16.26	−17	6	12
	L Caudate Nucleus	16.24	−18	5	13
Cluster 3					
(113 voxels)	L Amygdala	20.24	−21	2	−15
Cluster 4					
(109 voxels)	R Putamen	21.78	35	−4	6
	R Putamen	20.46	35	−15	4
	R Putamen	20.12	33	−4	10
	R Insula Lobe	16.43	35	8	15
	R Putamen	15.04	33	2	10
Cluster 5					
(90 voxels)	L Caudate Nucleus	20.00	−17	24	0
	L Caudate Nucleus	18.97	−18	24	4
	L Caudate Nucleus	17.25	−14	23	−8
Cluster 6					
(79 voxels)	R Amygdala	20.62	24	3	−17
	R Amygdala	16.96	27	2	−14
	R Amygdala	15.80	21	−3	−9
	R Amygdala	14.35	23	−1	−11
Cluster 7					
(39 voxels)	L Hippocampus	16.47	−20	−13	−23
Cluster 8					
(34 voxels)	R Precuneus	17.90	8	−45	75
	R Paracentral Lobule	16.13	6	−37	75
Cluster 9					
(20 voxels)	L Insula Lobe	21.58	−30	6	12
Cluster 10					
(19 voxels)	L Posterior-Medial Frontal	19.28	−9	21	58
	L Posterior-Medial Frontal	14.83	−9	17	63
Cluster 11					
(19 voxels)	L Putamen	16.76	−33	−19	1
Cluster 12					
(19 voxels)	R Superial Temporal Gyrus	15.19	42	−4	−15
Cluster 13					
(18 voxels)	L Inferior Temporal Gyrus	15.26	−63	−31	−21
	L Inferior Temporal Gyrus	15.25	−63	−37	−21
Cluster 14					
(17 voxels)	R Globus Pallidum	15.64	11	6	1
Cluster 15					
(15 voxels)	L Middle Temporal Gyrus	15.55	−62	−25	−8
Cluster 16					
(14 voxels)	L Cingular gyrus	16.33	−18	−34	43
Cluster 17					
(13 voxels)	L Middle Temporal Gyrus	18.94	−65	-34	−15

A threshold of $P < 0.05$, corrected for multiple comparisons based on the false discovery rate (FDR), was applied to the resulting statistical parametric maps. Only clusters with a minimum extent of 10 contiguous voxels are reported. L, Left; R, Right.

increase in MRI subvolumes in the early stages of a pathology may reflect some structural adaptative processes that gradually decrease with the ongoing pathology. Such changes have already been observed in the striatum, more specifically within the bilateral caudate nucleus of patients with long-term neurosensory disorders (Casseb et al., 2019), just like an adaptative mechanism for chronic lack of proprioceptive and vibratory inputs. Since deafferentation increases the risk of falls (Saftari and Kwon, 2018), this may explain at least in part our present results. Of note, we also found here that fallers with MCI and dementia, but not the CHI, exhibited larger GM striatal subvolumes, suggesting an adaptative mechanism used by those with MCI and dementia to maintain operational high-level gait control despite cognitive decline. However, the design of our study did not correlate GM morphological changes to behavioral changes such as gait improvements or prevention of falls, which prevented the conclusion of a compensation mechanism according to Cabeza et al. (2018).

We found no changes in WM subvolumes according to the history of falls. This result is not inconsistent with previous literature supporting a possible contribution of white matter in fall risk, which did not examine white matter volumetry but the onset of white matter hyperintensities (WMH) that broke integrity of white matter fibers (Taylor et al., 2018). It has notably been shown that WMH progression may increase the risk of falls (Callisaya et al., 2015). Thus our findings provide novel information by supporting that the WM might not be responsible for the risk of falling but, if it was the case, it would be a mechanism other than atrophy, such as for example the loss of integrity or vitality of the WM, that would be involved.

To our knowledge, we provide here the first voxel-based morphometric analysis in a large sample of participants to examine the morphology of fallers' brain. Our sample seems to be representative of the general population of seniors; the clinical characteristics of fallers corresponding to what is known in previous literature and what we observe in clinical routine (No author list, 2001). Regardless, a number of limitations also exist. First, the study sample was restricted to older community-dwellers with cognitive complaints. Second, the search for falls

was based on self-report in our patients, which may be influenced by a possible recall bias. Third, our assessment did not include a detailed measure of gait or visual processing, which could have further enhanced our understanding of the underlying mechanisms explaining the association between falls and gray matter subvolumes. Fourth, the cross-sectional design of our study does not allow any causal inference. Fifth, VBM has difficulties with the segmentation and normalization that may result in problems in localization of regional volumes. We limited these defects by using DARTEL, a fluid deformation capable of precisely realigning brain structures (Klein et al., 2009).

In conclusion, we found that older fallers -mostly those with MCI and dementia- had greater subvolumes in bilateral striatum than non-fallers, principally within the caudate nucleus. These findings suggest a possible adaptative mechanism based on the enhancement of specific brain regions to maintain operational high-level gait control despite cognitive decline. Additional work is needed to better understand the neuroanatomical correlates of falls in older adults. Understanding higher-level gait disorders may offer a powerful mechanism to act on mobility decline and falls in older adults and to maintain function late in life.

MEMBERS OF THE SAM GROUP

Pierre Abraham, M.D., Ph.D.; Cédric Annweiler, M.D., Ph.D.; Mickael Dinomais, M.D., Ph.D.; Guillaume Duval, M.D., M.S.; Nicolas Lerolle, M.D., Ph.D.; Frédéric Noublanche, M.D., M.S.

DATA AVAILABILITY STATEMENT

The raw data supporting the conclusions of this article will be made available by the authors, without undue reservation.

ETHICS STATEMENT

The studies involving human participants were reviewed and approved by Ethical Committee of Angers University Hospital. The patients/participants provided their written informed consent to participate in this study.

AUTHOR CONTRIBUTIONS

CA had full access to all of the data in the study, took responsibility for the data, the analyses and interpretation and had the right to publish any and all data, separate and apart from the attitudes of the sponsors, performed the administrative, technical, or material support, and supervised the study. CA and ML conceived and designed the study and drafted the manuscript. CA, MA, and ML carried out the data acquisition. ML, PA, MD, and CA did the analysis and interpretation of data. PA, MA, DS-R, and MD critically revised the manuscript for the important intellectual content. PA, MD, and CA did the statistical expertise. All authors have read and approved the manuscript.

ACKNOWLEDGMENTS

We acknowledge Melinda Beaudenon, MSc, Jennifer Gautier, MSc, and Romain Simon, MSc, from the Research Center on Autonomy and Longevity, Angers University Hospital, France, for their daily assistance.

SUPPLEMENTARY MATERIAL

The Supplementary Material for this article can be found online at: https://www.frontiersin.org/articles/10.3389/fbioe.2021.610426/full#supplementary-material

REFERENCES

Albert, M. S., DeKosky, S. T., Dickson, D., Dubois, B., Feldman, H. H., Fox, N. C., et al. (2011). The diagnosis of mild cognitive impairment due to Alzheimer's disease: recommendations from the national institute on aging-Alzheimer's association workgroups on diagnostic guidelines for Alzheimer's disease. *Alzheimers Dement* 7, 270–279. doi: 10.1016/j.jalz.2011.03.008

Allali, G., Assal, F., Kressig, R. W., Dubost, V., Herrmann, F. R., and Beauchet, O. (2008). Impact of impaired executive function on gait stability. *Dement Geriatr. Cogn. Disord.* 26, 364–369. doi: 10.1159/000162358

Allali, G., van der Meulen, M., Beauchet, O., Rieger, S. W., Vuilleumier, P., and Assal, F. (2014). The neural basis of age-related changes in motor imagery of gait: an fMRI study. *J. Gerontol. Biol. Sci. Med. Sci.* 69, 1389–1398. doi: 10.1093/gerona/glt207

Andersson, C., Hamer, R. M., Lawler, C. P., Mailman, R. B., and Lieberman, J. A. (2002). Striatal volume changes in the rat following long-term administration of typical and atypical antipsychotic drugs. *Neuropsychopharmacology* 27, 143–151. doi: 10.1016/S0893-133X(02)00287-287

Annweiler, C., Beauchet, O., Bartha, R., Wells, J. L., Borrie, M. J., Hachinski, V., et al. (2013). Motor cortex and gait in mild cognitive impairment: a magnetic resonance spectroscopy and volumetric imaging study. *Brain* 136, 859–871. doi: 10.1093/brain/aws373

Annweiler, C., Maby, E., Meyerber, M., and Beauchet, O. (2014a). Hypovitaminosis D and executive dysfunction in older adults with memory complaint: a memory clinic-based study. *Dement Geriatr. Cogn. Disord* 37, 286–293. doi: 10.1159/000356483

Annweiler, C., Montero-Odasso, M., Bartha, R., Drozd, J., Hachinski, V., and Beauchet, O. (2014b). Association between gait variability and brain ventricle attributes: a brain mapping study. *Exp. Gerontol.* 57, 256–263. doi: 10.1016/j.exger.2014.06.015

Ashburner, J. (2007). A fast diffeomorphic image registration algorithm. *Neuroimage* 38, 95–113. doi: 10.1016/j.neuroimage.2007.07.007

Beauchet, O., Allali, G., Berrut, G., Hommet, C., Dubost, V., and Assal, F. (2008). Gait analysis in demented subjects: interests and perspectives. *Neuropsychiatr. Dis. Treat* 4, 155–160. doi: 10.2147/ndt.s2070

Beauchet, O., Allali, G., Launay, C., Herrmann, F. R., and Annweiler, C. (2013). Gait variability at fast-pace walking speed: a biomarker of mild cognitive impairment? *J. Nutr. Health Aging* 17, 235–239. doi: 10.1007/s12603-012-0394-394

Beauchet, O., Launay, C. P., Annweiler, C., and Allali, G. (2015). Hippocampal volume, early cognitive decline and gait variability: which association? *Exp. Gerontol.* 61, 98–104. doi: 10.1016/j.exger.2014.11.002

Beauchet, O., Launay, C. P., Barden, J., Liu-Ambrose, T., Chester, V. L., Szturm, T., et al. (2017). Association between falls and brain subvolumes: results from

a cross-sectional analysis in healthy older adults. *Brain Topogr.* 30, 272–280. doi: 10.1007/s10548-016-0533-z

Blumen, H. M., Brown, L. L., Habeck, C., Allali, G., Ayers, E., Beauchet, O., et al. (2019). Gray matter volume covariance patterns associated with gait speed in older adults: a multi-cohort MRI study. *Brain Imag. Behav.* 13, 446–460. doi: 10.1007/s11682-018-9871-9877

Cabeza, R., Albert, M., Belleville, S., Craik, F. I. M., Duarte, A., Grady, C. L., et al. (2018). Maintenance, reserve and compensation: the cognitive neuroscience of healthy ageing. *Nat. Rev. Neurosci.* 19, 701–710. doi: 10.1038/s41583-018-0068-62

Callisaya, M. L., Beare, R., Phan, T., Blizzard, L., Thrift, A. G., Chen, J., et al. (2015). Progression of white matter hyperintensities of presumed vascular origin increases the risk of falls in older people. *J. Gerontol. Biol. Sci. Med. Sci.* 70, 360–366. doi: 10.1093/gerona/glu148

Casseb, R. F., de Campos, B. M., Martinez, A. R. M., Castellano, G., and França Junior, M. C. (2019). Selective sensory deafferentation induces structural and functional brain plasticity. *NeuroImage: Clin.* 21:101633. doi: 10.1016/j.nicl.2018.101633

Dickerson, B. C., and Sperling, R. A. (2008). Functional abnormalities of the medial temporal lobe memory system in mild cognitive impairment and Alzheimer's disease: insights from functional MRI studies. *Neuropsychologia* 46, 1624–1635. doi: 10.1016/j.neuropsychologia.2007.11.030

Dinomais, M., Celle, S., Duval, G. T., Roche, F., Henni, S., Bartha, R., et al. (2016). Anatomic correlation of the mini-mental state examination: a voxel-based morphometric study in older adults. *PLoS One* 11:e0162889. doi: 10.1371/journal.pone.0162889

Dubois, B., Sarazin, M., Lehericy, S., Chupin, M., Tonelli, I., Garner, L., et al. (2009). P2a-4 etude hippocampe: evaluation de l'efficacité du donépézil versus placebo sur des marqueurs IRM et cliniques chez des patients présentant des troubles cognitifs légers. *Revue Neurol.* 165, 66–67. doi: 10.1016/S0035-3787(09)72632-72633

Eickhoff, S. B., Stephan, K. E., Mohlberg, H., Grefkes, C., Fink, G. R., Amunts, K., et al. (2005). A new SPM toolbox for combining probabilistic cytoarchitectonic maps and functional imaging data. *Neuroimage* 25, 1325–1335. doi: 10.1016/j.neuroimage.2004.12.034

Fortea, J., Sala-Llonch, R., Bartrés-Faz, D., Bosch, B., Lladó, A., Bargalló, N., et al. (2010). Increased cortical thickness and caudate volume precede atrophy in PSEN1 mutation carriers. *J. Alzheimers Dis.* 22, 909–922. doi: 10.3233/JAD-2010-100678

Gillespie, L. D., Robertson, M. C., Gillespie, W. J., Sherrington, C., Gates, S., Clemson, L. M., et al. (2012). Interventions for preventing falls in older people living in the community. *Cochrane Database Syst. Rev.* 9:CD007146. doi: 10.1002/14651858.CD007146.pub3

Good, C. D., Johnsrude, I. S., Ashburner, J., Henson, R. N., Friston, K. J., and Frackowiak, R. S. (2001). A voxel-based morphometric study of ageing in 465 normal adult human brains. *Neuroimage* 14, 21–36. doi: 10.1006/nimg.2001.0786

Gur, R. E., Maany, V., Mozley, P. D., Swanson, C., Bilker, W., and Gur, R. C. (1998). Subcortical MRI volumes in neuroleptic-naive and treated patients with schizophrenia. *Am. J. Psychiatry* 155, 1711–1717. doi: 10.1176/ajp.155.12.1711

Guze, S. B. (1995). Diagnostic and statistical manual of mental disorders, 4th ed. (DSM-IV). *AJP* 152, 1228–1228. doi: 10.1176/ajp.152.8.1228

Helmich, R. C., Derikx, L. C., Bakker, M., Scheeringa, R., Bloem, B. R., and Toni, I. (2010). Spatial remapping of cortico-striatal connectivity in Parkinson's disease. *Cereb. Cortex* 20, 1175–1186. doi: 10.1093/cercor/bhp178

Hsu, C. L., Best, J. R., Chiu, B. K., Nagamatsu, L. S., Voss, M. W., Handy, T. C., et al. (2016). Structural neural correlates of impaired mobility and subsequent decline in executive functions: a 12-month prospective study. *Exp. Gerontol.* 80, 27–35. doi: 10.1016/j.exger.2016.04.001

Katz, R., and Shah, P. (2010). The patient who falls: challenges for families, clinicians, and communities. *JAMA* 303, 273–274. doi: 10.1001/jama.2009.2016

Klein, A., Andersson, J., Ardekani, B. A., Ashburner, J., Avants, B., Chiang, M.-C., et al. (2009). Evaluation of 14 nonlinear deformation algorithms applied to human brain MRI registration. *Neuroimage* 46, 786–802. doi: 10.1016/j.neuroimage.2008.12.037

Kreitzer, A. C., and Malenka, R. C. (2008). Striatal plasticity and basal ganglia circuit function. *Neuron* 60, 543–554. doi: 10.1016/j.neuron.2008.11.005

Krings, T., Foltys, H., Meister, I. G., and Reul, J. (2003). Hypertrophic olivary degeneration following pontine haemorrhage: hypertensive crisis or cavernous haemangioma bleeding? *J. Neurol. Neurosurg. Psychiatry* 74, 797–799. doi: 10.1136/jnnp.74.6.797

Macfarlane, M. D., Looi, J. C. L., Walterfang, M., Spulber, G., Velakoulis, D., Styner, M., et al. (2015). Shape abnormalities of the caudate nucleus correlate with poorer gait and balance: results from a subset of the LADIS study. *Am. J. Geriatr. Psychiatry* 23, 59–71.e1. doi: 10.1016/j.jagp.2013.04.011

Maidan, I., Droby, A., Jacob, Y., Giladi, N., Hausdorff, J. M., and Mirelman, A. (2020). The neural correlates of falls: alterations in large-scale resting-state networks in elderly fallers. *Gait Posture* 80, 56–61. doi: 10.1016/j.gaitpost.2020.05.023

Muir, S. W., Beauchet, O., Montero-Odasso, M., Annweiler, C., Fantino, B., and Speechley, M. (2013). Association of executive function impairment, history of falls and physical performance in older adults: a cross-sectional population-based study in eastern France. *J. Nutr. Health Aging* 17, 661–665. doi: 10.1007/s12603-013-0045-44

No author list (2001). Guideline for the prevention of falls in older persons. american geriatrics society, british geriatrics society, and american academy of orthopaedic surgeons panel on falls prevention. *J. Am. Geriatr. Soc.* 49, 664–672.

Postuma, R. B., and Dagher, A. (2006). Basal ganglia functional connectivity based on a meta-analysis of 126 positron emission tomography and functional magnetic resonance imaging publications. *Cereb. Cortex* 16, 1508–1521. doi: 10.1093/cercor/bhj088

Rubenstein, L. Z., Powers, C. M., and MacLean, C. H. (2001). Quality indicators for the management and prevention of falls and mobility problems in vulnerable elders. *Ann. Intern. Med.* 135, 686–693. doi: 10.7326/0003-4819-135-8_part_2-200110161-200110167

Saftari, L. N., and Kwon, O.-S. (2018). Ageing vision and falls: a review. *J. Physiol. Anthropol.* 37:11. doi: 10.1186/s40101-018-0170-171

Smith, J. C., Nielson, K. A., Antuono, P., Lyons, J.-A., Hanson, R. J., Butts, A. M., et al. (2013). Semantic memory functional MRI and cognitive function after exercise intervention in mild cognitive impairment. *J. Alzheimers Dis.* 37, 197–215. doi: 10.3233/JAD-130467

Taylor, M. E., Lord, S. R., Delbaere, K., Wen, W., Jiang, J., Brodaty, H., et al. (2018). White matter hyperintensities are associated with falls in older people with dementia. *Brain Imaging Behav.* 13, 1265–1272. doi: 10.1007/s11682-018-9943-9948

Tinetti, M. E., Speechley, M., and Ginter, S. F. (1988). Risk factors for falls among elderly persons living in the community. *N. Engl. J. Med.* 319, 1701–1707. doi: 10.1056/NEJM198812293192604

Whalley, L. J., Deary, I. J., Appleton, C. L., and Starr, J. M. (2004). Cognitive reserve and the neurobiology of cognitive aging. *Ageing Res. Rev.* 3, 369–382. doi: 10.1016/j.arr.2004.05.001

Conflict of Interest: The authors declare that the research was conducted in the absence of any commercial or financial relationships that could be construed as a potential conflict of interest.

frontiers in Bioengineering and Biotechnology

ORIGINAL RESEARCH
published: 11 March 2021
doi: 10.3389/fbioe.2021.639337

Balance Impairments as Differential Markers of Dementia Disease Subtype

Ríona Mc Ardle[1,2], Stephanie Pratt[1], Christopher Buckley[3], Silvia Del Din[1], Brook Galna[4], Alan Thomas[1], Lynn Rochester[1,5] and Lisa Alcock[1]*

[1] Translational and Clinical Research Institute, Newcastle University, Newcastle upon Tyne, United Kingdom, [2] Population Health Sciences Institute, Newcastle University, Newcastle upon Tyne, United Kingdom, [3] Department of Sport, Exercise and Rehabilitation, Northumbria University, Newcastle upon Tyne, United Kingdom, [4] School of Biomedical, Nutritional and Sports Sciences, Newcastle University, Newcastle upon Tyne, United Kingdom, [5] Newcastle upon Tyne Hospitals, National Health Service Foundation Trust, Newcastle upon Tyne, United Kingdom

OPEN ACCESS

Edited by:
Martina Mancini, Oregon Health & Science University, United States

Reviewed by:
Wan-Tai Au-Yeung, Oregon Health & Science University, United States
Yuri Agrawal, Johns Hopkins University, United States
Richard Camicioli, University of Alberta, Canada

***Correspondence:**
Ríona Mc Ardle
riona.mcardle@ncl.ac.uk

Specialty section:
This article was submitted to Biomechanics, a section of the journal Frontiers in Bioengineering and Biotechnology

Received: *08 December 2020*
Accepted: *29 January 2021*
Published: *11 March 2021*

Citation:
Mc Ardle R, Pratt S, Buckley C, Del Din S, Galna B, Thomas A, Rochester L and Alcock L (2021) Balance Impairments as Differential Markers of Dementia Disease Subtype. Front. Bioeng. Biotechnol. 9:639337. doi: 10.3389/fbioe.2021.639337

Background: Accurately differentiating dementia subtypes, such as Alzheimer's disease (AD) and Lewy body disease [including dementia with Lewy bodies (DLB) and Parkinson's disease dementia (PDD)] is important to ensure appropriate management and treatment of the disease. Similarities in clinical presentation create difficulties for differential diagnosis. Simple supportive markers, such as balance assessments, may be useful to the diagnostic toolkit. This study aimed to identify differences in balance impairments between different dementia disease subtypes and normal aging using a single triaxial accelerometer.

Methods: Ninety-seven participants were recruited, forming four groups: cognitive impairment due to Alzheimer's disease (AD group; $n = 31$), dementia with Lewy bodies (DLB group; $n = 26$), Parkinson's disease dementia (PDD group; $n = 13$), and normal aging controls ($n = 27$). Participants were asked to stand still for 2 minutes in a standardized position with their eyes open while wearing a single triaxial accelerometer on their lower back. Seven balance characteristics were derived, including jerk (combined, mediolateral, and anterior–posterior), root mean square (RMS; combined, mediolateral, and anterior–posterior), and ellipsis. Mann–Whitney *U* tests identified the balance differences between groups. Receiver operating characteristics and area under the curve (AUC) determined the overall accuracy of the selected balance characteristics.

Results: The PDD group demonstrated higher RMS [combined ($p = 0.001$), mediolateral ($p = 0.005$), and anterior–posterior ($p = 0.001$)] and ellipsis scores ($p < 0.002$) than the AD group (AUC = 0.71–0.82). The PDD group also demonstrated significantly impaired balance across all characteristics ($p \leq 0.001$) compared to the controls (AUC = 0.79–0.83). Balance differences were not significant between PDD and DLB (AUC = 0.69–0.74), DLB and AD (AUC = 0.50–0.65), DLB and controls (AUC = 0.62–0.68), or AD and controls (AUC = 0.55–0.67) following Bonferroni correction.

Discussion: Although feasible and quick to conduct, key findings suggest that an accelerometer-based balance during quiet standing does not differentiate dementia disease subtypes accurately. Assessments that challenge balance more, such as gait or standing with eyes closed, may prove more effective to support differential diagnosis.

Keywords: dementia, Alzheimer's disease, Lewy body disease, Parkinson's disease, balance, accelerometer, postural control

INTRODUCTION

Assessing motor performance, such as gait and balance, in the aging population may be a useful clinical tool for predicting a range of clinical outcomes, such as falls risk, neurological disorders, cognitive impairment, and mortality (Fritz and Lusardi, 2009; Schoneburg et al., 2013; Creaby and Cole, 2018; Buckley et al., 2019; Modarresi et al., 2019; Peel et al., 2019). Recently, motor performance has been reported as a potential supportive marker of differentiating Lewy body disease (LBD) from Alzheimer's disease (AD) (Fritz et al., 2016; Mc Ardle et al., 2019, 2020). Identifying supportive clinical tools to differentiate dementia subtypes, such as LBD [which includes dementia with Lewy bodies (DLB) and Parkinson's disease dementia (PDD)], is of critical importance to ensure accurate and appropriate treatment and care provision for people with dementia (Palmqvist et al., 2009). This is particularly apparent for people with DLB, as DLB is underdiagnosed and may be misdiagnosed as AD due to similarities in clinical presentation (Palmqvist et al., 2009; Kane et al., 2018). As such, quick and easy-to-use diagnostic tools may be welcome additions to the clinician's toolkit.

Motor assessments that require minimal space and time may be an avenue of interest for differential diagnosis, such as balance assessment. Maintaining postural control (i.e., balance) requires coordination from multiple body systems, including the vestibular, cognitive, visual, somatosensory, and motor systems (Mancini and Horak, 2010); balance impairments may therefore arise from changes to the aforementioned systems, such as neuropathology and cognitive decline. Greater sway and larger sway velocities have been reported in both mild cognitive impairment and dementia (Bahureksa et al., 2017), suggesting that balance impairments may be a marker of cognitive disorders. This is supported by the reported associations between balance impairments with slower information processing and greater executive dysfunction in Parkinson's disease (PD) (Fernandes et al., 2016).

With the advent of accelerometer-based wearable technology, conducting balance assessments in constrained settings such as a clinic is increasingly feasible (Mancini et al., 2011b, 2012b). Accelerometer-based balance characteristics are reported as useful measures of postural instability in neurodegenerative populations such as PD (Mancini et al., 2011a). Balance impairments may therefore be useful markers of neurodegenerative disease type and progression, with measures of sway jerkiness (i.e., jerk) in the mediolateral direction significantly impaired in PD compared to controls (Mancini et al., 2012a), and jerk, root mean square (RMS; the magnitude of accelerometer traces), and ellipsis (the area which includes 95% of the mediolateral and anteroposterior accelerometer trajectories) increasing as the disease progresses (Mancini et al., 2012a; Pantall et al., 2018). However, there is a dearth of research examining the ability of balance assessment to discriminate between dementia disease subtypes, with only clinical measures of balance assessment used to report worse balance performance in LBD compared to AD and in PDD compared to DLB (Allan et al., 2005; Fritz et al., 2016; Scharre et al., 2016).

As such, the primary aims of this study were to (1) examine differences in the accelerometer-derived balance characteristics between dementia disease subtypes (i.e., AD, DLB, and PDD) and (2) between dementia disease subtypes and normal aging. A secondary aim was to (3) explore the associations between clinical and cognitive characteristics with balance characteristics in dementia disease subtypes. We hypothesize that (1) Lewy body disease groups (i.e., DLB and PDD) will demonstrate significantly larger jerk, RMS, and ellipsis compared to AD; (2) all dementia disease subtypes will have significantly worse postural instability compared to controls; and (3) slower information processing, greater executive dysfunction, worse motor performance, and lower balance confidence will be significantly correlated with impaired balance characteristics in all dementia disease subtypes.

MATERIALS AND METHODS

Participants

Participants with probable mild cognitive impairment (MCI) or probable dementia due to AD, DLB, and PDD and older adult controls were recruited to the GaitDem Study at Newcastle University. Participants were identified by clinicians in old age psychiatry, geriatric medicine, or neurology services, recruited from a local research case register (the North East DeNDRoN Case Register), or *via* ongoing research studies. The inclusion/exclusion criteria can be found elsewhere (Mc Ardle et al., 2019). All participants had capacity to consent and provided written informed consent. The NHS Local Research Ethics Committee, Newcastle and North Tyneside 1, approved this study.

The disease diagnosis of all participants was verified by two independent clinicians *via* review of medical notes and assessments; disagreements were adjudicated by a third clinician. The relevant diagnostic criteria for dementia due to AD (McKhann et al., 2011), DLB (McKeith et al., 2017), and PDD (Emre et al., 2007) and for MCI due to AD (Albert et al., 2011), DLB (McKeith et al., 2020), and PDD (Litvan et al., 2012) were applied.

Clinical and Cognitive Assessment

Sex, age, height, and body mass were recorded. Dementia disease stage was assessed with the Clinical Dementia Rating Scale (CDR) (Morris, 1997). Premorbid IQ was measured with the National Adult Reading Test (NART) (Nelson and Willison, 1991). Comorbidities were assessed with the Cumulative Illness Rating Scale – Geriatrics (CIRS-G) (Linn et al., 1968), while motor disease severity was determined using the Movement Disorders Society Unified Parkinson's Disease Rating Scale (MDS-UPDRS) (Goetz et al., 2008). Functional dependence was assessed using the Bristol Activities of Daily Living Scale (BADLS) (Bucks et al., 1996). Balance confidence was measured using the Activities Balance Confidence (ABC) Scale (Powell and Myers, 1995). Faller status was recorded (i.e., if the participant had experienced a fall within the previous 12 months).

Global cognition was measured using both the standardized Mini Mental State Examination (sMMSE) (Molloy and Standish, 1997) and the Addenbrooke's Cognitive Examination III (ACE-III) (Noone, 2015), which has subscales measuring attention, language, memory, fluency, and visuospatial abilities. Information processing speed was assessed using the Trail Making Test A (TMT-A) (Bowie and Harvey, 2006). The F-A-S Verbal Fluency test assessed verbal fluency and executive function (Borkowski et al., 1967), and the computerized simple reaction time test measured attention.

Balance Assessment

A small accelerometer-based wearable (Axivity AX3, York, United Kingdom; dimensions, 23.0 mm × 32.5 mm × 7.6 mm; weight, 11 g; accuracy, 20 ppm; sampling frequency, 100 Hz) was attached to the participants' lower back in the L5 position using a double-sided hydrogel adhesive and a Hypafix medical plaster. Participants were asked to stand with heels 10 cm apart, maintaining an upright position with arms by their sides and eyes open for 2 min. Participants wore shoes during the assessment. Researchers stood close by in case of adverse events.

Following assessment, the data were downloaded to a computer and processed with a customized MATLAB® script. Accelerations in the anteroposterior and mediolateral planes were of particular interest. Data were filtered using fourth-order zero phase, low-pass Butterworth filter. The cutoff frequency was 3.5 Hz (Del Din et al., 2015). Data were transformed to a horizontal–vertical coordinate system, following which the balance outcomes were extracted in the mediolateral, anteroposterior, and combined directions.

Balance Characteristics

Seven balance characteristics were derived. Three characteristics related to jerk in the mediolateral, anteroposterior, and combined directions (i.e., the rate of change of acceleration, considered a measure of dynamic stability) (Mancini et al., 2011b). Three characteristics corresponded to RMS in the mediolateral, anteroposterior, and combined directions (i.e., the magnitude of accelerometer traces) (Mancini et al., 2011b). Ellipsis was also derived (i.e., the area which includes 95% of the mediolateral and anteroposterior acceleration trajectories) (Del Din et al., 2015). Data were normalized over the duration of the standing balance test to account for any differences in standing time.

Data Analysis

Normality of data was assessed using the Shapiro–Wilk test and inspection of the histograms and box plots. Chi-squared tests identified differences between groups for sex and faller status. Kruskal–Wallis tests and one-way analysis of variance (ANOVA) examined differences between groups for all demographic, cognitive, and clinical variables. Mann–Whitney U tests and independent t tests identified where the differences lay between groups. As all balance characteristics were not normally distributed, Kruskal–Wallis tests and Mann–Whitney U tests were used to identify differences between groups. Bonferroni corrections ($p \leq 0.007$) were applied to account for multiple comparisons. There was one significant outlier in the control group; we assessed group differences with and without the outlier and found no difference to our interpretation of results, so we retained this participant. Receiver operating characteristics and area under the curve (AUC) were used to determine the accuracy of discrete balance characteristics and were interpreted as follows: 0.5–0.7 = low accuracy, 0.7–0.9 = acceptable accuracy, and 0.9–1 = high accuracy. As the data were not normally distributed, Spearman's correlations were used to explore associations between balance impairments and the demographic, clinical, and cognitive measures.

RESULTS

Demographics

One hundred twenty-five participants were recruited to the study; 97 participants were included in this analysis. The reasons for exclusion were as follows: clinical diagnosis other than AD, DLB, PDD, or control (vascular dementia = 7, non-dementia = 4, control with suspected cognitive impairment = 1), withdrawal from the study (n = 3), and inability to complete the balance assessment (n = 13).

As the dementia disease groups included people with MCI or dementia (see **Table 1**), we initially examined the differences in balance characteristics within each dementia disease group, comparing MCI and dementia. As there were no significant differences found between MCI and dementia within each subtype, it was deemed feasible to include both disease stages within each dementia disease group (i.e., AD, DLB, and PDD). The demographics and clinical and cognitive information are illustrated in **Table 1**, with significant between-group differences reported.

Differences in Balance Characteristics Between Dementia Disease Subtypes

Compared to the AD group, the PDD group demonstrated significantly larger jerk in the combined, anteroposterior (AP), and mediolateral (ML) directions (see **Tables 2**, **3** for statistical significance), larger RMS in the combined, ML, and AP directions, and larger ellipsis (see **Figure 1**). They also

TABLE 1 | Demographics and clinical and cognitive data for dementia disease groups and controls.

	Controls	AD	DLB	PDD	*p*	Between-group differences
n	27	31	26	13		
Age (years)	74 ± 9	77 ± 6	76 ± 6	79 ± 6	0.326	
Sex (male/female)	11/16	14/17	22/4	12/1	**<0.001**	a, b, c, d, e
NART	123 (117–126)	117 (101–125)	116 (101–124)	121 (105–124)	**<0.001**	a, b, c
CIRS-G	4 (0–11)	8 (3–16)	10 (5–16)	10 (3–17)	**<0.001**	a, b, c, d, e
MDS-UPDRS III	1 (0–11)	7 (0–19)	26 (0–57)	40 (20–70)	**<0.001**	a, b, c, d, e
Faller status (%)	20%	45%	59%	69%	**0.009**	a, b, c
ABC (%)	94 (52–100)	90 (37–100)	86 (42–100)	75 (21–94)	**<0.001**	a, b, c, e
% Mild cognitive impairment	N/a	39	33	46	0.732	
% Dementia	N/a	61	67	54	0.732	
sMMSE (/30)	30 (25–30)	23 (14–29)	24 (16–30)	24 (12–30)	**<0.001**	a, b, c
ACE-III Total (/100)	97 (87–100)	74 (48–90)	75 (15–95)	79 (49–95)	**<0.001**	a, b, c
ACE-III Attention (/18)	18 (17–18)	14 (6–18)	15 (8–18)	14 (7–18)	**<0.001**	a, b, c
ACE-III Memory (/26)	25 (19–26)	14 (6–23)	17 (0–26)	20 (9–26)	**<0.001**	a, b, c, d, e
ACE-III Fluency (/14)	13 (5–14)	9 (2–13)	8 (3–13)	7 (2–12)	**<0.001**	a, b, c
ACE-III Language (/26)	26 (24–26)	23 (11–26)	23 (0–26)	25 (17–26)	**<0.001**	a, b, c
ACE-III Visuospatial (/16)	16 (13–16)	14 (6–16)	12 (0–16)	11 (9–16)	**<0.001**	a, b, c, d, e
FAS (*n*)	47 (29–75)	35 (3–61)	31 (7–58)	19 (11–48)	**<0.001**	a, b, c, e
TMT-A (s)	30 (19–65)	51 (29–306)	109 (28–835)	95 (24–955)	**<0.001**	a, b, c, d, e
RT Single Task (ms)	373 (291–493)	415 (287–773)	446 (287–1,071)	558 (387–3,792)	**<0.001**	a, b, c, d, e

Data displayed as mean ± SD were analyzed using one-way ANOVA and post hoc t tests. Data displayed as median (min–max) were analyzed using Kruskal–Wallis tests and post hoc Mann–Whitney U tests. Significant differences are as follows: a = controls vs. AD, b = controls vs. DLB, c = controls vs. PDD, d = AD vs. DLB, and e = AD vs. PDD. AD, Alzheimer's disease; DLB, dementia with Lewy bodies; PDD, Parkinson's disease dementia; NART, National Adult Reading Test; CIRS-G, Cumulative Illness Rating Scale – Geriatrics; MDS-UPDRS III, Movement Disorders Society Unified Parkinson's Disease Rating Scale; ABC, Activities Balance Confidence Scale; sMMSE, standardized Mini Mental State Examination; ACE-III, Addenbrooke's Cognitive Examination III; FAS, FAS Verbal Fluency Test; TMT-A, Trail Making Task Part A; RT, reaction time. Bold p-values indicate statistically significant results.

demonstrated significantly larger RMS ML compared to the DLB group. No differences were found between the AD and DLB groups. When Bonferroni corrections were applied, only differences in RMS, RMS AP, and ellipsis remained statistically significant between the AD and PDD groups. ROC curve analysis demonstrated acceptable–excellent accuracy to discriminate PDD from AD (AUC = 0.71–0.82), acceptable accuracy to discriminate PDD from DLB (AUC = 0.69–0.74), and low accuracy to discriminate DLB from AD (AUC = 0.50–0.65) for all balance characteristics (see **Table 3**).

Differences in Balance Characteristics Between Dementia Disease Subtypes and Controls

Compared to the controls, both the PDD and DLB groups demonstrated significantly larger jerk in the combined, AP, and ML directions, larger RMS in the combined and AP directions, and larger ellipsis (see **Tables 2**, **3** and **Figure 1**). The PDD group also demonstrated greater RMS ML compared to the controls. The AD group had greater jerk AP compared to the controls. When Bonferroni corrections were applied, only differences between the controls and PDD for all characteristics remained statistically significant. ROC curve analysis demonstrated excellent accuracy to discriminate PDD (AUC = 0.79–0.83) from the controls and low accuracy to discriminate AD (AUC = 0.55–0.67) and DLB (AUC = 0.62–0.68) from the controls for all balance characteristics (see **Table 3**).

Associations Between Balance Characteristics and Clinical and Cognitive Measures in Dementia Disease Subtypes

Alzheimer's Disease

In AD, older age was associated with greater combined (rho = 0.424, $p = 0.018$) and AP RMS (rho = 0.438, $p = 0.014$) and larger ellipsis (rho = 0.404, $p = 0.024$). Greater motor problems, as measured by UPDRS-III, was associated with greater RMS AP (rho = 0.428, $p = 0.018$; see **Figure 2**). Worse verbal fluency, as measured by ACE-III Fluency, was significantly associated with greater combined (rho = 0.422, $p = 0.018$), ML (rho = 0.406, $p = 0.024$), and AP jerk (rho = 0.426, $p = 0.017$), greater combined (rho = 0.373, $p = 0.039$) and ML RMS (rho = 0.369, $p = 0.041$), and larger ellipsis (rho = 0.378, $p = 0.036$). Similar findings were found between the FAS verbal fluency test with jerk AP (rho = 0.377, $p = 0.037$) and RMS ML (rho = 0.374, $p = 0.038$). Slower information processing, as measured by TMT-A, was significantly associated with greater combined (rho = 0.461, $p = 0.009$), ML (rho = 0.416, $p = 0.020$), and AP jerk (rho = 0.454, $p = 0.010$).

Dementia With Lewy Bodies

In DLB, better visuospatial abilities (rho = 0.423, $p = 0.035$), as measured by the ACE-III visuospatial subscale, and quicker information processing (rho = 0.539, $p = 0.026$) were associated

TABLE 2 | Balance differences between dementia disease groups and controls.

	Controls	Alzheimer's disease	Dementia with Lewy bodies	Parkinson's disease dementia	*p*	Between-group differences
n	27	31	26	13		
Jerk combined ($m^2\ s^{-6}$)	0.063 (0.027–3.942)	0.075 (0.038–0.383)	0.080 (0.023–0.726)	0.203 (0.050–1.10)	**0.003**	a
Jerk ML ($m^2\ s^{-6}$)	0.029 (0.006–2.669)	0.030 (0.013–0.180)	0.037 (0.002–0.414)	0.062 (0.019–0.625)	0.008	
Jerk AP ($m^2\ s^{-6}$)	0.035 (0.016–1.274)	0.044 (0.024–0.202)	0.047 (0.019–0.312)	0.109 (0.031–0.471)	**0.002**	a
RMS combined ($m\ s^{-3}$)	0.0008 (0.0004–0.0061)	0.0009 (0.0006–0.0027)	0.0012 (0.0006–0.0039)	0.0022 (0.0005–0.0044)	**0.001**	a, b
RMS ML ($m\ s^{-3}$)	0.0004 (0.0001–0.0039)	0.0005 (0.0003–0.0016)	0.0005 (0.0001–0.0019)	0.0012 (0.0004–0.0023)	**0.006**	a, b
RMS AP ($m\ s^{-3}$)	0.0007 (0.0004–0.0049)	0.0008 (0.0006–0.0022)	0.0011 (0.0006–0.0034)	0.0018 (0.0004–0.0039)	**0.001**	a, b
Ellipsis ($m^2\ s^{-5}$)	0.0007 (0.0001–0.0410)	0.0008 (0.0004–0.0061)	0.0011 (0.0001–0.0142)	0.0043 (0.0003–0.0116)	**0.001**	a, b

Data are reported as median (minimum–maximum). Kruskal–Wallis tests were used to identify differences between groups. Mann–Whitney U tests were used to identify where differences lay. Bonferroni correction ($p < 0.007$) applied. Significant differences are as follows: a = PDD vs. controls and b = PDD vs. AD. ML, mediolateral; AP, anteroposterior; RMS, root mean square. Bold p-values indicate statistically significant results.

TABLE 3 | Area under the curve values of discrete balance characteristics between groups based on receiver operator curve analysis.

	AD vs. DLB				AD vs. PDD				PDD vs. DLB			
	Area	***p***	**CI lower**	**CI upper**	**Area**	***p***	**CI lower**	**CI upper**	**Area**	***p***	**CI lower**	**CI upper**
Jerk combined	0.531	0.689	0.377	0.685	0.73	0.017	0.55	0.909	0.698	0.046	0.511	0.886
Jerk ML	0.545	0.564	0.391	0.699	0.722	0.021	0.538	0.907	0.695	0.049	0.512	0.878
Jerk AP	0.535	0.654	0.381	0.689	0.715	0.026	0.531	0.898	0.692	0.053	0.502	0.883
RMS combined	0.655	0.045	0.503	0.807	0.811	**0.001**	0.63	0.992	0.734	0.019	0.546	0.922
RMS ML	0.574	0.336	0.418	0.731	0.779	**0.004**	0.608	0.95	0.731	0.02	0.546	0.915
RMS AP	0.656	0.044	0.505	0.807	0.824	**0.001**	0.649	0.999	0.743	0.015	0.557	0.928
Ellipsis	0.624	0.109	0.471	0.778	0.804	**0.002**	0.624	0.984	0.71	0.034	0.524	0.896
	AD vs. Controls				**DLB vs. Controls**				**PDD vs. Controls**			
	Area	***p***	**CI lower**	**CI upper**	**Area**	***p***	**CI lower**	**CI upper**	**Area**	***p***	**CI lower**	**CI upper**
Jerk combined	0.652	0.047	0.51	0.794	0.682	0.023	0.534	0.831	0.821	**0.001**	0.667	0.974
Jerk ML	0.626	0.1	0.481	0.771	0.67	0.034	0.518	0.821	0.792	**0.003**	0.613	0.971
Jerk AP	0.675	0.022	0.534	0.816	0.687	0.02	0.539	0.834	0.838	**0.001**	0.707	0.968
RMS combined	0.558	0.45	0.406	0.71	0.695	0.015	0.552	0.839	0.818	**0.001**	0.646	0.989
RMS ML	0.584	0.272	0.435	0.734	0.628	0.109	0.472	0.785	0.795	**0.003**	0.626	0.963
RMS AP	0.56	0.431	0.408	0.713	0.684	0.022	0.538	0.83	0.823	**0.001**	0.657	0.99
Ellipsis	0.578	0.307	0.43	0.727	0.668	0.036	0.517	0.819	0.826	**0.001**	0.664	0.988

Bonferroni correction ($p < 0.007$) applied. Bold p-values indicate statistically significant results.

with greater jerk ML (see **Figure 2**). Worse verbal fluency was associated with greater jerk AP (rho = 0.433, $p = 0.035$).

Parkinson's Disease Dementia

In PDD, worse balance confidence, as measured by the ABC scale, was associated with greater jerk ML (rho = 0.578, $p = 0.039$; see **Figure 2**). Slower information processing was associated with greater RMS ML (rho = 0.566, $p = 0.044$).

DISCUSSION

This is the first study to examine the differences in accelerometer-derived balance characteristics between dementia disease subtypes and normal aging. The key results demonstrate that people with PDD could be discriminated with acceptable accuracy from both people with AD and cognitively intact older adults based on balance impairments. However, differentiating between DLB and AD is more clinically challenging, and therefore, discriminative markers for these groups are considered a research priority (Kane et al., 2018). Our results demonstrated that balance assessment could not acceptably discriminate DLB from any other subtype, nor could it differentiate normal aging from AD or DLB.

Balance Assessment as a Differential Marker of Dementia Disease Subtype

In partial agreement with hypothesis 1, the PDD group demonstrated greater RMS in the combined and mediolateral directions and larger ellipsis compared to people with AD. This is consistent with findings from clinical measures (Allan et al., 2005; Fritz et al., 2016; Scharre et al., 2016). However, no differences were found between DLB and either AD or PDD once multiple

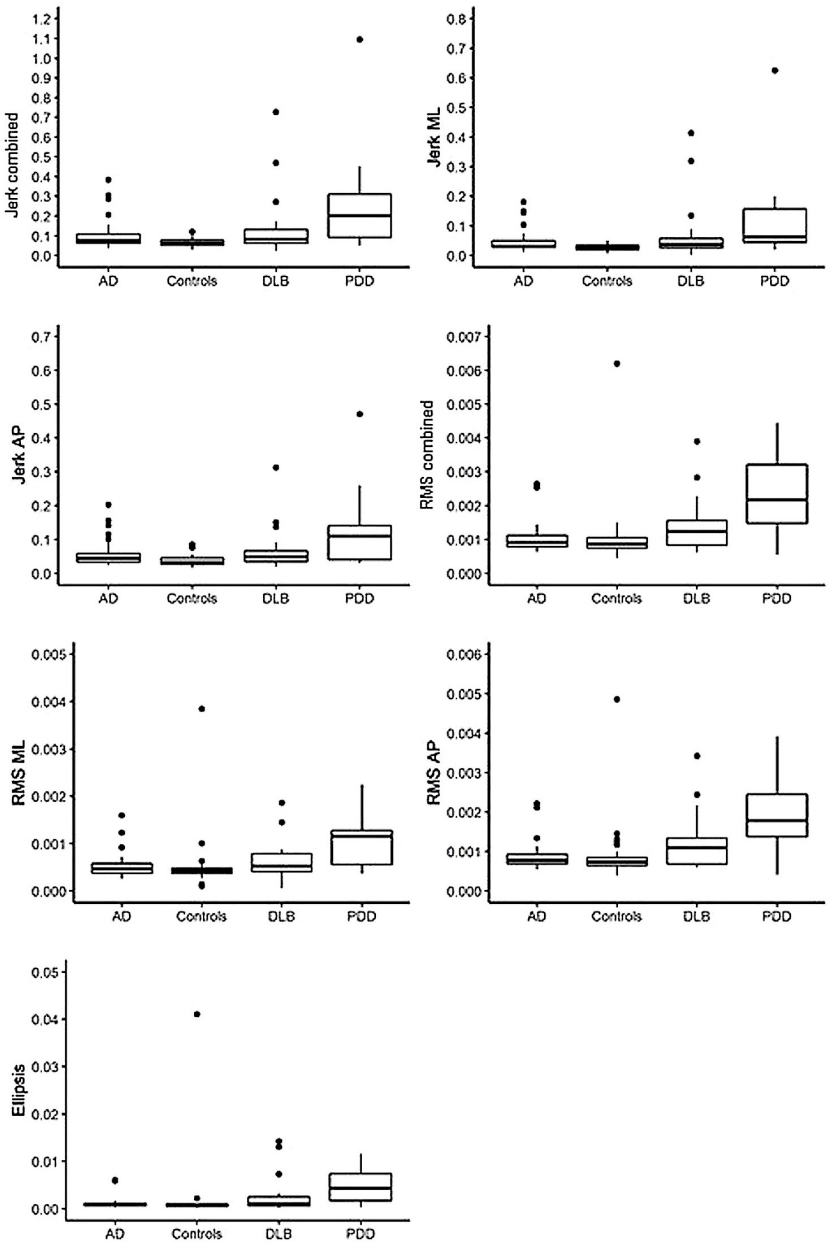

FIGURE 1 | Illustration of balance data across dementia disease subtypes and controls. AD, Alzheimer's disease; DLB, dementia with Lewy bodies; PDD, Parkinson's disease dementia; ML, mediolateral; AP, anteroposterior; RMS, root mean square. Dots denote outliers.

comparison corrections were applied. Although this is the first study to quantitatively examine balance impairments across dementia disease subtypes, these findings contrast with findings of significant differences in balance performance between all three dementia subtypes when assessed with an observational clinical measure (i.e., the Tinetti Balance subscale) (Allan et al., 2005; Fritz et al., 2016; Scharre et al., 2016). Confirmation bias introduced by clinical measures may explain the discrepancy in the findings, as examiners may subjectively expect greater balance problems in cohorts with clinically defined motor problems such as LBD (Emre et al., 2007; McKeith et al., 2017) compared to conditions that are not traditionally considered to have motor impairments such as AD (Allan et al., 2005). Based on our results, we do not recommend an eyes-open accelerometer-based balance assessment as a differential tool for AD and DLB.

Balance Assessment as a Differential Marker of Cognitive Impairment

In disagreement with hypothesis 2, only the PDD group demonstrated significant differences across all balance characteristics compared to cognitively intact controls. These

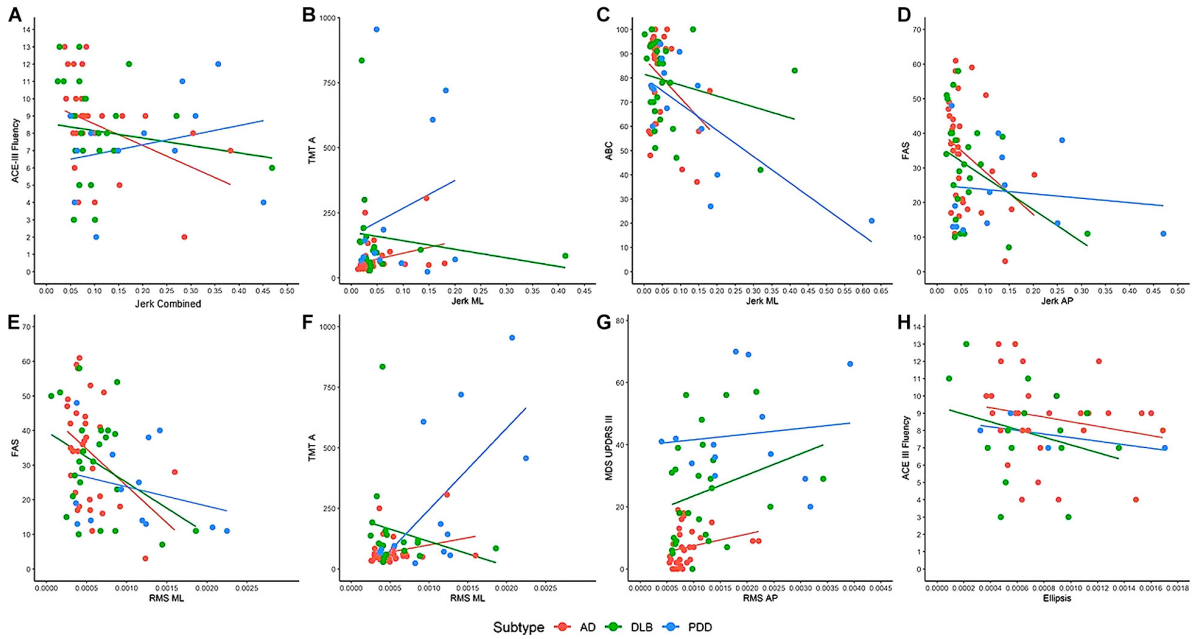

FIGURE 2 | Examples of the associations between clinical and cognitive variables with balance characteristics. **(A)** ACE-III Fluency associated with jerk vertical in AD (rho = 0.422, p = 0.018). **(B)** TMT-A associated with jerk ML in AD (rho = 0.416, p = 0.020) and DLB (rho = 0.539, p = 0.035). **(C)** ABC associated with jerk ML in PDD (rho = 0.578, p = 0.039). **(D)** FAS associated with jerk AP in AD (rho = 0.377, p = 0.037) and DLB (rho = 0.433, p = 0.035). **(E)** FAS associated with RMS ML in AD (rho = 0.374, p = 0.038). **(F)** TMT-A is associated with RMS ML in PDD (rho = 0.566, p = 0.044). **(G)** MDS UPDRS-III is associated with RMS AP in AD (rho = 0.428, p = 0.018). **(H)** ACE-III Fluency is associated with ellipsis in AD (rho = 0.378, p = 0.036). AD, Alzheimer's disease; DLB, dementia with Lewy bodies; PDD, Parkinson's disease dementia; ML, mediolateral; AP, anteroposterior; RMS, root mean square; ACE-III, Addenbrooke's Cognitive Examination; TMT-A, Trail Making Test A; ABC, Activities Balance Confidence Scale; FAS, FAS Verbal Fluency Test; MDS-UPDRS III, Movement Disorders Society Unified Parkinson's Disease Rating Scale. Dots denote outliers.

results support previous findings that accelerometer-based balance assessment is useful for differentiating PD from normal aging and for monitoring disease progression and cognitive decline in people with PD (Mancini et al., 2012a; Schoneburg et al., 2013; Del Din et al., 2015; Pantall et al., 2018). However, static eyes-open balance assessment did not appear significantly impaired in other dementia disease subtypes and, therefore, may not be a good marker of general cognitive impairment; this contrasts previous literature (Bahureksa et al., 2017). It should be noted that our cohort was a predominately mild dementia group, composed of both MCI and dementia participants, and this may have impacted our results. The review of Bahureksa et al. (2017) found limited differences in static balance performance in the MCI groups compared to normal aging in eyes-open conditions, suggesting that these groups use visual feedback to appropriately maintain their postural stability. As such, balance differences under these conditions may be apparent in the later stages of dementia disease. However, this is not useful to support early diagnosis of cognitive impairment, which is required to better manage the condition, ensure patients and carers can appropriately plan for the future, and to improve researchers' understanding of early disease stages in order to develop novel targets for therapeutics (Kenigsberg et al., 2016). We therefore suggest alternative motor performance measures to support differential diagnosis. For example, gait assessment has demonstrated acceptable accuracy to discriminate AD and DLB and may therefore be an effective easy-to-use supportive diagnostic marker (Mc Ardle et al., 2019, 2020).

Relationships Between Discrete Clinical and Cognitive Characteristics With Balance

To aid interpretation of the results, we examined associations between clinical and cognitive measures with balance performance. Partially agreeing with hypothesis 3, correlations were found between cognitive impairments and balance impairments. This was most apparent in the AD group, with slower information processing and worse verbal fluency (often considered a measure of executive function) (Williams-Gray et al., 2009) associated with poor balance performance. This is supported by the literature in PD (Fernandes et al., 2016), suggesting that balance relies on these discrete cognitive processes to maintain postural stability. For example, executive function may be important for planning and set-shifting during standing balance and may inhibit inappropriate postural responses (Schoneburg et al., 2013). Interestingly, associations between greater motor disease and worse balance were only found in the AD group, and associations between worse balance confidence and balance were only found in the PDD group; however, trends indicated similar directionality in all groups (see **Figure 2**). As the PDD group demonstrated significantly slower

information processing, worse verbal fluency, greater motor disease burden, and worse balance confidence compared to the AD group, this may somewhat account for their poorer balance performance. Overall, static balance may not be challenging to cognitive and motor abilities, particularly in lab-based environments which lack complexities experienced in the real word that may increase cognitive demands, such as constrained spaces, moving objects, and visual stimuli. The results may have been different if static balance performance was examined under different conditions. For example, eyes-closed static balance assessments increase reliance on the vestibular system and decreases compensatory visual and cognitive input for the maintenance of balance, potentially revealing greater balance impairments (Schoneburg et al., 2013; Bahureksa et al., 2017). Similarly, static balance assessments on uneven surfaces have demonstrated significantly worse balance in AD compared to normal aging (Suttanon et al., 2012). Standing statically on uneven surfaces, such as foam, requires consistent and quick postural adaptions to maintain balance (yeun Lee et al., 2011) and may reveal significant impairments when participants have discrete cognitive deficits, such as slower information processing that slows their anticipatory postural adjustments. Other studies have also employed cognitive dual tasks to static balance assessment in people with AD (Manckoundia et al., 2006). This places competition on cognitive resources, as participants are trying to maintain balance while carrying out an additional cognitive task, and produces greater balance impairments compared to single-task balance assessments. Future research could consider the impact of different conditions such as those outlined on balance in people with cognitive impairments. However, the findings from this study suggest that eyes-open static balance assessments will not be useful additions to the diagnostic toolkit.

Limitations and Directions for Future Research

A main strength of this study was that all participants' diagnoses were confirmed by clinicians' consensus based on clinical notes and well-characterized clinical and cognitive profiles. However, while this lends confidence to our results, diagnosis of dementia subtype can only be confirmed postmortem, which was beyond the scope of this study. We also looked at groups across the spectrum of cognitive impairment, which was deemed feasible as the MCI and dementia participants were indistinguishable in terms of balance impairments. However, there are limits to this approach; although we applied validated criteria for MCI due to dementia disease subtype (Litvan et al., 2012; McKeith et al., 2020), not all MCI participants may progress to dementia, and it was beyond the scope of this study to determine whether participants with MCI due to Lewy body disease went on to develop DLB or PDD. Additionally, although this is the first study of its kind, our sample size was small, causing difficulties to the generalizability of the findings, and outliers may have affected the results. Raw data were checked to ensure that outlier data were correct, highlighting the skewed distribution of balance performance. As our data were not normally distributed, we used non-parametric analysis to explore differences between groups. This limited our ability to account for potential confounders, such as age and sex, which may have improved our interpretation of results. Larger studies are required to account for these issues with generalizability and skewed distribution and would strengthen the findings described here. Our results suggest that a 2-min static eyes-open balance assessment is not a useful differential marker of dementia disease subtype or cognitive impairment. Studies in PD have indicated that balance impairments may be time-dependent, with shorter bouts producing more sensitive results (Del Din et al., 2015). However, we examined postural stability across different bout lengths (e.g., <30 and <60 s) and found that it did not change our interpretation. Additionally, we did not assess visual acuity in this study. As vision plays a significant role in the maintenance of balance, our lack of insight into participants' visual acuities is considered a limitation (Hill et al., 2016; Baydan et al., 2020; Hunter et al., 2020). To ensure participant safety, a researcher stood close to the participants who were visibly unstable or worried about their balance; this may also have influenced the results as it provided more security and confidence for the participants. It should be noted that static balance is only one element of balance; dynamic balance assessments require faster postural adjustments and may be significantly more compromised by cognitive impairments (Liaw et al., 2009). As we did not assess dynamic balance, we cannot draw conclusions on the efficacy of such assessments to detect cognitive impairment or dementia disease subtype. Finally, there is growing interest in classification methods, such as machine learning, which involve combining different disease features and assessing the best combinations for discriminating diseases. In the future, these methods could be applied in larger studies to combinations of balance characteristics, such as those described in this article, or to a combination of balance characteristics with other motor performance measures, such as gait or dynamic balance performance.

CONCLUSION

In conclusion, this study found that static eyes-open balance assessments could only acceptably differentiate PDD from AD and controls. Static eyes-open balance assessment is not a useful differential marker of AD and DLB or for distinguishing general cognitive impairment from normal ageing. In line with previous work in PD, associations were found between slower information processing and greater executive dysfunction with balance impairments, suggesting that cognition may play a role in safely maintaining balance. Future research could examine the impact of alternative conditions, such as eyes closed or dual tasks, on balance across dementia disease subtypes as this may prove a more fruitful endeavor.

DATA AVAILABILITY STATEMENT

The datasets generated and analyzed for this study can be made available by request with permission of the GaitDem Data Management team (lynn.rochester@ncl.ac.uk).

ETHICS STATEMENT

The studies involving human participants were reviewed and approved by the NHS Local Research Ethics Committee, Newcastle and North Tyneside 1. The patients/participants provided their written informed consent to participate in this study.

AUTHOR CONTRIBUTIONS

LR, BG, AT, LA, and RM contributed to the conception and design of this study. RM and LA collected the data for this study. RM, CB, SD, and LA organized the database. RM and SP performed the statistical analysis and wrote the first draft of the manuscript. All authors contributed to the manuscript revision and read and approved the submitted version.

FUNDING

This work was supported by the Alzheimer's Society (ADSTC2014007) and the National Institute for Health Research (NIHR) Newcastle Biomedical Research Centre based at Newcastle upon Tyne Hospitals NHS Foundation Trust and Newcastle University (BH152398/PD0617). This work was also supported by the NIHR/Wellcome Trust Clinical Research Facility (CRF) infrastructure at Newcastle upon Tyne Hospitals NHS Foundation Trust. RM was supported by a grant (MR/N029941/1) from the National Institute for Health Research (NIHR) and the Medical Research Council (MRC). The views expressed are those of the author(s) and not necessarily those of the NIHR or the Department of Health and Social Care or the funders.

ACKNOWLEDGMENTS

The research team acknowledges the support of the National Institute for Health Research Clinical Research Network (NIHR CRN) with the recruitment of participants. The research team would like to acknowledge Prof. John Paul Taylor and Dr. Paul Donaghy for their support in consensus diagnoses.

REFERENCES

Albert, M. S., DeKosky, S. T., Dickson, D., Dubois, B., Feldman, H. H., Fox, N. C., et al. (2011). The diagnosis of mild cognitive impairment due to Alzheimer's disease: recommendations from the national institute on aging-Alzheimer's association workgroups on diagnostic guidelines for Alzheimer's disease. *Alzheimer's Dementia.* 7, 270–279. doi: 10.1016/j.jalz.2011.03.008

Allan, L. M., Ballard, C. G., Burn, D. J., and Kenny, R. A. (2005). Prevalence and severity of gait disorders in Alzheimer's and non-Alzheimer's dementias. *J. Am. Geriatr. Soc.* 53, 1681–1687. doi: 10.1111/j.1532-5415.2005.53552.x

Bahureksa, L., Najafi, B., Saleh, A., Sabbagh, M., Coon, D., Mohler, M. J., et al. (2017). The impact of mild cognitive impairment on gait and balance: a systematic review and meta-analysis of studies using instrumented assessment. *Gerontology* 63, 67–83. doi: 10.1159/000445831

Baydan, M., Caliskan, H., Balam-Yavuz, B., Aksoy, S., and Boke, B. (2020). The interaction between mild cognitive impairment with vestibulo-ocular reflex, dynamic visual acuity and postural balance in older adults. *Exp. Gerontol.* 130:110785. doi: 10.1016/j.exger.2019.110785

Borkowski, J. G., Benton, A. L., and Spreen, O. (1967). Word fluency and brain damage. *Neuropsychologia* 5, 135–140. doi: 10.1016/0028-3932(67)90015-2

Bowie, C. R., and Harvey, P. D. (2006). Administration and interpretation of the trail making test. *Nat. Protoc.* 1, 2277–2281. doi: 10.1038/nprot.2006.390

Buckley, C., Alcock, L., McArdle, R., Rehman, R. Z. U., Del Din, S., Mazza, C., et al. (2019). The role of movement analysis in diagnosing and monitoring neurodegenerative conditions: insights from gait and postural control. *Brain Sci.* 9:34. doi: 10.3390/brainsci9020034

Bucks, R. S., Ashworth, D. L., Wilcock, G. K., and Siegfried, K. (1996). Assessment of activities of daily living in dementia: development of the bristol activities of daily living scale. *Age Ageing* 25, 113–120. doi: 10.1093/ageing/25.2.113

Creaby, M. W., and Cole, M. H. (2018). Gait characteristics and falls in Parkinson's disease: a systematic review and meta-analysis. *Parkinsonism Relat. Disord.* 57, 1–8. doi: 10.1016/j.parkreldis.2018.07.008

Del Din, S., Godfrey, A., Coleman, S., Galna, B., Lord, S., and Rochester, L. (2015). Time-dependent changes in postural control in early Parkinson's disease: what are we missing? *Med. Biol. Eng. Comp.* 54, 401–410. doi: 10.1007/s11517-015-1324-5

Emre, M., Aarsland, D., Brown, R., Burn, D. J., Duyckaerts, C., Mizuno, Y., et al. (2007). Clinical diagnostic criteria for dementia associated with Parkinson's disease. *Mov. Disord.* 22, 1689–1707. doi: 10.1002/mds.21507

Fernandes, A., Mendes, A., Rocha, N., and Tavares, J. M. (2016). Cognitive predictors of balance in Parkinson's disease. *Somatosens Mot. Res.* 33, 67–71. doi: 10.1080/08990220.2016.1178634

Fritz, N. E., Kegelmeyer, D. A., Kloos, A. D., Linder, S., Park, A., Kataki, M., et al. (2016). Motor performance differentiates individuals with lewy body dementia, Parkinson's and Alzheimer's disease. *Gait Posture.* 50, 1–7. doi: 10.1016/j.gaitpost.2016.08.009

Fritz, S., and Lusardi, M. (2009). White paper:"walking speed: the sixth vital sign". *J. Geriat. Phys. Ther.* 32, 2–5. doi: 10.1519/00139143-200932020-00002

Goetz, C. G., Tilley, B. C., Shaftman, S. R., Stebbins, G. T., Fahn, S., Martinez-Martin, P., et al. (2008). Movement disorder society-sponsored revision of the unified parkinson's disease rating scale (MDS-UPDRS): scale presentation and clinimetric testing results. *Mov. Disord.* 23, 2129–2170. doi: 10.1002/mds.22340

Hill, E., Stuart, S., Lord, S., Del Din, S., and Rochester, L. (2016). Vision, visuo-cognition and postural control in Parkinson's disease: an associative pilot study. *Gait Posture* 48, 74–76. doi: 10.1016/j.gaitpost.2016.04.024

Hunter, S. W., Divine, A., Madou, E., Omana, H., Hill, K. D., Johnson, A. M., et al. (2020). Executive function as a mediating factor between visual acuity and postural stability in cognitively healthy adults and adults with Alzheimer's dementia. *Arch. Gerontol. Geriatr.* 89:104078. doi: 10.1016/j.archger.2020.104078

Kane, J. P. M., Surendranathan, A., Bentley, A., Barker, S. A. H., Taylor, J. P., Thomas, A. J., et al. (2018). Clinical prevalence of Lewy body dementia. *Alzheimers Res. Ther.* 10:19. doi: 10.1186/s13195-018-0350-6

Kenigsberg, P. A., Aquino, J. P., Berard, A., Gzil, F., Andrieu, S., Banerjee, S., et al. (2016). Dementia beyond: knowledge and uncertainties. *Dementia (London)* 2016, 6–21. doi: 10.1177/1471301215574785

Liaw, M. Y., Chen, C. L., Pei, Y. C., Leong, C. P., and Lau, Y. C. (2009). Comparison of the static and dynamic balance performance in young, middle-aged, and elderly healthy people. *Chang Gung Med. J.* 32, 297–304.

Linn, B. S., Linn, M. W., and Gurel, L. (1968). Cumulative illness rating scale. *J. Am. Geriatr. Soc.* 16, 622–626. doi: 10.1111/j.1532-5415.1968.tb02103.x

Litvan, I., Goldman, J. G., Troster, A. I., Schmand, B. A., Weintraub, D., Petersen, R. C., et al. (2012). Diagnostic criteria for mild cognitive impairment in Parkinson's disease: movement disorder society task force guidelines. *Mov. Disord.* 27, 349–356. doi: 10.1002/mds.24893

Mancini, M., Carlson-Kuhta, P., Zampieri, C., Nutt, J. G., Chiari, L., and Horak, F. B. (2012a). Postural sway as a marker of progression in Parkinson's disease: a

pilot longitudinal study. *Gait Posture* 36, 471–476. doi: 10.1016/j.gaitpost.2012.04.010

Mancini, M., Salarian, A., Carlson-Kuhta, P., Zampieri, C., King, L., Chiari, L., et al. (2012b). Isway: a sensitive, valid and reliable measure of postural control. *J. Neuroeng. Rehabil.* 9:59. doi: 10.1186/1743-0003-9-59

Mancini, M., and Horak, F. B. (2010). The relevance of clinical balance assessment tools to differentiate balance deficits. *Eur. J. Phys. Rehabil. Med.* 46, 239–248.

Mancini, M., Horak, F. B., Zampieri, C., Carlson-Kuhta, P., Nutt, J. G., and Chiari, L. (2011a). Trunk accelerometry reveals postural instability in untreated Parkinson's disease. *Parkinsonism Relat. Disord.* 17, 557–562. doi: 10.1016/j.parkreldis.2011.05.010

Mancini, M., King, L., Salarian, A., Holmstrom, L., McNames, J., and Horak, F. B. (2011b). Mobility lab to assess balance and gait with synchronized body-worn sensors. *J. Bioeng. Biomed. Sci.* 12(Suppl. 1):007.

Manckoundia, P., Pfitzenmeyer, P., d'Athis, P., Dubost, V., and Mourey, F. (2006). Impact of cognitive task on the posture of elderly subjects with Alzheimer's disease compared to healthy elderly subjects. *Mov. Disord.* 21, 236–241. doi: 10.1002/mds.20649

Mc Ardle, R., Del Din, S., Galna, B., Thomas, A., and Rochester, L. (2020). Differentiating dementia disease subtypes with gait analysis: feasibility of wearable sensors? *Gait Posture* 76, 372–376. doi: 10.1016/j.gaitpost.2019.12.028

Mc Ardle, R., Galna, B., Donaghy, P., Thomas, A., and Rochester, L. (2019). Do Alzheimer's and Lewy body disease have discrete pathological signatures of gait? *Alzheimers Dement* 15, 1367–1377. doi: 10.1016/j.jalz.2019.06.4953

McKeith, I. G., Boeve, B. F., Dickson, D. W., Halliday, G., Taylor, J. P., Weintraub, D., et al. (2017). Diagnosis and management of dementia with Lewy bodies: fourth consensus report of the DLB Consortium. *Neurology* 89, 88–100. doi: 10.1212/WNL.0000000000004058

McKeith, I. G., Ferman, T. J., Thomas, A. J., Blanc, F., Boeve, B. F., Fujishiro, H., et al. (2020). Research criteria for the diagnosis of prodromal dementia with Lewy bodies. *Neurology* 94, 743–755. doi: 10.1212/WNL.0000000000009323

McKhann, G. M., Knopman, D. S., Chertkow, H., Hyman, B. T., Jack, C. R. Jr., Kawas, CH. et al. (2011). The diagnosis of dementia due to Alzheimer's disease: recommendations from the National Institute on Aging-Alzheimer's Association workgroups on diagnostic guidelines for Alzheimer's disease. *Alzheimer's Dementia* 7, 263–269. doi: 10.1016/j.jalz.2011.03.005

Modarresi, S., Divine, A., Grahn, J. A., Overend, T. J., and Hunter, S. W. (2019). Gait parameters and characteristics associated with increased risk of falls in people with dementia: a systematic review. *Int. Psychogeriat.* 31, 1287–1303. doi: 10.1017/S1041610218001783

Molloy, D. W., and Standish, T. I. (1997). A guide to the standardized mini-mental state examination. *Int. Psychogeriatr.* 9(Suppl. 1), 87–94. doi: 10.1017/S1041610297004754

Morris, J. C. (1997). Clinical dementia rating: a reliable and valid diagnostic and staging measure for dementia of the Alzheimer type. *Int. Psychogeriatr.* 9(Suppl. 1), 173–176. doi: 10.1017/S1041610297004870

Nelson, H. E., and Willison, J. (1991). *National Adult Reading Test (NART)*. Windsor: Nfer-Nelson.

Noone, P. (2015). Addenbrooke's cognitive examination-III. *Occup. Med. (Lond)* 65, 418–420. doi: 10.1093/occmed/kqv041

Palmqvist, S., Hansson, O., Minthon, L., and Londos, E. (2009). Practical suggestions on how to differentiate dementia with Lewy bodies from Alzheimer's disease with common cognitive tests. *Int. J. Geriatr. Psychiatry* 24, 1405–1412. doi: 10.1002/gps.2277

Pantall, A., Suresparan, P., Kapa, L., Morris, R., Yarnall, A., Del Din, S., et al. (2018). Postural dynamics are associated with cognitive decline in Parkinson's disease. *Front. Neurol.* 9:1044. doi: 10.3389/fneur.2018.01044

Peel, N. M., Alapatt, L. J., Jones, L. V., and Hubbard, R. E. (2019). The association between gait speed and cognitive status in community-dwelling older people: a systematic review and meta-analysis. *J. Gerontol.: Series A.* 74, 943–948. doi: 10.1093/gerona/gly140

Powell, L. E., and Myers, A. M. (1995). The Activities-specific Balance Confidence (ABC) scale. *J. Gerontol. A Biol. Sci. Med. Sci.* 50A, M28–M34. doi: 10.1093/gerona/50A.1.M28

Scharre, D. W., Chang, S. I., Nagaraja, H. N., Park, A., Adeli, A., Agrawal, P., et al. (2016). Paired studies comparing clinical profiles of lewy body dementia with Alzheimer's and Parkinson's Diseases. *J. Alzheimers Dis.* 54, 995–1004. doi: 10.3233/JAD-160384

Schoneburg, B., Mancini, M., Horak, F., and Nutt, J. G. (2013). Framework for understanding balance dysfunction in Parkinson's disease. *Mov. Disord.* 28, 1474–1482. doi: 10.1002/mds.25613

Suttanon, P., Hill, K. D., Said, C. M., Logiudice, D., Lautenschlager, N. T., and Dodd, K. J. (2012). Balance and mobility dysfunction and falls risk in older people with mild to moderate Alzheimer disease. *Am. J. Phys. Med. Rehabil.* 91, 12–23. doi: 10.1097/PHM.0b013e31823caeea

Williams-Gray, C. H., Evans, J. R., Goris, A., Foltynie, T., Ban, M., Robbins, T. W., et al. (2009). The distinct cognitive syndromes of Parkinson's disease: 5 year follow-up of the CamPaIGN cohort. *Brain* 132(Pt 11), 2958–2969. doi: 10.1093/brain/awp245

yeun Lee, J., Park, J., Lee, D., and Roh, H. (2011). The effects of exercising on unstable surfaces on the balance ability of stroke patients. *J. Phys. Therapy Sci.* 23, 789–792. doi: 10.1589/jpts.23.789

Conflict of Interest: The authors declare that the research was conducted in the absence of any commercial or financial relationships that could be construed as a potential conflict of interest.

frontiers in Bioengineering and Biotechnology

ORIGINAL RESEARCH
published: 15 April 2021
doi: 10.3389/fbioe.2021.627481

Detection of Motor Dysfunction With Wearable Sensors in Patients With Idiopathic Rapid Eye Movement Disorder

*Lin Ma[1†], Shu-Ying Liu[1†], Shan-Shan Cen[1], Yuan Li[1], Hui Zhang[1], Chao Han[2], Zhu-Qin Gu[3], Wei Mao[1], Jing-Hong Ma[1], Yong-Tao Zhou[1], Er-He Xu[1] and Piu Chan[1,2,3,4,5]**

[1] Department of Neurobiology, Neurology and Geriatrics, Xuanwu Hospital of Capital Medical University, Beijing Institute of Geriatrics, Beijing, China, [2] National Clinical Research Center for Geriatric Disorders, Beijing, China, [3] Clinical and Research Center for Parkinson's Disease, Capital Medical University, Beijing, China, [4] Key Laboratory for Neurodegenerative Disease of the Ministry of Education, Beijing Key Laboratory for Parkinson's Disease, Parkinson Disease Center of Beijing Institute for Brain Disorders, Beijing, China, [5] Advanced Innovation Center for Human Brain Protection, Capital Medical University, Beijing, China

OPEN ACCESS

Edited by:
Egon Perilli,
Flinders University, Australia

Reviewed by:
Emilia Scalona,
Institute of Neuroscience, National Research Council (CNR), Italy
Rami Al-Dirini,
Flinders University, Australia

***Correspondence:**
Piu Chan
pbchan@hotmail.com

[†] These authors have contributed equally to this work

Specialty section:
This article was submitted to Biomechanics, a section of the journal Frontiers in Bioengineering and Biotechnology

Received: 09 November 2020
Accepted: 29 March 2021
Published: 15 April 2021

Citation:
Ma L, Liu S-Y, Cen S-S, Li Y, Zhang H, Han C, Gu Z-Q, Mao W, Ma J-H, Zhou Y-T, Xu E-H and Chan P (2021) Detection of Motor Dysfunction With Wearable Sensors in Patients With Idiopathic Rapid Eye Movement Disorder. Front. Bioeng. Biotechnol. 9:627481. doi: 10.3389/fbioe.2021.627481

Patients with idiopathic rapid eye movement sleep behavior disorder (iRBD) are at high risk for conversion to synucleinopathy and Parkinson disease (PD). This can potentially be monitored by measuring gait characteristics of iRBD patients, although quantitative data are scarce and previous studies have reported inconsistent findings. This study investigated subclinical gait changes in polysomnography-proven iRBD patients compared to healthy controls (HCs) during 3 different walking conditions using wearable motor sensors in order to determine whether gait changes can be detected in iRBD patients that could reflect early symptoms of movement disorder. A total 31 iRBD patients and 20 HCs were asked to walk in a 10-m corridor at their usual pace, their fastest pace, and a normal pace while performing an arithmetic operation (dual-task condition) for 1 min each while using a wearable gait analysis system. General gait measurements including stride length, stride velocity, stride time, gait length asymmetry, and gait variability did not differ between iRBD patients and HCs; however, the patients showed decreases in range of motion ($P = 0.004$) and peak angular velocity of the trunk ($P = 0.001$) that were significant in all 3 walking conditions. iRBD patients also had a longer step time before turning compared to HCs ($P = 0.035$), and the difference between groups remained significant after adjusting for age, sex, and height. The decreased trunk motion while walking and increased step time before turning observed in iRBD may be early manifestations of body rigidity and freezing of gait and are possible prodromal symptoms of PD.

Keywords: Idiopathic REM sleep behavior disorder, gait, quantitative measurement, prodromal stage, wearable sensors

INTRODUCTION

Rapid eye movement (REM) sleep behavior disorder (RBD) is characterized by episodes of vigorous movements during REM sleep, usually accompanied by unpleasant dreams and violent limb movements (Iranzo et al., 2016). Up to 97% of patients with idiopathic (i) RBD progress within 14.2 years to synucleinopathies such as Parkinson disease (PD), multiple system atrophy, and dementia with Lewy bodies (Galbiati et al., 2019). According to the Movement Disorder Society Research Criteria for Prodromal Parkinson's Disease, polysomnography (PSG)-proven RBD is the most significant risk factor for prodromal PD (Heinzel et al., 2019). Thus, patients diagnosed with iRBD are potential candidates for clinical trials of neuroprotective therapies (Postuma et al., 2015).

Wearable sensors can provide reliable and unbiased data on subtle changes in gait. Previous studies have used sensors to objectively analyze gait abnormality in PD (Silva de Lima et al., 2017; Suzuki et al., 2017) and other types of parkinsonism (Raccagni et al., 2018). These studies demonstrated that quantitative gait characteristics can be used to identify prodromal PD, and that higher gait variability and asymmetry during a single task at the usual walking speed can predict time to PD conversion (Del Din et al., 2019).

There have been few studies of quantitative motor assessment in RBD patients, and the results are inconsistent. One study found that probable RBD diagnosed with the Mayo Sleep Questionnaire was associated with decreased velocity and cadence and increased stride time variability as measured using the GAITRite system (a 5.0 × 0.7-m pressure sensor walkway) (McDade et al., 2013); however, decreases in gait velocity, rhythm, and gait variability were observed by real-world gait monitoring of PSG-proven iRBD patients using a tri-axial accelerometer (Del Din et al., 2020). In another study in which a 6.1 m × 0.61 m Zeno pressure sensor walkway was used to measure gait, no differences in step length and velocity were observed between PSG-proven iRBD patients and healthy controls (HCs); however, during fast-paced walking, iRBD patients showed greater gait asymmetry and in the dual-task walking condition, step width variability was increased (Ehgoetz Martens et al., 2019). iRBD patients also showed impairment in biomechanical measures of self-initiated stepping including reductions in the posterior shift of the center of pressure during the anticipatory and propulsive phases of gait initiation that resembled the freezing of gait (FOG) observed in PD (Alibiglou et al., 2016).

Most studies have used pressure sensors to measure RBD patients' gait. Wearable sensors are composed of a tri-axial accelerometer, gyroscope, and magnetometer and have the advantages of being small and lightweight with wireless transmission, which make the devices portable and convenient to use outside the laboratory and in long-term daily monitoring; moreover, the devices can be used to collect data on trunk and arm movements.

In this study, we used wearable motor sensors to detect subclinical gait changes and quantitatively analyze motor performance of PSG-confirmed iRBD patients compared to HC subjects. We also examined whether iRBD patients with greater gait abnormality were at a higher risk of conversion to synucleinopathy. Our results indicate that iRBD is associated with decreased trunk motion while walking and increased step time before turning, which may be prodromal symptoms of PD.

PATIENTS AND METHODS

Participants

The iRBD patients were recruited from the neurology clinic of Xuanwu Hospital, Beijing, China (Li et al., 2019) and HCs were recruited from a community-based cohort study conducted in Beijing (Ji et al., 2020) over a 3-year period (2013–2015). iRBD patients were PSG-confirmed and had not been diagnosed with any neurodegenerative disease. Patients were excluded if they had a total score < 18 for the Rapid Eye Movement (REM) Sleep Behavior Disorder Questionnaire – Hong Kong (RBDQ-HK) (Li et al., 2010), obstructive sleep apnea-hypopnea syndrome or any other sleep disorder, musculoskeletal conditions, or prior surgeries that could influence gait. The study was approved by the Ethics Committee of Xuanwu Hospital Capital Medical and all participants provided written, informed consent.

Procedures

Demographic data and medical history were recorded. All participants underwent a comprehensive neurologic assessment that included Part III of the Unified Parkinson's Disease Rating Scale (UPDRS III) to assess motor symptoms, Montreal Cognitive Assessment (MoCA) to assess cognitive state, RBDQ-HK to screen for RBD, a 5-odor olfactory detection array to evaluate the threshold of olfactory identification (TOI) (Cao et al., 2016), and Non-motor Symptoms Scale (NMSS) to measure the number and severity of non-motor symptoms.

Gait Assessment

Participants completed 3 walking trials with a wearable system for quantitative gait analysis comprising 6 wearable gyroscope and accelerometer sensors (APDM; Mobility Lab, Portland, OR, United States). The sensors were placed at bilateral wrists and ankles, the anterior sternum, and lower back (**Figure 1**). Participants were asked to walk in a corridor with a 10-m effective distance at their usual pace, fastest pace, and a normal pace while subtracting 7 from 100 (dual-task condition) for 1 min each (an average of 22 valid strides per walking condition). Participants were instructed to walk past a line marked with tape and turn during each task.

The following parameters were examined in the study based on previous reports (Salarian et al., 2010; Washabaugh et al., 2017).

- Normalized stride length, which is the distance between 2 consecutive footfalls at the moment of initial contact; the value is normalized for height and averaged for left and right sides.
- Normalized stride velocity, which is the participant's walking speed normalized to his/her height and averaged for left and right sides.

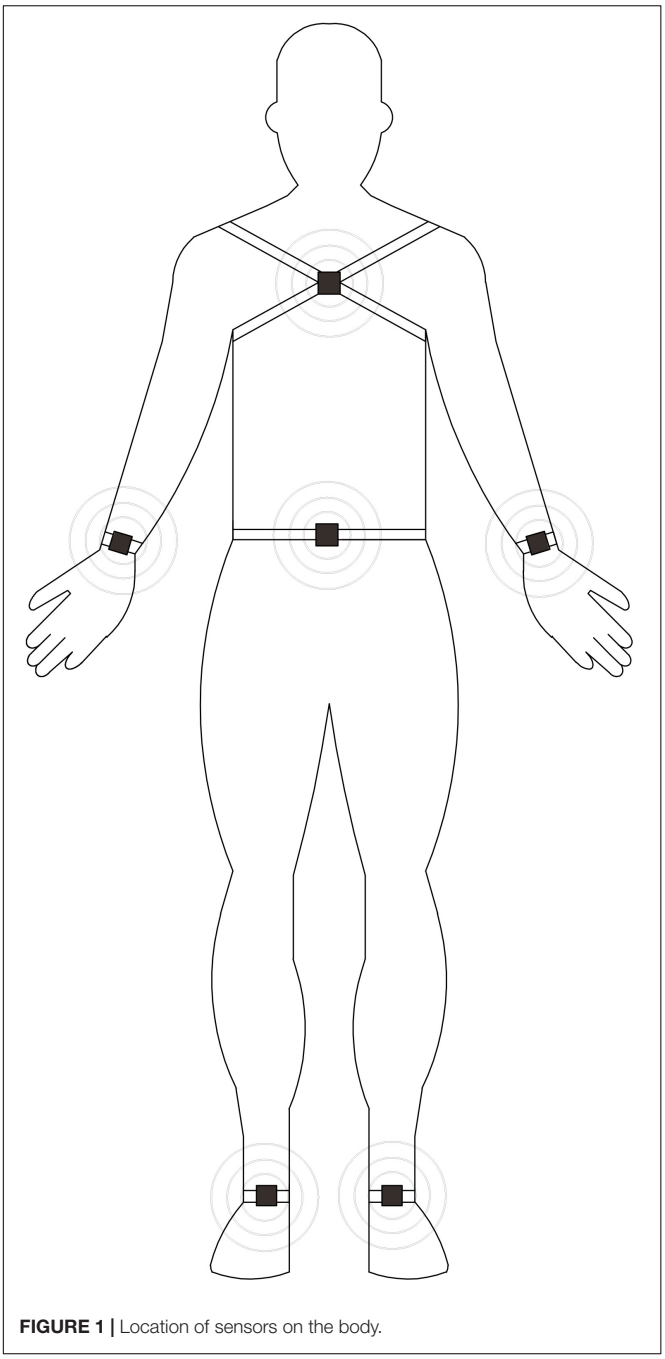

FIGURE 1 | Location of sensors on the body.

- Stride time, which is the duration of a complete gait cycle (defined as the period between 2 consecutive initial contacts [heel strikes] of the right foot).
- Range of motion of the trunk in the sagittal plane, which is the angular range of the thoracic spine in the anterior–posterior plane (i.e., moving back and forth).
- Range of motion of the trunk in the horizontal plane, which is the angular range of the thoracic spine in the head–feet plane (i.e., moving up and down).
- Peak angular velocity of the trunk in the sagittal or horizontal plane, which is the peak angular speed of the thoracic spine motion in the sagittal or horizontal plane, respectively.
- Step time before turning, which is the duration of the last step immediately before a turn.
- Stride length asymmetry, which is the mean asymmetry of the left and right stride lengths and is calculated as $100 \times \left|\ln\left\{\frac{\min(stride\ length\ L,\ stride\ length\ R)}{\max(stride\ length\ L,\ stride\ length\ R)}\right\}\right|$ (Sant'Anna et al., 2011).
- Coefficient of variation of stride length, which is the stride length variability of multiple consecutive strides and is calculated as 100 × standard deviation / mean value of stride length.
- Coefficient of variation of stride time, which is the stride time variability of multiple consecutive strides and is calculated as 100 × standard deviation / mean value of stride time.

Statistical Analysis

All parameters were checked for normality and homoscedasticity within groups. Repeated-measures analysis of variance was used to assess between-group effects (iRBD vs. HC), the effect of the walking condition (usual, fast, or dual-task), and any interactions between group and walking condition. When group or walking condition effect differences were significant, posthoc analyses were performed with Bonferroni correction. The covariance analysis method was used to adjust for covariates; normalized stride length and velocity were adjusted for age and sex as they were already normalized by height; the other variables were adjusted for age, sex, and height. The independent-samples *t* test and Mann–Whitney *U* test were performed to compare demographic and clinical characteristics between iRBD patients and HCs, and between iRBD patients with abnormal gait parameters and those with normal gait. Pearson's correlation coefficient was used to analyze the relationship between gait parameters and clinical characteristics. Statistical analyses were performed with SPSS v19 software (SPSS Inc, Chicago, IL, United States). $P < 0.05$ was considered statistically significant; correlations were determined based on | r| values as follows: 0.8–1.0, very strong; 0.6–0.8, strong; 0.4–0.6, moderate; 0.2–0.4, weak; and 0.0–0.2 very weak/no correlation.

RESULTS

Demographic and Clinical Characteristics of the Study Population

A total of 51 participants (31 iRBD and 20 HCs) were enrolled. There were no statistically significant differences in age, body mass index, and MoCA score between the iRBD patients and HCs; the percentage of females was lower in the iRBD group than in the HC group as expected. iRBD patients had significantly higher UPDRS III score ($U = 471$, $P = 0.001$), TOI score ($T_{49} = -4.023$, $P < 0.001$), NMSS ($U = 606.5$, $P < 0.001$), and RBDQ-HK score ($U = 617.5$, $P < 0.001$) compared to HCs (**Table 1**). The UPDRS III score of iRBD patients ranged from 0 to 5.

TABLE 1 | Demographic and clinical characteristics of iRBD patients and healthy controls.

	iRBD (n = 31)	HC (n = 20)	P value
Age, years	69 (63, 73)	70 (67, 73)	0.602*
Sex, female	5 (16.1%)	11 (55%)	0.003
Height, cm	169.0 ± 7.8	162.0 ± 6.7	0.002
BMI	24.63 ± 3.35	24.68 ± 3.26	0.957
UPDRSIII	2 (0, 3)	0 (0, 0)	0.001*
MoCA	24 ± 3	25 ± 3	0.330
TOI	2.8 ± 0.5	2.2 ± 0.6	< 0.001
RBDQ-HK	39 (30, 46)	4 (3, 6.75)	< 0.001*
NMSS	37 (25, 46)	8 (2, 11)	< 0.001*

Data are presented as mean value ± standard deviation for normally distributed data or as median (upper quartile, lower quartile) for non-normally distributed data.
**P value calculated with the Mann–Whitney U test.*
BMI, body mass index; F, female; HC, healthy control; iRBD, idiopathic rapid eye movement sleep behavior disorder; MoCA, Montreal Cognitive Assessment; NMSS, Non-motor Symptoms Scale; RBDQ-HK, Rapid Eye Movement Sleep Behavior Disorder Questionnaire – Hong Kong; TOI, threshold of olfactory identification; UPDRS III, Unified Parkinson's Disease Rating Scale Part III.

Differences in Gait Measures Between iRBD Patients and HCs

Group Effect

General gait measures including normalized stride length, normalized stride velocity, stride time, stride length asymmetry, stride length variability, and stride time variability did not differ between iRBD patients and HCs under usual, fast, and dual-task walking conditions (**Table 2**). However, iRBD patients had a significantly decreased range of motion of the trunk in the sagittal plane compared to HCs ($F_{2,152}$ = 9.383, P = 0.004), especially in the usual and dual-task conditions (3.86 ± 0.77 vs. 4.50 ± 0.79, P = 0.006; 4.13 ± 0.89 vs. 4.96 ± 1.09, P = 0.004) (**Table 3**). The corresponding peak angular velocity of the trunk in the sagittal plane was also reduced in the patients ($F_{2,152}$ = 11.588, P = 0.001). As expected, trunk motion in the horizontal plane did not differ between groups. An increase in the time for the last step before turning was observed in iRBD patients compared to controls ($F_{2,152}$ = 4.724, p = 0.035), which was more prominent under usual and fast walking conditions. The difference between groups was also significant after adjusting for age, sex, and height (**Table 3**). Comparisons of gait measures between groups under different walking conditions are shown in **Figure 2**.

Walking Condition Effect

There was significant walking condition effect on all general gait parameters examined in this study including stride length, stride velocity, stride time, stride length asymmetry, stride length variability, and stride time variability. Both iRBD patients and HCs walked more rapidly as instructed in the fast condition and slowed down in the dual-task condition (P < 0.001; **Table 2**). However, stride length asymmetry and variability of stride length and time increased under both conditions compared to the baseline (i.e., usual walking condition) in both groups, and the time of the last step before turning was increased in the dual-task test (P < 0.001). There was no interaction between group and walking condition for any parameter.

TABLE 2 | Differences in general gait measures between iRBD patients and healthy controls.

Parameter	iRBD	HC	P	P*
Normalized stride length, % height				
Usual	84.03 ± 5.19	83.25 ± 4.99		
Fast	85.95 ± 5.45	84.82 ± 5.12		
Dual-task	82.06 ± 6.82	80.19 ± 5.49		
Group effect			0.414	0.727
Condition effect			< 0.001	< 0.001
Interaction: group × condition			0.409	
Normalized stride velocity, % height/s				
Usual	79.33 ± 6.89	81.86 ± 5.89		
Fast	88.04 ± 8.02	90.28 ± 5.66		
Dual-task	74.44 ± 9.57	72.50 ± 7.19		
Group effect			0.617	0.614
Condition effect			< 0.001	< 0.001
Interaction: group × condition			0.099	
Stride time, s				
Usual	1.06 ± 0.08	1.02 ± 0.05		
Fast	0.98 ± 0.08	0.94 ± 0.04		
Dual-task	1.11 ± 0.11	1.12 ± 0.09		
Group effect			0.143	0.238
Condition effect			< 0.001	< 0.001
Interaction: group × condition			0.176	
Stride length asymmetry, %				
Usual	0.97 ± 0.28	1.07 ± 0.55		
Fast	1.04 ± 0.34	1.22 ± 0.56		
Dual-task	1.20 ± 0.49	1.43 ± 0.57		
Group effect			0.102	0.085
Condition effect			< 0.001	0.004
Interaction: group × condition			0.710	
Stride length coefficient of variation, %				
Usual	2.11 ± 0.65	2.43 ± 1.94		
Fast	2.23 ± 1.00	2.47 ± 1.04		
Dual-task	3.08 ± 2.23	3.29 ± 1.85		
Group effect			0.352	0.711
Condition effect			0.007	0.002
Interaction: group × condition			0.973	
Stride time coefficient of variation, %				
Usual	2.00 ± 0.63	1.75 ± 0.71		
Fast	2.36 ± 1.55	2.36 ± 1.20		
Dual-task	3.85 ± 3.48	4.00 ± 3.33		
Group effect			0.934	0.512
Condition effect			0.001	< 0.001
Interaction: group × condition			0.798	

Data are presented as mean value ± standard deviation.
**P values for stride length (% height) and velocity (% height/s) were adjusted for age and sex; the other parameters were adjusted for age, sex, and height.*
HC, healthy control; iRBD, idiopathic rapid eye movement sleep behavior disorder.

Comparisons of iRBD Patients With or Without Gait Abnormality

In order to determine whether iRBD patients with greater gait abnormality were at higher risk of conversion to synucleinopathy, the iRBD group was divided into patients with and those without gait abnormality based on the mean value of peak angular velocity of the trunk in the sagittal plane. Patients with gait abnormality

TABLE 3 | Differences in gait measures related to trunk motion and turning initiation between iRBD patients and healthy controls.

Parameter	iRBD	HC	*P*	*P**
Range of motion of the trunk in the sagittal plane, °				
Usual	3.86 ± 0.77	4.50 ± 0.79	0.006	0.113
Fast	4.03 ± 0.72	4.52 ± 0.75	0.023	0.254
Dual-task	4.13 ± 0.89	4.96 ± 1.09	0.004	0.097
Group effect			0.004	0.009
Condition effect			< 0.001	0.106
Interaction: group × condition			0.409	
Peak angular velocity of trunk in the sagittal plane, °/s				
Usual	22.75 ± 4.71	27.53 ± 4.19	0.001	0.007
Fast	26.93 ± 6.18	32.38 ± 5.96	0.003	0.027
Dual-task	22.45 ± 5.50	26.04 ± 5.45	0.027	0.246
Group effect			0.001	< 0.001
Condition effect			< 0.001	< 0.001
Interaction: group × condition			0.099	
Range of motion of the trunk in the horizontal plane, °				
Usual	6.85 ± 1.59	6.80 ± 1.29		
Fast	6.72 ± 1.79	6.54 ± 1.10		
Dual-task	7.57 ± 1.73	7.94 ± 1.74		
Group effect			0.912	0.287
Condition effect			< 0.001	0.002
Interaction: group × condition			0.176	
Peak angular velocity of trunk in the horizontal plane, °/s				
Usual	21.17 ± 5.52	21.86 ± 3.87		
Fast	24.35 ± 6.23	24.91 ± 4.33		
Dual-task	23.64 ± 6.06	24.59 ± 4.70		
Group effect			0.605	0.509
Condition effect			< 0.001	0.009
Interaction: group × condition			0.710	
Step time before turn, s				
Usual	0.54 ± 0.04	0.51 ± 0.02	0.005	0.033
Fast	0.50 ± 0.04	0.48 ± 0.02	0.018	0.090
Dual-task	0.56 ± 0.06	0.55 ± 0.03	0.445	0.768
Group effect			0.035	0.034
Condition effect			< 0.001	< 0.001
Interaction: group × condition			0.973	

Data are presented as mean value ± standard deviation.
**P values were adjusted for age, sex, and height.*
HC, healthy control; iRBD, idiopathic rapid eye movement sleep behavior disorder.

had a higher NMSS score and higher number of non-motor symptoms as well as a longer RBD duration compared to patients with normal gait, but the differences were not statistically significant. UPDRS III score, MoCA, TOI, and RBDQ-HK score did not differ between the 2 groups (**Table 4**).

Correlations Between Gait Parameters and Clinical Characteristics of iRBD Patients

Negative correlations were observed between age and normalized stride length ($r = -0.555$, $P = 0.001$) and between age and peak angular velocity of the trunk in the sagittal plane ($r = -0.386$, $P = 0.032$; **Supplementary Table 1**). Stride length asymmetry showed a moderate negative correlation with MoCA score ($r = -0.412$, $P = 0.021$) and a weak positive correlation with RBDQ-HK score ($r = 0.368$, $P = 0.041$) (**Supplementary Table 1**).

DISCUSSION

In this cross-sectional study, we investigated subclinical changes in gait characteristics in PSG-confirmed iRBD patients compared to HCs using wearable motor sensors. While there were no differences in stride length, stride velocity, stride time, stride length asymmetry, and stride length and stride time variability in the 3 walking conditions, iRBD patients showed a significantly decreased range of motion and peak angular velocity of the trunk and had a longer step time before turning than HCs. These differences were significant even after adjusting for age, sex, and height. Because of the type of sensor that was used, we did not examine step width variability in this study. There were no differences in NMSS score, number of non-motor symptoms, UPDRS III score, MoCA, TOI, RBDQ-HK score, or RBD duration between iRBD patients with and those without abnormal gait.

Previous findings on quantitative gait characteristics in iRBD patients have been inconsistent. One study found a lack of difference in step length and velocity between PSG-proven iRBD patients and HCs but when walking at a fast pace, iRBD patients showed increased gait asymmetry as well as an increase of step width variability in the dual-task walking condition (Ehgoetz Martens et al., 2019). On the contrary, decreases in velocity and cadence and an increase in stride time variability were reported in patients with probable RBD who were diagnosed with the Mayo Sleep Questionnaire (McDade et al., 2013). Meanwhile, a real-world gait monitoring study of PSG-proven iRBD patients found decreases in gait velocity, variability, and rhyme (Del Din et al., 2020). These results are at odds with our data. The inconsistency in primary gait parameters across studies may be attributable to the different gait detection methods that were used and the heterogeneity of the disease stage among RBD patients, and suggests that these parameters lack specificity and sensitivity for predicting phenoconversion to PD in iRBD patients.

In contrast to the lack of difference in general gait parameters, we observed an increase in step time before turning in iRBD patients, suggesting that they need a longer time to prepare for a change in walking direction. Moreover, this could indicate a slower initiation of gait or FOG, which is characterized by difficulty in step initiation and turning. A previous study of gait initiation in RBD patients found that during the propulsive phase, a posterior shift in the center of pressure occurred only in iRBD patients and PD patients with FOG and not in controls or PD patients without FOG (Alibiglou et al., 2016). Thus, it is possible that some iRBD patients develop difficulty in initiating turning prior to the emergence of full motor symptoms. In fact, the pathophysiologic mechanisms of RBD and gait disturbance both involve upper brainstem structures such as the pedunculopontine nucleus (PPN) (Steriade, 2004). Activity in the PPN increases during REM sleep, which plays an important role in turning on REM sleep and maintaining atonia during this sleep stage (Rye, 1997). Moreover, the PPN is one of the nuclei that is affected by

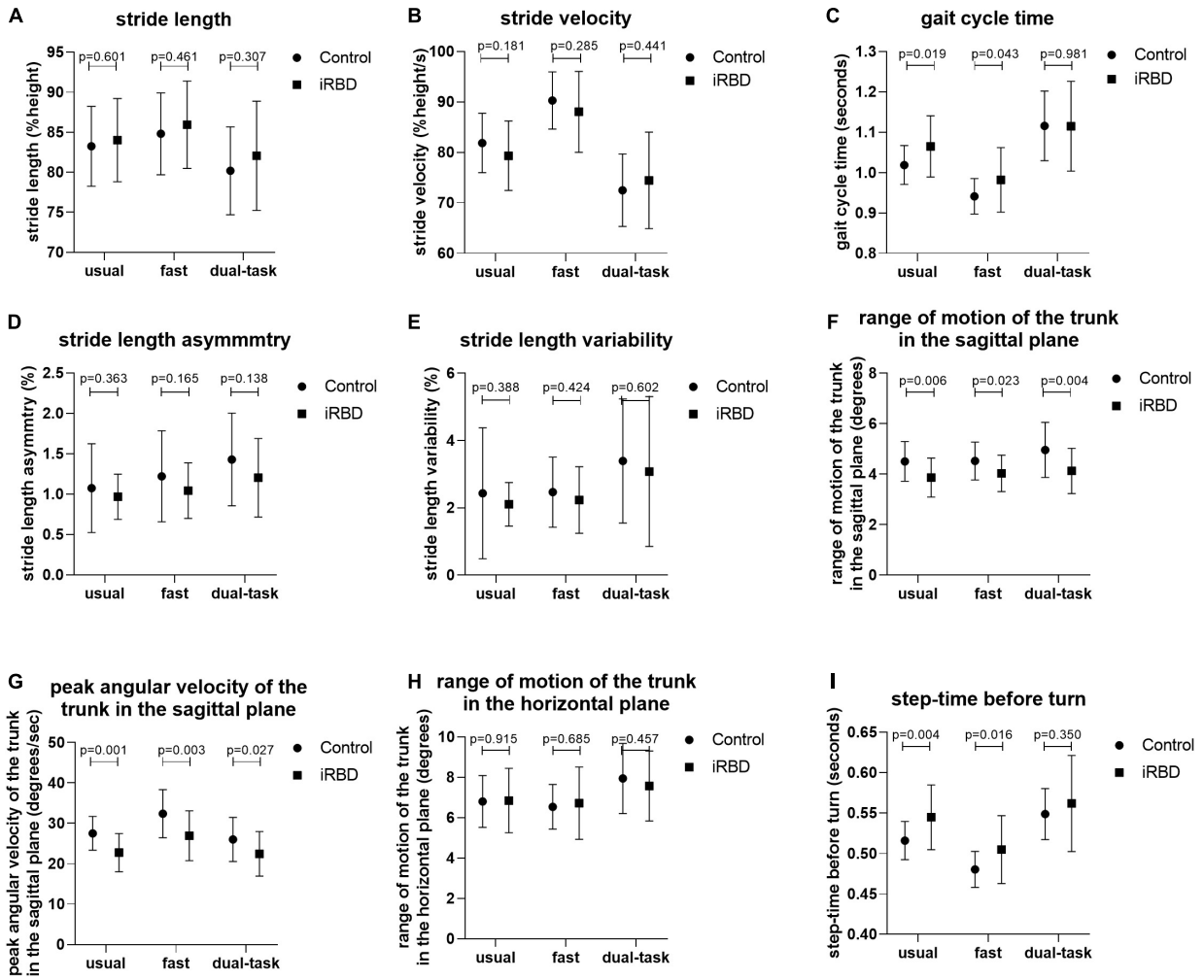

FIGURE 2 | Comparison of gait measures between groups under different walking conditions. **(A–I)** Group differences in stride length **(A)**, stride velocity **(B)**, stride time **(C)**, stride length asymmetry **(D)**, stride length variability **(E)**, range of motion of the trunk in the sagittal plane **(F)**, peak angular velocity of the trunk in the sagittal plane **(G)**, range of motion of the trunk in the horizontal plane **(H)**, and step time before turn **(I)** between iRBD patients and HCs under the usual pace, fast pace, and dual-task walking conditions.

alpha-synuclein aggregation in the prodromal stage of PD, which is consistent with the elevated risk of parkinsonism associated with iRBD. Deep brain stimulation of PPN was shown to improve gait disturbance (including FOG) in PD patients (Ferraye et al., 2010; Moro et al., 2010; Thevathasan et al., 2018), and a functional magnetic resonance imaging study using gait imagery demonstrated that PD patients with FOG had higher activity in the mesencephalic locomotor region (Snijders et al., 2011), which comprises the PPN and midbrain extrapyramidal area (Alam et al., 2011). Neurotransmitter systems may also provide a link between iRBD and FOG. Gait disturbance is generally dopamine-resistant and animal experiments have indicated that it is more closely related to the cholinergic system (Karachi et al., 2010), which was found to be dysregulated in patients with PD or iRBD and associated with RBD symptoms (Müller and Bohnen, 2013). Whether the increase in step time before turning observed in iRBD patients in our study was caused by the degeneration of cholinergic neurons that occurs in the prodromal stage of PD remains to be determined; however, our finding that iRBD patients had impaired olfactory identification compared to HCs supports a mechanistic link, as degeneration of cholinergic neurons in the basal forebrain was shown to be associated with olfactory dysfunction (Doty, 2017).

Another finding of our study is that both the range of motion and peak angular velocity of the trunk in the sagittal plane were decreased in iRBD patients, indicating that patients' trunk was more rigid and inflexible compared to that of HC subjects while walking. Several studies have reported that PD patients with RBD have more prominent axial symptoms and a postural instability and gait dysfunction (PIGD) phenotype. A large community-based longitudinal study found that PD patients with probable RBD tended to have higher axial UPDRS III subscores (Duarte Folle et al., 2019). Moreover, motor symptoms deteriorated more rapidly in patients with RBD with the PIGD phenotype

TABLE 4 | Differences in demographic and clinical characteristics between iRBD patients with and those without gait abnormality.

	Normal gait (*n* = 14)	Abnormal gait (*n* = 17)	*P* value
Age, years	67 ± 6	70 ± 6	0.188
Sex, female	4 (28.6%)	1 (5.9%)	0.087
UPDRSIII	2 (0.75, 3)	2 (0, 3)	0.922*
MoCA	24 ± 3	24 ± 3	0.784
RBD duration	8 (4.75, 9.25)	8.5 (2, 12)	0.710*
TOI	2.9 ± 0.4	2.8 ± 0.5	0.411
RBDQ-HK	42 (29.25, 44.5)	38 (30, 49)	0.570*
NMSS	36.5 (27.5, 47)	38 (24, 55.5)	0.769*
Number of non-motor symptoms	10 ± 4	11 ± 5	0.586

*Data are presented as mean value ± standard deviation for normally distributed data or as median (upper quartile, lower quartile) for non-normally distributed data. *P value calculated with the Mann–Whitney U test.*

F, female; HC, healthy control; iRBD, idiopathic rapid eye movement sleep behavior disorder; MoCA, Montreal Cognitive Assessment; NMSS, Non-motor Symptoms Scale; RBDQ-HK, Rapid Eye Movement Sleep Behavior Disorder Questionnaire – Hong Kong; TOI, threshold of olfactory identification; UPDRS III, Unified Parkinson's Disease Rating Scale Part III.

(Duarte Folle et al., 2019). A cross-sectional study showed that the prevalence of PIGD was higher in PD patients who reported having past or present RBD symptoms (Bugalho et al., 2011), and a cluster study of PD subtypes based on non-motor symptoms found that patients with the highest incidence (92%) of RBD symptoms exhibited the most severe gait disturbance and had the highest rate of FOG and falls (Fereshtehnejad et al., 2015). Our study provides additional evidence that iRBD patients have increased rigidity and gait disorder (i.e., the PIGD phenotype) even at the very early stage of disease.

The results of this study demonstrate the effectiveness of wearable sensors for the early quantitative detection of gait abnormality in iRBD patients, which can potentially reveal prodromal symptoms of PD and predict the time to conversion owing to the objective and sensitive nature of quantitative gait measurements (Del Din et al., 2019). Prodromal PD symptoms usually occur together because of the clustered anatomic location of brainstem structures; thus, gait abnormality in iRBD patients may reflect a more advanced disease stage and may be accompanied by additional non-motor symptoms. iRBD patients with a longer disease duration or who are progressing to synucleinopathy may be more likely to demonstrate gait abnormality. In this study we did not observe differences in NMSS score, number of non-motor symptoms, or RBD duration between iRBD patients with and those without gait abnormality, possibly because of the small sample size and variable time course of phenoconversion to PD. As expected, we found no difference in UPDRS III score between iRBD patients with vs. those without gait abnormality, as this scale is less objective and sensitive than quantitative gait measurements. We also found that gait parameters of iRBD patients were associated with older age, cognitive impairment, and the severity of non-motor and RBD symptoms, possibly reflecting the extent of neurodegeneration in this group.

Major limitations of our study were the small sample size and cross-sectional design. We are still following the iRBD cohort annually and additional studies are underway to better characterize motor symptoms and phenoconversion in the iRBD cohort.

In summary, we found that PSG-confirmed iRBD patients exhibited decreased trunk motion while walking and increased step time before turning, which may be early manifestations of body rigidity and possible FOG as prodromal symptoms of PD. Comprehensive analyses of gait and postural balance are necessary in the follow-up of our patients to monitor for potential progression to PD. Additionally, a large longitudinal study of iRBD patients is needed to determine whether the PIGD phenotype and axial symptoms persist after conversion to PD.

DATA AVAILABILITY STATEMENT

The raw data supporting the conclusions of this article will be made available by the authors, without undue reservation.

ETHICS STATEMENT

The studies involving human participants were reviewed and approved by Ethics Committee of Xuanwu Hospital Capital Medical. The patients/participants provided their written informed consent to participate in this study.

AUTHOR CONTRIBUTIONS

S-YL and PC designed the study. S-SC, YL, HZ, Z-QG, WM, J-HM, Y-TZ, and E-HX collected the data. CH provided guidance on statistical methods. LM and S-YL performed statistical analyses and drafted the manuscript. PC reviewed and critiqued the manuscript. All authors read and approved the final version of the manuscript for publication.

FUNDING

This work was supported by the National Key R&D Program of China (Grant Nos. 2018YFC1312001, 2017ZX09304018, and 2017YFC1310203), Beijing Municipal Science & Technology Commission (Grant No. Z171100000117013), and National Natural Science Foundation of China (Grant No. 81901285).

ACKNOWLEDGMENTS

We thank all study participants and Zi-Wen Zhou for assistance with the artwork in **Figure 1**.

SUPPLEMENTARY MATERIAL

The Supplementary Material for this article can be found online at: https://www.frontiersin.org/articles/10.3389/fbioe.2021.627481/full#supplementary-material

REFERENCES

Alam, M., Schwabe, K., and Krauss, J. K. (2011). The pedunculopontine nucleus area: critical evaluation of interspecies differences relevant for its use as a target for deep brain stimulation. *Brain* 134, 11–23. doi: 10.1093/brain/awq322

Alibiglou, L., Videnovic, A., Planetta, P. J., Vaillancourt, D. E., and MacKinnon, C. D. (2016). Subliminal gait initiation deficits in rapid eye movement sleep behavior disorder: A harbinger of freezing of gait? *Mov Disord* 31, 1711–1719. doi: 10.1002/mds.26665

Bugalho, P., da Silva, J. A., and Neto, B. (2011). Clinical features associated with REM sleep behavior disorder symptoms in the early stages of Parkinson's disease. *J Neurol* 258, 50–55. doi: 10.1007/s00415-010-5679-0

Cao, M., Gu, Z. Q., Li, Y., Zhang, H., Dan, X. J., Cen, S. S., et al. (2016). Olfactory dysfunction in Parkinson's disease patients with the LRRK2 G2385R variant. *Neurosci Bull* 32, 572–576. doi: 10.1007/s12264-016-0070-5

Del Din, S., Elshehabi, M., Galna, B., Hobert, M. A., Warmerdam, E., Suenkel, U., et al. (2019). Gait analysis with wearables predicts conversion to parkinson disease. *Ann Neurol* 86, 357–367. doi: 10.1002/ana.25548

Del Din, S., Yarnall, A. J., Barber, T. R., Lo, C., Crabbe, M., Rolinski, M., et al. (2020). Continuous real-world gait monitoring in idiopathic REM sleep behavior disorder. *J Parkinsons Dis* 10, 283–299. doi: 10.3233/jpd-191773

Doty, R. L. (2017). Olfactory dysfunction in neurodegenerative diseases: Is there a common pathological substrate? *Lancet Neurol* 16, 478–488. doi: 10.1016/s1474-4422(17)30123-0

Duarte Folle, A., Paul, K. C., Bronstein, J. M., Keener, A. M., and Ritz, B. (2019). Clinical progression in Parkinson's disease with features of REM sleep behavior disorder: A population-based longitudinal study. *Parkinsonism Relat Disord* 62, 105–111. doi: 10.1016/j.parkreldis.2019.01.018

Ehgoetz Martens, K. A., Matar, E., Hall, J. M., Phillips, J., Szeto, J. Y. Y., Gouelle, A., et al. (2019). Subtle gait and balance impairments occur in idiopathic rapid eye movement sleep behavior disorder. *Mov Disord* 34, 1374–1380. doi: 10.1002/mds.27780

Fereshtehnejad, S. M., Romenets, S. R., Anang, J. B., Latreille, V., Gagnon, J. F., and Postuma, R. B. (2015). New clinical subtypes of Parkinson disease and their longitudinal progression: A prospective cohort comparison with other phenotypes. *JAMA Neurol* 72, 863–873. doi: 10.1001/jamaneurol.2015.0703

Ferraye, M. U., Debû, B., Fraix, V., Goetz, L., Ardouin, C., Yelnik, J., et al. (2010). Effects of pedunculopontine nucleus area stimulation on gait disorders in Parkinson's disease. *Brain* 133(Pt 1), 205–214. doi: 10.1093/brain/awp229

Galbiati, A., Verga, L., Giora, E., Zucconi, M., and Ferini-Strambi, L. (2019). The risk of neurodegeneration in REM sleep behavior disorder: A systematic review and meta-analysis of longitudinal studies. *Sleep Med Rev* 43, 37–46. doi: 10.1016/j.smrv.2018.09.008

Heinzel, S., Berg, D., Gasser, T., Chen, H., Yao, C., and Postuma, R. B. (2019). Update of the MDS research criteria for prodromal Parkinson's disease. *Mov Disord* 34, 1464–1470. doi: 10.1002/mds.27802

Iranzo, A., Santamaria, J., and Tolosa, E. (2016). Idiopathic rapid eye movement sleep behaviour disorder: diagnosis, management, and the need for neuroprotective interventions. *Lancet Neurol* 15, 405–419. doi: 10.1016/s1474-4422(16)00057-0

Ji, S., Wang, C., Qiao, H., Gu, Z., Gan-Or, Z., Fon, E. A., et al. (2020). Decreased penetrance of Parkinson's disease in elderly carriers of glucocerebrosidase gene L444P/R mutations: A community-based 10-year longitudinal study. *Mov Disord* 35, 672–678. doi: 10.1002/mds.27971

Karachi, C., Grabli, D., Bernard, F. A., Tandé, D., Wattiez, N., Belaid, H., et al. (2010). Cholinergic mesencephalic neurons are involved in gait and postural disorders in Parkinson disease. *J Clin Invest* 120, 2745–2754. doi: 10.1172/jci42642

Li, S. X., Wing, Y. K., Lam, S. P., Zhang, J., Yu, M. W., Ho, C. K., et al. (2010). Validation of a new REM sleep behavior disorder questionnaire (RBDQ-HK). *Sleep Med* 11, 43–48. doi: 10.1016/j.sleep.2009.06.008

Li, Y., Zhang, H., Mao, W., Liu, X., Hao, S., Zhou, Y., et al. (2019). Visual dysfunction in patients with idiopathic rapid eye movement sleep behavior disorder. *Neurosci Lett* 709, 134360. doi: 10.1016/j.neulet.2019.134360

McDade, E. M., Boot, B. P., Christianson, T. J., Pankratz, V. S., Boeve, B. F., Ferman, T. J., et al. (2013). Subtle gait changes in patients with REM sleep behavior disorder. *Mov Disord* 28, 1847–1853. doi: 10.1002/mds.25653

Moro, E., Hamani, C., Poon, Y. Y., Al-Khairallah, T., Dostrovsky, J. O., Hutchison, W. D., et al. (2010). Unilateral pedunculopontine stimulation improves falls in Parkinson's disease. *Brain* 133(Pt 1), 215–224. doi: 10.1093/brain/awp261

Müller, M. L., and Bohnen, N. I. (2013). Cholinergic dysfunction in Parkinson's disease. *Curr Neurol Neurosci Rep* 13, 377. doi: 10.1007/s11910-013-0377-9

Postuma, R. B., Gagnon, J. F., Bertrand, J. A., Genier Marchand, D., and Montplaisir, J. Y. (2015). Parkinson risk in idiopathic REM sleep behavior disorder: Preparing for neuroprotective trials. *Neurology* 84, 1104–1113. doi: 10.1212/wnl.0000000000001364

Raccagni, C., Gaßner, H., Eschlboeck, S., Boesch, S., Krismer, F., Seppi, K., et al. (2018). Sensor-based gait analysis in atypical parkinsonian disorders. *Brain Behav* 8, e00977. doi: 10.1002/brb3.977

Rye, D. B. (1997). Contributions of the pedunculopontine region to normal and altered REM sleep. *Sleep* 20, 757–788. doi: 10.1093/sleep/20.9.757

Salarian, A., Horak, F. B., Zampieri, C., Carlson-Kuhta, P., Nutt, J. G., Aminian, K., et al. (2010). iTUG, a sensitive and reliable measure of mobility. *IEEE Trans Neural Syst Rehabil Eng* 18, 303–310. doi: 10.1109/tnsre.2010.2047606

Sant'Anna, A., Salarian, A., and Wickström, N. (2011). A new measure of movement symmetry in early Parkinson's disease patients using symbolic processing of inertial sensor data. *IEEE Trans Biomed Eng* 58, 2127–2135. doi: 10.1109/tbme.2011.2149521

Silva de Lima, A. L., Evers, L., Hahn, T., Bataille, L., Hamilton, J. L., Little, M. A., et al. (2017). Freezing of gait and fall detection in Parkinson's disease using wearable sensors: A systematic review. *J Neurol* 264, 1642–1654. doi: 10.1007/s00415-017-8424-0

Snijders, A. H., Leunissen, I., Bakker, M., Overeem, S., Helmich, R. C., Bloem, B. R., et al. (2011). Gait-related cerebral alterations in patients with Parkinson's disease with freezing of gait. *Brain* 134, 59–72. doi: 10.1093/brain/awq324

Steriade, M. (2004). Acetylcholine systems and rhythmic activities during the waking–sleep cycle. *Prog Brain Res* 145, 179–196. doi: 10.1016/s0079-6123(03)45013-9

Suzuki, M., Mitoma, H., and Yoneyama, M. (2017). Quantitative analysis of motor status in Parkinson's disease using wearable devices: From methodological considerations to problems in clinical applications. *Parkinsons Dis* 2017, 6139716. doi: 10.1155/2017/6139716

Thevathasan, W., Debu, B., Aziz, T., Bloem, B. R., Blahak, C., Butson, C., et al. (2018). Pedunculopontine nucleus deep brain stimulation in Parkinson's disease: A clinical review. *Mov Disord* 33, 10–20. doi: 10.1002/mds.27098

Washabaugh, E. P., Kalyanaraman, T., Adamczyk, P. G., Claflin, E. S., and Krishnan, C. (2017). Validity and repeatability of inertial measurement units for measuring gait parameters. *Gait Posture* 55, 87–93. doi: 10.1016/j.gaitpost.2017.04.013

Conflict of Interest: The authors declare that the research was conducted in the absence of any commercial or financial relationships that could be construed as a potential conflict of interest.

frontiers in Bioengineering and Biotechnology

ORIGINAL RESEARCH
published: 27 April 2021
doi: 10.3389/fbioe.2021.617028

Pupillary Response to Postural Demand in Parkinson's Disease

Melike Kahya[1], Kelly E. Lyons[2], Rajesh Pahwa[2], Abiodun E. Akinwuntan[3,4], Jianghua He[5] and Hannes Devos[4]*

[1] Hinda and Arthur Marcus Institute for Aging Research, Harvard Medical School, Boston, MA, United States, [2] Department of Neurology, School of Medicine, University of Kansas Medical Center, Kansas City, KS, United States, [3] Office of the Dean, School of Health Professions, University of Kansas Medical Center, Kansas City, KS, United States, [4] Department of Physical Therapy and Rehabilitation Science, School of Health Professions, University of Kansas Medical Center, Kansas City, KS, United States, [5] Department of Biostatistics and Data Science, University of Kansas Medical Center, Kansas City, KS, United States

OPEN ACCESS

Edited by:
Martina Mancini, Oregon Health and Science University, United States

Reviewed by:
Antonio Nardone, Istituti Clinici Scientifici Maugeri (ICS Maugeri), Italy
Eduardo Normando, Western Eye Hospital, United Kingdom
Fabio Augusto Barbieri, São Paulo State University, Brazil

***Correspondence:**
Melike Kahya
melikekahya@hsl.harvard.edu

Specialty section:
This article was submitted to Biomechanics, a section of the journal Frontiers in Bioengineering and Biotechnology

Received: *13 October 2020*
Accepted: *09 March 2021*
Published: *27 April 2021*

Citation:
Kahya M, Lyons KE, Pahwa R, Akinwuntan AE, He J and Devos H (2021) Pupillary Response to Postural Demand in Parkinson's Disease. Front. Bioeng. Biotechnol. 9:617028. doi: 10.3389/fbioe.2021.617028

Background: Individuals with Parkinson's disease (PD) may need to spend more mental and physical effort (i.e., cognitive workload) to maintain postural control. Pupillary response reflects cognitive workload during postural control tasks in healthy controls but has not been investigated as a measure of postural demand in PD.

Objectives: To compare pupillary response during increased postural demand using vision occlusion and dual tasking between individuals with PD and healthy controls.

Methods: Thirty-three individuals with PD and thirty-five healthy controls were recruited. The four conditions lasted 60 s and involved single balance task with eyes open; single balance task with eyes occluded; dual task with eyes open; dual task with eyes occluded. The dual task comprised the Auditory Stroop test. Pupillary response was recorded using an eye tracker. The balance was assessed by using a force plate. Two-way Repeated Measures ANOVA and LSD *post-hoc* tests were employed to compare pupillary response and Center of Pressure (CoP) displacement across the four conditions and between individuals with PD and healthy controls.

Results: Pupillary response was higher in individuals with PD compared to healthy controls ($p = 0.009$) and increased with more challenging postural conditions in both groups ($p < 0.001$). The *post-hoc* analysis demonstrated increased pupillary response in the single balance eyes occluded ($p < 0.001$), dual task eyes open ($p = 0.01$), and dual task eyes occluded ($p < 0.001$) conditions compared to single task eyes open condition.

Conclusion: Overall, the PD group had increased pupillary response with increased postural demand compared to the healthy controls. In the future, pupillary response can be a potential tool to understand the neurophysiological underpinnings of falls risk in the PD population.

Keywords: pupillary response, posture, balance, vision, dual tasking, Parkinson's disease

INTRODUCTION

Falls are a common problem for individuals with Parkinson's disease (PD). A fall is defined as an event in which an individual comes to rest involuntarily on a lower surface, such as the ground or floor (Kellogg, 1987). It has been reported that 50–68% of the PD population fall annually (Huse et al., 2005), which is three times more often than the fall rate of the older population in general (Lord et al., 1993). In addition, 67% of fallers in the PD population have had more than one fall since diagnosis (Contreras and Grandas, 2012). The increased rate of falls suggests that individuals with PD have impaired skills to accurately react and initiate appropriate compensatory postural strategies to prevent falls.

Falls are not only associated with physical function and well-being, but they also share a strong association with cognitive function (Halliday et al., 2018). Higher order executive skills, such as shifting attention, cognitive flexibility, and inhibition, are needed to initiate appropriate postural control strategies (Liu-Ambrose et al., 2008). Studies have shown that fallers with and without PD exhibit increased prefrontal hemodynamic activation while performing walking and cognitive tasks at the same time (Maidan et al., 2016; Verghese et al., 2017). This increased hemodynamic activation is associated with performance on executive tasks (Ranchet et al., 2020). In addition, studies have shown that individuals who have lower cognitive scores on executive function and attention tasks are more likely to fall up to three times than those with higher cognitive scores (Herman et al., 2010). It is possible that cognitive functioning mediates the relationship between reduced postural control and falls in older adults and individuals with PD.

One way to stress the brain to assess its capacity is using a dual task paradigm. Most activities of daily living require performing two tasks simultaneously such as standing while talking or processing information. In such dual tasking conditions, upright stance posture is a basic yet essential motor skill to accomplish various motor and cognitive tasks concurrently (Burki et al., 2017). Although maintaining an upright stance posture seems autonomous and effortless in healthy individuals, it may become challenging and cognitively effortful due to the impaired automatic control process in individuals with PD (Kelly et al., 2012). PD pathology affects subcortical pathways leading to impaired automatic control of movement, which is suggested to be accompanied by a compensatory shift to more voluntary cortical control (Wu et al., 2015). In addition, studies have shown that individuals with PD heavily rely on visual feedback to maintain postural control due to impaired proprioception (Tagliabue et al., 2009; Lahr et al., 2015). While the motor contributions to postural control are well-studied in PD, fewer studies have investigated non-motor contributions such as cognition and vision. It is important to investigate the neurophysiological mechanism of impaired postural control associated with visual occlusion and dual tasking to better understand fall risk and to develop appropriate rehabilitation interventions.

Pupillary response is a non-intrusive, real-time neurophysiological measure of cognitive workload (or mental effort). The reliability and validity of pupillary response to measure cognitive workload were established in individuals without and with PD (Steinhauer and Hakerem, 1992; Pomplun and Sunkara, 2003; Kahya et al., 2020). Increased pupillary response due to cognitive workload stems from increased activation of the locus coeruleus (Beatty, 1982; Sirois and Brisson, 2014). The locus coeruleus plays an essential role in the regulation of physiological arousal and cognition (Sara, 2009). When activated, the locus coeruleus sends inhibitory projections to the parasympathetic Edinger-Westphal nucleus. The Edinger-Westphal nucleus subsequently inhibits the sphincter pupillae muscle, resulting in pupil dilation (Beatty and Lucero-Wagoner, 2000). Increased activity of the locus coeruleus also triggers the sympathetic nervous system, which results in additional pupil dilation due to the activation of the dilator pupillae muscle. Both pupillary response and activation of noradrenergic neurons in the locus coeruleus have been shown to increase in a correlated manner with increased cognitive workload (Varazzani et al., 2015). Although locus coeruleus is one of the first areas undergoing degeneration due to the PD pathophysiology (Micieli et al., 1991; Paredes-Rodriguez et al., 2020), dopamine replacement therapy has been shown to restore pupillary response in individuals with PD (Manohar and Husain, 2015). Also, a previous study showed that pupillary response during "ON" medication reflects cognitive workload in individuals with PD (Kahya et al., 2018a). The pattern of pupillary response in PD to cognitive demand was similar to that of healthy controls, suggesting that early PD pathology does not affect the accuracy of pupillary response in challenging cognitive tasks.

In addition, pupillary response to cognitive workload has been shown to be sensitive to changes in postural demand. Pupillary response increased from a single task to dual task balance conditions in healthy young adults (Kahya et al., 2018b). Also, previous work by our group has shown that pupillary response is a reliable and valid tool of cognitive workload during postural demanding tasks in individuals with PD (Kahya et al., 2020). However, it is not known whether pupillary response is different between individuals with PD and healthy controls during increased postural demand. A better understanding of the cognitive workload measured by pupillary response during postural demand in PD may inform more adequate assessment and treatment strategies to mitigate the effect of increased cognitive workload on balance impairments and falls. Therefore, the purpose of this study was to investigate neurophysiological changes, indexed by pupillary response, during postural demanding tasks between individuals with PD and healthy controls. Previous research in the PD population showed that individuals with PD had higher brain hemodynamic activation and increased brain power with increased postural demand compared to healthy controls (Maidan et al., 2016, 2019). Therefore, we hypothesized that individuals with PD would demonstrate higher pupillary response compared to healthy controls. An exploratory aim was to investigate the differences in pupillary response during postural demand between three groups: PD fallers, PD non-fallers, and healthy controls.

MATERIALS AND METHODS

Thirty-three individuals with PD and thirty-five age- and sex-matched healthy controls were recruited. Power analysis was performed for sample size estimation based on data from our previous study (Kahya et al., 2018a). The effect size (f) in this study was 0.26, which is considered a moderate effect size based on Cohen's criteria (Cohen, 1988). Using this effect size, 56 participants (n = 28 PD and n = 28 healthy controls) were needed to detect a moderate effect size of f = 0.26 with 80% power using a Two-way Repeated-Measures ANOVA, with two groups (between-factor) and four conditions of measurement (within-factor). To account for the possibility of random missing data, we recruited 20% more participants than our sample size calculation. Hence, we recruited 68 (n = 33 PD and n = 35 healthy controls) participants.

Participants with PD were categorized into fallers (n = 14, number of falls > 0) or non-fallers (n = 19, number of falls = 0) based on their self-reported fall history in the past 12 months (Lindholm et al., 2016). Patients with PD were recruited from the University of Kansas Medical Center Parkinson's Disease and Movement Disorder Center between 08/2018 and 02/2019. Diagnosis of idiopathic PD was established according to the United Kingdom Parkinson's Disease Society Brain Bank Clinical Diagnostic Criteria (Hughes et al., 1992). Healthy controls were the spouse/significant others of the participants with PD or members of the community.

Inclusion criteria for the PD group were (1) voluntary consent, (2) ability to speak and understand the English language, and (3) mild to moderate disease severity (Hoehn and Yahr stage II and III). Exclusion criteria were (1) diagnosis of mild cognitive impairment or dementia, (2) atypical parkinsonism, (3) history of neurological or vestibular conditions unrelated to PD, (4) current visual acuity problems that cannot be resolved by corrective lenses or visual field problems, (5) severe trunk and head dyskinesia or dystonia in the medication "on" state, (6) blepharospasm, (7) deep brain stimulation, (8) unpredictable motor fluctuations, and (9) any musculoskeletal condition that might affect standing and balance activities. Inclusion criteria for the healthy controls were (1) voluntary consent and (2) ability to speak and understand the English language. We excluded individuals who (1) had or currently have neurological or vestibular problems, (2) any musculoskeletal problems that might affect balance activities, and (3) visual acuity problems that cannot be resolved by corrective lenses or visual field problems.

This study was approved by the Human Subjects Committee at the University of Kansas Medical Center. Participants were asked to make one visit to the University of Kansas Medical Center Parkinson's Disease and Movement Disorder Center. Prior to enrollment written informed consent was obtained from all study participants. Study testing lasted for a total of 2 h including consent and breaks. All assessments were done in the medication "on" state. Participants with PD were tested approximately 30–45 min after medication intake to minimize the possibility of wearing-off, which could potentially affect the test results. It is reported that individuals with PD had better recognition of wearing-off based on their self-reported exacerbated motor and non-motor symptoms compared to a PD specialist (Stacy et al., 2005). Therefore, if the medication wore off based on participants' self-report during the assessment, the assessment was stopped until approximately 30 min after the next medication dose when the participant was again in the medication "on" state. The "on" medication for clinical assessments was defined as the patients taking their normal daily medications in the optimally medicated state, as determined by both the patient and the researcher.

Demographic characteristics and medical history were collected from the participants. A list of prescribed and unprescribed medications was obtained from the participants' medical records. Levodopa Equivalent Daily dose was calculated to tally antiparkinsonian related medication usage (Deuschl et al., 2006). Global cognitive functioning was measured through the Montreal Cognitive Assessment (MoCA) (Nasreddine et al., 2005). Restrictions in activities of daily living and motor impairments were evaluated through the Movement Disorders Society-Unified Parkinson's Disease Rating Scale (MDS-UPDRS) Part II (motor experiences of daily living) and Part III (motor examination) (Goetz et al., 2008). The Hoehn and Yahr (H&Y) Scale (Hoehn and Yahr, 1967) was used to assess PD severity. The Scales for Outcomes in Parkinson's Disease-Autonomic Dysfunction (SCOPA-AUT) (Visser et al., 2004) was conducted to assess autonomic symptoms as dysautonomia may potentially influence pupillary response in PD. Lastly, fear of falling was measured through the Falls Efficacy Scale-International (FES-I).

All participants were asked to wear Tobii Pro 2 glasses (Tobii Technologies, Inc.) to measure pupillary response during the testing. Participants were tested in a room with no windows. The temperature and lighting conditions of the room were identical for each participant. A force plate was used (AMTI OPT464508-1000, Advanced Mechanical Technology, Inc.) to assess Center of Pressure (CoP) displacement with a sampling frequency of 100 Hz. Participants were instructed to stand with their shoes on by placing their feet oriented at 14° with heel centers 17 cm apart. The assessment and testing took around 2 h and we mitigated the effect of fatigue by giving breaks and by allowing participants to have rest periods anytime during the study. Participants were asked to complete the following conditions in randomized order.

1. Single balance eyes open condition: Participants stood on a force plate and were instructed to maintain an upright standing posture for 60 s.
2. Single balance eyes occluded condition: Participants were instructed to stand on a force plate for 60 s while their eyes were occluded with a sleep mask. The sleep mask was placed in front of the eye-tracking glasses. Participants were instructed to keep their eyes open throughout the condition.
3. Dual task eyes open condition: Participants were instructed to stand on the force plate for 60 s while concurrently completing an Auditory Stroop test.
4. Dual task eyes occluded condition: Participants were instructed to stand on a force plate for 60 s while simultaneously completing an Auditory Stroop test with their eyes occluded.

The Auditory Stroop test was shown to be one of the key determinants of dual task performance in individuals with PD (Strouwen et al., 2016). Therefore, the Auditory Stroop test was conducted to stress the executive function and cognitive flexibility abilities of the participants. During the Auditory Stroop test, participants heard the word "high" or "low" in a high or low pitch and were instructed to name the pitch of the stimulus, while ignoring the meaning of the word. Participants heard congruent stimuli where the word and pitch are equal (e.g., "high" at a high pitch) or incongruent stimuli where the word and pitch differ (e.g., "high" at a low pitch) in a random order for 60 s. There were 30 stimuli presented at 2-s intervals for 60 s. Participants were instructed to respond as accurately and as fast as possible. To standardize the test, participants wore headphones and the stimuli were played by a digital recorder.

After testing, the pupillary response data were extracted at 60 Hz from EyeWorks Analyze software. By solely measuring the change of the raw pupil dilation, there are potential limitations such as the light reflex and movement artifacts interfering with the pupil size. We minimized these potential confounders by keeping lighting in the room constant and having participants focus on a picture of dots on the wall to minimize eye movements to better capture pupil dilation. In addition, we used the Index of Cognitive Activity (ICA) algorithm, calculated through the EyeWorks Analyze software to differentiate pupillary response due to workload from the light reflex (Marshall, 2007). In this study, pupil dilation was measured by an eye-tracker, and ICA analysis was conducted to compare cognitive workload across the conditions. This algorithm computes the number of unusual increments in pupil size per second. These values are then transformed into a continuous scale ranging between 0 (no cognitive workload) and 1 (maximum cognitive workload). Based on this algorithm the noisy signals are reduced to nearly zero (Marshall, 2007). The mean ICA was calculated after each condition for all groups.

In addition, the CoP displacement in the anterior-posterior (AP) and medio-lateral (ML) directions were calculated by using NetForce Ver. 3.5.3 software for each condition. We included several functional mobility tests to better understand an individual's risk of falling and provide a standardized assessment of disability and functional limitations. The APDM Movement Monitoring inertial sensor system (APDM Inc., Portland, OR, United States) was used to objectively characterize balance and gait impairments. After calibration, six synchronized Opal inertial sensors were fitted on each participant via elastic straps [sternum, waist (at the level of the fifth lumbar spine), dorsal surface of bilateral wrists and top of each foot]. Participants were asked to complete the Timed Up and Go (TUG) test and TUG-cognitive (TUG-COG) while wearing the sensors. TUG is a widely used, reliable, and valid test to examine functional mobility and falls risk in individuals with PD (Morris et al., 2001). This test also assesses multiple postural components such as balance control, physical mobility, and gait; therefore, we decided to use this test to better characterize fall risk and to confirm the classification of self-reported fallers and non-fallers. Participants were asked to sit on a chair to start the TUG test and instructed to stand up from the chair, walk 3 m at normal speed, turn back, walk back to the chair, and then sit down. The test was done three times and the average turning and completion time was calculated. It has been shown that both TUG turning duration and TUG completion time provide a good understanding of functional impairments and fall risk in individuals with PD (Mancini et al., 2015). During TUG-COG, individuals were asked to count backward by 7 starting from a random three-digit number while standing up from the chair, walking 3 m at normal speed, turning back, walking back to the chair and then sitting

TABLE 1 | Demographic and clinical characteristics.

Variables	PD fallers (*n* = 14)	PD non-fallers (*n* = 19)	Healthy controls (*n* = 35)	*p*-value
Age (years)	69.9 ±6.8	68.8 ± 6.9	68.5 ± 6.2	0.8
Sex (female/male, n)	7/7	7/12	21/14	0.3
Education (years)	15.2 ± 2.2	15.5 ± 2.1	17.3± 3.5	0.02
MoCA [0–30]	26.8 ± 3.8	26.3 ± 2.3	26.6± 2.3	0.8
MDS-UPDRS II [0–52]	14.3 ±8.3	10.1 ±7.9	N/A	0.1
MDS-UPDRS III [0–72]	47.4 ± 12.4	41.5 ± 16.4	N/A	0.3
Modified H&Y scale [1–5]	2.4 ± 0.6	2.2 ± 0.4	N/A	0.2
LED (mg)	312.2± 302.6	294.5± 236.8	N/A	0.9
SCOPA-AUT [0–69]	16.6 ±10.2	14.3 ± 8.2	N/A	0.5
FES-I [16–64]	30.6±11.6	23.3 ±7.5	18.3 ± 2.1	<0.001
TUG turning time (sec)	2.7 ± 0.5	2.6 ± 0.6	2.3 ± 0.3	0.01
TUG total time (sec)	15.1 ± 5.2	13.2 ± 3.2	11.6± 1.8	0.01
TUG-COG turning time (sec)	2.8 ± 0.5	2.6 ± 0.6	2.3± 0.4	0.02
TUG-COG total time (sec)	15.8 ±0.3	17.3 ± 12.1	14.4 ±5.4	0.44

PD, Parkinson's disease; MoCA, Montreal Cognitive Assessment; MDS-UPDRS II, Movement Disorder Society Unified Parkinson Disease Rating Scale motor experiences of daily living; MDS-UPDRS III, Movement Disorder Society Unified Parkinson Disease Rating Scale motor examination; H&Y, Hoehn and Yahr; LED, Levodopa Equivalent Dose; SCOPA-AUT, Scales for Outcomes in Parkinson's Disease-Autonomic questionnaire; N/A, Not Applicable. FES-I, Falls Efficacy Scale-International, TUG, Timed Up and Go; TUG-COG, Timed Up and Go-Cognitive. The results are presented as mean ± standard deviation except for the sex variable. The ranges of each scale were presented in the brackets.

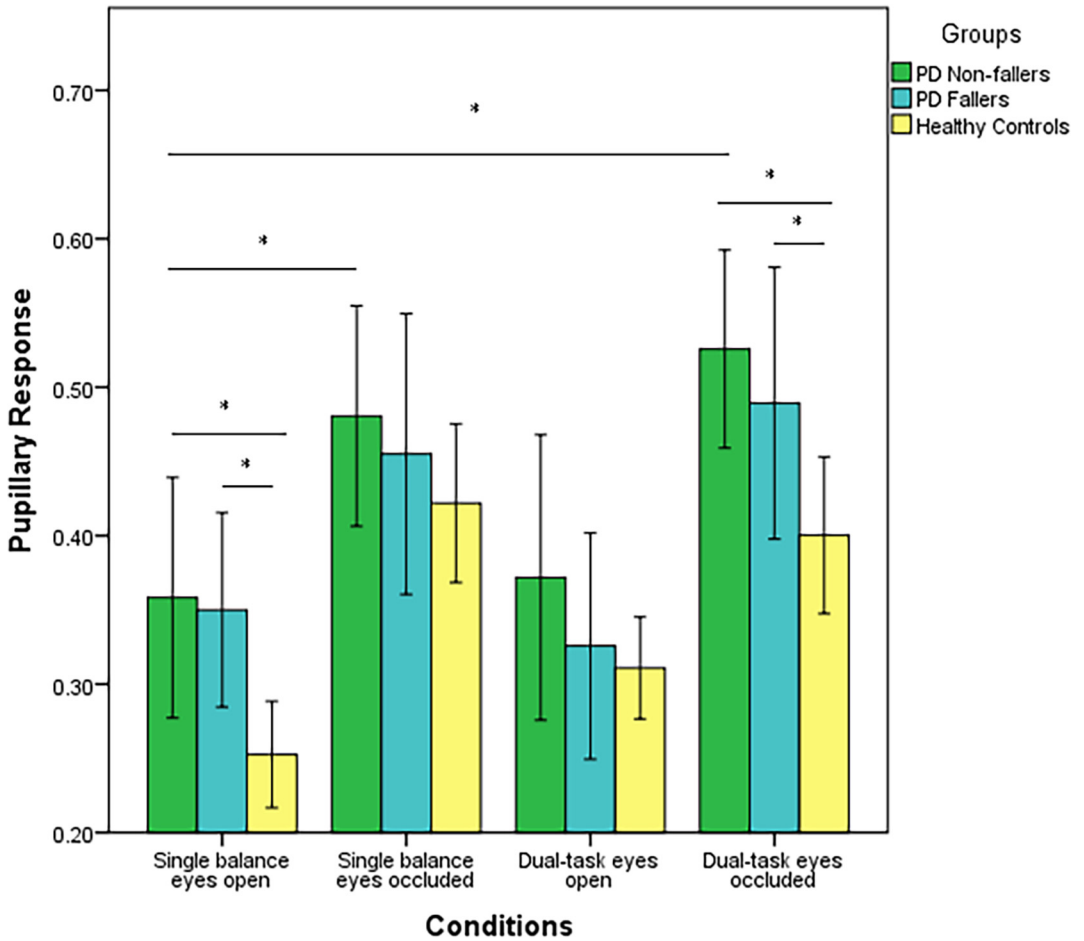

FIGURE 1 | Mean values (range 0–1) and standard error of the mean (SEM) of pupillary response of PD fallers, PD non-fallers, and healthy controls across the conditions. *$p < 0.01$.

down. The TUG-COG was done three times and average turning and completion times were calculated. Signals were automatically processed and calculated via the corresponding Mobility Lab^{TM} software package.

STATISTICAL ANALYSIS

Homogeneity of variance between groups was verified using Levene's test. Independent *t*-tests were used to compare demographic and clinical variables between individuals with PD and healthy controls. One-way Analysis of Variance (ANOVA) was used to compare demographic and clinical variables between PD fallers, PD non-fallers, and healthy controls. Fisher's exact test was used to compare nominal variables. Independent *t*-tests were used to compare disease-specific variables between PD fallers and PD non-fallers. Two-way Repeated Measures ANOVA and LSD *post-hoc* tests were employed to compare pupillary response and CoP displacement across the four conditions and between individuals with PD and healthy controls. The same test was run to compare pupillary response and CoP displacement between PD fallers, PD non-fallers, and healthy controls. Pearson's correlation was used to analyze the relationship between pupillary response and CoP displacement. The results were interpreted as follows: >0.70 is strong, 0.50–0.70 is moderate, 0.30–0.50 is weak (Hinkle et al., 1988). All statistical analyses were performed with the IBM SPSS Statistics v.26 software (IBM, Armonk, NY, United States). Bonferroni correction was applied to adjust multiple pairwise comparisons and $p < 0.01$ were considered statistically significant.

RESULTS

A summary of the demographic and clinical characteristics of two groups are shown in **Table 1**. Individuals with PD had mild to moderate disease severity ($n = 24$ in H&Y stage II; $n = 9$ H&Y stage III) and MDS-UPDRS II and III scores (**Supplementary Table S1**). There were no significant differences in demographic variables between the groups except that healthy controls had more years of education. In addition, PD fallers had significantly higher FES-I scores, TUG turning and total time, and TUG-COG

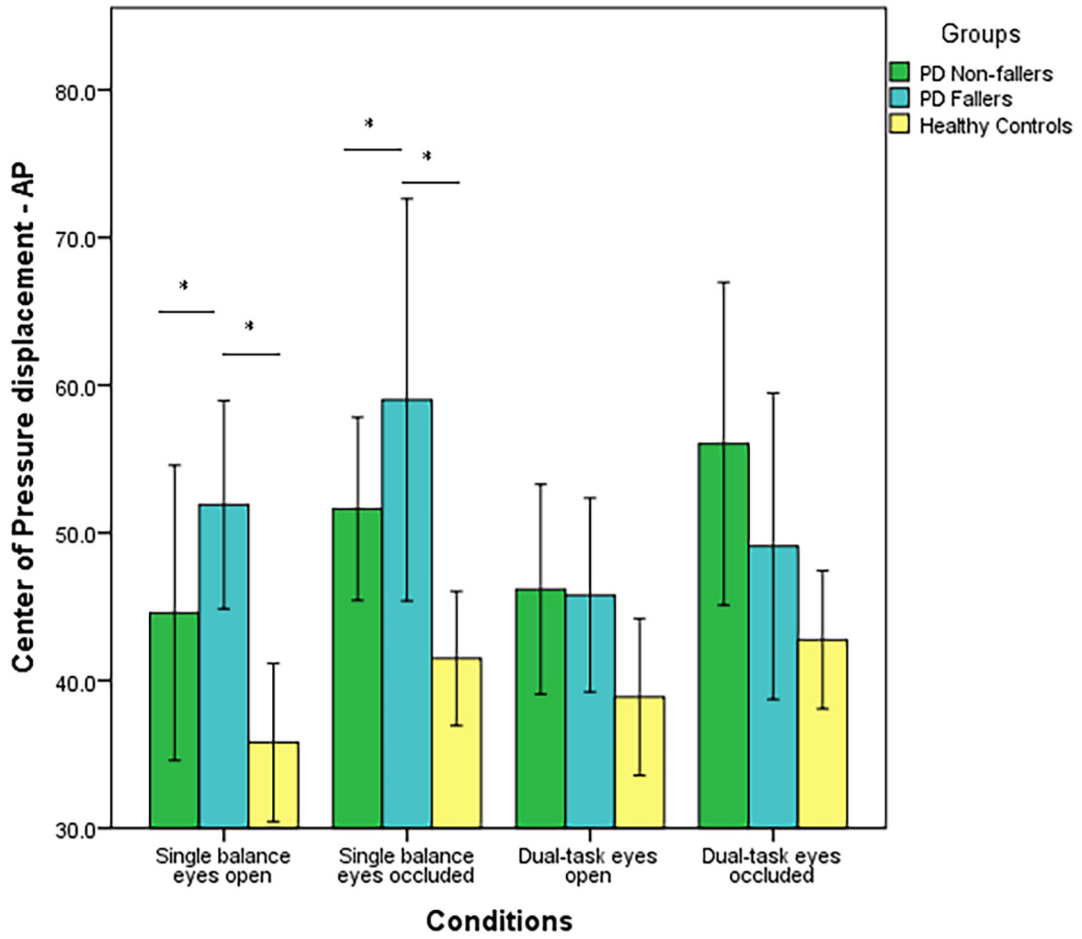

FIGURE 2 | Mean values (in mm^2/s) and standard error of the mean (SEM) of Center of Pressure (CoP) displacement in the Anterior-Posterior (AP) direction of PD fallers, PD non-fallers, and healthy controls across the conditions. *$p < 0.01$.

turning time compared to PD non-fallers and healthy controls. However, there was no significant difference in the TUG-COG total time between the groups.

We first conducted a two-way repeated measures ANOVA with main effects of group (PD vs. controls), condition, and interaction effect of group × condition. Individuals with PD had a higher pupillary response compared to healthy controls ($p = 0.009$). In addition, a significant within-condition effect was observed, indicating that pupillary response increased with increased postural demand ($p < 0.001$). The *post-hoc* analysis demonstrated that pupillary response was significantly larger in the single balance eyes occluded ($p < 0.001$), dual task eyes open ($p = 0.01$), and dual task eyes occluded ($p < 0.001$) conditions compared to single task eyes open condition. No other *post-hoc* within group differences were observed. Lastly, there was a trend in the interaction effect of group × condition ($p = 0.06$), suggesting cognitive workload as a result of postural demand manifests differently in participants with PD compared to healthy controls (**Supplementary Figure S1**).

Next, two-way repeated measures ANOVA was employed to compare pupillary response between PD fallers, PD non-fallers, and controls across the four conditions. Pupillary response was significantly different between the groups ($p < 0.001$). The *post-hoc* analysis demonstrated that PD non-fallers ($p = 0.001$) and PD fallers ($p = 0.01$) exhibited greater pupillary response compared to healthy controls over all the conditions. Although there was no significant difference between PD non-fallers and PD fallers between-group grand averages of the four conditions, the comparison of mean and standard deviation demonstrated that PD non-fallers (mean ± s.d.) (0.43 ± 0.2) exhibited greater pupillary response compared to the PD fallers (0.38 ± 0.2) and healthy controls (0.34 ± 0.1) ($p = 0.25$). Pupillary response significantly increased with increased postural demand, especially from eyes open to eyes occluded conditions ($p < 0.001$). However, no interaction effect was observed ($p = 0.77$) (**Figure 1**).

CoP displacement in the AP direction was significantly different between the three groups ($p < 0.001$). The *post-hoc* analysis demonstrated there was a significant difference between PD non-fallers and healthy controls ($p = 0.001$) as well as between PD fallers and healthy controls ($p = 0.001$). However, there was no difference between PD non-fallers and PD fallers ($p = 0.61$). Also, there was not a significant within-condition effect ($p = 0.04$). There was not an interaction effect of group × condition ($p = 0.48$) (**Figure 2**). Lastly, there were no significant

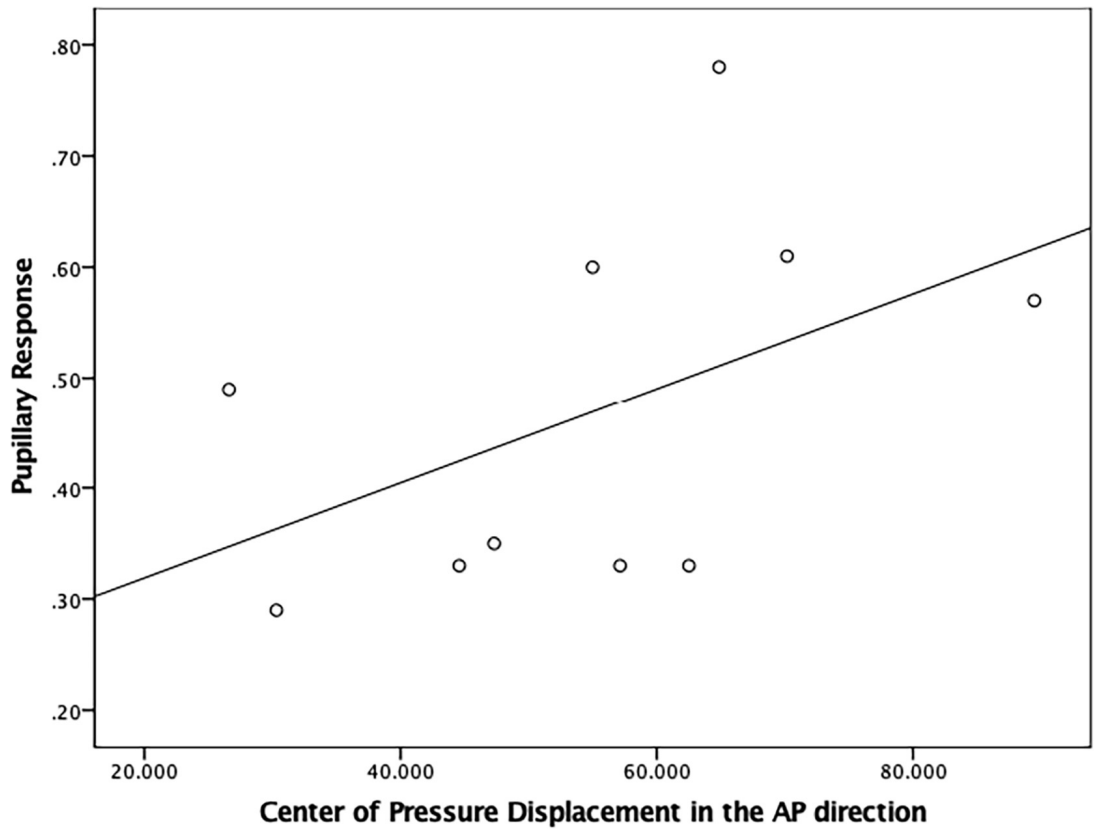

FIGURE 3 | Correlation analysis between pupillary response and Center of Pressure (CoP) displacement (in mm^2/s) in the Anterior-Posterior direction in PD fallers.

between-group ($p = 0.25$) or within-group ($p = 0.02$) differences for the CoP displacement in the ML direction.

There was a moderately strong, positive, but non-significant correlation ($r = 0.50$; $p = 0.15$) between pupillary response and CoP displacement in PD fallers group during single balance eyes occluded (**Figure 3**). Also, a moderate negative correlation was observed between pupillary response and CoP displacement in healthy controls during single balance eyes occluded ($r = -0.51$; $p = 0.006$) (**Figure 4**). No other moderate or strong correlations were observed between pupillary response and COP displacement. Lastly, the Auditory Stroop results demonstrated that both individuals with PD and healthy controls responded correctly to 75% of the questions during the test both in dual task eyes open and dual-task eyes occluded conditions.

DISCUSSION

To our knowledge, this is the first study that investigated pupillary response as a measure of cognitive workload to changes in postural demand in individuals with PD. The findings of this study demonstrated that, overall, individuals with PD exhibited higher cognitive workload measured by pupillary response compared to healthy controls. In addition, a significant condition effect was observed suggesting that individuals with PD and healthy controls displayed increased pupillary response from single balance eyes open to dual task eyes open condition and to dual task eyes occluded conditions. Our results demonstrate that pupillary response is a sensitive neurophysiological measure of postural demand in both individuals with PD and healthy controls. The results imply that vision occlusion and secondary cognitive task impose additional cognitive workload that can be adequately captured through the pupillary response.

Pupillary response was sensitive to incremental difficulty levels of postural demand in both groups. In addition, the PD group exhibited greater postural demand for all tasks compared to the healthy controls. These findings were similar to previous studies, which measured brain activation by using functional near-infrared spectroscopy (fNIRS) or electroencephalogram during dual-tasking in PD. Studies have shown that individuals with PD had higher brain activation perhaps to compensate for the neurodegeneration compared to healthy older adults (Maidan et al., 2016, 2019). Increased pupillary response in individuals with PD might be related to a neurodegeneration process leading to limited cognitive resources to exert during balance tasks compared to the healthy controls. A greater understanding of the amount of cortical workload involved in balance tasks with PD-related neurodegeneration will allow the development of PD-specific interventions targeting cortical activity and eventually decrease fall risk in these individuals. The novelty of our study

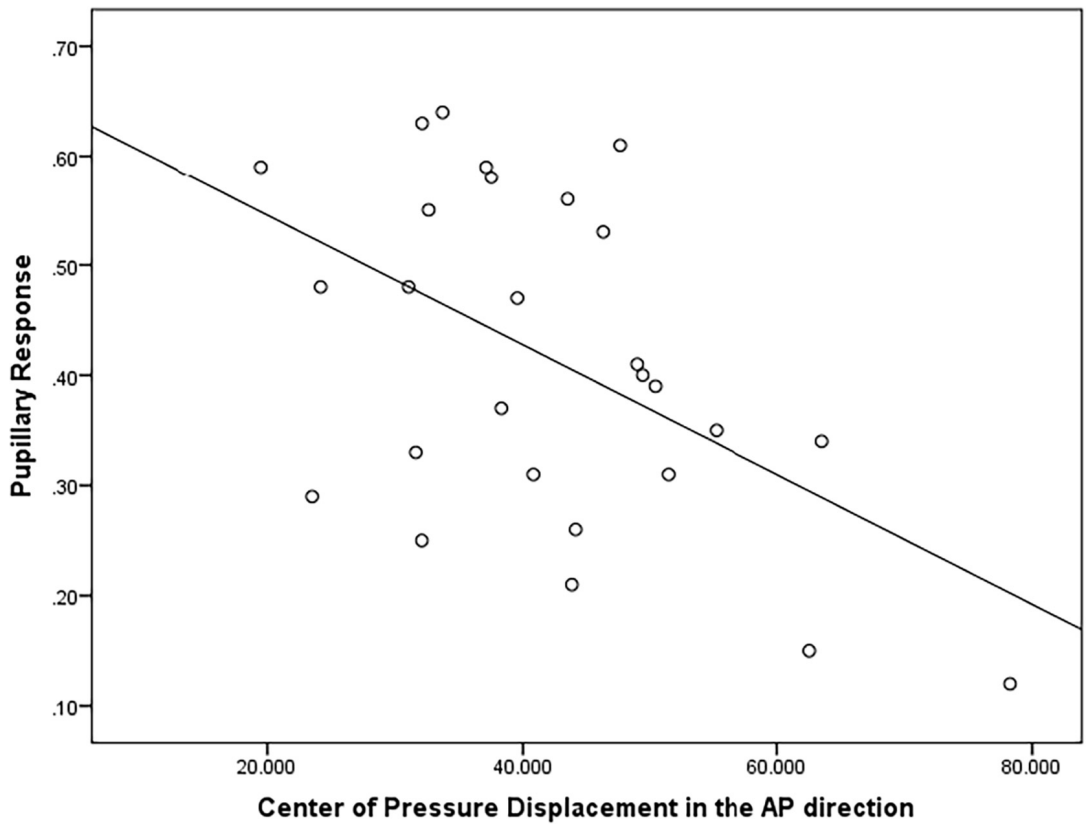

FIGURE 4 | Correlation analysis between pupillary response and Center of Pressure (CoP) displacement (in mm^2/s) in the Anterior-Posterior direction in healthy controls.

is to use pupillary response, which may offer an inexpensive, less intrusive alternative to other neurophysiological tools, such as fNIRS or electroencephalogram, in unraveling brain activation during postural demand in individuals with PD. In the future, pupillary response can be a potential tool to understand the neurophysiological underpinnings of falls risk in the PD population.

Although the results were not significant, PD non-fallers exhibited higher mean pupillary response compared to PD fallers and healthy controls. These results are important to discuss since there is a need to objectively characterize falls risk in clinical practice for individuals with PD. Our results were contradictory to previous studies, which have shown that PD fallers and older adults who are fallers had higher brain activation, measured by fNIRS, in the prefrontal cortex compared to their non-fallers group during dual task gait activities (Halliday et al., 2018; Maidan et al., 2018). One possible explanation is that PD fallers may need to use additional brain networks from the prefrontal cortex as a compensatory strategy to maintain their balance. In our study, we used pupillary response to understand cognitive workload, which has a greater temporal resolution compared to fNIRS (Numata et al., 2019). Therefore, it is possible that pupillary response better corresponds to the timing of the actual brain activity compared to the fNIRS.

PD fallers and PD non-fallers had higher CoP displacement in the AP direction, higher fear of falling, and longer time to complete TUG compared to healthy controls. In the literature, similar results were published. Studies showed higher fear of falling and increased time to complete TUG and TUG-COG in PD fallers compared to PD non-fallers (Vance et al., 2015; Kader et al., 2016). Higher fear of falling is a predictor of future falls and associated with worse motor symptoms and lower quality of life in the PD population (Jonasson et al., 2018). Therefore, it was not surprising that our data demonstrated higher fear of falling and worse outcomes in clinical fall risk assessments in PD fallers. In addition, Matinolli et al. (2007) demonstrated that individuals with PD who are fallers had higher postural sway and CoP displacement compared to PD non-fallers and healthy controls. Other studies demonstrated increased CoP displacement with visual deprivation and additional cognitive load in individuals with PD (Marchese et al., 2003; Holmes et al., 2010; Morenilla et al., 2020). In the present study, **Figure 2** demonstrated increased CoP displacement in PD fallers with visual occlusion; however, the effect of additional cognitive load was absent measured by CoP displacement. Also, PD fallers had increased CoP displacement during single tasks but showed decreased displacement during the dual task conditions, whereas PD non-fallers had a similar pattern of CoP displacement

compared to healthy controls. This might suggest that PD fallers demonstrated a rigid posture to maintain their balance during dual task activities. In PD, it is typical to observe increased CoP displacement and postural sway during balance but also a high and unadaptable axial tone (rigidity), which both negatively impact postural balance (Cohen et al., 2015). Based on our results, increased rigidity perhaps contributes more to falls, which suggests that PD fallers are unable to react and initiate appropriate compensatory postural strategies to prevent falls. Alternatively, decreased CoP displacement during the dual task conditions can be explained as individuals prioritize and divert their attention to the motor task since during the Auditory Stroop test individuals responded wrongly to 25% of the questions. These results might suggest that both individuals with PD and healthy older adults exhibited cognitive-motor interference resulting in decreased performance in one or both tasks under dual task conditions.

Lastly, it is important to couple behavioral and neurophysiological results to increase our understanding of brain-behavior interaction. A moderate positive correlation was observed between pupillary response and CoP displacement in PD fallers, whereas a moderate negative correlation was observed between pupillary response and CoP displacement in healthy controls during single balance eyes occluded. It is possible that impaired posture control is associated with higher cognitive workload in individuals with PD who are fallers, whereas healthy controls exhibit higher cognitive workload as a compensatory strategy to maintain their posture. Future studies are needed to better understand the relationship between neurophysiological and behavioral results in healthy and disease population.

This study has several limitations. PD fallers and non-fallers were grouped based on their self-report of falls. However, the clinical fall risk assessments demonstrated that PD fallers had significantly higher TUG and TUG-COG completion time and fear of falling compared to PD non-fallers and healthy controls. Therefore, we assume that individuals were assigned to correct groups based on their self-reported falls. In addition, we did not control the number of falls in our analysis in healthy controls. Only five individuals reported a history of falls out of 35 participants; therefore, we assume that history of falls in healthy controls was not a major confounding factor in our results. Although we measured subjects' cognition by MoCA and years of education as proxies of cognitive capacity, future studies should consider formally measuring cognitive capacity, for example, through the cognitive reserve index questionnaire (Nucci et al., 2012), to better understand the neurophysiological response of the brain to increased postural demand in aging and age-related neurodegenerative conditions. Lastly, during the dual task conditions individuals engaged with triple tasks including balance, cognition, and speaking to respond Auditory Stroop test. It is possible that individuals allocated a small amount of cognitive resources for speaking. However, the main idea of using dual task paradigms is to challenge individuals' ability to more than one task at the same time. The Auditory Stroop task in combination with a postural test requires a significant cognitive capacity for older adults and individuals with PD. Also, during the Auditory Stroop test individuals only responded by saying "low" or "high." Therefore, in this study, we believe that individuals did not allocate significant cognitive capacity to speaking.

CONCLUSION

Pupillary response is a non-intrusive, objective, and sensitive neurophysiological measure of cognitive workload during postural demand in older adults with and without PD. Individuals with PD exerted greater pupillary response to remain standing still under visual occlusion and dual tasking conditions. In the future, pupillary response can be a potential tool to understand the neurophysiological underpinnings of falls and falls risk in the PD population.

DATA AVAILABILITY STATEMENT

The raw data supporting the conclusions of this article will be made available by the authors, without undue reservation.

ETHICS STATEMENT

This study was approved by the Human Subjects Committee at the University of Kansas Medical Center. The patients/participants provided their written informed consent to participate in this study.

AUTHOR CONTRIBUTIONS

MK: conception, organization, and execution for the research project, design and execution for the statistical analysis, and writing of the first draft for manuscript preparation. KL: conception and organization for the research project, review and critique for the statistical analysis, and manuscript preparation. RP: organization for the research project, review and critique for the statistical analysis, and manuscript preparation. AA: conception for the research project, review and critique for the statistical analysis, and manuscript preparation. JH: conception for the research project, design, review, and critique for the statistical analysis, and review and critique for the manuscript preparation. HD: conception, organization, and execution for the research project, design, review, and critique for the statistical analysis, and review and critique for the manuscript preparation. All authors contributed to the article and approved the submitted version.

FUNDING

This study was funded in part by T32HD057850 from the Eunice Kennedy Shriver National Institute of Child Health and Human Development and by Mabel A. Woodyard Fellowship in Neurodegenerative Disorders (MK) and by the National Institute on Aging of the National Institutes of Health under Award Number K01AG058785 (HD).

ACKNOWLEDGMENTS

We would like to thank Lisa Landis, SPT (University of Kansas Medical Center) and Maddi Hughes-Zahner, SPT (University of Kansas Medical Center) for their help with the data collection.

SUPPLEMENTARY MATERIAL

The Supplementary Material for this article can be found online at: https://www.frontiersin.org/articles/10.3389/fbioe.2021.617028/full#supplementary-material

Supplementary Figure 1 | Mean values (range 0–1) and standard error of the mean (SEM) of pupillary response of individuals with PD and healthy controls accross the conditions. $^{*}p < 0.01$.

Supplementary Table 1 | Demographic and ClinicalCharacteristics.
PD = Parkinson's disease; MoCA = Montreal Cognitive Assessment; MDS-UPDRS II = Movement Disorder Society Unified Parkinson Disease Rating Scalemotor experiences of daily living; MDS-UPDRS III = Movement Disorder Society Unified Parkinson Disease Rating Scalemotor examination; H&Y = Hoehn and Yahr; LED = Levodopa Equivalent Dose; SCOPA-AUT = Scales for Outcomes in Parkinson's Disease-Autonomic questionnaire; N/A = Not Applicable. FES-I = Falls Efficacy Scale-International, TUG = Timed Up and Go; TUG-COG = Timed Up and Go-Cognitive. The results are presented as mean ± standard deviation except for the sex variable.

REFERENCES

Beatty, J. (1982). Task-evoked pupillary responses, processing load, and the structure of processing resources. *Psychol. Bull.* 91:276. doi: 10.1037/0033-2909.91.2.276

Beatty, J., and Lucero-Wagoner, B. (2000). The pupillary system. *Handb. Psychophysiol.* 2, 142–162.

Burki, C. N., Bridenbaugh, S. A., Reinhardt, J., Stippich, C., Kressig, R. W., and Blatow, M. (2017). Imaging gait analysis: an fMRI dual task study. *Brain Behav.* 7:e00724.

Cohen, J. (1988). *Statistical Power Analysis for the Behavioral Sciences.* 2nd Edn. CityplaceHillsdale, StateNJ: Lawrence Erlbaum Associates Inc.

Cohen, R. G., Gurfinkel, V. S., Kwak, E., Warden, A. C., and Horak, F. B. (2015). Lighten up: specific postural instructions affect axial rigidity and step initiation in patients with Parkinson's Disease. *Neurorehabil. Neural Repair.* 29, 878–888. doi: 10.1177/1545968315570323

Contreras, A., and Grandas, F. (2012). Risk of falls in Parkinson's disease: a cross-sectional study of 160 patients. *Parkinson's Disease* 2012:362572.

Deuschl, G., Schade-Brittinger, C., Krack, P., Volkmann, J., Schäfer, H., Bötzel, K., et al. (2006). A randomized trial of deep-brain stimulation for Parkinson's disease. *N. Engl. J. Med.* 355, 896–908.

Goetz, C. G., Tilley, B. C., Shaftman, S. R., Stebbins, G. T., Fahn, S., Martinez-Martin, P., et al. (2008). Movement Disorder Society-sponsored revision of the Unified Parkinson's Disease Rating Scale (MDS-UPDRS): scale presentation and clinimetric testing results. *Movement Dis.* 23, 2129–2170. doi: 10.1002/mds.22340

Halliday, D. W., Hundza, S. R., Garcia-Barrera, M. A., Klimstra, M., Commandeur, D., Lukyn, T. V., et al. (2018). Comparing executive function, evoked hemodynamic response, and gait as predictors of variations in mobility for older adults. *J. Clin. Exp. Neuropsychol.* 40, 151–160. doi: 10.1080/13803395.2017.1325453

Herman, T., Mirelman, A., Giladi, N., Schweiger, A., and Hausdorff, J. M. (2010). Executive control deficits as a prodrome to falls in healthy older adults: a prospective study linking thinking, walking, and falling. *J. Gerontol. Ser. A: Biomed. Sci. Med. Sci.* 65, 1086–1092. doi: 10.1093/gerona/glq077

Hinkle, D. E., Wiersma, W., and Jurs, S. G. (1988). *Solutions Manual: Applied Statistics for the Behavioral Sciences*. placeCityBoston: Houghton Mifflin.

Hoehn, M. M., and Yahr, M. D. (1967). Parkinsonism: onset, progression and mortality. *Neurology* 17, 427–442. doi: 10.1212/wnl.17.5.427

Holmes, J. D., Jenkins, M. E., Johnson, A. M., Adams, S. G., and Spaulding, S. J. (2010). Dual-task interference: the effects of verbal cognitive tasks on upright postural stability in Parkinson's disease. *Parkinsons Dis.* 2010:696492.

Hughes, A. J., Daniel, S. E., Kilford, L., and Lees, A. J. (1992). Accuracy of clinical diagnosis of idiopathic Parkinson's disease: a clinico-pathological study of 100 cases. *J. Neurol. Neurosurg. Psychiatry* 55, 181–184. doi: 10.1136/jnnp.55.3.181

Huse, D. M., Schulman, K., Orsini, L., Castelli-Haley, J., Kennedy, S., and Lenhart, G. (2005). Burden of illness in Parkinson's disease. *Movement Dis.* 20, 1449–1454.

Jonasson, S. B., Nilsson, M. H., Lexell, J., and Carlsson, G. (2018). Experiences of fear of falling in persons with Parkinson's disease–a qualitative study. *BMC Geriatr.* 18:44. doi: 10.1186/s12877-018-0735-1

Kader, M., Iwarsson, S., Odin, P., and Nilsson, M. H. (2016). Fall-related activity avoidance in relation to a history of falls or near falls, fear of falling and disease severity in people with Parkinson's disease. *BMC Neurol.* 16:84. doi: 10.1186/s12883-016-0612-5

Kahya, M., Lyons, K. E., Pahwa, R., Akinwuntan, A. E., He, J., and Devos, H. (2020). Reliability and validity of pupillary response during dual-task balance in Parkinson Disease. *Arch. Phys. Med. Rehabil.* 102, 448–455. doi: 10.1016/j.apmr.2020.08.008

Kahya, M., Moon, S., Lyons, K. E., Pahwa, R., Akinwuntan, A. E., and Devos, H. (2018a). Pupillary response to cognitive demand in parkinson's disease: a pilot study. *Front. Aging Neurosci.* 10:90. doi: 10.3389/fnagi.2018.00090

Kahya, M., Wood, T. A., Sosnoff, J. J., and Devos, H. (2018b). Increased postural demand is associated with greater cognitive workload in healthy young adults: a pupillometry study. *Front. Hum. Neurosci.* 12:288. doi: 10.3389/fnhum.2018.00288

Kellogg (1987). The prevention of falls in later life. a report of the kellogg international work group on the prevention of falls by the elderly. *Dan. Med. Bull.* 34(Suppl. 4), 1–24.

Kelly, V. E., Eusterbrock, A. J., and Shumway-Cook, A. (2012). A review of dual-task walking deficits in people with Parkinson's disease: motor and cognitive contributions, mechanisms, and clinical implications. *Parkinson's Disease* 2012:918719.

Lahr, J., Pereira, M. P., Pelicioni, P. H., De Morais, L. C., and Gobbi, L. T. (2015). Parkinson's disease patients with dominant hemibody affected by the disease rely more on vision to maintain upright postural control. *Percept. Mot. Skills* 121, 923–934. doi: 10.2466/15.pms.121c26x0

Lindholm, B., Nilsson, M. H., Hansson, O., and Hagell, P. (2016). External validation of a 3-step falls prediction model in mild Parkinson's disease. *J. Neurol.* 263, 2462–2469. doi: 10.1007/s00415-016-8287-9

Liu-Ambrose, T. Y., Ashe, M. C., Graf, P., Beattie, B. L., and Khan, K. M. (2008). Increased risk of falling in older community-dwelling women with mild cognitive impairment. *Phys. Therapy* 88, 1482–1491. doi: 10.2522/ptj.20080117

Lord, S. R., Ward, J. A., Williams, P., and Anstey, K. J. (1993). An epidemiological study of falls in older community-dwelling women: the placeCityRandwick falls and fractures study. *Aus. J. Public Health* 17, 240–245. doi: 10.1111/j.1753-6405.1993.tb00143.x

Maidan, placeI., Fahoum, F., Shustak, S., Gazit, E., Patashov, D., Tchertov, D., et al. (2019). Changes in event-related potentials during dual task walking in aging and Parkinson's disease. *Clin. Neurophysiol.* 130, 224–230. doi: 10.1016/j.clinph.2018.11.019

Maidan, placeI., Nieuwhof, F., Bernad-Elazari, H., Klimstra, M., Commandeur, D., Lukyn, T. V., et al. (2018). Evidence for differential effects of 2 forms of exercise on prefrontal plasticity during walking in Parkinson's Disease. *Neurorehabil. Neural Repair.* 32, 200–208. doi: 10.1177/1545968318763750

Maidan, placeI., Nieuwhof, F., Bernad-Elazari, H., Reelick, M. F., Bloem, B. R., Giladi, N., et al. (2016). The role of the frontal lobe in complex walking among patients with parkinson's disease and healthy older adults: an fNIRS study. *Neurorehabil. Neural Repair.* 30, 963–971. doi: 10.1177/1545968316650426

Mancini, M., El-Gohary, M., Pearson, S., McNames, J., Schlueter, H., Nutt, J. G., et al. (2015). Continuous monitoring of turning in Parkinson's disease: rehabilitation potential. *NeuroRehabilitation* 37, 3–10. doi: 10.3233/nre-151236

Manohar, S., and Husain, M. (2015). Reduced pupillary reward sensitivity in Parkinson's disease. *NPJ Parkinson's Disease* 1:15026.

Marchese, R., Bove, M., and Abbruzzese, G. (2003). Effect of cognitive and motor tasks on postural stability in Parkinson's disease: a posturographic study. *Mov. Disord.* 18, 652–658. doi: 10.1002/mds.10418

Marshall, S. P. (2007). Identifying cognitive state from eye metrics. *Aviat. Space Environ. Med.* 78, B165–B175.

Matinolli, M., Korpelainen, J. T., Korpelainen, R., Sotaniemi, K. A., Virranniemi, M., and Myllyla, V. V. (2007). Postural sway and falls in Parkinson's disease: a regression approach. *Mov. Dis.* 22, 1927–1935. doi: 10.1002/mds.21633

Micieli, G., Tassorelli, C., Martignoni, E., Pacchetti, C., Bruggi, P., Magri, M., et al. (1991). Disordered pupil reactivity in Parkinson's disease. *Clin. Auton Res.* 1, 55–58. doi: 10.1007/bf01826058

Morenilla, L., Márquez, G., Sánchez, J. A., Bello, O., López-Alonso, V., Fernández-Lago, H., et al. (2020). Postural stability and cognitive performance of subjects with Parkinson's disease during a dual-task in an upright stance. *Front. Psychol.* 11:1256. doi: 10.3389/fpsyg.2020.01256

Morris, S., Morris, M. E., and Iansek, R. (2001). Reliability of measurements obtained with the Timed "Up & Go" test in people with Parkinson disease. *Phys. Ther.* 81, 810–818. doi: 10.1093/ptj/81.2.810

Nasreddine, Z. S., Phillips, N. A., Bedirian, V., Charbonneau, S., Whitehead, V., Collin, placeI., et al. (2005). The placeCitymontreal cognitive assessment, MoCA: a brief screening tool for mild cognitive impairment. *J. Am. Geriatr. Soc.* 53, 695–699. doi: 10.1111/j.1532-5415.2005.53221.x

Nucci, M., Mapelli, D., and Mondini, S. (2012). Cognitive Reserve Index questionnaire (CRIq): a new instrument for measuring cognitive reserve. *Aging Clin. Exp. Res.* 24, 218–226.

Numata, T., Kiguchi, M., and Sato, H. (2019). Multiple-Time-Scale analysis of attention as revealed by EEG, NIRS, and pupil diameter signals during a free recall task: a multimodal measurement approach. *Front. Neurosci.* 13:1307. doi: 10.3389/fnins.2019.01307

Paredes-Rodriguez, E., Vegas-Suarez, S., Morera-Herreras, T., De Deurwaerdere, P., and Miguelez, C. (2020). The noradrenergic system in Parkinson's Disease. *Front. Pharmacol.* 11:435. doi: 10.3389/fphar.2020.00435

Pomplun, M., and Sunkara, S. (2003). "Pupil dilation as an indicator of cognitive workload in human-computer interaction," in *Proceedings of the International Conference on HCI*, (CityBoston, StateMA: PlaceTypeplaceUniversity of PlaceNameMassachusetts).

Ranchet, M., Hoang, placeI., Cheminon, M., Derollepot, R., Devos, H., Perrey, S., et al. (2020). Changes in prefrontal cortical activity during walking and cognitive functions among patients With Parkinson's Disease. *Front. Neurol.* 11:601686. doi: 10.3389/fneur.2020.601686

Sara, S. J. (2009). The locus coeruleus and noradrenergic modulation of cognition. *Nat. Rev. Neurosci.* 10:211. doi: 10.1038/nrn2573

Sirois, S., and Brisson, J. (2014). Pupillometry. *Wiley Interdisciplinary Rev. Cogn. Sci.* 5, 679–692. doi: 10.1002/wcs.1323

Stacy, M., Bowron, A., Guttman, M., Hauser, R., Hughes, K., Larsen, J. P., et al. (2005). Identification of motor and nonmotor wearing-off in Parkinson's disease: comparison of a patient questionnaire versus a clinician assessment. *Mov. Dis.* 20, 726–733. doi: 10.1002/mds.20383

Steinhauer, S. R., and Hakerem, G. (1992). The pupillary response in cognitive psychophysiology and schizophrenia a. *Annals N Y Acad. Sci.* 658, 182–204. doi: 10.1111/j.1749-6632.1992.tb22845.x

Strouwen, C., Molenaar, E. A., Keus, S. H., Münks, L., Heremans, E., Vandenberghe, W., et al. (2016). Are factors related to dual-task performance in people with Parkinson's disease dependent on the type of dual task? *Parkinsonism Related Disorders* 23, 23–30. doi: 10.1016/j.parkreldis.2015.11.020

Tagliabue, M., Ferrigno, G., and Horak, F. (2009). Effects of Parkinson's disease on proprioceptive control of posture and reaching while standing. *Neuroscience* 158, 1206–1214. doi: 10.1016/j.neuroscience.2008.12.007

Vance, R. C., Healy, D. G., Galvin, R., and French, H. P. (2015). Dual tasking with the timed "up & go" test improves detection of risk of falls in people with Parkinson disease. *Phys. Ther.* 95, 95–102. doi: 10.2522/ptj.20130386

Varazzani, C., San-Galli, A., Gilardeau, S., and Bouret, S. (2015). Noradrenaline and dopamine neurons in the reward/effort trade-off: a direct electrophysiological comparison in behaving monkeys. *J. Neurosci.* 35, 7866–7877. doi: 10.1523/jneurosci.0454-15.2015

Verghese, J., Wang, C., Ayers, E., Izzetoglu, M., and Holtzer, R. (2017). Brain activation in high-functioning older adults and falls: prospective cohort study. *Neurology* 88, 191–197. doi: 10.1212/wnl.0000000000003421

Visser, M., Marinus, J., Stiggelbout, A. M., and Van Hilten, J. J. (2004). Assessment of autonomic dysfunction in Parkinson's disease: the SCOPA-AUT. *Mov. Disorders* 19, 1306–1312. doi: 10.1002/mds.20153

Wu, T., Hallett, M., and Chan, P. (2015). Motor automaticity in Parkinson's disease. *Neurobiol. Disease* 82, 226–234. doi: 10.1016/j.nbd.2015.06.014

Conflict of Interest: MK holds a fellowship through NIH T32 Harvard Translational Research in Aging Training Program. KL reports consultancies with Abbott and Acorda. RP reports consultancies with Abbott, AbbVie, ACADIA, Acorda, Adamas, Amneal, CalaHealth, Global Kinetics, Impel Neuropharma, Kyowa, Lundbeck, Mitsubishi, Neurocrine, Orbis Bioscience, PhotoPharmics, Prilenia, Sunovion, Teva Neuroscience, US World Meds and research support from Abbott, AbbVie, Addex, Biogen, Biohaven, Boston Scientific, EIP, Global Kinetics, Impax, Lilly, Neuroderm, Neuraly, Parkinson's Foundation, Pharma 2B, Prelinia, Roche, SIS, Sun Pharma, Sunovion, Theranexus, Theravance, US WorldMeds, and Voyager/Neurocrine. AA has received honoraria for being a member of the National Advisory Board for the NIH National Center for Medical Rehabilitation Research and has royalties from a scientific invention with license held by the University of Kansas Medical Center. HD holds research grants from National Institute for Aging, Parkinson's Foundation, National Multiple Sclerosis Society, Georgia CTSA, and royalties for the sale of the Portable Driving Simulator.

The remaining author declares that the research was conducted in the absence of any commercial or financial relationships that could be construed as a potential conflict of interest.

frontiers in Bioengineering and Biotechnology

ORIGINAL RESEARCH
published: 03 May 2021
doi: 10.3389/fbioe.2021.634327

Biomechanical-Based Protocol for *in vitro* Study of Cartilage Response to Cyclic Loading: A Proof-of-Concept in Knee Osteoarthritis

Paolo Caravaggi[1], Elisa Assirelli[2], Andrea Ensini[3], Maurizio Ortolani[1], Erminia Mariani[2,4], Alberto Leardini[1], Simona Neri[2] and Claudio Belvedere[1]*

[1] Movement Analysis Laboratory, Istituto di Ricovero e Cura a Carattere Scientifico (IRCCS) Istituto Ortopedico Rizzoli, Bologna, Italy, [2] Laboratory of Immunorheumatology and Tissue Regeneration, Istituto di Ricovero e Cura a Carattere Scientifico (IRCCS) Istituto Ortopedico Rizzoli, Bologna, Italy, [3] I Orthopaedic and Traumatologic Clinic, Istituto di Ricovero e Cura a Carattere Scientifico (IRCCS) Istituto Ortopedico Rizzoli, Bologna, Italy, [4] Department of Medical and Surgical Sciences, Alma Mater Studiorum-Università di Bologna, Bologna, Italy

OPEN ACCESS

Edited by:
Simone Tassani, Pompeu Fabra University, Spain

Reviewed by:
Matteo Berni, Rizzoli Orthopedic Institute (IRCCS), Italy
Himadri Shikhar Gupta, Queen Mary University of London, United Kingdom

***Correspondence:**
Simona Neri
simona.neri@ior.it

Specialty section:
This article was submitted to Biomechanics, a section of the journal Frontiers in Bioengineering and Biotechnology

Received: *27 November 2020*
Accepted: *08 April 2021*
Published: *03 May 2021*

Citation:
Caravaggi P, Assirelli E, Ensini A, Ortolani M, Mariani E, Leardini A, Neri S and Belvedere C (2021) Biomechanical-Based Protocol for in vitro Study of Cartilage Response to Cyclic Loading: A Proof-of-Concept in Knee Osteoarthritis. Front. Bioeng. Biotechnol. 9:634327. doi: 10.3389/fbioe.2021.634327

Osteoarthritis (OA) is an evolving disease and a major cause of pain and impaired mobility. A deeper understanding of cartilage metabolism in response to loading is critical to achieve greater insight into OA mechanisms. While physiological joint loading helps maintain cartilage integrity, reduced or excessive loading have catabolic effects. The main scope of this study is to present an original methodology potentially capable to elucidate the effect of cyclic joint loading on cartilage metabolism, to identify mechanisms involved in preventing or slowing down OA progression, and to provide preliminary data on its application. In the proposed protocol, the combination of biomechanical data and medical imaging are integrated with molecular information about chondrocyte mechanotransduction and tissue homeostasis. The protocol appears to be flexible and suitable to analyze human OA knee cartilage explants, with different degrees of degeneration, undergoing *ex vivo* realistic cyclic joint loading estimated via gait analysis in patients simulating mild activities of daily living. The modulation of molecules involved in cartilage homeostasis, mechanotransduction, inflammation, pain and wound healing can be analyzed in chondrocytes and culture supernatants. A thorough analysis performed with the proposed methodology, combining *in vivo* functional biomechanical evaluations with *ex vivo* molecular assessments is expected to provide new insights on the beneficial effects of physiological loading and contribute to the design and optimization of non-pharmacological treatments limiting OA progression.

Keywords: osteoarthritis, knee cartilage, chondrocyte mechanotransduction, knee biomechanics, knee loading

INTRODUCTION

Osteoarthritis (OA) is considered the sixth-leading cause of disability in the world (Kloppenburg and Berenbaum, 2020). It is an evolving disease and a major cause of impaired mobility leading to an important reduction of the quality of life and increased costs on healthcare systems (World Health Organization, 2003; Piscitelli et al., 2012). Since OA is non-reversible, its prevalence

increases significantly with age, although with differences between genders. In particular, worldwide estimates report that 9.6% of male and 18% of females aged above 60 years show symptomatic OA (Woolf and Pfleger, 2003; World Health Organization, 2003). Weight-bearing joints, such as the hip and knee, are the most affected anatomical structures. In particular, knee OA was ranked the 11th highest contributor to global disability showing a global age-standardized prevalence of 3.8% (Cross et al., 2014). While walking and exercise therapy are considered effective for pain relief (Huang et al., 2003; Beckwee et al., 2013; Juhl et al., 2014; Fransen et al., 2015) and are generally recommended (Fernandes et al., 2013; Bruyere et al., 2014; McAlindon et al., 2014; Nelson et al., 2014), most patients suffering from severe OA will eventually need surgical treatments. Though partial- or total-joint-replacement become necessary for pain relief and for restoring the original joint function, they involve complex invasive surgical procedures with high social costs. As far as the knee, its complex joint mechanics makes the outcome of surgical procedures not always fully satisfying, as a number of patient-specific anatomical and kinematic factors can affect duration of the implant (Ensini et al., 2012), which may require revision surgery over time. In the European Union, OA has been reported to be the main cause for surgical intervention (Merx et al., 2003).

In this context, a deeper understanding of the joint cartilage wear patterns is of paramount importance to achieve greater insight into the main causes of knee OA (Andriacchi et al., 2004). The knee has a rather complex movement with respect to the simple ball-and-socket hip joint. The lateral femoral condyle presents a pronounced posterior translation during knee flexion, which is consistent with the simultaneous internal tibial rotation; this has been referred to as a medial-pivoting motion (Asano et al., 2001). This combination of rolling and sliding motion is unique in the human body and, combined to the large loads acting on the knee in some of the daily living activities (Kutzner et al., 2010; Qi et al., 2013), can result in permanent damages to OA-prone knee cartilage. The analysis of the main biomechanical factors affecting knee cartilage loading and biological response is critical to identify effective conservative treatments capable to delay OA progression and related surgeries. Among the most important factors affecting knee OA are the severity of the degenerative changes due to biomechanical factors, such as the lower limb mechanical axis and abnormal knee joint kinematics (Moschella et al., 2006). In this perspective, a thorough *in vivo* biomechanical analysis to estimate the knee internal joint forces and contact areas during locomotion is essential to fully understand knee functioning (Hinterwimmer et al., 2005; Berti et al., 2006; Edwards et al., 2008; Morimoto et al., 2009; Hosseini et al., 2010; Scheys et al., 2013; Battaglia et al., 2014). This has been conducted mostly *in vivo* using gait analysis, though mainly for hip and knee joint replacements (Belvedere et al., 2014). The still-unclear association between molecular cartilage homeostasis and effects of cycling joint loading during motor activities requires further investigation to achieve better understanding of OA pathomechanics. Filling this gap becomes essential for efficient OA management. In order to counteract the irreversibility of OA, a reasonable medical approach may be focused on the prevention of this disease or, at least, on slowing down its progression.

By the biological point of view, accumulating literature evidence points to the ambivalent effect of joint loading on cartilage: physiologic loading promotes cartilage anabolism whereas reduced or excessive loading stimulate tissue catabolism (Leong et al., 2011; Sun et al., 2011). Duration, frequency and magnitude of the load applied to the articular cartilage are critical for tissue homeostasis and can stimulate matrix-protein remodeling and biosynthesis, improve mechanical properties and sustain chondrocyte differentiation (Sun, 2010). The underlying mechanisms are only partially elucidated, mostly on *in vitro* or animal models, whereas, to our knowledge, few studies exist on *ex vivo* dynamic stimulation of human cartilage tissue (Huang et al., 2007; Bougault et al., 2008; Haudenschild et al., 2010; Ramachandran et al., 2011; Jeon et al., 2012; Kawakita et al., 2012; Griebel et al., 2013; Bougault et al., 2014). A variety of cellular structures and cell surface molecules including integrins, cell adhesion receptors, and ion channels have been implicated in mechanotransduction in cartilage (O'Conor et al., 2014). Moreover, cartilage extracellular matrix components and matrix enzymes play a pivotal role in cartilage response to mechanotransduction. In a recent study we demonstrated that compression of OA human cartilage modulates the inflammatory milieu by differently affecting the expression of components and homeostasis regulators of cartilage extracellular matrix (Dolzani et al., 2019). Future challenges include better characterization of the signaling and transcriptional pathways involved and identification of the molecular mechanisms that differentiate degenerative responses from protective and beneficial effects of exercise treatments (demonstrated by clinical evidence) (Abramoff and Caldera, 2020).

The main scope of this study is to offer an original investigation methodology in mechanotransduction for the *in vitro* testing of human explanted knee cartilage tissue based on physiological biomechanical data, and according to cartilage scoring. A feasibility proof of the proposed methodological protocol has been here originally performed as concerning the extraction of molecular information about chondrocyte mechanotransduction and tissue homeostasis by high throughput gene expression analysis.

PROPOSED INVESTIGATION PROTOCOL

The main activities of the proposed investigation protocol on mechanotransduction for *in vitro* testing of human explanted knee cartilage are summed up in **Figure 1**.

In the first phase (P1), a biomechanical analysis is performed on a defined number of subjects (P1-1), healthy or suffering from knee OA, depending on the project plan. Biomechanical data recruitment is essential to estimate the magnitude and direction of physiological joint loading, during the execution of motor tasks of daily living, using a combination of kinematic analysis via stereo-photogrammetry, and detailed kinetic analysis of the ground reaction force via force and pressure plates (P1-2). Lower limb kinematic data and measured external forces during

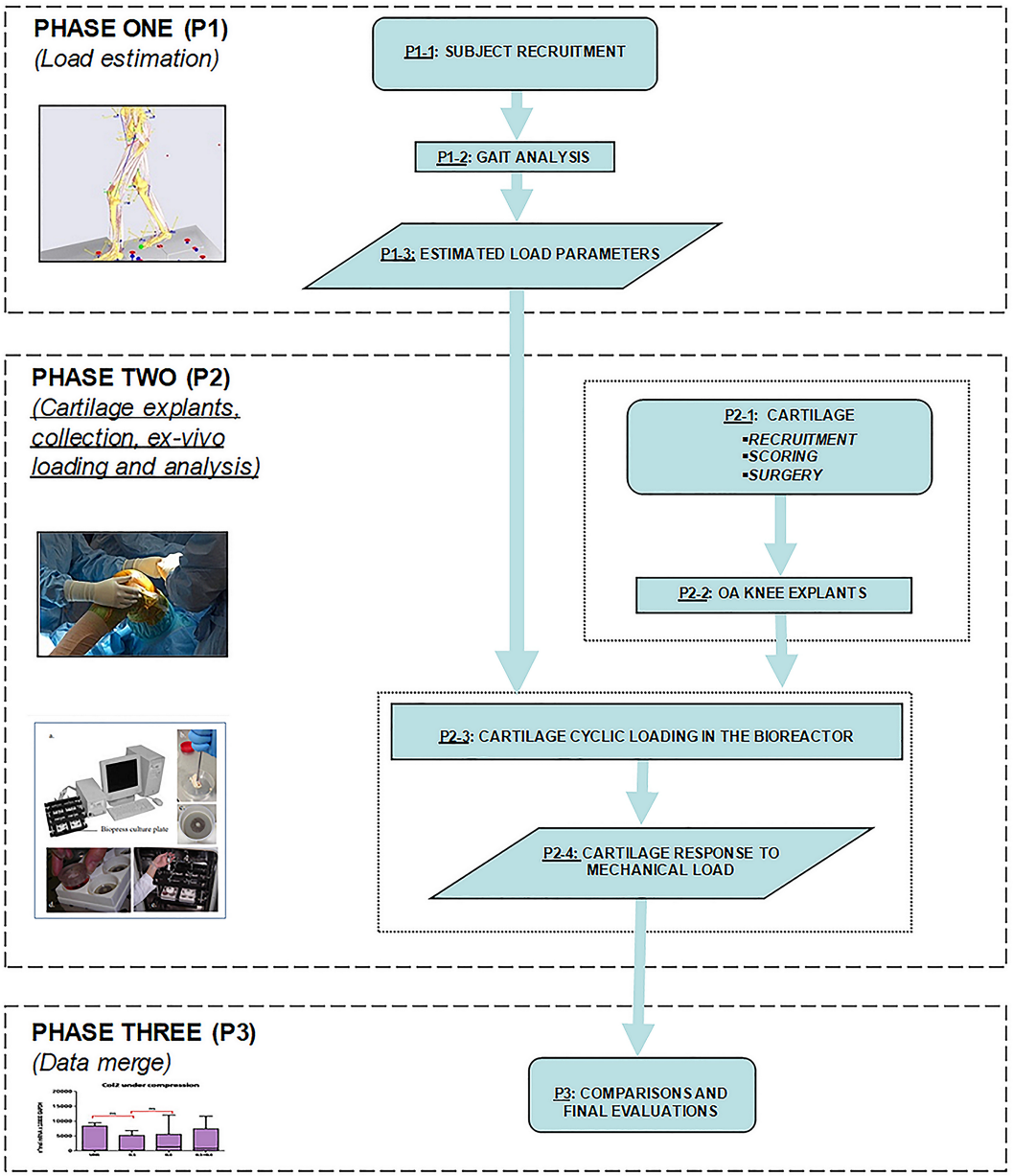

FIGURE 1 | Proposed Investigation Workflow reporting the sequence of all phases.

mild motor activities or exercises can be applied to a model of the knee joint to estimate the internal forces and moments (P1-3). In this phase, the investigator can take advantage of several supporting data reported in the relevant literature and briefly summed up here below. Kinematic and kinetic data are intended to set up an effective and realistic loading regime to be applied *ex vivo* to cartilage explants. In particular, the estimated axial component of the internal loading on the distal femur are converted into the corresponding compression values to be applied *ex vivo*, in order to obtain a more precise simulation of the mechanical stimulation experienced by the knee articular cartilage *in vivo*. In accordance with the biomechanical analysis, different loading regimes can be applied to the cartilage samples.

In the second phase (P2) cartilage (P2-1) is recruited after appropriate macroscopic scoring, possibly including also inspections based on MRI. In detail, OA cartilage samples can be obtained from OA patients undergoing knee surgery, such as total knee replacement. Collection of healthy cartilage is a demanding task, due to possible ethical and regulatory issues specific for each single country. For example, cartilage samples can be obtained from oncological patients subjected to surgical removal at the knee level, under appropriate inclusion and exclusion criteria. Image-based inspection is

helpful to characterize the areas of the knee with different cartilage alteration. The latter can be performed via routine MRI-based protocol with additional sagittal T1rho and T2 sequences and mapping. MRI images from all examinations must be reviewed by expert musculoskeletal radiologists to determine the presence, the extent, and the features of cartilage lesions on the femoral articular surfaces. To further enhance the precise identification of the area of cartilage explantation, and for geometric characterization of the whole articular cartilage under testing, the surgeon can take advantage of state-of-the-art systems for computer-aided knee-based surgery (Belvedere et al., 2014). Moreover, cartilage degeneration is visually inspected by the surgeon, attributing a macroscopic score that will be subsequently confirmed by microscopic scoring through histological evaluation. The biological assessment of the explants is always performed in P2. Cylinders of cartilage are cut with a coring tool from the femoral condyles, and then grouped according to both the original anatomical location, and to the degree of cartilage degeneration (based on MRI and/or macroscopic scores). The cartilage samples are then exposed to *ex vivo* cyclic loading in a bioreactor (P2-3), in agreement with the estimated *in vivo* knee joint loads. Subsequently, the corresponding cartilage response to the mechanical load is evaluated (P2-4) in terms of modulation of cartilage homeostasis marker expression. Cartilage samples and culture supernatants are recovered for downstream analyses, including morphological analyses on explants (histology, immunohistochemistry), molecular analyses on explants (RNA extraction followed by gene expression analysis) or on supernatants (protein expression analysis). Data obtained from compressed samples are compared to the same paired samples (same topographical areas and same score) maintained in unloaded conditions.

In the last phase (P3), all obtained data are meant to be merged for overall comparison and final evaluations.

MATERIALS AND METHODS

In the following sections we are reporting the assumptions made for the application of the different steps of the proposed protocol. A pilot application to test the feasibility of high throughput gene expression analysis is also presented.

Estimation of Knee Joint Loading (Phase P1)

Knowledge of the forces and moments acting at the knee during common motor activities, along with information about the tibio-femoral contact areas, are essential to identify reference input data (e.g., pressure, axial load, load frequency) to perform corresponding knee cartilage stress analysis using *ad-hoc* devices such as a bioreactor.

Measuring physiological knee joint loading *in vivo* is complex, and most of the data reported in the literature are based on musculoskeletal (McLean et al., 2003; Fregly et al., 2012) or EMG-driven modeling approaches (Buchanan et al., 2004). Two studies by some of the authors of the present study (D'Angeli et al., 2014) were aimed at contributing to this knowledge using an original non-invasive methodology. Gait analysis and 3D anatomical-based data were recorded in 20 healthy young volunteers and used to estimate the moments about the femoral and the tibial shaft during common motor activities (e.g., level walking, squatting, stair ascending/descending). While an instrumented knee prosthesis has also been proposed for direct measurement of internal knee forces (D'Lima et al., 2006), the largest collection of knee joint loading data is from the open OrthoLoad database (Julius Wolff Institute and Charité – Universitätsmedizin Berlin, 2020). An instrumented knee prosthesis with telemetric data transmission allowed to measure axial (compression), medio-lateral and antero-posterior (shear) forces between femoral and tibial components in several patients and for several activities of daily living (Heinlein et al., 2009). The combination of knee loading data and knee joint contact areas allows to estimate the pressure exerted at the tibio-femoral joint. As far as the latter, **Table 1** is reporting a critical review of the relevant literature by taking into account only those studies reporting information on the methodological approach, sample size, tibio-femoral joint flexion angle and loading conditions, and differentiation between medial and lateral knee compartments. Studies differ in terms of axial loading applied to the knee, knee flexion angle, instruments for force estimation, and *in vivo* or *in vitro* approach. The reported average knee medial compartment contact area ranges from 235 to 670 mm^2 across all studies. Liu et al. (2010) reported the most complete dataset measured *in vivo* using 3D video-fluoroscopy and MRI in 8 subjects (age 32–49 years; average BMI 23.5 kg/m^2), including medial compartment contact area at five gait time-points.

While standard gait-analysis instrumentation does not allow to measure *in vivo* joint loading, this has been found to be significantly correlated to the knee external adduction moment (Kutzner et al., 2013), which is commonly measured via force plate measurements and knee kinematics. A linear relationship between the medial tibio-femoral contact force (Fmed) and the External Knee Adduction Moment (EAM) during stance phase duration has been inferred using data from 9 subjects (age 70 ± 5 years; BMI = 30.6 ± 4.6 kg/m^2) (Kutzner et al., 2013):

$$Fmed = 100 + 26 * EAM$$

where Fmed is reported in % of Body Weight (%BW), and EAM in % of BW*height.

This relationship (R^2 = 0.56 and RMS error = 0.28*BW, in Kutzner et al., 2013) has been used here to estimate the average knee loading (**Figure 2A**) in an exemplary patient (M; age 52 years; weight 73 kg; height 1.73 m; Body Mass Index 24.4) suffering from knee OA. Average tibio-femoral joint flexion angles and adduction/abduction moments were obtained from 5 walking trials recorded during comfortable walking-speed at 100 Hz (**Figures 2A,C**). Data were obtained using a validated lower limb skin-marker based kinematic protocol (Leardini et al., 2007) and angles calculated according to the joint coordinate system (Grood and Suntay, 1983; Cappozzo et al., 1995), as recommended by the International Society of Biomechanics. By assuming the knee contact area to vary continuously and

TABLE 1 | Knee joint contact areas as from a critical literature review.

Studies	Technique	Sample size	External load (N) applied	Knee flexion angle (°)	Contact area (mm^2)	
					Medial compartment	Lateral compartment
Fukubayashi and Kurosawa (1980)	*In vitro*, sensor sheets	7	500	0	240	160
Henderson et al. (2011)	*In vivo*, MRI	1	365	Full extension in weight bearing	511 ± 143.1	256 ± 40.3
Hinterwimmer et al. (2005)	*In vivo*, MRI	12	0	0	487 ± 103	220 ± 72
				30	404 ± 98	299 ± 58
				90	302 ± 79	255 ± 51
Hosseini et al. (2010)	*In vivo*, MRI combined with video-fluoroscopy analysis during single-leg upright standing for 300 s	6	Full body weight	Full extension in weight bearing	From 47.0 ± 21.2 (at 0 s) to 263.2 ± 19.6 (at 300 s)	From 20.3 ± 20.0 (at 0 s) to 135.6 ± 20.8 (at 300 s)
Kettelkamp and Jacobs	*In vitro*, roentgenography	14	23–79	0–35	480	300
Liu et al. (2010)	*In vivo*, MRI combined with gait and 3D video-fluoroscopy analysis during a standard gait cycle	8	Not reported	Heel strike	235 ± 11	200 ± 84
				30%	467 ± 61	411 ± 159
				50%	354 ± 97	329 ± 97
				80%	428 ± 87	451 ± 109
				Toe-off	260 ± 140	331 ± 167
Morimoto et al. (2009)	*In vitro*, axial testing machine and pressure-sensitive film	22	1,000	0	578.3 ± 177.0 (3.6 ± 0.4)[#]	443.1 ± 121.0 (3.9 ± 0.5)[#]
				15	488.5 ± 140.4 (3.5 ± 0.3)[#]	495.3 ± 146.4 (3.6 ± 0.4)[#]
				30	449.9 ± 151.4 (3.4 ± 0.3)[#]	507.0 ± 189.2 (3.7 ± 0.4)[#]
				65	468.4 ± 143.1 (3.7 ± 0.5)[#]	507.8 ± 152.6 (3.6 ± 0.6)[#]
Patel et al. (2004)	*In vivo*, MRI	10	133	60	374	276
Périé and Hobatho (1998)	*In vivo*, MRI and FEM	1	0	Full extension	293 ± 72	111 ± 57
Yao et al. (2008)	*In vitro*, MRI	10	0	−4	670 ± 140*	600 ± 80*
				134	560 ± 110*	375 ± 75*

**Average data including contact with the meniscus.*
[#]In brackets corresponding measured mean pressure data in MP.

smoothly over stance duration—which is acceptable for most time-dependent biomechanical and biological variables—the mean temporal profile of the knee contact area was approximated by a cubic spline interpolating the five contact-area points (**Figure 2B**) reported in Liu et al. (2010). Pressure at the knee medial compartment (**Figure 2C**) was estimated by dividing the knee contact force (**Figure 2A**) by the contact area (**Figure 2B**) across normalized stance-phase duration.

Cartilage Explants Collection, *ex vivo* Loading and Analysis (Phase P2 and P3)

Sample Recruitment

In order to test the protocol, 9 mono-compartmental knee OA cases (2 F, 7 M; age ± SD: 69.6 ± 8.7 years; mean BMI ± SD: 28.0 ± 4.2 kg/m^2) were recruited. Out of these, 6 cases (2 F, 4 M; age ± SD: 69.6 ± 9.8 were used to check for macroscopic scoring reliability and 3 cases (3 M; age ± SD: 74.3 ± 6.0 years; BMI: 24.2; 26.6; and 32 kg/m^2, respectively) were used to test the feasibility of high throughput gene expression analysis. The study was carried out in compliance with the Helsinki declaration, and approved by the local Ethic Committee (CE-AVEC Prot. Kneeload N. EM603-2018_89/2015/Sper/IOR_EM1), including documentation of written patient consent. Medial and lateral femoral condyles were collected at time of knee replacement surgery. For each knee condylar explant (medial and lateral) four topographical areas (corresponding to the original anatomical location and, therefore, exposed to different *in vivo* loading

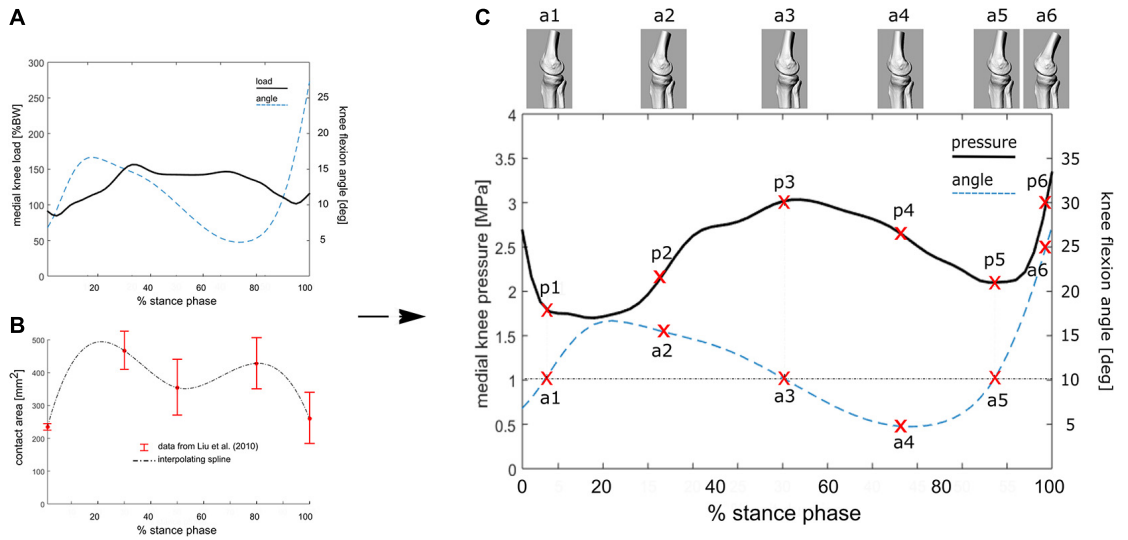

FIGURE 2 | (A) Knee flexion angle and the estimated internal tibio-femoral joint forces during stance phase of walking using the linear relationship between EAM and knee forces reported in the equation. EAM and knee kinematics were calculated as the average across five walking trials for a subject with knee OA. **(B)** Interpolated temporal profile of cartilage contact area over stance phase duration, using data from Liu et al. (2010). **(C)** Estimated temporal profile of tibio-femoral contact pressure over stance phase of walking for the knee OA patient; the curve is obtained by dividing the contact force **(A)** by the contact area **(B)**. 3D representations of the tibio-femoral joint angle (a1–a6) at different time frames are shown. The knee is flexed 10° at three times of the of the stance phase, while the relevant cartilage region is subjected to pressure p1, p3 and p5.

conditions) were identified: medial anterior, medial posterior, lateral anterior and lateral posterior (**Figure 3A**). Cartilage samples from six out of the nine recruited donors were processed for histology, while the samples from the remaining three donors were cored after subchondral bone removal. Obtained fresh cartilage cylinders were cultured overnight and then exposed to *ex vivo* controlled compression (**Supplementary Tables 1, 2**).

Macro- and Microscopic Cartilage Scoring

The surgeon in charge for total knee replacement attributed macroscopic scoring to the cartilage areas according to the Collins grading system of disease severity (from 0 to 4, with 0 corresponding to apparently normal cartilage, and 4 corresponding to completely degenerated tissue) (Pritzker et al., 2006). Each of the four condylar topographical areas (lateral anterior, lateral posterior, medial anterior and medial posterior) can be homogeneous, or further zoned in sub-areas, according to the macroscopic score (**Figure 3A**). Samples of full thickness cartilage were freshly recovered from all identified sub-areas and scored after conventional Safranin O-staining. Briefly, 5 μm thick sections of FFPE samples were rehydrated and stained with Haematoxylin/Eosin, 0.1% Safranin-O and 0.02% Fast Green (SIGMA-ALDRICH, Munich, Germany). Three representative slices from each sub-area (homogeneous for macroscopic score and anatomical position) were independently analyzed by two experienced biologists for histopathology grading score attribution following the OARSI criteria (from grade 0, corresponding to intact cartilage, to grade 6, corresponding to complete cartilage degradation and bone deformation). The mean of three different positions for each sub-area was recorded (Pritzker et al., 2006; **Figure 3B**). Evaluations were performed with an Eclipse 90i microscope and NIS elements software (NIKON CORPORATION, Tokyo, Japan).

Pearson's correlation was used to compare macroscopic and microscopic scores from 22 samples (areas with homogeneous macroscopic score obtained from 6 donors). The macroscopic score provided by the surgeon was compared to the microscopic mean score of three representative slices for each of the 22 areas (**Supplementary Table 1**).

Controlled Cartilage Compression

Within phase P2 the knee loading parameters estimated in Phase P1 are applied to fresh cartilage samples. To evaluate the effect of mechanical compression on articular OA cartilage in relationship to the level of cartilage degeneration, samples from different topographical areas and with different macroscopic score are separately recovered, then cylinders of 2.5 mm diameter cartilage tissue are cored with a biopsy needle. Cartilage explants in D-MEM medium (SIGMA, Sigma Aldrich, St. Louis, United States) are serum starved for 24 h, then exposed to unconfined controlled compression in a computer-regulated bioreactor (FlexCell FX-4000C, Flexcell International Corporation, United States). The system allows for control of duration, frequency and intensity of the applied load in order to simulate different motor tasks and to span physiologic and extra-physiologic stimulations. Compression regimes are performed in an incubator under controlled temperature (37°C) and CO_2 level (5%). The assembly of the compression unit and sample accommodation in the compression well has been described elsewhere (Dolzani et al., 2019). Multiple loading positions in compressed plates allow for simultaneous compression of paired samples in basal or stimulated conditions (such as in the presence of pro- or anti-inflammatory mediators

like IL-1β and IL-4, respectively) (Dolzani et al., 2019). After compression, fresh tissue samples can be dedicated to histological, immunohistochemical and/or molecular analyses that can be performed individually or in parallel, the only limit being the available tissue.

As exemplary application of the above-described protocol, here we run a compression experiment on three knee OA cases using the estimated knee loading parameters during normal walking (1 Hz loading sinusoid). Fresh cartilage samples were cored and cartilage cylinders with homogeneous macroscopic degeneration score (0–1) were serum starved overnight in the incubator, then exposed to loading. Compression was implemented by setting the flexcell apparatus with a force sinusoid—1 Hz frequency—for 45 min, applied to the superior surface of a single cartilage cylinder per well, vertically arranged as to reproduce the cyclic pressure established in the biomechanical evaluation (3 MPa). Paired uncompressed samples were used as controls.

Array-Based Gene Expression Analysis

Molecular analyses were performed on total RNA by array-based gene expression analysis to provide proof of concept of applicability of this kind of high throughput analysis to these challenging samples. We performed a pilot experiment on cartilage cylinders from three donors. Cartilage explants from areas with macroscopic score corresponding to 0–1 were used. Cartilage explants are cylinders of 2.5 mm diameter and variable height (ranging from 1 to 3–4 mm) and weight (ranging from about 20 to about 40 mg) depending on tissue zonal thickness and degeneration. Two uncompressed/unstimulated samples were run in duplicate to test for assay reproducibility, while two samples were also analyzed after compression and in absence or presence of IL1-β stimulation (2 ng/ml). Cartilage areas and donors used for these analyses are specified in **Supplementary Table 2**.

Fresh explants were immediately recovered and liquid nitrogen frozen, then pulverized using the Mikro-Dismembrator S grinding mill (Sartorius Stedim Italy SpA, Italy) in 5 ml PFTE shaking flasks with a stainless-steel grinding ball (2,000 rpm, 45″). Total cellular RNA was purified from pulverized explants with Trizol isolation reagent (Thermo Scientific, Germany) and spectrophotometric quantification was performed (mean recovery 2.5 μg, range 0.8–5.4 μg). Total RNA was treated with the RNase-Free DNase Set (Qiagen, Germany), cleaned-up in RNeasy mini columns (Qiagen) following manufacturer's instructions to deplete contaminating DNA and reverse transcribed by the RT2 First strand kit (Qiagen). The expression of a focused panel of 84 genes involved in wound healing together with five housekeeping genes (actin beta-ACTB; Beta-2-microglobulin-B2M; Glyceraldehyde-3-phosphate dehydrogenase-GAPDH; Hypoxanthine phosphoribosyltransferase 1-HPRT1; Ribosomal protein large P0-RPLP0) was evaluated by the RT2 Profiler PCR Array PAHS-121Z (Qiagen) in a Rotor-gene 6000 real-time analyzer (Corbett, Concorde, NSW, Australia), following manufacturer's instructions. The system includes genomic DNA control, reverse transcription control and positive and negative controls.

The threshold cycle (Ct) values for all the genes were calculated by the software of the real time PCR instrumentation and considered as a negative call when ≥35 or not detected. To compare Ct values across different runs, a single baseline within the exponential growth phase of the reaction curves was manually set. Relative gene expressions were calculated by the $\Delta\Delta$Ct method relative to the housekeeping genes showing Ct value consistency (ACTB; B2M; GAPDH; RPLP0). Differences between groups were analyzed by the Web-based PCR Array Data Analysis Software (SABiosciences™, Frederick, MD) available at https://dataanalysis.qiagen.com/pcr/arrayanalysis.php. Variations in gene expression in uncompressed vs. compressed samples were calculated by the $\Delta\Delta$Ct method, in which ΔCt is the difference between the gene of interest (GOI) Ct and the average of housekeeping gene (HKG) Ct. Fold-Change ($2^{-\Delta\Delta Ct}$) is the ratio between the normalized gene expression ($2^{-\Delta Ct}$) in the compressed sample and the normalized gene expression ($2^{-\Delta Ct}$) in the uncompressed sample. A twofold change threshold for up- and down-regulation was considered. Genes were excluded from the fold change analysis if more than two conditions gave negative results.

RESULTS

Estimated Knee Loading Conditions

The calculated EAM and knee flexion-extension angle for the knee OA patient analyzed here are generally consistent with physiological kinematic and kinetic data during walking. The knee shows a peak of flexion at heel strike, followed by continuous extension up to about 80% of stance, and flexion again prior to toe-off (**Figure 2A**). The shape of the interpolated temporal profile of cartilage contact area (**Figure 2B**) is consistent with that of the vertical ground reaction forces in walking, with two peaks at around 20 and 80% of the stance phase duration. These are also rather consistent with the estimated knee contact force shown in **Figure 2A**. **Figure 2C** is reporting the estimated pressure (MPa) at the knee medial compartment for the knee OA patient recruited in this study during gait. The pressure waveform varies between 1.5 and about 3.5 MPa over stance duration, showing two minima at around 20 and 80% of stance which is consistent with the larger contact area at these two time frames (**Figure 2B**). However, due to the knee flexion/extension motion in gait, a different joint cartilage region is subjected to a specific pressure at each time frame (**Figure 4**). Anterior and central cartilage regions may undergo multiple contacts during each walking cycle. For example, the anterior-central region of the cartilage compressed when the knee is flexed 10° (**Figure 4**), is subjected to pressure p1, p3 and p5, respectively, during the stance phase (**Figure 2C**). Whereas the cartilage in the posterior region, which is compressed for knee flexion angles larger than 20° (**Figures 2C**, **4**), is loaded just once over stance duration.

The chosen input parameters used here for the bioreactor were those related to the posterior region cartilage region. Due also to the apparatus specifications, a sinusoid with 1 Hz

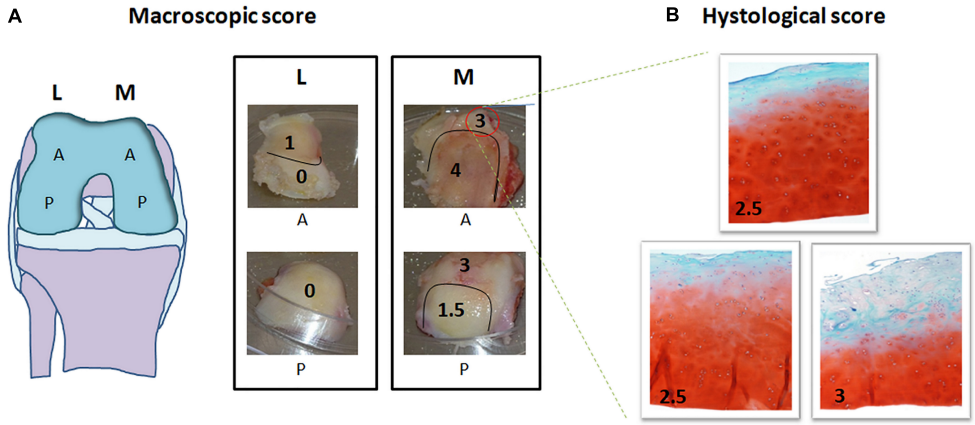

FIGURE 3 | Macroscopic and histological scoring of femoral condyles from a representative mono-compartmental knee OA patient. **(A)** Schematic drawing of the knee and images of the four condyle areas: femoral condyles (medial, M and lateral, L) removed by the surgeon were divided each in anterior (A) and posterior (P). Each of the four areas was scored by the surgeon based on macroscopic degeneration of the cartilage tissue by Collins grading system, thus obtaining further zoning. **(B)** For each zone identified, histological evaluation was performed in triplicate in three subareas. Macroscopic and histological scores attributed are indicated in each picture, histological images being at 10× magnification.

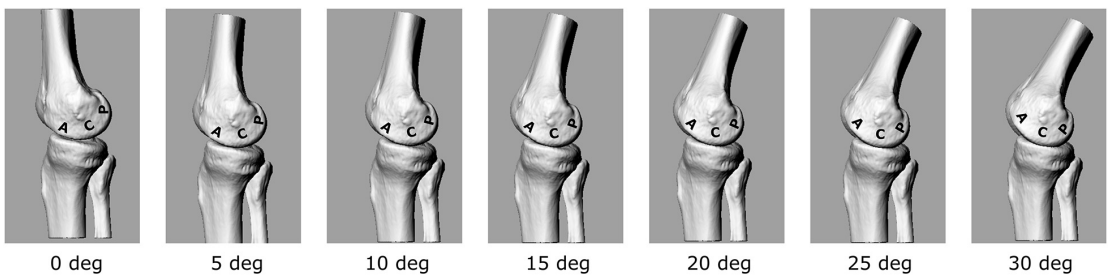

FIGURE 4 | 3D representation of the tibio-femoral joint at different knee flexion angles (0°–30°). A different cartilage region (Posterior, Central, Anterior) is loaded at each flexion angle.

frequency and amplitude of about 3 MPa was chosen to test the cartilage explants.

Correlation Between Macro and Microscopic Scoring

Comparison between macro and microscopic cartilage scoring was performed in samples from 6 donors to check for correlation between macroscopic scoring and actual cartilage degeneration, as assessed by histological evaluation. This provides evidence of correct assignment of samples to different groups. Macro and microscopic scores were compared by Pearson's correlation analysis. Particularly, the correlation between Collins macroscopic score and OARSI histological score was evaluated on 22 different condyle areas from 6 OA donors (see **Supplementary Table 1**). Areas with completely degraded cartilage and subchondral bone exposure were excluded from the analysis due to the absence of cartilage tissue to be used for histology. The two scoring systems showed a high correlation coefficient $R = 0.887$, supporting the reliability and usefulness of the macroscopic score as criterion for cartilage area identification according to degeneration severity (**Figure 5**).

Array-Based Gene Expression Analysis

To assess the feasibility of array-based gene expression approaches on limited amounts of OA cartilage exposed to mechanical compression, two cartilage cylinders per sample (from a single area per sample, macroscopic score = 0–1) were used for RNA extraction and gene expression pattern analysis of 84 human wound healing-related genes by RT-PCR arrays.

We firstly performed the analysis on unstimulated uncompressed samples from 2 OA patients to test the reproducibility of our protocol (**Supplementary Table 2**). Each sample was run in duplicate and the Ct variation coefficient (CV) of each analyzed gene was calculated. The average percentage CV of the two analyzed samples was 0.66 and 0.27%, respectively, indicating a very high reproducibility of our results. All internal quality controls met the requirements. Among the housekeeping genes included in the analysis, beta actin showed the higher stability.

To assess the effect of compression on wound healing-related gene expression we performed the same array-based analysis on 2 patients in basal conditions (uncompressed) and after compression. This was also done in presence of a

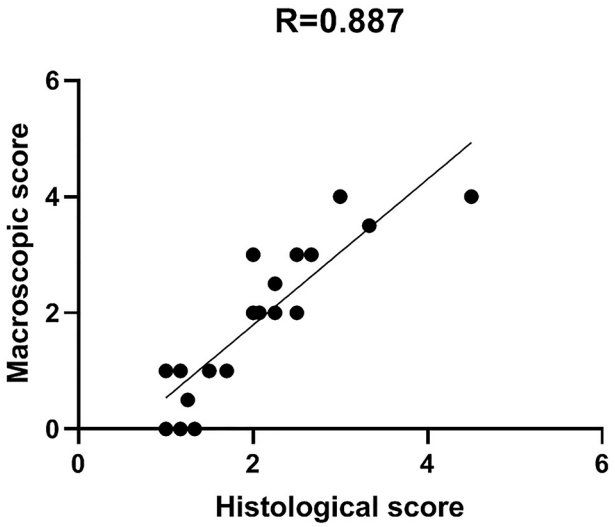

FIGURE 5 | Macro and microscopic cartilage score correlation. Scatter plot representation of the correlation between macroscopic and histological scores for the evaluation of cartilage degeneration. Histological score is the mean of triplicate evaluations from the same area, performed by two independent researchers.

pro-inflammatory stimulus (IL-1β). Sample used for this analysis are shown in **Supplementary Table 2**.

The applied compression regime corresponds to the estimated knee loading parameters during normal walking. Cartilage cylinders exposed to this unconfined compression were significantly deformed at the end of the loading regime (with a final reduction in height of about 60%).

In **Figure 6**, gene expression analysis results are shown. The heatmap (**Figure 6A**) represents relative expression of the 55 expressed genes in the four experimental conditions (NC, C, NC+ IL1-β, C+IL1-β) as referred to the control group (NC) (see **Supplementary Table 3** for detailed fold change values, while raw data are shown in **Supplementary Table 4**). Gene expression levels clearly differ after compression, both in unstimulated and in IL1-β-stimulated condition. Non-supervised hierarchical clustering of the four groups indicates that NC samples are more similar to C+IL1-β samples than the other groups. If considering a threshold fold change of at least 2 for both up and down-regulation, we observed that 89% of the genes were modulated by compression, 61% of them showing upregulation. Among the upregulated genes, Chemokine (C-C motif) ligand 7 (CCL7), CD40 ligand (CD40L), collagen 1 a2 (COL1A2), colony stimulating factor 3 (granulocyte) (CSF3), integrin alpha V (vitronectin receptor, alpha polypeptide, antigen CD51) (ITGAV), Integrin beta 1 (ITGB1), Integrin beta 6 (ITGB6), Mitogen-activated protein kinase 3 (MAPK3) and plasminogen receptor (PLAUR) appeared more than fivefold increased in compressed samples compared to controls. Array-based gene expression analysis is therefore feasible in the presented experimental model, despite the challenging tissue samples to be analyzed.

DISCUSSION

Mechanical stimulation plays a central role in the maintenance of cartilage homeostasis, and it is also involved in the pathogenesis of OA. The complex biological and mechanical scenario characterizing the knee joint homeostasis is generally based on several mechano-transduction mechanisms that elicit neutral, positive or negative biological responses in the subchondral bone and cartilage. Describing these mechanisms is a complex task for the number of biological and kinetic variables affecting this phenomenon. *In vitro* models of knee joint cartilage mechanotransduction are therefore particularly valuable as these allow to control the kinetic input, i.e., loading, and to measure the biological response under the same protocol conditions, and across a large population of homogeneous cartilage samples.

The present study aimed at proposing a novel methodological approach for the analysis of the knee cartilage response subjected to mechanical stimuli simulating common motor tasks of daily living. In particular, the theoretical loading parameters to be used as input for the bioreactor testing device were estimated by integrating the most comprehensive literature data on *in vivo* internal knee loading and cartilage contact area during gait. Gait data acquired in an exemplary patient suffering from knee OA were used to estimate theoretical loading parameters for the bioreactor. The superimposition of the temporal profiles of the *in vivo* knee sagittal-plane motion and cartilage pressure has allowed to reveal some interesting mechanical aspects which characterize the knee joint cartilage during walking. According to the anatomical region of interest, the cartilage appears to be subjected to different loading patterns, either in terms of loading frequency and/or magnitude. The anterior-central region of the cartilage, i.e., the region in contact from 0 to about 20° of knee flexion, is subjected to three pressure values (p1, p3, and p5) over the stance phase of walking. Conversely, the central-posterior region of the femoral cartilage (flexion angles larger than 20°) is subjected to just one pressure value over the stance phase. Therefore, in order to accurately simulate the *in vivo* tibio-femoral cartilage mechanics, it may be plausible to establish different cyclic pressure waveforms, both in terms of amplitude and frequency, according to the anatomical region the cartilage samples were explanted from. The amplitude of the theoretical cyclic pressure waveform would need to be set according to the location of the explants. In line with the kinetics of the exemplary OA patient used here, cartilage pressure ranges approximately between 1.5 and 3.5 MPa according to the stance time frame and thus to the cartilage location. In terms of cycle frequency, since the gait cycle time of comfortable walking is about 1 s, the bioreactor loading frequency could range between 1 Hz (for the posterior region cartilage samples) to about 5–10 Hz (for the central region cartilage samples).

Since the response of cartilage to loading is strictly dependent on the characteristics of the applied forces (frequency, intensity and duration) (Leong et al., 2011; Sun et al., 2011), these parameters need to be chosen and set with particular attention in order to reproduce the real forces occurring *in vivo*. In the proposed protocol, we applied compression loading to human cartilage explants *ex vivo* simulating the loading acting

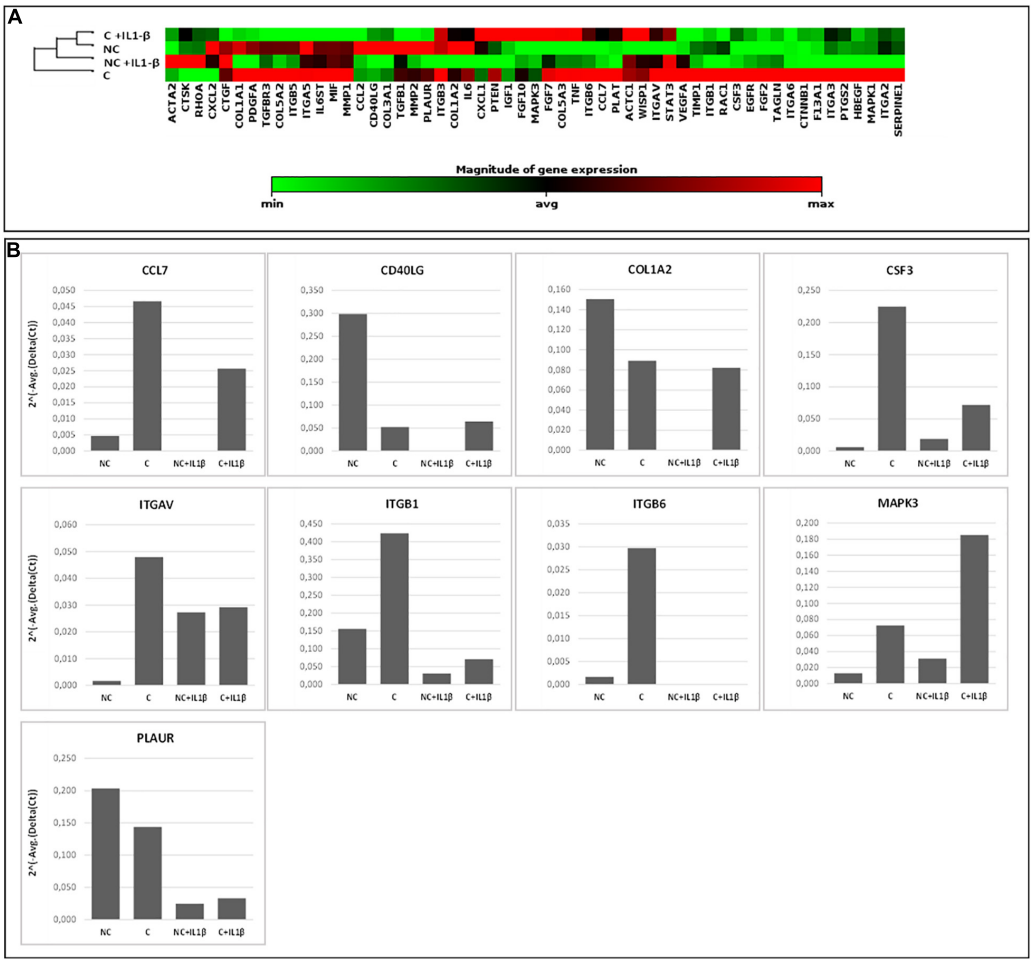

FIGURE 6 | Array-based gene expression analysis of OA cartilage samples. A focused panel of 84 genes involved in wound healing was analyzed. Four experimental conditions were tested: (1) NC (not compressed cartilage, control group); (2) C (compressed cartilage); (3) NC+IL1-β (not compressed cartilage stimulated with the pro-inflammatory factor IL1-β); and (4) C+IL1-β (compressed cartilage stimulated with the pro-inflammatory factor IL1-β). Each group consists of two samples from two different donors. **(A)** Heatmap of the unsupervised hierarchical cluster analysis. Red indicates high levels of expression and green indicates low levels of expression; **(B)** Variations of selected genes after OA cartilage compression for 45 min at 1 Hz and 3 MPa and with addition of pro-inflammatory stimulation (IL1-β 2 ng/ml). Genes with a fold change of at least 5 in one out of 4 conditions are showed.

on the knee cartilage during walking following a thorough biomechanical analysis based on *in vivo* knee forces. Input parameters were run on a pilot case series of human OA cartilage cylinders in a bioreactor, differentiating samples according to tissue scoring and original anatomical position. In general, studies on human cartilage response to loading suffer from the reduced amount of available tissue and from the reduced number of cells normally present in the cartilage. Moreover, the anatomical and qualitative differentiation used here further reduces tissue availability for molecular analyses, thus representing the principal challenge to perform gene expression analysis in the presented experimental model. For this reason, high throughput multiple gene approaches (such as gene expression arrays) are likely to be a valuable tool to evaluate a significant number of molecules with reduced starting material. The drawback of such approaches is the need of higher quality RNA. Here we demonstrated that small cylinders of cartilage can be efficiently used for array-based gene expression analysis, giving reproducible results, and allowing to detect differences before and after compression. In the proposed protocol we were able to obtain sufficient amount of high-quality RNA to carry out the analysis of complex molecular pathways that can increase the understanding of the biomolecular mediators underlying the response to mechanical stimulation and possibly involved in cartilage integrity maintenance. In this proof-of-concept study, cartilage samples from two donors only were analyzed for gene expression, therefore attention should be paid before generalizing the results. We choose to analyze genes involved in the wound healing process to assess the effect of compression in cartilage tissue repair. Some of the genes most involved in mechanotransduction and regulated by compression forces are Integrins and the MAPK3 (Zhao et al., 2020), chemokines and factors involved in the inflammatory processes (CD40L, CCL7 and CSF3), the receptor for the matrix degradative enzyme

plasminogen (PLAUR) and a component of cartilage matrix (COL1A2) (see **Supplementary Table 3** for details on genes). As shown by non-supervised hierarchical clustering (**Figure 6**) NC samples are more similar to C+IL1-β samples than the other groups. Similarly to what observed in previous experiments (Dolzani et al., 2019), these results suggest a counteracting effect of compression against the pro-inflammatory stimulus.

The protocol proposed in this study can be applied to explore other molecular pathways implicated in the development of OA such as low-grade inflammation and innate immunity (Sokolove and Lepus, 2013; Silawal et al., 2018). Furthermore, in this study we hypothesized that chondrocytes from areas with distinct degrees of tissue alteration respond to loading differently. A very good correlation was obtained between macroscopic and microscopic scores. This confirms that a simple method such as macroscopic scoring, obtained by cartilage observation at the time of sample collection, could be a reliable method to quantify different degrees of degeneration.

The analysis conducted here to establish a set of biomechanical parameters to be used as loading inputs for a bioreactor should be interpreted with respect to some limitations. Although the relationship between EAM and internal knee forces used to estimate the knee force in our OA patient is rather accurate at early and mid-stance, it fails to accurately predict knee forces at late stance even considering the effect of covariates, such as walking speed and limb alignment (Kutzner et al., 2013). Thus, knee force and pressure temporal profiles should be considered to be reliable up to about 80% of stance phase, as the knee joint is almost fully unloaded at push-off. In addition, the temporal pattern of medial knee cartilage contact area over stance duration was estimated by interpolation of 5 points only. A more complete dataset of cartilage contact area throughout stance duration of walking should be sought to improve the accuracy in pressure estimation. In this proof-of concept study we validated different steps of the protocol with different samples without performing a complete workflow with a unique case series. We acknowledge that the characteristics and clinical history of the single knee OA patient recruited here, and thus the measured kinematic and kinetic data in gait, may not be fully representative of the average knee OA population. Specifically, the age of the OA patient (52 years) is lower than that of the *ex vivo* analysis cohort (69.6 ± 8.7 years); however, since the BMI (24.4 kg/m^2) is within 1 SD of the mean in the cohort, we do not believe these differences compromise the generalizability of our results and significantly affect the conclusions. Ideally, a cohort of knee OA patients should be assessed via gait analysis to estimate the average physiological cartilage pressure and application frequency—according to the cartilage region; this data should be used as loading conditions in the bioreactor to test the explanted cartilage samples from the same cohort.

CONCLUSION

In conclusion, we have here proposed an integrated protocol where *in vivo* estimated knee joint loading was used as compression regime applied *in vitro* to human cartilage. The molecular response to these stimulations has been analyzed to gain more insight into cartilage mechanobiology. A pilot application of this protocol to knee OA has also been presented. The combination of biomechanical and biological data may provide a significant added value to improve our understanding of knee cartilage mechanotransduction, by allowing to control the main parameters affecting the physiological condition. The proposed approach can be applied to different motor tasks (different compression regimes) or to specific cartilage samples (different anatomical regions or with different degrees of degeneration), and therefore could become a flexible tool to study different aspects of cartilage mechanotransduction.

DATA AVAILABILITY STATEMENT

The raw data supporting the conclusions of this article will be made available by the authors, without undue reservation.

ETHICS STATEMENT

The studies involving human participants were reviewed and approved by CE-AVEC. The patients/participants provided their written informed consent to participate in this study.

AUTHOR CONTRIBUTIONS

EA, CB, PC, and SN: conceptualization, writing—original draft preparation, writing, review and editing, and project administration. EA, CB, PC, AE, and SN: investigation. AL and EM: resources and funding acquisition. EA, CB, PC, SN, and MO: data curation. EA, CB, PC, AE, SN, and MO: methodology. All authors have read and agreed to the published version of the manuscript.

FUNDING

This study was funded by the Italian Health Ministry "5 per mille" fund and by the Italian Health Ministry grant "Ricerca Finalizzata" (Grant No. RF-2018-12368274).

ACKNOWLEDGMENTS

This is a short text to acknowledge the contributions of specific colleagues, institutions, or agencies that aided the efforts of the authors.

SUPPLEMENTARY MATERIAL

The Supplementary Material for this article can be found online at: https://www.frontiersin.org/articles/10.3389/fbioe.2021.634327/full#supplementary-material

REFERENCES

Abramoff, B., and Caldera, F. E. (2020). Osteoarthritis: pathology, diagnosis, and treatment options. *Med. Clin. North Am.* 104, 293–311.

Andriacchi, T. P., Mundermann, A., Smith, R. L., Alexander, E. J., Dyrby, C. O., and Koo, S. (2004). A framework for the in vivo pathomechanics of osteoarthritis at the knee. *Ann. Biomed. Eng.* 32, 447–457. doi: 10.1023/b:abme.0000017541.82498.37

Asano, T., Akagi, M., Tanaka, K., Tamura, J., and Nakamura, T. (2001). In vivo three-dimensional knee kinematics using a biplanar image-matching technique. *Clin. Orthop. Relat. Res.* 388, 157–166. doi: 10.1097/00003086-200107000-00023

Battaglia, S., Belvedere, C., Jaber, S. A., Affatato, S., D'angeli, V., and Leardini, A. (2014). A new protocol from real joint motion data for wear simulation in total knee arthroplasty: stair climbing. *Med. Eng. Phys.* 36, 1605–1610. doi: 10.1016/j.medengphy.2014.08.010

Beckwee, D., Vaes, P., Cnudde, M., Swinnen, E., and Bautmans, I. (2013). Osteoarthritis of the knee: why does exercise work? A qualitative study of the literature. *Ageing Res. Rev.* 12, 226–236. doi: 10.1016/j.arr.2012.09.005

Belvedere, C., Ensini, A., Leardini, A., Dedda, V., Feliciangeli, A., Cenni, F., et al. (2014). Tibio-femoral and patello-femoral joint kinematics during navigated total knee arthroplasty with patellar resurfacing. *Knee Surg. Sports Traumatol. Arthrosc.* 22, 1719–1727. doi: 10.1007/s00167-013-2825-0

Berti, L., Benedetti, M. G., Ensini, A., Catani, F., and Giannini, S. (2006). Clinical and biomechanical assessment of patella resurfacing in total knee arthroplasty. *Clin. Biomech. (Bristol, Avon)* 21, 610–616. doi: 10.1016/j.clinbiomech.2006.01.002

Bougault, C., Paumier, A., Aubert-Foucher, E., and Mallein-Gerin, F. (2008). Molecular analysis of chondrocytes cultured in agarose in response to dynamic compression. *BMC Biotechnol.* 8:71. doi: 10.1186/1472-6750-8-71

Bougault, C., Priam, S., Houard, X., Pigenet, A., Sudre, L., Lories, R. J., et al. (2014). Protective role of frizzled-related protein B on matrix metalloproteinase induction in mouse chondrocytes. *Arthritis Res. Ther.* 16:R137.

Bruyere, O., Cooper, C., Pelletier, J. P., Branco, J., Luisa Brandi, M., Guillemin, F., et al. (2014). An algorithm recommendation for the management of knee osteoarthritis in Europe and internationally: a report from a task force of the European Society for Clinical and Economic Aspects of Osteoporosis and Osteoarthritis (ESCEO). *Semin. Arthritis Rheum* 44, 253–263. doi: 10.1016/j.semarthrit.2014.05.014

Buchanan, T. S., Lloyd, D. G., Manal, K., and Besier, T. F. (2004). Neuromusculoskeletal modeling: estimation of muscle forces and joint moments and movements from measurements of neural command. *J. Appl. Biomech.* 20, 367–395. doi: 10.1123/jab.20.4.367

Cappozzo, A., Catani, F., Croce, U. D., and Leardini, A. (1995). Position and orientation in space of bones during movement: anatomical frame definition and determination. *Clin. Biomech. (Bristol, Avon)* 10, 171–178. doi: 10.1016/0268-0033(95)91394-t

Cross, M., Smith, E., Hoy, D., Nolte, S., Ackerman, I., Fransen, M., et al. (2014). The global burden of hip and knee osteoarthritis: estimates from the global burden of disease 2010 study. *Ann. Rheum Dis.* 73, 1323–1330. doi: 10.1136/annrheumdis-2013-204763

D'Angeli, V., Belvedere, C., Ortolani, M., Giannini, S., and Leardini, A. (2014). Load along the tibial shaft during activities of daily living. *J. Biomech.* 47, 1198–1205. doi: 10.1016/j.jbiomech.2014.01.045

D'Lima, D. D., Patil, S., Steklov, N., Slamin, J. E., and Colwell, C. W. Jr. (2006). Tibial forces measured in vivo after total knee arthroplasty. *J. Arthroplasty* 21, 255–262. doi: 10.1016/j.arth.2005.07.011

Dolzani, P., Assirelli, E., Pulsatelli, L., Meliconi, R., Mariani, E., and Neri, S. (2019). Ex vivo physiological compression of human osteoarthritis cartilage modulates cellular and matrix components. *PLoS One* 14:e0222947. doi: 10.1371/journal.pone.0222947

Edwards, W. B., Gillette, J. C., Thomas, J. M., and Derrick, T. R. (2008). Internal femoral forces and moments during running: implications for stress fracture development. *Clin. Biomech. (Bristol, Avon)* 23, 1269–1278. doi: 10.1016/j.clinbiomech.2008.06.011

Ensini, A., Catani, F., Biasca, N., Belvedere, C., Giannini, S., and Leardini, A. (2012). Joint line is well restored when navigation surgery is performed for total knee arthroplasty. *Knee Surg. Sports Traumatol. Arthrosc.* 20, 495–502. doi: 10.1007/s00167-011-1558-1

Fernandes, L., Hagen, K. B., Bijlsma, J. W., Andreassen, O., Christensen, P., Conaghan, P. G., et al. (2013). EULAR recommendations for the non-pharmacological core management of hip and knee osteoarthritis. *Ann. Rheum Dis.* 72, 1125–1135.

Fransen, M., Mcconnell, S., Harmer, A. R., Van Der Esch, M., Simic, M., and Bennell, K. L. (2015). Exercise for osteoarthritis of the knee: a cochrane systematic review. *Br. J. Sports Med.* 49, 1554–1557.

Fregly, B. J., Besier, T. F., Lloyd, D. G., Delp, S. L., Banks, S. A., Pandy, M. G., et al. (2012). Grand challenge competition to predict in vivo knee loads. *J. Orthop. Res.* 30, 503–513. doi: 10.1002/jor.22023

Fukubayashi, T., and Kurosawa, H. (1980). The contact area and pressure distribution pattern of the knee. A study of normal and osteoarthrotic knee joints. *Acta Orthop. Scand.* 51, 871–879. doi: 10.3109/17453678008990887

Griebel, A. J., Trippel, S. B., and Neu, C. P. (2013). Noninvasive dualMRI-based strains vary by depth and region in human osteoarthritic articular cartilage. *Osteoarthr. Cartil.* 21, 394–400. doi: 10.1016/j.joca.2012.11.009

Grood, E. S., and Suntay, W. J. (1983). A joint coordinate system for the clinical description of three-dimensional motions: application to the knee. *J. Biomech. Eng.* 105, 136–144. doi: 10.1115/1.3138397

Haudenschild, D. R., Chen, J., Pang, N., Lotz, M. K., and D'lima, D. D. (2010). Rho kinase-dependent activation of SOX9 in chondrocytes. *Arthritis Rheum* 62, 191–200. doi: 10.1002/art.25051

Heinlein, B., Kutzner, I., Graichen, F., Bender, A., Rohlmann, A., Halder, A. M., et al. (2009). ESB Clinical Biomechanics Award 2008: complete data of total knee replacement loading for level walking and stair climbing measured in vivo with a follow-up of 6-10 months. *Clin. Biomech. (Bristol, Avon)* 24, 315–326. doi: 10.1016/j.clinbiomech.2009.01.011

Henderson, C. E., Higginson, J. S., and Barrance, P. J. (2011). Comparison of MRI-based estimates of articular cartilage contact area in the tibiofemoral joint. *J. Biomech. Eng.* 133:014502.

Hinterwimmer, S., Gotthardt, M., Von Eisenhart-Rothe, R., Sauerland, S., Siebert, M., Vogl, T., et al. (2005). In vivo contact areas of the knee in patients with patellar subluxation. *J. Biomech.* 38, 2095–2101. doi: 10.1016/j.jbiomech.2004.09.008

Hosseini, A., Van De Velde, S. K., Kozanek, M., Gill, T. J., Grodzinsky, A. J., Rubash, H. E., et al. (2010). In-vivo time-dependent articular cartilage contact behavior of the tibiofemoral joint. *Osteoarthr. Cartil.* 18, 909–916. doi: 10.1016/j.joca.2010.04.011

Huang, J., Ballou, L. R., and Hasty, K. A. (2007). Cyclic equibiaxial tensile strain induces both anabolic and catabolic responses in articular chondrocytes. *Gene* 404, 101–109. doi: 10.1016/j.gene.2007.09.007

Huang, M. H., Lin, Y. S., Yang, R. C., and Lee, C. L. (2003). A comparison of various therapeutic exercises on the functional status of patients with knee osteoarthritis. *Semin. Arthritis Rheum* 32, 398–406. doi: 10.1053/sarh.2003.50021

Jeon, J. E., Schrobback, K., Hutmacher, D. W., and Klein, T. J. (2012). Dynamic compression improves biosynthesis of human zonal chondrocytes from osteoarthritis patients. *Osteoarthr. Cartil.* 20, 906–915. doi: 10.1016/j.joca.2012.04.019

Juhl, C., Christensen, R., Roos, E. M., Zhang, W., and Lund, H. (2014). Impact of exercise type and dose on pain and disability in knee osteoarthritis: a systematic review and meta-regression analysis of randomized controlled trials. *Arthritis Rheumatol.* 66, 622–636. doi: 10.1002/art.38290

Julius Wolff Institute and Charité – Universitätsmedizin Berlin (2020). *2020 OrthoLoad Database [Online]*. Available online at: https://orthoload.com/ (accessed 2020).

Kawakita, K., Nishiyama, T., Fujishiro, T., Hayashi, S., Kanzaki, N., Hashimoto, S., et al. (2012). Akt phosphorylation in human chondrocytes is regulated by p53R2 in response to mechanical stress. *Osteoarthr. Cartil.* 20, 1603–1609. doi: 10.1016/j.joca.2012.08.022

Kloppenburg, M., and Berenbaum, F. (2020). Osteoarthritis year in review 2019: epidemiology and therapy. *Osteoarthr. Cartil.* 28, 242–248. doi: 10.1016/j.joca.2020.01.002

Kutzner, I., Heinlein, B., Graichen, F., Bender, A., Rohlmann, A., Halder, A., et al. (2010). Loading of the knee joint during activities of daily living measured in vivo in five subjects. *J. Biomech.* 43, 2164–2173. doi: 10.1016/j.jbiomech.2010.03.046

Kutzner, I., Trepczynski, A., Heller, M. O., and Bergmann, G. (2013). Knee adduction moment and medial contact force–facts about their correlation during gait. *PLoS One* 8:e81036. doi: 10.1371/journal.pone.0081036

Leardini, A., Sawacha, Z., Paolini, G., Ingrosso, S., Nativo, R., and Benedetti, M. G. (2007). A new anatomically based protocol for gait analysis in children. *Gait Posture* 26, 560–571. doi: 10.1016/j.gaitpost.2006.12.018

Leong, D. J., Hardin, J. A., Cobelli, N. J., and Sun, H. B. (2011). Mechanotransduction and cartilage integrity. *Ann. N. Y. Acad. Sci.* 1240, 32–37. doi: 10.1111/j.1749-6632.2011.06301.x

Liu, F., Kozanek, M., Hosseini, A., Van De Velde, S. K., Gill, T. J., Rubash, H. E., et al. (2010). In vivo tibiofemoral cartilage deformation during the stance phase of gait. *J. Biomech.* 43, 658–665. doi: 10.1016/j.jbiomech.2009.10.028

McAlindon, T. E., Bannuru, R. R., Sullivan, M. C., Arden, N. K., Berenbaum, F., Bierma-Zeinstra, S. M., et al. (2014). OARSI guidelines for the non-surgical management of knee osteoarthritis. *Osteoarthr. Cartil.* 22, 363–388. doi: 10.1016/j.joca.2014.01.003

McLean, S. G., Su, A., and Van Den Bogert, A. J. (2003). Development and validation of a 3-D model to predict knee joint loading during dynamic movement. *J Biomech Eng* 125, 864–874. doi: 10.1115/1.1634282

Merx, H., Dreinhofer, K., Schrader, P., Sturmer, T., Puhl, W., Gunther, K. P., et al. (2003). International variation in hip replacement rates. *Ann. Rheum Dis.* 62, 222–226. doi: 10.1136/ard.62.3.222

Morimoto, Y., Ferretti, M., Ekdahl, M., Smolinski, P., and Fu, F. H. (2009). Tibiofemoral joint contact area and pressure after single- and double-bundle anterior cruciate ligament reconstruction. *Arthroscopy* 25, 62–69. doi: 10.1016/j.arthro.2008.08.014

Moschella, D., Blasi, A., Leardini, A., Ensini, A., and Catani, F. (2006). Wear patterns on tibial plateau from varus osteoarthritic knees. *Clin. Biomech. (Bristol, Avon)* 21, 152–158. doi: 10.1016/j.clinbiomech.2005.09.001

Nelson, A. E., Allen, K. D., Golightly, Y. M., Goode, A. P., and Jordan, J. M. (2014). A systematic review of recommendations and guidelines for the management of osteoarthritis: the chronic osteoarthritis management initiative of the U.S. bone and joint initiative. *Semin. Arthritis Rheum* 43, 701–712. doi: 10.1016/j.semarthrit.2013.11.012

O'Conor, C. J., Leddy, H. A., Benefield, H. C., Liedtke, W. B., and Guilak, F. (2014). TRPV4-mediated mechanotransduction regulates the metabolic response of chondrocytes to dynamic loading. *Proc. Natl. Acad. Sci. U.S.A.* 111, 1316–1321. doi: 10.1073/pnas.1319569111

Patel, V. V., Hall, K., Ries, M., Lotz, J., Ozhinsky, E., Lindsey, C., et al. (2004). A three-dimensional MRI analysis of knee kinematics. *J. Orthop. Res.* 22, 283–292. doi: 10.1016/j.orthres.2003.08.015

Périé, D., and Hobatho, M. C. (1998). In vivo determination of contact areas and pressure of the femorotibial joint using non-linear finite element analysis. *Clin. Biomech. (Bristol, Avon)* 13, 394–402. doi: 10.1016/s0268-0033(98)00091-6

Piscitelli, P., Iolascon, G., Di Tanna, G., Bizzi, E., Chitano, G., Argentiero, A., et al. (2012). Socioeconomic burden of total joint arthroplasty for symptomatic hip and knee osteoarthritis in the Italian population: a 5-year analysis based on hospitalization records. *Arthritis Care Res. (Hoboken)* 64, 1320–1327. doi: 10.1002/acr.21706

Pritzker, K. P., Gay, S., Jimenez, S. A., Ostergaard, K., Pelletier, J. P., Revell, P. A., et al. (2006). Osteoarthritis cartilage histopathology: grading and staging. *Osteoarthr. Cartil.* 14, 13–29. doi: 10.1016/j.joca.2005.07.014

Qi, W., Hosseini, A., Tsai, T. Y., Li, J. S., Rubash, H. E., and Li, G. (2013). In vivo kinematics of the knee during weight bearing high flexion. *J. Biomech.* 46, 1576–1582. doi: 10.1016/j.jbiomech.2013.03.014

Ramachandran, M., Achan, P., Salter, D. M., Bader, D. L., and Chowdhury, T. T. (2011). Biomechanical signals and the C-type natriuretic peptide counteract catabolic activities induced by IL-1beta in chondrocyte/agarose constructs. *Arthritis Res. Ther.* 13:R145.

Scheys, L., Leardini, A., Wong, P. D., Van Camp, L., Callewaert, B., Bellemans, J., et al. (2013). Three-dimensional knee kinematics by conventional gait analysis for eleven motor tasks of daily living: typical patterns and repeatability. *J. Appl. Biomech.* 29, 214–228. doi: 10.1123/jab.29.2.214

Silawal, S., Triebel, J., Bertsch, T., and Schulze-Tanzil, G. (2018). Osteoarthritis and the complement cascade. *Clin. Med. Insights Arthritis Musculoskelet Disord.* 11:1179544117751430.

Sokolove, J., and Lepus, C. M. (2013). Role of inflammation in the pathogenesis of osteoarthritis: latest findings and interpretations. *Ther. Adv. Musculoskelet Dis.* 5, 77–94. doi: 10.1177/1759720x12467868

Sun, H. B. (2010). Mechanical loading, cartilage degradation, and arthritis. *Ann. N. Y. Acad. Sci.* 1211, 37–50. doi: 10.1111/j.1749-6632.2010.05808.x

Sun, H. B., Cardoso, L., and Yokota, H. (2011). Mechanical intervention for maintenance of cartilage and bone. *Clin. Med. Insights Arthritis Musculoskelet Disord.* 4, 65–70.

Woolf, A. D., and Pfleger, B. (2003). Burden of major musculoskeletal conditions. *Bull. World Health Organ.* 81, 646–656.

World Health Organization (2003). *The Burden of Musculoskeletal Conditions at the Start of the New Millenium.* WHO Tecnical Report Series 919. Geneva: World Health Organization.

Yao, J., Lancianese, S. L., Hovinga, K. R., Lee, J., and Lerner, A. L. (2008). Magnetic resonance image analysis of meniscal translation and tibio-menisco-femoral contact in deep knee flexion. *J. Orthop. Res.* 26, 673–684. doi: 10.1002/jor.20553

Zhao, Z., Li, Y., Wang, M., Zhao, S., Zhao, Z., and Fang, J. (2020). Mechanotransduction pathways in the regulation of cartilage chondrocyte homoeostasis. *J. Cell Mol. Med.* 24, 5408–5419. doi: 10.1111/jcmm.15204

Conflict of Interest: The authors declare that the research was conducted in the absence of any commercial or financial relationships that could be construed as a potential conflict of interest.

frontiers in Bioengineering and Biotechnology

ORIGINAL RESEARCH
published: 05 May 2021
doi: 10.3389/fbioe.2021.613616

Experimental and Modeling Analyses of Human Motion Across the Static Magnetic Field of an MRI Scanner

Davide Gurrera[1,2], Alberto Leardini[3], Maurizio Ortolani[3], Stefano Durante[3], Vittorio Caputo[4], Karmenos K. Gallias[4], Boris F. Abbate[4], Calogero Rinaldi[5], Giuseppina Iacoviello[4], Giuseppe Acri[6], Giuseppe Vermiglio[7] and Maurizio Marrale[2]*

[1] Advanced Radiation Oncology Department, Cancer Care Center, Istituto di Ricovero e Cura a Carattere Scientifico (IRCCS) Sacro Cuore Don Calabria Hospital, Negrar di Valpolicella, Italy, [2] Dipartimento di Fisica e Chimica, Università degli Studi di Palermo, Palermo, Italy, [3] Istituto di Ricovero e Cura a Carattere Scientifico (IRCCS) Istituto Ortopedico Rizzoli, Movement Analysis Laboratory, Bologna, Italy, [4] Azienda Ospedaliera di Rilievo Nazionale e di Alta Specializzazione (A.R.N.A.S.) Civico–Di Cristina–Benfratelli, Unità Operativa Complessa (U.O.C.) Fisica Sanitaria, Palermo, Italy, [5] Villa Santa Teresa, Unità Operativa (U.O.) Fisica Sanitaria, Bagheria, Italy, [6] Dipartimento di Scienze Biomediche, Odontoiatriche e delle Immagini Morfologiche e Funzionali (BIOMORF), Università degli Studi di Messina, Messina, Italy, [7] Scuola di Specializzazione in Fisica Medica, Università degli Studi di Messina, Messina, Italy

It is established that human movements in the vicinity of a permanent static magnetic field, such as those in magnetic resonance imaging (MRI) scanners induce electric fields in the human body; this raises potential severe risks of health to radiographers and cleaners exposed routinely to these fields in MRI rooms. The relevant directives and parameters, however, are based on theoretical models, and accurate studies on the simulation of the effects based on human movement data obtained in real conditions are still lacking. Two radiographers and one cleaner, familiar with MRI room activities and these directives, were gait analyzed during the execution of routine job motor tasks at different velocities. Full body motion was recorded in a gait laboratory arranged to reproduce the workspace of a room with an MRI full-body scanner. Body segments were tracked with clusters of at least three markers, from which position and velocity of the centroids were calculated. These were used as input in an established computer physical model able to map the stray field in an MRI room. The spatial peak values of the calculated electric field induced by motion of the head and of the entire body during these tasks, for both the health and sensory effects, were found smaller than the thresholds recommended by the European directives, for both 1.5 T and 3.0 T MRI. These tasks therefore seem to guarantee the safety of MRI room operators according to current professional good practice for exposure risks. Physical modeling and experimental measures of human motion can also support occupational medicine.

Keywords: human movement analysis, static magnetic fields, exposure limit values, MRI personnel safety, Directive 2013/35/EU

OPEN ACCESS

Edited by:
Simone Tassani,
Pompeu Fabra University, Spain

Reviewed by:
Xiaojun Chen,
Shanghai Jiao Tong University, China
Michele Raggi,
Turingsense EU Lab s.r.l, Italy

****Correspondence:***
Davide Gurrera
davide.gurrera@sacrocuore.it

Specialty section:
This article was submitted to Biomechanics, a section of the journal Frontiers in Bioengineering and Biotechnology

Received: *02 October 2020*
Accepted: *10 March 2021*
Published: *05 May 2021*

Citation:
Gurrera D, Leardini A, Ortolani M, Durante S, Caputo V, Gallias KK, Abbate BF, Rinaldi C, Iacoviello G, Acri G, Vermiglio G and Marrale M (2021) Experimental and Modeling Analyses of Human Motion Across the Static Magnetic Field of an MRI Scanner. Front. Bioeng. Biotechnol. 9:613616. doi: 10.3389/fbioe.2021.613616

1. INTRODUCTION

Magnetic resonance imaging (MRI) is used largely worldwide to assess the status of tissues in patients with musculoskeletal and other diseases. There are ∼50,000 MRI machines worldwide, with about 5,000 new units sold every year. Forty million scans are performed annually in the United States, and the number of examinations in 2017 has the peak of 143 per 1,000 population in Germany (Mikulic, 2019). It is also established that movements in the vicinity of a permanent

static magnetic field, such as that of an MRI scanner, induce electric fields in the human body. This raises potential severe risks of health to the persons working routinely in MRI rooms, such as radiographers and cleaners. There are directives for these workers on how to move in these rooms, but today these are based on theoretical models only (inter alii, Hartwig et al., 2014, 2019; Zilberti et al., 2015, 2016; Sannino et al., 2017). In other words, accurate simulation studies based on human movement data obtained in real conditions able to provide estimations of the exact effects of these fields are still lacking. The scope of the present experimental and modeling study is to provide these estimations for the first time by enhancing with experimental data the analysis provided in a previous modeling work (Gurrera et al., 2019). The general aim is to support general good practice methods for exposure assessment of personnel moving across the permanent static magnetic field straying from MRI scanners.

This previous work in fact (Gurrera et al., 2019) suffers from some limitations. The MRI operators were supposed to move translationally and at a constant speed, with relevant parameters derived on the basis of general studies reporting allegedly normal walking speeds (Bohannon and Williams Andrews, 2011). Thus, there is still a lack of specialized literature or experiments dealing with motion analysis of MRI operators. Moreover, the exposure assessment did not include any 3.0 T facilities. What would be necessary for the enhancement of the previous work is a full body, i.e., from head to foot, kinematic characterization of real MRI operators at work. This would provide the most realistic estimation of the electric field induced by these movements, easily extendable to the scanners of 3.0 T or more.

This kinematic characterization is obtained usually by human movement analysis (HMA) using stereophotogrammetry, an established technique which allows for accurate 3D tracking in space of body segments during the execution of locomotion tasks or elementary exercises or even high-performance sport activities (Cappozzo et al., 2005). This is achieved by instrumenting the subject under analysis with small spherical markers stuck on the skin possibly according to standard protocols (Ferrari et al., 2008; Kainz et al., 2017), and in case by arranging the gait analysis laboratory with the necessary furnishing for the simulation of the required environment according to the activity under investigation (chairs, steps, stairs, obstacles, etc.).

As mentioned, given an inertial reference frame in which the magnet is at rest, electric charges movements within the body of an MRI operator may occur because of body segment voluntary movements of the subjects; other organ and tissue motion within the body (Herman, 2016) are here ignored. The motion-induced field within the body of an MRI operator is addressed in the guidelines of the International Commission on Non-Ionizing Radiation Protection (ICNIRP) (International Commission on Non-Ionizing Radiation Protection, 2014). Unfortunately, for these estimations, questionable approximations were used, and an alleged "conversion factor" should be accounted, associated to "the location within the body, the size of the body, the shape of the body, electrical properties of the tissue" as well as "the direction and distribution of the magnetic field." Direct measurements of body segment motion of MRI operators are therefore necessary to quantify these effects.

The present work wants to contribute in this respect. In particular, the hypothesis is that the exposure of MRI personnel to static magnetic fields does comply with the current European Directive 2013/35/EU, and for both 1.5 T and 3.0 T MRI machines.

2. MATERIALS AND METHODS

2.1. The Theoretical Basis

The theoretical basis, introduced and discussed in Gurrera et al. (2019), is here briefly summarized.

1. Given an inertial reference frame in which the magnet is at rest, electric charges within the body of an MRI operator may be moving because of two reasons: natural movements within the body as those related to blood flow and nervous communication system (Herman, 2016), which are ignored in the present study, and the voluntary movements of the body segments and joints associated to locomotion and upper body maneuvers according to the tasks to be performed.
2. Let $\gamma(t)$ be an oriented closed conducting wire moving across a static magnetic field $\vec{B}_{\text{ext}}$, $\vec{v}$ the velocity of each point of the wire, $S_{\gamma(t)}$ an arbitrary surface enclosed by $\gamma(t)$.

   Then, according to the Faraday–Neumann's law:

$$\oint_{\gamma(t)} \vec{E} \cdot \hat{t}\, dl = -\iint_{S_{\gamma(t)}} \frac{\partial \vec{B}}{\partial t} \cdot \hat{n}\, dS \tag{1}$$

   or equivalently:

$$\oint_{\gamma(t)} (\vec{E} + \vec{v} \times \vec{B}) \cdot \hat{t}\, dl = -\frac{d}{dt} \iint_{S_{\gamma(t)}} \vec{B} \cdot \hat{n}\, dS \tag{2}$$

   where $\vec{E}$ and $\vec{B}$ are the electric field and the overall magnetic field, respectively. The rest of the notation is assumed to be familiar to the reader.

   If the inductance of the wire is negligible, then it is possible to assume that $\vec{B} = \vec{B}_{\text{ext}}$ and there is no time dependence. Therefore, according to Equation (1), the generated electric

TABLE 1 | Specific job and other details of the three MRI operators who volunteered to participate the study.

Operator	Job	Gender	Age	Height (cm)	Weight (kg)
MRIR1	Radiographer	Male	31	189	115
MRIR2	Radiographer	Female	27	150	49
MRIC	Cleaner	Male	54	172	61

field comes out to be irrotational and, as a consequence, has to be caused only by a continuous charge redistribution within the wire. And such a redistribution is imposed by the action of the Lorentz' force. The complete cause and effect picture is as follows. Free charges within the conductor start moving across the external magnetic field with a mean velocity that, at each point, is equal to the velocity of the wire.

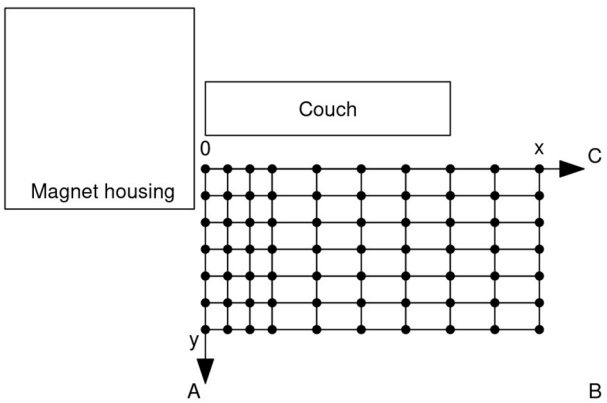

FIGURE 1 | Measurement environment where the three volunteers executed the tasks listed in **Table 2**. In order to account for different MRI room arrangements, A–C indicate the possible position of the door. In the actual MRI room, the modulus of the stray field was measured in each of the indicated points and at each of three different heights. The short and long steps in the net are 20 and 40 cm long, respectively. The map lies as close as possible to the bore and the couch.

Then the Lorentz' force accelerates them and causes a charge separation that produces an electrostatic field $\vec{E}$ opposing further accumulation, i.e., opposing the electromotive field $\vec{v} \times \vec{B}$. Except for particular given arrangements of $\vec{B}_{\text{ext}}$ and $\vec{v}$, equilibrium is not reached and a time-varying density current flows along the wire. As far as the magnetic field produced by this induced current may be neglected, there will be only an electromotive field $\vec{v} \times \vec{B}$ and a reaction electrostatic field ($\nabla \times \vec{E} = \vec{0}$). Now, a human body moving inside an MRI room may be considered as a special instance of a massive extended non-ferromagnetic conductor for which all the reasoning above applies. Particularly, the motion-induced "electric field" to be tested against the exposure limit values (ELVs) of the directive will be the sum of the electromotive field $\vec{v} \times \vec{B}$ and the reaction electrostatic field $\vec{E}$. If the latter, which even a computational model accounting for the electrical properties of the human body could only approximate, is neglected, then an overestimation of the induced field may be expected. But that even results in a precautionary approach.

To summarize, an electric charge moving in a magnetic field $\vec{B}$, with overall instantaneous velocity $\vec{v}$, is subjected to the Lorentz' force and the related electromotive field $\vec{v} \times \vec{B}$ may be regarded as the best approximation for the motion-induced field within the body of an MRI operator. Indeed, the induced field suggested in the guidelines of the International Commission on Non-Ionizing Radiation Protection (ICNIRP) (International Commission on Non-Ionizing Radiation Protection, 2014)

TABLE 2 | Selected representative job motor tasks, involved in normal and emergency scenarios, executed by the MRI operators who volunteered to participate the study.

Task code	Involved operators	Task title	Task description
N1	Radiographers	Entering/Leaving A	The operator enters the MRI room through Door A, reaches the control panel on the magnet housing, then leaves the room through the same door.
N2	Radiographers	Entering/Leaving B	As in N1, but through Door B.
N3	Radiographers	Entering/Leaving C	As in N1, but through Door C.
N4	Radiographers	Head coil preparation	The operator enters the MRI room through Door A and places the head coil on the couch near the bore entrance, then leaves the room through the same door.
N5	Radiographers	Patient centering	The operator is near the bore entrance, bends over the patient and positions the head coil, centers and checks the patient, then leaves the room through Door A.
N6	Radiographers	Object recovering	The operator enters the MRI room through Door A, bends over the floor next to the bore entrance and picks up an object, then leaves the room through the same door.
E1	Radiographers	Emergency entering A	Patient alarm on. The operator enters the MRI room through Door A and checks the patient lying inside the bore, then leaves the room through the same door.
E2	Radiographers	Emergency entering B	As in E1, but through Door B.
E3	Radiographers	Emergency entering C	As in E1, but through Door C.
E4	Radiographers	Emergency patient extraction	Patient alarm on. The operator enters the MRI room through Door A, checks the patient lying inside the bore, then rapidly extracts the couch manually and finally leaves the room through the same door.
C1	Cleaner	Floor sweeping	The operator enters the MRI room through Door A and sweeps the floor (from the door toward the couch and then back), then leaves the room through the same door.
C2	Cleaner	Floor mopping	The operator enters the MRI room through Door A and mops the floor (from the couch toward the door), then leaves the room through the same door.

*Refer to **Figure 1** for a sketch of the measurement environment. The words "MRI room," "door," "control panel," "magnet housing," "coil," "couch," "bore," and "patient" are used only evocatively. However, during the acquisition the floor was really swept and mopped by the cleaner and the patient alarm was really heard during the emergency scenarios.*

$$E_{\mathrm{i}} = C\frac{\mathrm{d}B}{dt} \tag{3}$$

may be considered as an unnecessary coarse approximation of it (and, possibly, an overestimation), C being a "conversion factor" that should account for "the location within the body, the size of the body, the shape of the body, electrical properties of the tissue" as well as "the direction and distribution of the magnetic field." In fact, in a static magnetic field, the electric field induced in a moving conducting loop is irrotational (see also Bringuier, 2002). Therefore, the Faraday–Neumann's law simplifies to:

$$\oint \vec{v} \times \vec{B} \cdot \hat{t}\, dl = -\frac{d}{dt} \iint \vec{B} \cdot \hat{n}\, dS \tag{4}$$

and calculating the rate of change of the magnetic flux is tantamount to calculate the circulation of $\vec{v} \times \vec{B}$.

3. A magnetic dipole may provide (if data confirming evidence is obtained) a parsimonious, but still adequate, 3D approximation of the magnetic field straying from a closed full-body MRI scanner, its specific architecture details being unknown (see also Sannino et al., 2017).

2.2. Mapping Relevant Velocities in an MRI Room

In May 2019, three healthy MRI operators, specific job and other details provided in **Table 1**, volunteered to contribute the current study and to be observed and recorded during the execution of routine job tasks at the Movement Analysis Laboratory of the Istituto Ortopedico Rizzoli in Bologna (Italy). This was instrumented with an 8-TV-camera stereophotogrammetric system (Vicon Motion Systems, Oxford, UK) and related processing software and opportunely arranged, as sketched in **Figure 1**, to reproduce a typical workspace of an MRI closed full-body scanner. The subjects were given instructions and time to familiarize with the room environment and then were asked to execute twice each of the representative job motor tasks, involved in normal and emergency scenarios, listed in **Table 2**.

State-of-the-art stereophotogrammetric HMA was performed during the execution of the tasks. Established protocols were used to track lower limbs and pelvis segments (Leardini et al., 2007), trunk and shoulders (Leardini et al., 2011), head, and upper limbs (according to Plug-in-Gait protocol, Vicon Motion Systems, Oxford, UK). All together, combining the three protocols, a total of 47 spherical reflective markers, 14 mm diameter, were stuck on the skin in correspondence of palpable anatomical landmarks, each tracked in space at 100 Hz by the stereophotogrammetric system during movement. Six of these markers served only for anatomical calibration of those landmarks necessary for body segment analysis and were removed after a single static posture acquisition in double-leg stance. Marker trajectories were smoothed by the standard software tools within the motion capture system, according to established algorithms (Woltring, 1985). Then, from each cluster of markers stuck in a single body segment, the corresponding centroid was also derived.

TABLE 3 | Selected points in the body of the three operators whose instantaneous position and velocity during the execution of the tasks are used for the exposure assessment.

Point number	Point type	Point position
1	Centroid	Head
2	Centroid	Trunk
3	Centroid	Pelvis
4	Centroid	Right thigh
5	Centroid	Left thigh
6	Centroid	Right tibia
7	Centroid	Left tibia
8	Centroid	Right foot
9	Centroid	Left foot
10	Centroid	Right hand
11	Centroid	Left hand
12	Marker	Right temple
13	Marker	Left temple
14	Marker	Right side of occipital bone
15	Marker	Left side of occipital bone
16	Marker	Second thoracic vertebra
17	Marker	Midpoint between the inferior angles of most caudal points of the two scapulae
18	Marker	Neck in between jugular veins
19	Marker	Xiphoid process
20	Marker	Right anterior superior iliac spine
21	Marker	Left anterior superior iliac spine
22	Marker	Right posterior superior iliac spine
23	Marker	Left posterior superior iliac spine

From each marker and centroid trajectory, the corresponding velocity was computed. In particular, instantaneous position and velocity during the execution of the tasks were obtained for each of the 23 representative body points listed in **Table 3**.

2.3. Mapping the Stray Field in an MRI Room

The model proposed in Gurrera et al. (2019) for the static magnetic field straying inside an MRI room was applied in the present study to a closed full-body 3.0 T scanner, the modulus of the magnetic field being mapped, in order to fit the model, as described in the paper and by the same three-axis Hall magnetometer. Particularly, the modulus of the magnetic field was measured according to the map shown in **Figure 1**, positioned as close as possible to the bore and the couch and whose short and long steps are 20 and 40 cm long, respectively. These measurements were recorded in each of the 70 indicated points and at each of three different heights from the floor level: 72, 119, and 156 cm. Therefore, a three-dimensional map composed of 210 measures was produced for the scanner. The modulus of the generated magnetic dipole and its height above the floor level, i.e., the preliminary estimations

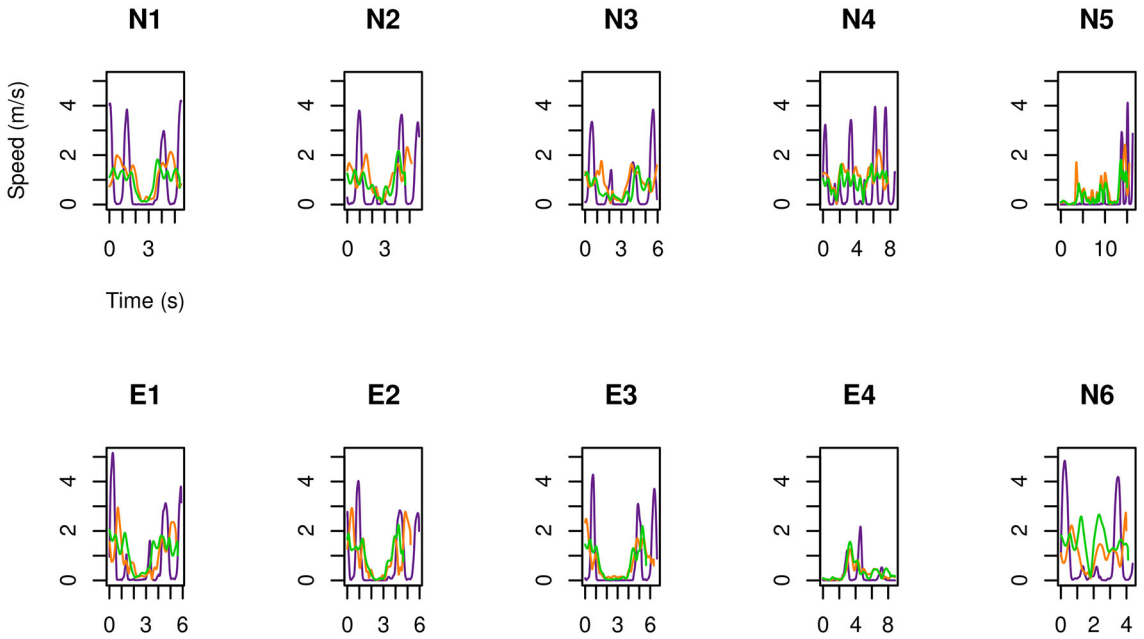

FIGURE 2 | For MRIR1 (**Table 1**), speed of the head and of the limbs as a function of time during the execution of each of the recurrent selected tasks (**Table 2**). Particularly, the green line refers to the marker on the right temple, the orange line to the right hand, and the violet line to the right foot.

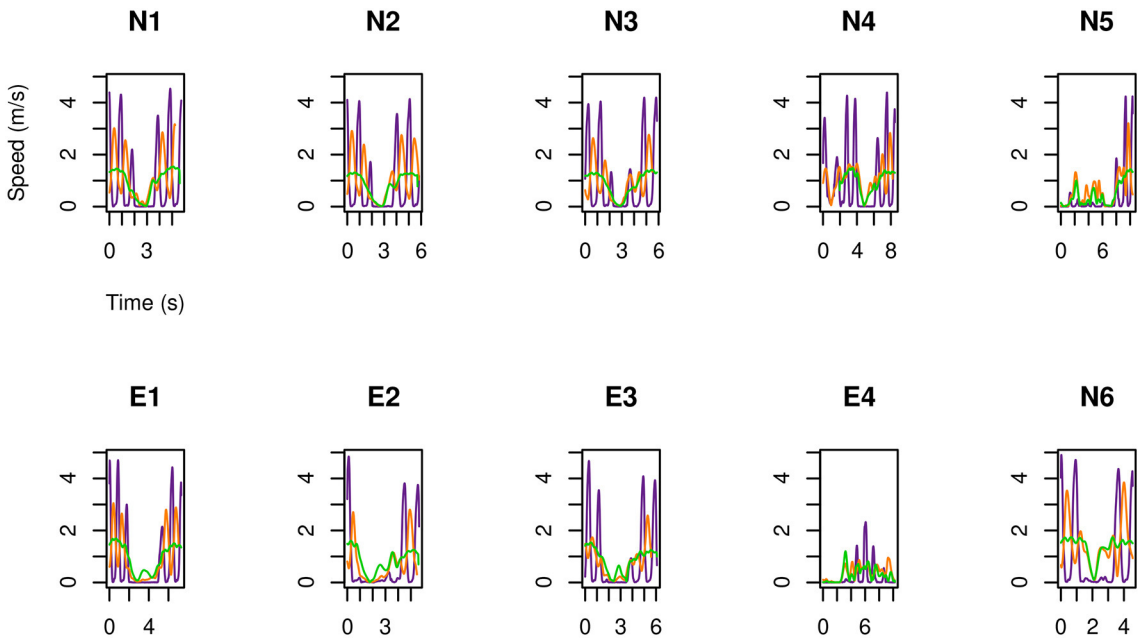

FIGURE 3 | As in **Figure 2**, but for MRIR2.

necessary for the fit (Gurrera et al., 2019), are 1.06 MA m^2 and 100 cm, respectively.

2.4. Implementation

What follows was carried out in the R environment for statistical computing and visualization (R Core Team, 2018) by *ad hoc* in-house developed code.

3. RESULTS

3.1. MRI Operators: How Fast Do They Move?

As a first result of the HMA, displayed in **Figures 2–4** is the speed, as a function of time, of each of the three examined operators (**Table 1**) during the second execution of each of their

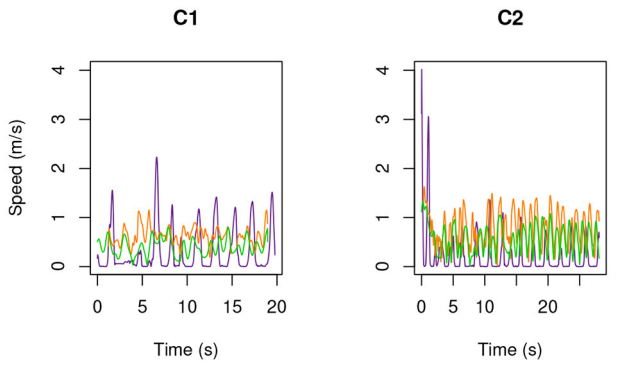

FIGURE 4 | As in **Figure 2**, but for MRIC.

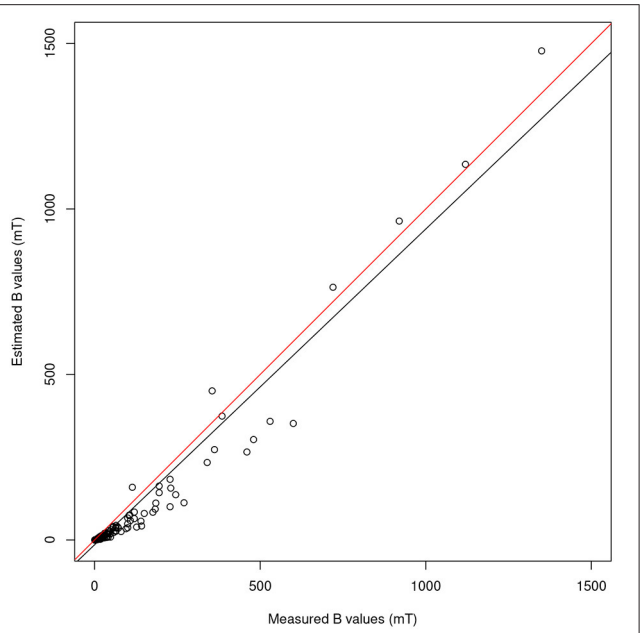

FIGURE 5 | For the 3.0 T machine, scatter plot of all the 210 values of B estimated by the model proposed in Gurrera et al. (2019) vs. the raw measures. The black straight line shows the best fit, while the other represents "perfect" modeling, i.e., $y = x$.

tasks (**Table 2**). No significant difference was observed between the first and the second execution of each task. Specifically, position and velocity of the body segments here analyzed showed a good inter-trial repeatability, consistent with previous work from these authors (Manca et al., 2010; Caravaggi et al., 2011) where standard deviations of gait-analysis patterns are in the range $2 \div 4\%$.

The following results are drawn.

1. The feet are the part of the body that move fastest: up to $5\,\mathrm{m\,s^{-1}}$. Then come the hands: up to $3.5\,\mathrm{m\,s^{-1}}$.
2. Head marker on MRIR2 moved always slower than $2\,\mathrm{m\,s^{-1}}$, while this speed was occasionally exceeded by MRIR1. In the case of MRIC, head speed did not exceed $1\,\mathrm{m\,s^{-1}}$.
3. For the two radiographers, a U-shaped speed profile is observed: operators move fast when entering and leaving the room, while they slow down as they approach the magnet.

3.2. The Fit

Once conformed to the measured values, the dipole model in Gurrera et al. (2019) provides, in the case of the 3.0 T machine here analyzed, the response shown in **Figure 5**, displaying the scatter plot of all the estimated B values vs. the raw measures. Also displayed in the figure are two almost coincident straight lines, the black one being the best fit line, the other representing "perfect" modeling, i.e., $y = x$. As a result, despite the inherent heteroscedasticity, adherence to the model as measured by the Pearson's correlation coefficient is 0.97 (as it was in the case of the 1.5 T machines analyzed in Gurrera et al., 2019). The estimated values for the two unknowns Δx and Δy (Gurrera et al., 2019) are 69 and 8 cm, respectively.

3.3. Assessing the Whole-Body Exposure

By making use of the position and velocity map of each of the 23 tracked points in the body of the three volunteers (**Table 3**) and of the $\vec{B}$ map provided by the model, in **Figures 6–8** the peak value $\max_{i=1,\ldots,23} |\vec{v}_i(t) \times \vec{B}|$ is shown during the (second) execution of each task. Results are given for the 3.0 T machine analyzed in this work, hereafter Machine 3.0, and for the 1.5 T Machine A analyzed in Gurrera et al. (2019).

For each operator and for each task, exposure results far below the $1.1\,\mathrm{V\,m^{-1}}$ ELV prescribed in European Union (2013) to account for possible health effects.

3.4. Assessing the Head Exposure

By making use of the position and velocity map of each of the five tracked points in the head of the three volunteers (**Table 3**) and of the $\vec{B}$ map provided by the model, in **Figures 9–11** the peak value $\max_{i=1,12,\ldots,15} |\vec{v}_i(t) \times \vec{B}|$ is shown during the (second) execution of each task.

Only "object recovering" (N6) deserves being considered in detail and therefore in **Figure 12** the induced pulse for MRIR1 and MRIR2 is shown in the case of Machine 3.0, along with the proper ELV adjusted by the motion-related frequency [1.43 and 1.14 Hz, respectively, as estimated by the spectral centroid of the corresponding periodogram (Massar et al., 2011)].

For each operator and for each task, exposure did not exceed the ELV prescribed in European Union (2013) to account for possible sensory effects, i.e., $0.7/f\,\mathrm{V\,m^{-1}}$, where f is the motion-related frequency.

4. DISCUSSION

In view of the obtained results, a limited risk margin (to exceed the ELV for the sensory effects) appeared only in the case of a 3.0 T machine. This raises questions about the opportunity of using lighter approaches. In fact, the

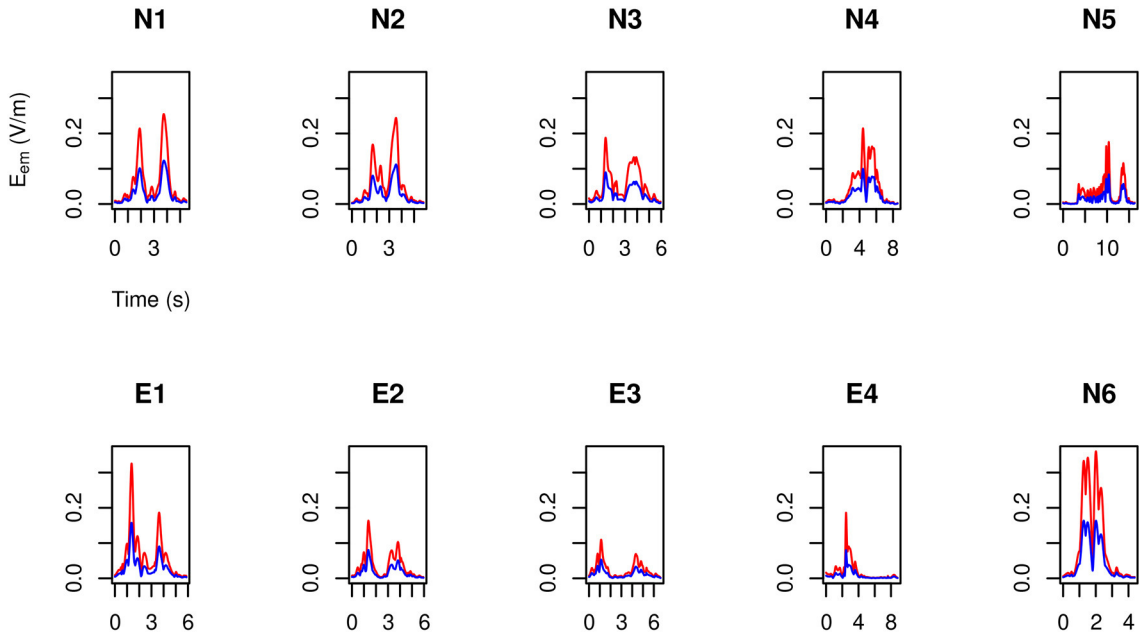

FIGURE 6 | For MRIR1 (**Table 1**), body peak value of the motion induced electromotive field E_{em} during the execution of each of the recurrent selected tasks (**Table 2**). Particularly, the red line refers to the 3.0 T machine analyzed in this work, while the blue line refers to the 1.5 T Machine A analyzed in Gurrera et al. (2019).

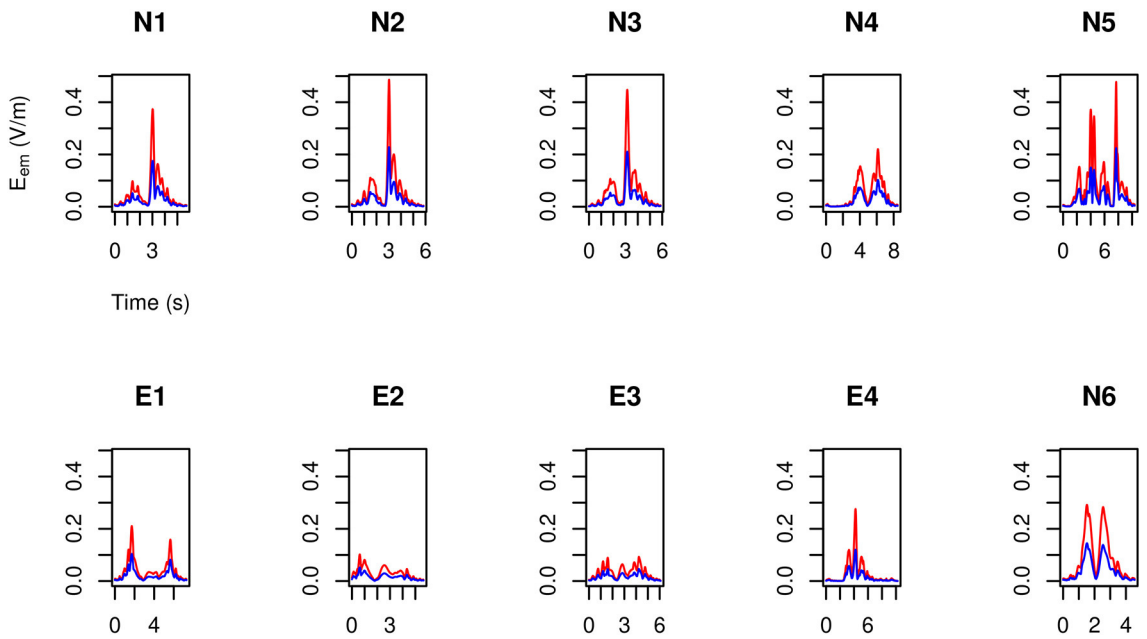

FIGURE 7 | As in **Figure 6**, but for MRIR2.

"practical" reference levels in International Commission on Non-Ionizing Radiation Protection (2014) "for determining compliance with the basic restrictions for the induced internal electric field," along with a practical but severe approximation of it (Equation 3), have proved to lead to alarming conclusions (inter alii, Acri et al., 2018 and Hartwig et al., 2019), while the estimation of the proper motion induced field introduced in Gurrera et al. (2019), once reliable

measures of the components of the involved velocities and of the stray magnetic field are obtained, is definitely not less practical.

Here, in order to obtain realistic positions and velocities, a state-of-the-art HMA was used, able to track single reflective markers and relevant centroids with an accuracy smaller than 1 mm, and applied to three real MRI operators whose specific training and daily experience may be expected to replicate usual activities though in a simulated environment. Moreover, in order to span different typologies of workers, a man and a woman of very different height were recruited from a number of available radiographers. In this study, the "skin motion artifact," due to the undesired displacements between the external markers on the skin and the underlying bone (Leardini et al., 2005), is not expected to affect the final results significantly, particularly the centroids, calculated from the external skin markers, and thus overall less sensible to this source of error.

In order to obtain the stray magnetic field, the simple dipole model already proposed in Gurrera et al. (2019) was used, which—once properly conformed to accurate static measures—has proved to yield reliable estimates of the three components of $\vec{B}$ also for a 3.0 T machine.

Of course, different scenarios other than those depicted here may occur in an MRI room and other different MRI facilities should be analyzed. The obtained results appear robust and suggest that, even in the case of a 3.0 T machine, a controlled behavior in the close proximity of the magnet might easily prevent electric pulses beyond the thresholds prescribed in the Directive 2013/35/EU. In any case, the present work represents an original cross-disciplinary interaction between physical models and human motion analysis, made nowadays more necessary for the complexities implied in these approaches, and casts light on the current lack of general consensus (Stam and Yamaguchi-Sekino, 2018). In fact, this lack appears to be due to three main reasons: (i) the ICNIRP has missed the fundamental role of the Lorentz' force; (ii) a lack of specialized studies dealing with the motion analysis of MRI operators; (iii) a lack of standardized MRI personnel training throughout the European Union. Particularly, the last point appears to be fundamental since, in view of the obtained results, it would provide safe working conditions at least up to 3.0 T machines for all MRI

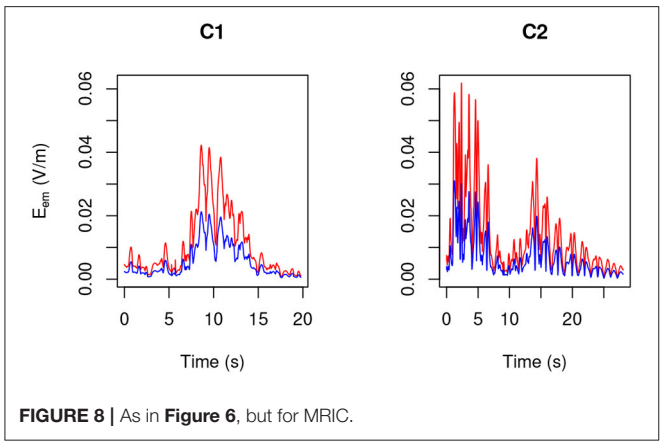

FIGURE 8 | As in **Figure 6**, but for MRIC.

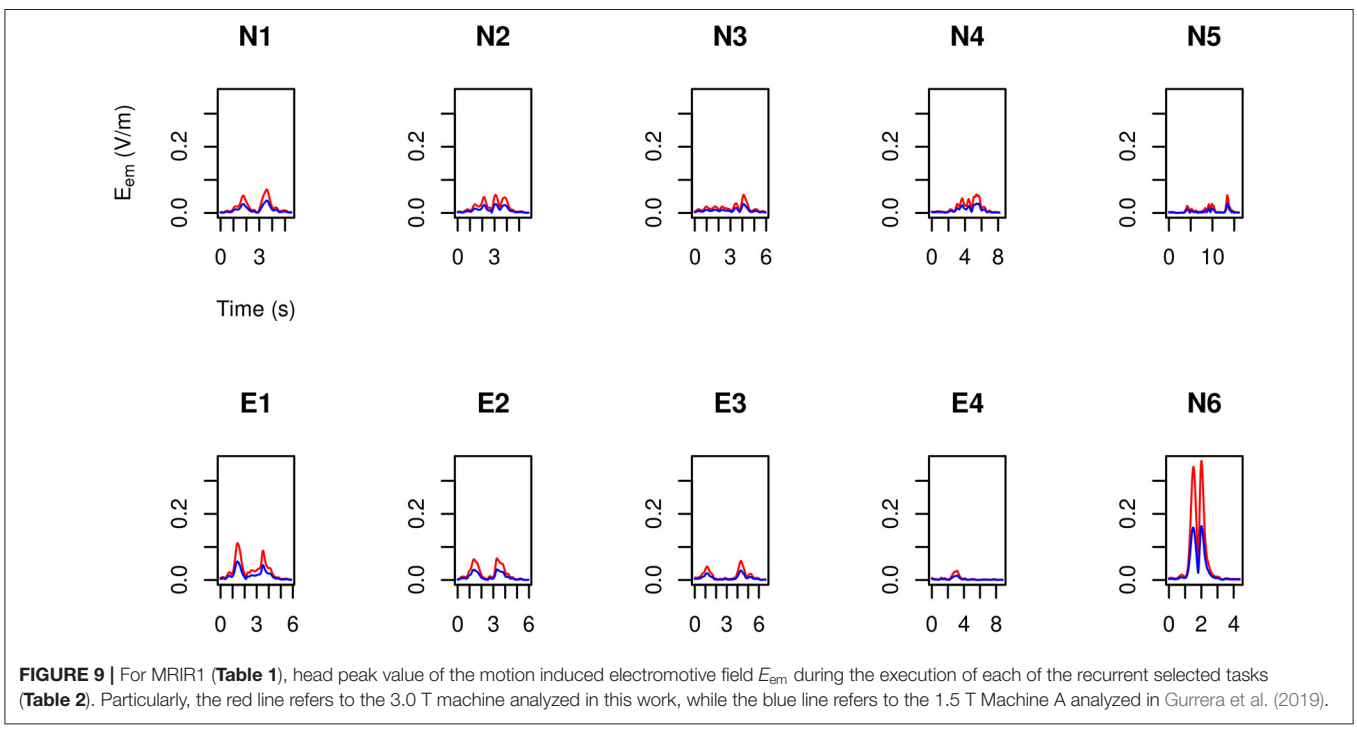

FIGURE 9 | For MRIR1 (**Table 1**), head peak value of the motion induced electromotive field E_{em} during the execution of each of the recurrent selected tasks (**Table 2**). Particularly, the red line refers to the 3.0 T machine analyzed in this work, while the blue line refers to the 1.5 T Machine A analyzed in Gurrera et al. (2019).

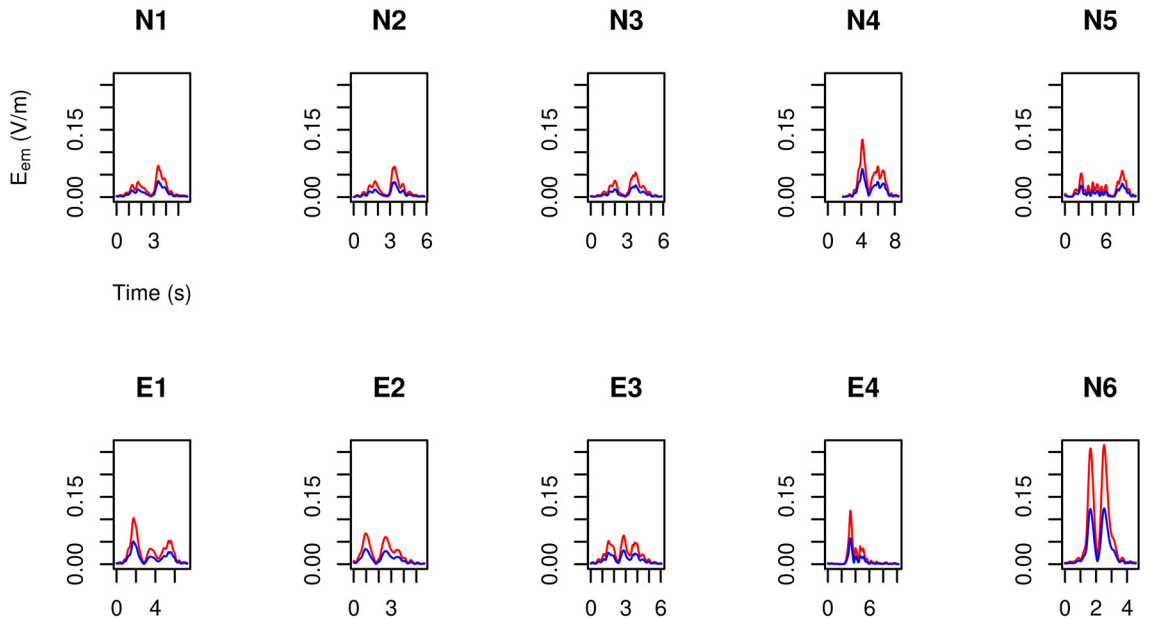

FIGURE 10 | As in **Figure 9**, but for MRIR2.

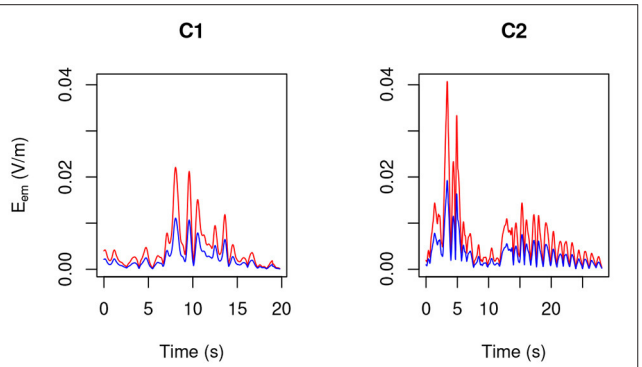

FIGURE 11 | As in **Figure 9**, but for MRIC.

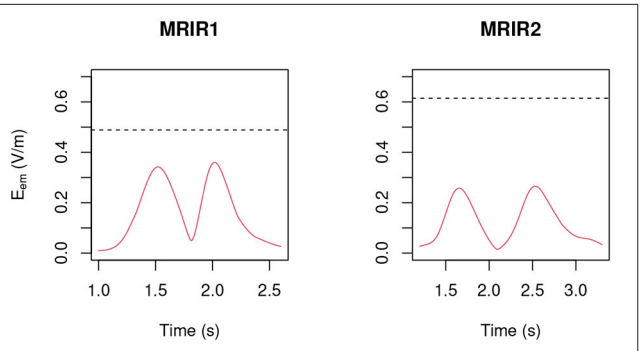

FIGURE 12 | Induced pulse during "object recovering" (N6) for the two radiographers in the case of Machine 3.0, along with the proper ELV (dashed black line) adjusted by the motion-related frequency.

operators. Of course, it should account for each possible task and for different statures.

5. CONCLUSIONS

The present study developed a method for introducing real human motion data into an established model now able to represent the induced electric field in the human body in the vicinity of an MRI scanner. This model, once applied to the two machines here analyzed—1.5 T one, 3.0 T the other—has resulted in a final positive compliance statement: both the health and sensory effects ELVs prescribed in the Directive 2013/35/EU are not exceeded. According to the present results, the introduction of specialized training protocols for MRI personnel throughout the European Union would prevent any possible risk to exceed the thresholds prescribed by the Directive currently in force, at least up to 3.0 T machines.

DATA AVAILABILITY STATEMENT

The raw data supporting the conclusions of this article will be made available by the authors, without undue reservation.

ETHICS STATEMENT

Ethical review and approval was not required for the study on human participants in accordance with the local legislation and institutional requirements. The patients/participants provided their written informed consent to participate in this study. Written informed consent was obtained from the individual(s) for the publication of any potentially identifiable images or data included in this article.

AUTHOR CONTRIBUTIONS

VC, DG, and AL conceived the study and were in charge of overall direction and planning. KG and BA conceived an *ad hoc* precision carpet to map the static magnetic field and DG realized it. CR fabricated an *ad hoc* precision support for the magnetometer. DG carried out the static magnetic field measurements with support from VC, KG, BA, GI, GA, and GV. AL and MO carried out the human movement analysis with support from SD and DG. DG and AL wrote the manuscript. DG designed the theoretical model, carried out its implementation, and analyzed the data. MM provided an in-depth reading and analysis of the manuscript. All authors provided critical feedback and helped shape the research and analysis.

FUNDING

This work was in part supported by the Italian Ministry of Economy and Finance, programme 5 per mille, and in part by the University of Palermo.

ACKNOWLEDGMENTS

The fundamental contribution to this study provided by the three MRI operators who volunteered their time and experience, namely, Pietro Urbani (MRIR1), Laura Federico (MRIR2), Massimo Doda (MRIC), was here deeply and gratefully acknowledged.

REFERENCES

Acri, G., Inferrera, P., Denaro, L., Sansotta, C., Ruello, E., Anfuso, C., et al. (2018). dB/dt Evaluation in MRI sites: is ICNIRP threshold limit (for workers) exceeded? *Int. J. Environ. Res. Public Health* 15:1298. doi: 10.3390/ijerph15071298

Bohannon, R. W., and Williams Andrews, A. (2011). Normal walking speed: a descriptive meta-analysis. *Physiotherapy* 97, 182–189. doi: 10.1016/j.physio.2010.12.004

Bringuier, E. (2002). Electrostatic charges in V × B fields and the phenomenon of induction. *Eur. J. Phys.* 24, 21–29. doi: 10.1088/0143-0807/24/1/304

Cappozzo, A., Della Croce, U., Leardini, A., and Chiari, L. (2005). Human movement analysis using stereophotogrammetry: part 1: theoretical background. *Gait Posture* 21, 186–196. doi: 10.1016/S0966-6362(04)00025-6

Caravaggi, P., Benedetti, M., Berti, L., and Leardini, A. (2011). Repeatability of a multi-segment foot protocol in adult subjects. *Gait Posture* 33, 133–135. doi: 10.1016/j.gaitpost.2010.08.013

European Union (2013). Directive 2013/35/EU of the European Parliament and of the Council of 26 June 2013 on the minimum health and safety requirements regarding the exposure of workers to the risks arising from physical agents (electromagnetic fields) (20th individual Directive within the meaning of Article 16(1) of Directive 89/391/EEC) and repealing Directive 2004/40/EC. *Off. J. Eur. Union* 56, 3–23. doi: 10.3000/19770677.L_2013.179.eng

Ferrari, A., Benedetti, M. G., Pavan, E., Frigo, C., Bettinelli, D., Rabuffetti, M., et al. (2008). Quantitative comparison of five current protocols in gait analysis. *Gait Posture* 28, 207–216. doi: 10.1016/j.gaitpost.2007.11.009

Gurrera, D., Gallias, K., Spanò, M., Abbate, B., D'Alia, F., Iacoviello, G., et al. (2019). Moving across the static magnetic field of a 1.5T MRI scanner: analysing compliance with Directive 2013/35/EU. *Phys. Med.* 57, 238–244. doi: 10.1016/j.ejmp.2018.11.004

Hartwig, V., Biagini, C., De Marchi, D., Flori, A., Gabellieri, C., Virgili, G., et al. (2019). The procedure for quantitative characterization and analysis of magnetic fields in magnetic resonance sites for protection of workers: a pilot study. *Ann. Work Exposures Health* 63, 1–9. doi: 10.1093/annweh/wxz002

Hartwig, V., Vanello, N., Giovannetti, G., Landini, L., and Santarelli, M. F. (2014). Estimation of occupational exposure to static magnetic fields due to usual movements in magnetic resonance units. *Concepts Magn. Reson. B Magn. Reson. Eng.* 44, 75–81. doi: 10.1002/cmr.b.21270

Herman, I. P. (2016). "Electrical and magnetic properties," in *Physics of the Human Body, Biological and Medical Physics, Biomedical Engineering* (Springer International Publishing), 819–871. doi: 10.1007/978-3-319-23932-3_12

International Commission on Non-Ionizing Radiation Protection (2014). Guidelines for limiting exposure to electric fields induced by movement of the human body in a static magnetic field and by time-varying magnetic fields below 1 Hz. *Health Phys.* 106, 418–425. doi: 10.1097/HP.0b013e31829e5580

Kainz, H., Graham, D., Edwards, J., Walsh, H. P., Maine, S., Boyd, R. N., et al. (2017). Reliability of four models for clinical gait analysis. *Gait Posture* 54, 325–331. doi: 10.1016/j.gaitpost.2017.04.001

Leardini, A., Biagi, F., Merlo, A., Belvedere, C., and Benedetti, M. G. (2011). Multi-segment trunk kinematics during locomotion and elementary exercises. *Clinical Biomech.* 26, 562–571. doi: 10.1016/j.clinbiomech.2011.01.015

Leardini, A., Chiari, L., Della Croce, U., and Cappozzo, A. (2005). Human movement analysis using stereophotogrammetry: part 3. Soft tissue artifact assessment and compensation. *Gait Posture* 21, 212–225. doi: 10.1016/j.gaitpost.2004.05.002

Leardini, A., Sawacha, Z., Paolini, G., Ingrosso, S., Nativo, R., and Benedetti, M. G. (2007). A new anatomically based protocol for gait analysis in children. *Gait Posture* 26, 560–571. doi: 10.1016/j.gaitpost.2006.12.018

Manca, M., Leardini, A., Cavazza, S., Ferraresi, G., Marchi, P., Zanaga, E., et al. (2010). Repeatability of a new protocol for gait analysis in adult subjects. *Gait Posture* 32, 282–284. doi: 10.1016/j.gaitpost.2010.05.011

Massar, M., Fickus, M., Bryan, E., Petkie, D., and Terzuoli, A. Jr. (2011). Fast computation of spectral centroids. *Adv. Comput. Math.* 35, 83–97. doi: 10.1007/s10444-010-9167-y

Mikulic, M. (2019). Number of examinations with magnetic resonance imaging (MRI) in selected countries in 2017. Available online at: https://www.statista.com/statistics/271470/mri-scanner-number-of-examinations-in-selected-countries/

R Core Team (2018). *R: A Language and Environment for Statistical Computing*. Vienna: R Foundation for Statistical Computing.

Sannino, A., Romeo, S., Scarfì, M., Massa, R., D'Angelo, R., Petrillo, A., et al. (2017). Exposure assessment and biomonitoring of workers in magnetic resonance environment: an exploratory study. *Front. Public Health* 5:344. doi: 10.3389/fpubh.2017.00344

Stam, R., and Yamaguchi-Sekino, S. (2018). Occupational exposure to electromagnetic fields from medical sources. *Ind. Health* 56, 96–105. doi: 10.2486/indhealth.2017-0112

Woltring, H. J. (1985). On optimal smoothing and derivative estimation from noisy displacement data in biomechanics. *Hum. Mov. Sci.* 4, 229–245. doi: 10.1016/0167-9457(85)90004-1

Zilberti, L., Bottauscio, O., and Chiampi, M. (2015). Motion-induced fields in magnetic resonance imaging: are the dielectric currents really negligible? *IEEE Magn. Lett.* 6, 1–4. doi: 10.1109/LMAG.2015.2429641

Zilberti, L., Bottauscio, O., and Chiampi, M. (2016). Assessment of exposure to MRI motion-induced fields based on the International Commission on Non-Ionizing Radiation Protection (ICNIRP) guidelines. *Magn. Reson. Med.* 76, 1291–1300. doi: 10.1002/mrm.26031

Conflict of Interest: The authors declare that the research was conducted in the absence of any commercial or financial relationships that could be construed as a potential conflict of interest.

frontiers in Bioengineering and Biotechnology

ORIGINAL RESEARCH
published: 12 July 2021
doi: 10.3389/fbioe.2021.696360

Statistical-Shape Prediction of Lower Limb Kinematics During Cycling, Squatting, Lunging, and Stepping—Are Bone Geometry Predictors Helpful?

*Joris De Roeck[1], Kate Duquesne[1], Jan Van Houcke[1,2] and Emmanuel A. Audenaert[1,2,3,4]**

[1] Department of Human Structure and Repair, Ghent University, Ghent, Belgium, [2] Department of Orthopedic Surgery and Traumatology, Ghent University Hospital, Ghent, Belgium, [3] Department of Trauma and Orthopedics, Addenbrooke's Hospital, Cambridge University Hospitals NHS Foundation Trust, Cambridge, United Kingdom, [4] Department of Electromechanics, Op3Mech Research Group, University of Antwerp, Antwerp, Belgium

Purpose: Statistical shape methods have proven to be useful tools in providing statistical predications of several clinical and biomechanical features as to analyze and describe the possible link with them. In the present study, we aimed to explore and quantify the relationship between biometric features derived from imaging data and model-derived kinematics.

Methods: Fifty-seven healthy males were gathered under strict exclusion criteria to ensure a sample representative of normal physiological conditions. MRI-based bone geometry was established and subject-specific musculoskeletal simulations in the Anybody Modeling System enabled us to derive personalized kinematics. Kinematic and shape findings were parameterized using principal component analysis. Partial least squares regression and canonical correlation analysis were then performed with the goal of predicting motion and exploring the possible association, respectively, with the given bone geometry. The relationship of hip flexion, abduction, and rotation, knee flexion, and ankle flexion with a subset of biometric features (age, length, and weight) was also investigated.

Results: In the statistical kinematic models, mean accuracy errors ranged from 1.60° (race cycling) up to 3.10° (lunge). When imposing averaged kinematic waveforms, the reconstruction errors varied between 4.59° (step up) and 6.61° (lunge). A weak, yet clinical irrelevant, correlation between the modes describing bone geometry and kinematics was observed. Partial least square regression led to a minimal error reduction up to 0.42° compared to imposing gender-specific reference curves. The relationship between motion and the subject characteristics was even less pronounced with an error reduction up to 0.21°.

Conclusion: The contribution of bone shape to model-derived joint kinematics appears to be relatively small and lack in clinical relevance.

Keywords: lower limb kinematics, bone geometry, musculoskeletal modeling, statistical shape model, SSM-based kinematics, model optimization

OPEN ACCESS

Edited by:
Simone Tassani,
Pompeu Fabra University, Spain

Reviewed by:
Luca Modenese,
Imperial College London, United Kingdom
Raphael Dumas,
Université Gustave Eiffel, France

***Correspondence:**
Emmanuel A. Audenaert
emmanuel.audenaert@ugent.be

Specialty section:
This article was submitted to Biomechanics, a section of the journal Frontiers in Bioengineering and Biotechnology

Received: *16 April 2021*
Accepted: *14 June 2021*
Published: *12 July 2021*

Citation:
De Roeck J, Duquesne K, Van Houcke J and Audenaert EA (2021) Statistical-Shape Prediction of Lower Limb Kinematics During Cycling, Squatting, Lunging, and Stepping—Are Bone Geometry Predictors Helpful? Front. Bioeng. Biotechnol. 9:696360. doi: 10.3389/fbioe.2021.696360

INTRODUCTION

Differences in motion patterns can be attributed to a large number of associated variables: velocity, proprioceptive, vestibular, and visual stimuli as well as neurocognitive and executive functions, body weight, sex, aging effects, and pathological deviations (Schwartz et al., 2004; Chau et al., 2005; Martin et al., 2013; Kobayashi et al., 2016; Reznick et al., 2020). While intuitively vital, the impact of bone and joint geometry on *in vivo* motor variability, nonetheless, remains controversial (Hoshino et al., 2012; Freedman and Sheehan, 2013; Lynch et al., 2020). Recent work on the knee, however, tends to indicate a significant relation between the joint anatomy and both experimentally and model-derived joint motions (Smoger et al., 2015; Nesbitt et al., 2018; Clouthier et al., 2019). Whether these findings can be extrapolated to a possible accurate statistical prediction of multi-body kinematics from mainly bone geometry predictors, remains to be investigated.

Recent advances in computational methodology allow for improved characterization of bone morphometry as well as motion at a population wide level. Statistical shape modeling enables to describe individualized bone geometry more precisely than consensus bone geometry or linearly scaled generic bone models (Audenaert et al., 2019a; Cerveri et al., 2020; Nolte et al., 2020). Similarly, statistical modeling of kinematics by non-linear methods as well as improvements in curve alignment methods during the pre-processing phase, might provide more reliable and stronger correlations between human anatomy and motion as opposed to previous reports (Freedman and Sheehan, 2013; Moissenet et al., 2019; De Roeck et al., 2020). Nevertheless, acquiring perfect kinematic data in an ethically responsible way remains a sticking point. *In vivo* kinematic data can be acquired by means of bone pins, radio-stereometric-analysis or fluoroscopy. However, these invasive and radiation exposing methods in healthy participants are cumbersome because of ethical concerns, and additionally they interfere with normal anatomy and physiological processes (Matsuki et al., 2017; Galvin et al., 2018). In contrast, skin-mounted marker motion capturing does not cause any associated hazards and therefore is the standard for healthy cohorts to date. However, the accuracy of marker-based or optoelectronic motion capture systems is affected by soft tissue artifacts (Andersen et al., 2009; Leardini et al., 2017; Begon et al., 2018; Galvin et al., 2018; Niu et al., 2018; Van Houcke et al., 2019; De Roeck et al., 2020). Several approaches have been developed to deal with these errors, such as multibody kinematics optimization methods (Lu and O'Connor, 1999; Andersen et al., 2009; Leardini et al., 2017; Begon et al., 2018) or by combining the motion tracking system with ultrasound (Niu et al., 2018).

Understanding how bone morphometry affects joint function might reveal fundamental insights into how geometrical features contribute to musculoskeletal disorders (Clouthier et al., 2019). However, the actual relationship between these two entities, kinematics and anatomical shape, remains largely unanswered in literature and low predictability of kinematics based on geometry characteristics has been reported (Lynch et al., 2020).

The objectives of this paper are therefore twofold. First, we intend to quantify individual differences for a wide range of activities of daily living (ADL) at a population-wide level. Statistical kinematic models that aim to describe the inter-subject variance in natural joint motion are appropriate for this purpose (Chau et al., 2005; Deluzio and Astephen, 2007; Leardini et al., 2017; Reznick et al., 2020; Duquesne et al., 2021). Secondly, we aspire to improve upon the understanding the extent to which segmented bone morphometry or subject characteristics are related to model-derived lower limb kinematics.

MATERIALS AND METHODS

Sample Recruitment

A group of able-bodied males aged between 18 and 25 years was recruited to establish the relationship between morphometric and motion variability. A healthy and homogeneous group was chosen to minimize potential bias from clinical (e.g., neurological and musculoskeletal pathology) origin or age-related differences. Therefore, individuals with musculoskeletal disorders or history of surgery were excluded. A second prerequisite to participate involved the absence of overweight (i.e., BMI less than 25 kg/m^2). An overview of population demographics ($n = 57$) is provided in **Table 1**. The study was approved by the Ghent University Hospital Ethics Committee and informed consent was obtained from all participants. As demonstrated in previous work on lunge dynamics, a minimal sample size of 50 is required to reproduce biomechanical waveform data at a population covering level (De Roeck et al., 2020).

Bone Geometry Segmentation and Modeling

The gold standard to obtain individualized bone geometry is the segmentation of shapes from high resolution 3D medical imaging (Nolte et al., 2020). Therefore, the pelvis and lower limb bones of the study cohort were scanned using a 3-Tesla MAGNETOM Trio-Tim System MRI device (Siemens AG, Erlangen, Germany). Following, segmentation procedures were applied to extract the underlying bone geometry. Automatic, model-based segmentation and registration was performed using the Ghent lower limb model (Audenaert et al., 2019b). For

TABLE 1 | General characteristics of the investigated population.

Population descriptors	Mean (95% CI)	Standard deviation
Age (years)	22.1 (21.5–22.7)	2.2
Length (cm)	181.4 (179.8–183.0)	6.3
Weight (kg)	71.5 (69.5–73.5)	7.8
CE angle (°)	28.2 (26.9–29.4)	4.8
Alpha angle (°)	64.5 (62.4–66.5)	8.1
CCD angle (°)	129.2 (128.0–130.3)	4.6
Femoral anteversion (°)	8.8 (6.8–10.9)	8.0

CI, confidence interval; CE angle, center-edge angle (hip acetabulum); CCD angle, caput-collum-diaphyseal angle or femoral neck-shaft angle.

the construction of this model, a total of 606 (left + right side) medical images were previously acquired and analyzed. We refer to the former work for detailed information on model construct and validation (Audenaert et al., 2019a, 2020). Shape model accuracy root-mean-square errors (RMSE) amounts 0.59 ± 0.08 mm, 0.59 ± 0.06 mm, and 0.59 ± 0.06 mm, for the pelvis, femur, and shank bones, respectively. To represent 95% of shape variance, the number of required shape modes in the pelvis, femur, and shank model was estimated at 33, 7, and 6 components, respectively (Audenaert et al., 2019b). By doing so, the combined bone geometry training set was assumed to be accurately described and compactly parameterized, at a population-covering level (Audenaert et al., 2019a). All of these modes were significant in the rank of roots permutation test developed by Vieira (2012). A combined shape model including femur (thighbone), tibia (shinbone), and fibula (calf bone) was additionally defined, with the aim to describe the entire lower limb for the canonical correlation analysis. All analyses were conducted in MATLAB (R2020b, Mathworks, Natick, MA, United States).

Motion Analysis

Twenty-seven skin beads (12 mm) were applied to the bony landmarks of the pelvis-leg apparatus and one at the vertebra prominens. Markers were placed by the same investigator and according to standardized protocols (Gorton et al., 2009; De Roeck et al., 2020). This is crucial as improper marker positioning can induce variability in the kinematics, particularly in the offsets between the kinematic curves of different subjects (Gorton et al., 2009). Spatial marker trajectories were measured using the marker-based 8-camera optical motion capture system from Optitrack (Natural Point Inc., Corvallis, OR, United States).

Subjects were asked to perform several ADL activities. More specifically, the motion analysis included stationary cycling, squat, lunge, and stair movements. Before motion tracking was initiated, each test subject received a brief training of the intended movements. The purpose of this instruction moment was to secure an adequate and smooth recording of the motor tasks. Then each movement was executed and recorded twice. All experiments were conducted in the same setting and under the same circumstances to limit the influence of external factors.

City Bike

To mimic the bicycle movements, a bike model was constructed. As provided in **Figure 1**, the bike model consisted of two pedals, a saddle, and steering handles. For standardization purposes, the test subjects received clear instructions on how to position themselves on the bike and changing the height of the steering handles and the saddle. Subsequently, the volunteers were asked to complete at least three full pedaling cycles.

Race Bike

Subjects were asked to take a seat on the bike model while maximally bending over, to mimic the posture of a professional cyclist. The height of the saddle was adjusted to be equal to the height of the hips of the subject, standing next to the model.

Squat

Squatting is one of the most challenging motions for the hip and knee joints as it generates considerably high reaction forces and it approximates the fully functional flexion range of the lower limb (Schellenberg et al., 2018; Van Houcke et al., 2019). Each subject slowly bent his legs while keeping his heels on the floor. Thereupon, the subjects were asked to hold the resulting position for 2 s, after which they returned to their original starting position.

Lunge

Like the squat, lunging is a closed-chain movement. The subjects stepped approximately 0.6–1.0 m forward with the right leg onto the other force plate. Consequently, both knees bent at the same time. Ultimately, the subjects stood still in this position for a few seconds and pushed off the right foot to rise. The recording ended when the starting position was reached.

Stair Movements

Subjects stood on a step and smoothly stepped up or down to the second step. As for the lunge, the volunteers were asked to use their right leg first. Both ascent and descent staircase motions were modeled individually. Given a previous study showed knee peak flexion angles to be correlated with the step height, the stair level was fixed (Niu et al., 2018).

Musculoskeletal Simulation Analysis

To simulate the ADL activities, the segmented bones, the position of the pelvic, thigh, and shank markers, the motion capture trajectories and force plate data were imported into the AMS (version 7.1.0). For each subject, individualized musculoskeletal models were created using the anybody managed model repository (AMMR) (version 2.0) and the Twente lower extremity model (TLEM) 2.0 (Carbone et al., 2015). Standard simplified joint definitions of the generic human body model were utilized, which include a 3 degree of freedom ball-and-socket joint for the hip joint, a 1 degree of freedom hinge joint for the knee joint, and a 2 degree of freedom condylar joint at the ankle (i.e., flexion and eversion). For the geometrical personalization of the lower limb, we employed a previously developed automated workflow (Van Houcke et al., 2019). Herein, first landmark correspondence between the individual bone geometry and the Anybody template bone geometry is established using the non-rigid registration algorithm of Audenaert et al. (2019b) and Audenaert (2021). Subsequently, automatic non-linear scaling of the musculoskeletal geometry based on the individualized bone geometries of the pelvis, right thigh, and right shank was performed. The left thigh and shank were assumed to be symmetric and were reconstructed through mirroring the corresponding right sided bones. For kinematic analysis, the position of the pelvic, thigh and shank reflective markers relative to the bone was directly imported in contrast to the normal workflow where the marker positions are estimated and optimized. As the positions of the skin markers are one of the factors highly influencing the joint kinematics, importing the positions eliminates one of these (El Habachi et al., 2015). Furthermore, to minimize skin shift effect an overdetermined

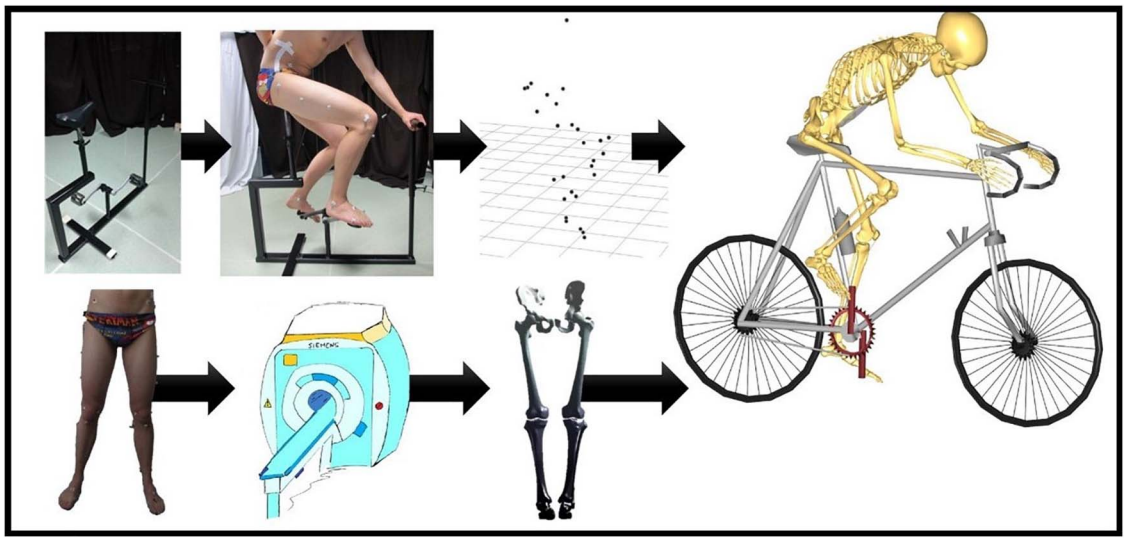

FIGURE 1 | Flow chart of the musculoskeletal simulation in the Anybody Modeling System. On the upper left, there is the bike model that was used by our test panel during the cycling experiments. Motion was recorded frame by frame through skin marker registration. Each subject underwent MRI for determination of the skin tags. Subsequently, Anybody calculated the kinematics for all the recorded frames. An identical workflow was applied for the simulation of squat, lunge, and stair movements.

kinematic solver tracking the experimental markers in a least-squares sense was used (Andersen et al., 2009).

Registration of Lower Limb Kinematics

We evaluated the hip flexion, hip abduction, hip rotation, knee flexion, and ankle flexion of the right leg in a single model for each movement. First, the simulation output from AMS was trimmed based on the knee flexion angles. As such, simulation output denoting subject immobility was rejected (Van Houcke et al., 2019; De Roeck et al., 2020). Then, each kinematic curve was discretized into 101 registration entries assigning 0–100% of movement progression (Sadeghi et al., 2003; Schwartz et al., 2004; Chau et al., 2005; Deluzio and Astephen, 2007; Kobayashi et al., 2016; Matsuki et al., 2017; Bouças et al., 2019; Moissenet et al., 2019; Van Houcke et al., 2019; De Roeck et al., 2020; Reznick et al., 2020; Duquesne et al., 2021; Warmenhoven et al., 2021). At last, a continuous registration (CR) method was applied to remove the phase variability of the curves (Sadeghi et al., 2003; Chau et al., 2005; Duquesne et al., 2021). CR is an alignment technique which converts the unaligned curves into perfectly aligned curves using a warping function. Curves are said to be perfectly aligned with a template curves if they only differ in amplitude. In an iterative process, CR tries to find a warping function that aligns the functional approximation of the waveforms perfectly with the estimated sample mean curve (the template curve). The process is repeated until the estimated sample mean (new template) does not differ significantly from the previously obtained estimated sample mean (the template curve). As such, the curve registration approach contributes to a reduction of the inter-subject variability (Sadeghi et al., 2003). Especially peak values and pronounced features in gait curves will be influenced after implementing the registration (Sadeghi et al., 2003; Duquesne et al., 2021). Regarding the cycling registrations, which curves imply a periodic nature, a Fourier basis was used as a functional approximation of the curves. For the curves of other movements, a spline basis was implemented to fit the kinematic data.

Parameterization of Lower Limb Kinematics

Once the pre-processing was completed, the registrations were parameterized. Therefore, all data was mean centered to examine the variability. To extract the leading dimensions in the kinematic curves, principal component analysis (PCA) of waveforms was applied. PCA of waveforms has been widely used in the literature for the modeling of gait curves (Chau et al., 2005; Deluzio and Astephen, 2007; Kobayashi et al., 2016; Warmenhoven et al., 2021). For each movement, a parameterized model was created based on covariance-based PCA. PCA decomposes the kinematics K into independent principal components (PC), corresponding to the eigenvector P of the covariance matrix $\left(K-\bar{K}\right)^T\left(K-\bar{K}\right)$, as outlined by Jolliffe (1986). $\bar{K}$ serves as the

TABLE 2 | Root-mean-square errors (RMSE ± standard deviation) from the kinematic parameterization.

RMSE (°)	Hip flexion	Hip abduction	Hip external rotation	Knee flexion	Ankle flexion
City bike	1.09 ± 0.07	1.56 ± 0.08	1.62 ± 0.08	1.44 ± 0.09	2.09 ± 0.13
Race bike	1.12 ± 0.08	1.51 ± 0.10	1.78 ± 0.10	1.22 ± 0.08	1.82 ± 0.12
Squat	2.58 ± 0.18	1.53 ± 0.08	2.19 ± 0.13	2.21 ± 0.15	1.80 ± 0.09
Lunge	2.82 ± 0.11	2.48 ± 0.12	2.77 ± 0.13	3.54 ± 0.17	3.33 ± 0.14
Step up	1.79 ± 0.09	1.91 ± 0.08	1.87 ± 0.10	2.12 ± 0.16	2.38 ± 0.10
Step down	1.82 ± 0.09	1.77 ± 0.08	1.93 ± 0.09	2.07 ± 0.09	2.16 ± 0.08

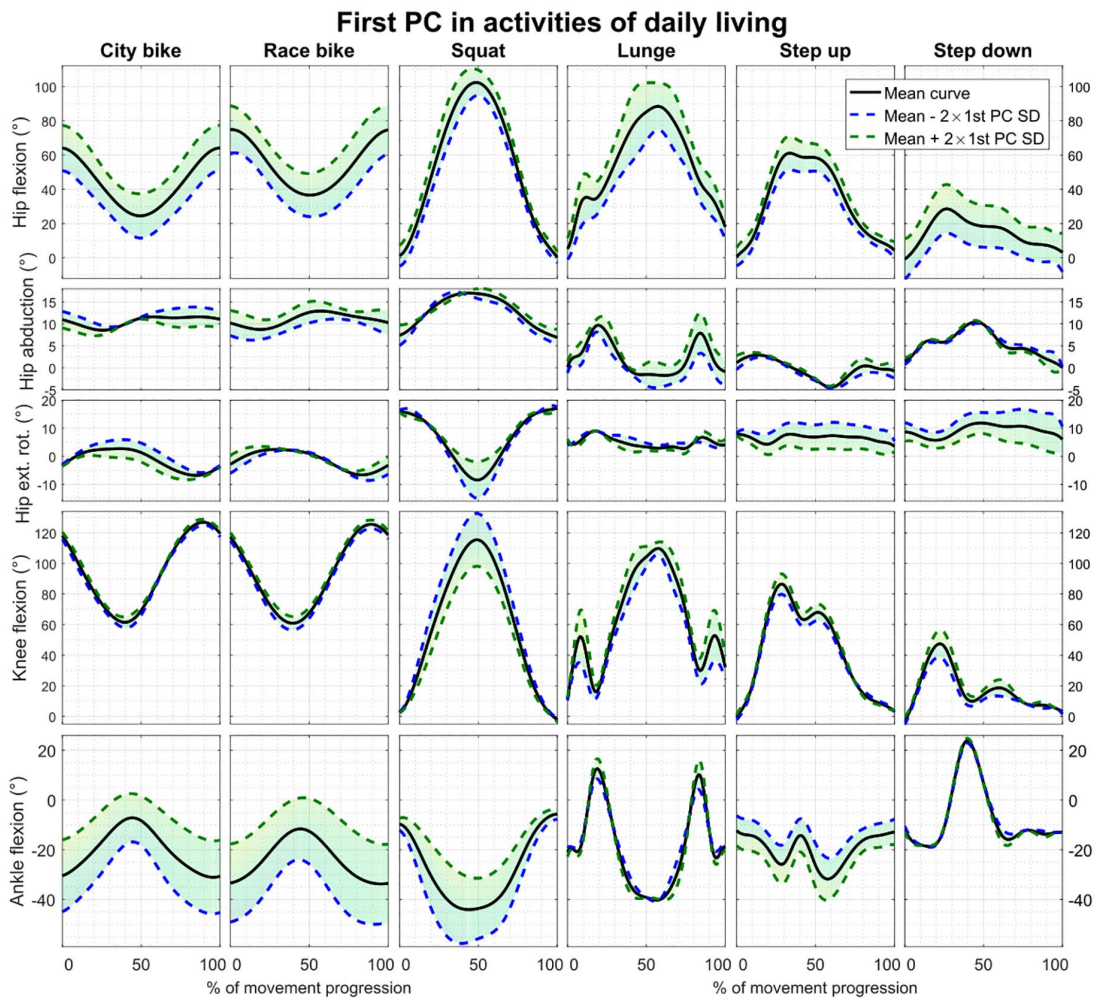

FIGURE 2 | First principal component of all the parameterized kinematic models based on PCA. Model training curves were first aligned by means of CR. The black line depicts the average motion curve, while the green and blue dashed line represent 2 standard deviations (SD) of the first kinematic mode.

average kinematic curve and b equals to the vector of PC weights or modes.

$$K = \bar{K} + Pb$$

The number of significant PC was derived by means of the rank of roots algorithm (Vieira, 2012). Model compactness and accuracy were calculated for each of the motion tasks. The compactness refers to the number of principal components involved in the model. Further, accuracies from our training dataset K consisting of n samples and 101 time frames t were presented by a RMSE.

$$RMSE = \frac{1}{101n} \sum_{i=1}^{n} \sum_{t=1}^{101} \| K_{model,\,i}(t) - K_i(t) \|^2$$

Correlation and Regression Analysis

Canonical correlation (CCA) and partial least squares regression (PLSR) are highly related to each other. However, the emphasis is slightly different. In CCA, the aim is to maximize correlation and to allow for a statistical interpretation of this correlation. CCA is a useful tool to understand the relationship between multiple explanatory variables and a set of response variables (Thompson, 2005). In contrast, PLSR maximizes the covariance, and is typically done for predictive purposes. Therefore, in this work CCA was used to report on the statistical correlation between the motion and shape modes, while PLSR was used to define the predictive value of bone shape.

Given the profound dominance of size in statistical shape models (Audenaert et al., 2019a), CCA was applied on the first PC weight vector from the kinematic model and the PC weights of the shape samples. Additionally, the correlation between a set of general demographic characteristics (i.e., age, length, and weight) of our test subjects and the main kinematic mode was established, similar to the gait prediction studies of Bouças et al. (2019) and Moissenet et al. (2019). Correlations were tested for significance by means of the Wilks' lambda likelihood ratio statistic ($\alpha = 0.05$). The null hypothesis states there is no correlation.

Partial least squares regression was used to predict the kinematic modes starting from the shape modes or the subject

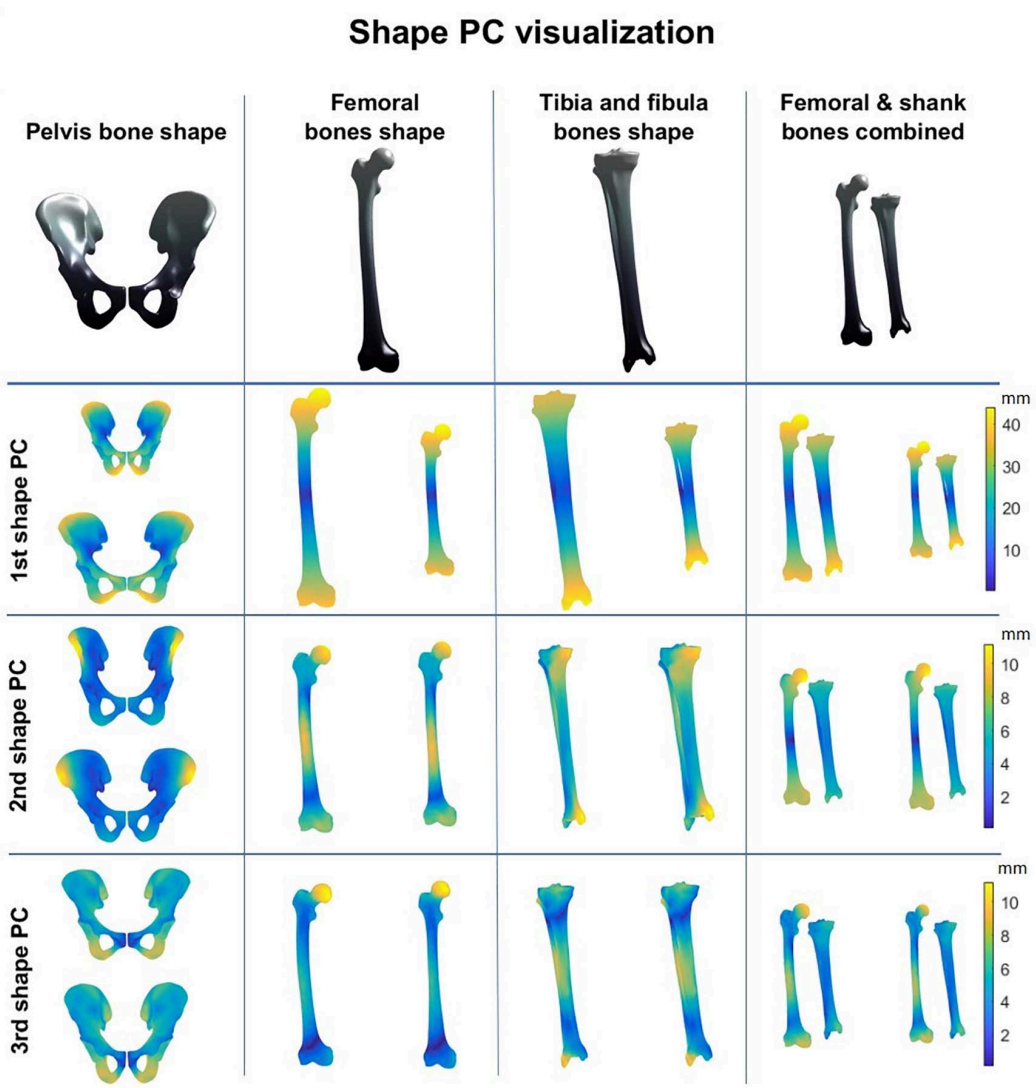

FIGURE 3 | Shape modes from the personalized bone shape models of pelvis, femur, shank (tibia + fibula), and femur and shank combined. Averaged geometry is displayed at the top while variation is represented with a color scheme (average shape ± 3 standard deviations of the shape principal components).

characteristics. To minimize overfitting of the data, only one partial least square regression component was used. To assess the regression fit, reconstruction errors of the shape-specific kinematic predictions were benchmarked again the RMSE when imposing the average curve for all subjects. Again, differences were tested by means of the two-tailed pairwise *t*-test ($\alpha = 0.05$).

$$RMSE = \frac{1}{101n}\sum_{i=1}^{n}\sum_{t=1}^{101} \| K_{prediction,\,i}(t) - K_i(t) \|^2$$

RESULTS

Reconstruction errors of the statistical kinematic models vary between 1.09° and 3.54° and are listed in **Table 2**. The city bike, race bike, and step up models all consist of five principal components retaining 92.43, 93.91, and 79.64% of population variance, respectively. Conversely, the squat, lunge, and step down models are composed of seven principal components having 88.22, 78.87, and 85.33% of population variance, respectively. The interpretation of the main principal component from the six kinematic models is outlined in **Figure 2**.

A combined shape model was introduced involving the femur, tibia and fibula bone geometry. Herein, the first 10 modes reproduce 95% of shape variance in the data and all of them are significant according to the rank of roots permutation test. The 3 dominant principal components from the 4 geometry models are shown in **Figure 3**. Furthermore, the results of the canonical correlation analyses are summarized in **Table 3**. Overall, canonical correlation coefficients are weak

and the correlations between the kinematic model and the pelvis geometry seem of interest, yet likely attributable to overfitting, considering the large amount of shape components required to describe pelvic anatomy.

Finally, the performance of the PLS regression is presented in **Table 4**. The RMSE on the predicted curves are all significantly lower compared to reference curve (i.e., average motion curves) benchmarking for each ADL. However, these corrections were modest and clinically insignificant, ranging from 0.14° to 0.41° when using bone shape as regression input and between 0.04° and 0.11° when subject characteristics serve as input variables. As such, only 1.4% (step down) up to 16.6% (race cycling) of kinematic variance could be explained by statistical shape models. On the other hand, merely 1.4% (step up) up to 7.3% (lunge) of kinematic variance could be explained by age, length, and weight.

DISCUSSION

The canonical correlations between the shape modes and kinematic modes are weak, even for the first mode which is predominantly representing the overall size. The association between the set of subject characteristics and kinematics is also found to be weak with still less explained kinematic variance, lower correlation coefficients and even less prediction ability. As such, our findings are similar to the trial from Moissenet et al. (2019) in which lower limb sagittal kinematics (hip, knee, and ankle flexions) during gait were predicted based on demographic parameters (walking speed, gender, age, and BMI) with errors exceeding 5°. In summary, when considering healthy Caucasian males aged between 20 and 25 years, correlation and predictions between shape and kinematic modes were not found to be clinically relevant. Hence, it seems that the applied modeling and statistical approaches are overkill methodology to the problem. In contrast, it appears that the statistical predictions based on some basic demographic parameters (i.e., without predictors based on bone geometry) might be as valid for the prediction of hip flexion, abduction, and rotation, knee flexion, and ankle flexion similar as reported in the literature for gait (Rasmussen et al., 2020).

While the presented methodology could not demonstrate important shape related variability in motion patterns, future work is mandatory to investigate such in pathological mixed groups, where the impact of bone geometry abnormalities is likely

TABLE 3 | Canonical correlation analysis between the significant shape PC weights or biometric variables and the first kinematic mode.

Kinematic model	Demographics/anatomy				
	Age, length, and weight	**Pelvis bone shape**	**Femoral bone shape**	**Tibia and fibula bones shape**	**Femur and shank bones combined**
Correlation measure	r^2 (p)	r^2 (p)	r^2 (p)	r^2 (p)	r^2 (p)
City bike	0.1479 (p = 0.036)	0.7012 (p = 0.060)	0.2420 (p = 0.249)	0.2170 (p = 0.355)	0.3578 (p = 0.245)
Race bike	0.0911 (p = 0.178)	0.6758 (p = 0.157)	0.2401 (p = 0.291)	0.2248 (p = 0.357)	0.4127 (p = 0.128)
Squat	0.0433 (p = 0.543)	0.7399 (p = 0.078)	0.2769 (p = 0.210)	0.1502 (p = 0.779)	0.4156 (p = 0.174)
Lunge	0.2559 (p = 0.002)	0.7787 (p = 0.009)	0.3364 (p = 0.053)	0.1731 (p = 0.619)	0.4902 (p = 0.026)
Step up	0.0643 (p = 0.331)	0.5881 (p = 0.498)	0.1873 (p = 0.544)	0.2570 (p = 0.227)	0.4555 (p = 0.057)
Step down	0.1129 (p = 0.093)	0.6210 (p = 0.276)	0.1202 (p = 0.850)	0.1795 (p = 0.549)	0.2943 (p = 0.509)

TABLE 4 | Partial least squares regression of the demographics and the combined femur and shank model PC weights to predict ADL kinematics.

	PLS regression based on bone geometry		**PLS regression based on age, length, and weight**		**RMSE ± SD when imposing reference curves (°)**
	RMSE ± SD (°)	**Explained kinematic variance (%)**	**RMSE ± SD (°)**	**Explained kinematic variance (%)**	
City bike	5.49 ± 2.18	12.9	5.84 ± 2.18	3.9	5.91 ± 2.19
Race bike	5.96 ± 2.23	16.6	6.29 ± 2.35	4.8	6.37 ± 2.35
Squat	6.11 ± 2.00	4.3	6.33 ± 1.99	2.3	6.40 ± 2.02
Lunge	6.26 ± 1.85	4.1	6.50 ± 1.95	7.3	6.61 ± 1.97
Step up	4.45 ± 1.31	1.8	4.55 ± 1.48	1.4	4.59 ± 1.50
Step down	4.95 ± 1.60	1.4	5.05 ± 1.68	5.7	5.11 ± 1.71

Predictions are benchmarked again the RMSE when imposing the average curve. All RMSE differences were significant at the 0.05 level. The percentages of explained kinematic variance by the regression models are also given. SD, standard deviation.

to be of higher importance. The presented methodology seems adequate to investigate these patterns.

The results of our research are affected by some limitations. Although further investigations might extend our findings, our study cohort represents a very selected group, especially with minimal age and height differences among subjects, and accordingly their kinematic variability was limited (Kobayashi et al., 2016). Furthermore, the sexual dimorphism of pelvic, femoral and tibial bone morphometry were not taken into account in the correlation analysis, since our study involved male subjects only (Audenaert et al., 2019a). While this approach minimized the impact of confounding variables and allowed us to deploy a well-controlled methodological pipeline, it limits the extent to which our conclusions can be extrapolated. Findings might be different in pathological conditions, with possibly more sources of variability and eventually with more meaningful and notable patterns. Clearly, more work in this area is needed.

Secondly, our findings are specific to the five model-derived joint angles approach used and the way the bone geometry is taken into account in the multibody kinematics optimization process. As such the study design aimed for the detection of obvious and large scale kinematic features such as walking with toes pointed outward. Our findings can therefore not be entirely generalized. For example, subtle relationships have been previously reported in the literature between joint shape and 6 degrees of freedom tibio-femoral kinematics (Smoger et al., 2015; Valente et al., 2015; Nesbitt et al., 2018; Clouthier et al., 2019; Martelli et al., 2020).

Furthermore, this study relies on the assumption that subject-specific motion can be predicted by a small set of parameters. Reconstruction errors of the statistical kinematic models generally range around 2 degrees, which corresponds to the inter-session error in the gait study from Schwartz et al. (2004) on lower-limb kinematics. Further, these errors are in line with the measurement errors classically found in optoelectronic experiments in a review from Leardini et al. (2017) comparing marker-based registrations to fluoroscopy and bone pins experiments.

Lastly, the sparse amount of data remains a major drawback in our investigation. Therefore, the regression analysis should be interpreted cautiously, and one must be aware of the potential risk of overfitting. Moreover, the pelvis shape model is notably less compact than the other models and therefore less suitable to regression analysis, particularly when having restricted numbers of training samples. Thereupon, pelvis bone morphometry was not incorporated into our combined shape model. Even though intra-subject variability was minimized by CR, no obvious patterns could be found here to link between bone morphometry and observable patterns in motion tasks. Alternatively, prediction performance may improve using deep learning methodology, however, such would require sample sizes to be substantially forced up (Bouças et al., 2019).

In conclusion, motion curves are not prominently related to subject characteristics or personal bone geometry in the present study. Furthermore, when benchmarked against average kinematic reference curves, personalization based on bone geometry appears to lack in clinical relevance.

DATA AVAILABILITY STATEMENT

The datasets generated for this study are available on reasonable request to the corresponding author.

ETHICS STATEMENT

The studies involving human participants were reviewed and approved by Ghent University Hospital Ethics Committee. The patients/participants provided their written informed consent to participate in this study.

AUTHOR CONTRIBUTIONS

JD, KD, and EA designed the algorithms. JD, JV, and EA assisted in the data collection and manipulation. JD and KD carried out the statistical analysis. JD wrote the first draft of the manuscript. All authors contributed to the manuscript revision and approved the submitted version.

FUNDING

EA was financially supported by a senior clinical fellowship from the Research Foundation Flanders.

REFERENCES

Andersen, M. S., Damsgaard, M., and Rasmussen, J. (2009). Kinematic analysis of over-determinate biomechanical systems. *Comput. Methods Biomech. Biomed. Engin.* 12, 371–384. doi: 10.1080/10255840802459412

Audenaert, E. (2021). *nonrigidICP–File Exchange–MATLAB Central*. Available online at: https://nl.mathworks.com/matlabcentral/fileexchange/41396-nonrigidicp (accessed February 1, 2021).

Audenaert, E. A., den Eynde, J., de Almeida, D. F., Steenackers, G., Vandermeulen, D., and Claes, P. (2020). Separating positional noise from neutral alignment in multicomponent statistical shape models. *Bone Rep.* 12:100243. doi: 10.1016/j.bonr.2020.100243

Audenaert, E. A., Pattyn, C., Steenackers, G., De Roeck, J., Vandermeulen, D., and Claes, P. (2019a). Statistical shape modeling of skeletal anatomy for sex discrimination: their training size, sexual dimorphism, and asymmetry. *Front. Bioeng. Biotechnol.* 7:302. doi: 10.3389/fbioe.2019.00302

Audenaert, E. A., Van Houcke, J., Almeida, D. F., Paelinck, L., Peiffer, M., Steenackers, G., et al. (2019b). Cascaded statistical shape model based segmentation of the full lower limb in CT. *Comput. Methods Biomech. Biomed. Engin.* 22, 644–657. doi: 10.1080/10255842.2019.1577828

Begon, M., Andersen, M. S., and Dumas, R. (2018). Multibody kinematics optimization for the estimation of upper and lower limb human joint kinematics: a systematized methodological review. *J. Biomech. Eng.* 140:03 0801.

Bouças, C., Ferreira, J. P., Coimbra, A. P., Crisóstomo, M. M., and Mendes, P. A. S. (2019). "Generating individual gait kinetic patterns using machine learning," in *Proceedings of the International Conference on Applied Technologies*, Cham: Springer, 53–64. doi: 10.1007/978-3-030-42520-3_5

Carbone, V., Fluit, R., Pellikaan, P., Van Der Krogt, M. M., Janssen, D., Damsgaard, M., et al. (2015). TLEM 2.0–A comprehensive musculoskeletal geometry dataset for subject-specific modeling of lower extremity. *J. Biomech.* 48, 734–741. doi: 10.1016/j.jbiomech.2014.12.034

Cerveri, P., Belfatto, A., and Manzotti, A. (2020). Predicting knee joint instability using a tibio-femoral statistical shape model. *Front. Bioeng. Biotechnol.* 8:253. doi: 10.3389/fbioe.2020.00253

Chau, T., Young, S., and Redekop, S. (2005). Managing variability in the summary and comparison of gait data. *J. Neuroeng. Rehabil.* 2, 1–20.

Clouthier, A. L., Smith, C. R., Vignos, M. F., Thelen, D. G., Deluzio, K. J., and Rainbow, M. J. (2019). The effect of articular geometry features identified using statistical shape modelling on knee biomechanics. *Med. Eng. Phys.* 66, 47–55. doi: 10.1016/j.medengphy.2019.02.009

De Roeck, J., Van Houcke, J., Almeida, D., Galibarov, P., De Roeck, L., and Audenaert, E. A. (2020). Statistical modeling of lower limb kinetics during deep squat and forward lunge. *Front. Bioeng. Biotechnol.* 8:233.

Deluzio, K. J., and Astephen, J. L. (2007). Biomechanical features of gait waveform data associated with knee osteoarthritis: an application of principal component analysis. *Gait Posture* 25, 86–93. doi: 10.1016/j.gaitpost.2006.01.007

Duquesne, K., De Roeck, J., Salazar-Torres, J.-J., and Audenaert, E. (2021). "Statistical kinematic modeling: concepts and model validity," in *Proceedings of the 26th Annual Meeting Gait and Clinical Movement Analysis Society*, West Chester, PA.

El Habachi, A., Moissenet, F., Duprey, S., Cheze, L., and Dumas, R. (2015). Global sensitivity analysis of the joint kinematics during gait to the parameters of a lower limb multi-body model. *Med. Biol. Eng. Comput.* 53, 655–667. doi: 10.1007/s11517-015-1269-8

Freedman, B. R., and Sheehan, F. T. (2013). Predicting three-dimensional patellofemoral kinematics from static imaging-based alignment measures. *J. Orthop. Res.* 31, 441–447. doi: 10.1002/jor.22246

Galvin, C. R., Perriman, D. M., Newman, P. M., Lynch, J. T., Smith, P. N., and Scarvell, J. M. (2018). Squatting, lunging and kneeling provided similar kinematic profiles in healthy knees—a systematic review and meta-analysis of the literature on deep knee flexion kinematics. *Knee* 25, 514–530. doi: 10.1016/j.knee.2018.04.015

Gorton, G. E. III, Hebert, D. A., and Gannotti, M. E. (2009). Assessment of the kinematic variability among 12 motion analysis laboratories. *Gait Posture* 29, 398–402. doi: 10.1016/j.gaitpost.2008.10.060

Hoshino, Y., Wang, J. H., Lorenz, S., Fu, F. H., and Tashman, S. (2012). The effect of distal femur bony morphology on in vivo knee translational and rotational kinematics. *Knee Surg. Sport Traumatol. Arthrosc.* 20, 1331–1338. doi: 10.1007/s00167-011-1661-3

Jolliffe, I. T. (1986). "Principal components in regression analysis," in *Principal Component Analysis*, (New York, NY: Springer), 129–155. doi: 10.1007/978-1-4757-1904-8_8

Kobayashi, Y., Hobara, H., Heldoorn, T. A., Kouchi, M., and Mochimaru, M. (2016). Age-independent and age-dependent sex differences in gait pattern determined by principal component analysis. *Gait Posture* 46, 11–17. doi: 10.1016/j.gaitpost.2016.01.021

Leardini, A., Belvedere, C., Nardini, F., Sancisi, N., Conconi, M., and Parenti-Castelli, V. (2017). Kinematic models of lower limb joints for musculo-skeletal modelling and optimization in gait analysis. *J. Biomech.* 62, 77–86. doi: 10.1016/j.jbiomech.2017.04.029

Lu, T. W., and O'Connor, J. J. (1999). Bone position estimation from skin marker co-ordinates using global optimisation with joint constraints. *J. Biomech.* 32, 129–134. doi: 10.1016/s0021-9290(98)00158-4

Lynch, J. T., Perriman, D. M., Scarvell, J. M., Pickering, M. R., Warmenhoven, J., Galvin, C. R., et al. (2020). Shape is only a weak predictor of deep knee flexion kinematics in healthy and osteoarthritic knees. *J. Orthop. Res* . 38, 2250–2261. doi: 10.1002/jor.24622

Martelli, S., Sancisi, N., Conconi, M., Pandy, M. G., Kersh, M. E., Parenti-Castelli, V., et al. (2020). The relationship between tibiofemoral geometry and musculoskeletal function during normal activity. *Gait Posture* 80, 374–382. doi: 10.1016/j.gaitpost.2020.06.022

Martin, K. L., Blizzard, L., Wood, A. G., Srikanth, V., Thomson, R., Sanders, L. M., et al. (2013). Cognitive function, gait, and gait variability in older people: a population-based study. *J. Gerontol. Ser. A Biomed. Sci. Med. Sci.* 68, 726–732. doi: 10.1093/gerona/gls224

Matsuki, K., Matsuki, K. O., Kenmoku, T., Yamaguchi, S., Sasho, T., and Banks, S. A. (2017). In vivo kinematics of early-stage osteoarthritic knees during pivot and squat activities. *Gait Posture* 58, 214–219. doi: 10.1016/j.gaitpost.2017.07.116

Moissenet, F., Leboeuf, F., and Armand, S. (2019). Lower limb sagittal gait kinematics can be predicted based on walking speed, gender, age and BMI. *Sci. Rep.* 9:9510.

Nesbitt, R. J., Bates, N. A., Rao, M. B., Schaffner, G., and Shearn, J. T. (2018). Effects of population variability on knee loading during simulated human gait. *Ann. Biomed. Eng.* 46, 284–297. doi: 10.1007/s10439-017-1956-8

Niu, K., Sluiter, V., Homminga, J., Sprengers, A., and Verdonschot, N. (2018). "A novel ultrasound-based lower extremity motion tracking system," in *Intelligent Orthopaedics*, eds G. Zheng, W. Tian, and X. Zhuang (Singapore: Springer), 131–142. doi: 10.1007/978-981-13-1396-7_11

Nolte, D., Ko, S.-T., Bull, A. M. J., and Kedgley, A. E. (2020). Reconstruction of the lower limb bones from digitised anatomical landmarks using statistical shape modelling. *Gait Posture* 77, 269–275. doi: 10.1016/j.gaitpost.2020.02.010

Rasmussen, J., Lund, M. E., and Waagepetersen, R. P. (2020). Data-based parametric biomechanical models for cyclic motions. *Adv. Transdiscipl. Eng.* 11, 372–379.

Reznick, E., Embry, K., and Gregg, R. D. (2020). "Predicting individualized joint kinematics over a continuous range of slopes and speeds," in *Proceedings of the 2020 8th IEEE RAS/EMBS International Conference for Biomedical Robotics and Biomechatronics (BioRob)*, New York, NY, 666–672.

Sadeghi, H., Mathieu, P. A., Sadeghi, S., and Labelle, H. (2003). Continuous curve registration as an intertrial gait variability reduction technique. *IEEE Trans. Neural Syst. Rehabil. Eng.* 11, 24–30. doi: 10.1109/tnsre.2003.810428

Schellenberg, F., Taylor, W. R., Trepczynski, A., List, R., Kutzner, I., Schütz, P., et al. (2018). Evaluation of the accuracy of musculoskeletal simulation during squats by means of instrumented knee prostheses. *Med. Eng. Phys Phys.* 61, 95–99. doi: 10.1016/j.medengphy.2018.09.004

Schwartz, M. H., Trost, J. P., and Wervey, R. A. (2004). Measurement and management of errors in quantitative gait data. *Gait Posture* 20, 196–203. doi: 10.1016/j.gaitpost.2003.09.011

Smoger, L. M., Fitzpatrick, C. K., Clary, C. W., Cyr, A. J., Maletsky, L. P., Rullkoetter, P. J., et al. (2015). Statistical modeling to characterize relationships between knee anatomy and kinematics. *J. Orthop. Res.* 33, 1620–1630. doi: 10.1002/jor.22948

Thompson, B. (2005). "Canonical correlation analysis," in *Encyclopedia of Statistics in Behavioral Science*, Vol. 1, eds B. Everitt and D. C. Howell (West Sussex: Wiley), 192–196.

Valente, G., Pitto, L., Stagni, R., and Taddei, F. (2015). Effect of lower-limb joint models on subject-specific musculoskeletal models and simulations of daily motor activities. *J. Biomech.* 48, 4198–4205. doi: 10.1016/j.jbiomech.2015.09.042

Van Houcke, J., Galibarov, P. E., Van Acker, G., Fauconnier, S., Allaert, E., Van Hoof, T., et al. (2019). Personalized hip joint kinetics during deep squatting in young, athletic adults. *Comput. Methods Biomech. Biomed. Engin.* 23, 23–32. doi: 10.1080/10255842.2019.1699539

Vieira, V. M. (2012). Permutation tests to estimate significances on principal components analysis. *Comput. Ecol. Softw.* 2:103.

Warmenhoven, J., Bargary, N., Liebl, D., Harrison, A., Robinson, M. A., Gunning, E., et al. (2021). PCA of waveforms and functional PCA: a primer for biomechanics. *J. Biomech.* 116: 110106. doi:10.1016/j.jbiomech.2020.110106

Conflict of Interest: The authors declare that the research was conducted in the absence of any commercial or financial relationships that could be construed as a potential conflict of interest.

frontiers in Bioengineering and Biotechnology

ORIGINAL RESEARCH
published: 21 July 2021
doi: 10.3389/fbioe.2021.679360

Subject-Specific Modeling of Femoral Torsion Influences the Prediction of Hip Loading During Gait in Asymptomatic Adults

Enrico De Pieri[1,2,3], Bernd Friesenbichler[4], Renate List[4], Samara Monn[4], Nicola C. Casartelli[4,5], Michael Leunig[6] and Stephen J. Ferguson[3]*

[1] Laboratory for Movement Analysis, University of Basel Children's Hospital, Basel, Switzerland, [2] Department of Biomedical Engineering, University of Basel, Basel, Switzerland, [3] Institute for Biomechanics, ETH Zurich, Zürich, Switzerland, [4] Human Performance Lab, Schulthess Clinic, Zürich, Switzerland, [5] Laboratory of Exercise and Health, ETH Zurich, Schwerzenbach, Switzerland, [6] Department of Orthopaedic Surgery, Schulthess Clinic, Zürich, Switzerland

OPEN ACCESS

Edited by:
Simone Tassani,
Pompeu Fabra University, Spain

Reviewed by:
Geoffrey Ng,
Imperial College London,
United Kingdom
Hans Kainz,
University of Vienna, Austria

***Correspondence:**
Enrico De Pieri
enrico.depieri@unibas.ch

Specialty section:
This article was submitted to Biomechanics, a section of the journal Frontiers in Bioengineering and Biotechnology

Received: *11 March 2021*
Accepted: *02 June 2021*
Published: *21 July 2021*

Citation:
De Pieri E, Friesenbichler B, List R, Monn S, Casartelli NC, Leunig M and Ferguson SJ (2021) Subject-Specific Modeling of Femoral Torsion Influences the Prediction of Hip Loading During Gait in Asymptomatic Adults. Front. Bioeng. Biotechnol. 9:679360. doi: 10.3389/fbioe.2021.679360

Hip osteoarthritis may be caused by increased or abnormal intra-articular forces, which are known to be related to structural articular cartilage damage. Femoral torsional deformities have previously been correlated with hip pain and labral damage, and they may contribute to the onset of hip osteoarthritis by exacerbating the effects of existing pathoanatomies, such as cam and pincer morphologies. A comprehensive understanding of the influence of femoral morphotypes on hip joint loading requires subject-specific morphometric and biomechanical data on the movement characteristics of individuals exhibiting varying degrees of femoral torsion. The aim of this study was to evaluate hip kinematics and kinetics as well as muscle and joint loads during gait in a group of adult subjects presenting a heterogeneous range of femoral torsion by means of personalized musculoskeletal models. Thirty-seven healthy volunteers underwent a 3D gait analysis at a self-selected walking speed. Femoral torsion was evaluated with low-dosage biplanar radiography. The collected motion capture data were used as input for an inverse dynamics analysis. Personalized musculoskeletal models were created by including femoral geometries that matched each subject's radiographically measured femoral torsion. Correlations between femoral torsion and hip kinematics and kinetics, hip contact forces (HCFs), and muscle forces were analyzed. Within the investigated cohort, higher femoral antetorsion led to significantly higher anteromedial HCFs during gait (medial during loaded stance phase and anterior during swing phase). Most of the loads during gait are transmitted through the anterior/superolateral quadrant of the acetabulum. Correlations with hip kinematics and muscle forces were also observed. Femoral antetorsion, through altered kinematic strategies and different muscle activations and forces, may therefore lead to altered joint mechanics and pose a risk for articular damage. The method proposed in this study, which accounts for both morphological and kinematic characteristics,

might help in identifying in a clinical setting patients who, as a consequence of altered femoral torsional alignment, present more severe functional impairments and altered joint mechanics and are therefore at a higher risk for cartilage damage and early onset of hip osteoarthritis.

Keywords: femoral torsion, hip osteoarthritis, hip contact forces, muscle lever arms, musculoskeletal modeling, EOS imaging

INTRODUCTION

Increased or abnormal intra-articular forces can lead to structural damages to the articular cartilage, loss of joint integrity, and tissue degeneration and thus to hip osteoarthritis (OA) (Solomon, 1976; Klaue et al., 1991; Tanzer and Noiseux, 2004; Ganz et al., 2008; Felson, 2013). The altered stresses in localized areas of the cartilage are often determined by a combination of overall excessive loading, due for instance to obesity or intense physical activities, as well as by morphological abnormalities in the hip joint structures (Felson, 2013).

Two main types of hip morphology have been identified as potential risk factors for developing hip OA: Hip dysplasia and morphologies associated with femoroacetabular impingement (FAI) syndrome, that is, cam morphology (reduced femoral head–neck offset) or pincer morphology (deep and/or retroverted acetabulum) (Thomas et al., 2012; Felson, 2013). However, other morphological features, such as femoral torsion, may contribute to the onset of hip OA, as it may exacerbate or diminish the effects of an existing cam and/or pincer morphology (Zeng et al., 2016). Indeed, femoral torsion can considerably affect impingement-free hip range of motion, aggravating or compensating excessive cartilage loading caused by concomitant cam/pincer deformities (Schmaranzer et al., 2019).

Femoral torsional and coronal deformities have previously been correlated with hip pain and labral damage (Tönnis and Heinecke, 1999). The presence of structural hip abnormalities is often observed in patients presenting labral tears (Wenger et al., 2004). Another study documented that among patients who underwent hip arthroscopy for labral pathology or FAI, the ones with higher femoral antetorsion presented larger and more anterior labral tears (Ejnisman et al., 2013). Femoral torsion is known to have a strong influence on the loading environment in the proximal femur and the hip (Heller et al., 2001). Increased femoral torsion has also been associated with complications in the adjacent joints, such as knee pain and OA (Eckhoff et al., 1997; Bretin et al., 2011), patellar instability, and pain (Powers, 2003; Stevens et al., 2014). Furthermore, abnormal values of femoral torsion could also represent a risk factor for hip dislocation (Upadhyay et al., 1985; Novais et al., 2019).

Femoral deformities that have been linked to hip joint degeneration are understood to represent developmental variations of normal human anatomy (Hogervorst et al., 2011, 2012). In particular, the amount of femoral torsion depends on age and sex (Hetsroni et al., 2013), starting approximatively at 40° at birth and ranging between 15° and 20° during adulthood (Fabry et al., 1973). Developmental torsional deformities of the lower limb in children and adolescents represent a frequent reason for consultation with pediatric orthopedic clinicians (Fabry, 2010). In addition to cosmetic considerations regarding their gait (Fabry, 2010), these deformities have been associated with the development of gait impairment and joint pain (Bruderer-Hofstetter et al., 2015). Nevertheless, there is no consistent definition of what can be considered excessive or pathological femoral antetorsion, with threshold values spanning between $> 30°$ and $> 50°$ (Jani et al., 1979; Cordier and Katthagen, 2000; Hefti, 2000; Alexander et al., 2019). Moreover, optimal surgical treatment for mechanically induced hip pain depends upon understanding the forces that are produced within the acetabulum and the potential mechanical consequences of femoral reorientation.

There is a general understanding that the rotational alignment of the whole lower limb plays a critical role in the onset of hip pathologies (Eckhoff, 1994; Keshmiri et al., 2016). Additionally, several kinematic compensatory strategies can be adopted at the hip (Bruderer-Hofstetter et al., 2015; Alexander et al., 2019), as a consequence of either pain avoidance (Leigh et al., 2016; Popovic et al., 2020) or lever arm dysfunction, particularly of the hip abductors (Arnold et al., 1997; van der Krogt et al., 2012; Boyer et al., 2016). Moreover, modeling excessive femoral antetorsion was shown to alter magnitude and orientation of predicted joint contact forces in pediatric pathological populations (Bosmans et al., 2014; Passmore et al., 2018), as well as in typically developing children (Kainz et al., 2020).

A complete understanding of the influence of femoral antetorsion on hip joint loading requires subject-specific morphometric and biomechanical data on the movement characteristics of individuals exhibiting varying degrees of femoral torsion. Musculoskeletal modeling allows us to estimate muscle activations and intra-articular joint forces (Erdemir et al., 2007) in relation to individual motion patterns and musculoskeletal geometry and represents therefore a suitable tool for a comprehensive evaluation of the lower-limb biomechanics in association with femoral torsional morphologies. Musculoskeletal models are commonly built starting from a cadaveric-based model template, which is scaled or morphed to match the overall anthropometrics of an individual subject (Andersen, 2021). However, these scaled models may not necessarily resemble the real anatomy of a subject, particularly when his/her bone morphology largely deviates from the baseline cadaveric template. The inclusion of additional subject-specific parameters, such as femoral torsion, may reduce the uncertainty associated with model scaling.

The aim of this study was to evaluate hip kinematics and kinetics, hip contact forces (HCFs), and muscle forces during gait in a group of asymptomatic adult subjects presenting a

heterogeneous range of femoral torsion. It was hypothesized that increased femoral torsion may lead to alterations in hip kinematics and loading. Specifically, higher femoral torsion was expected to alter muscle lever arms and potentially lead to kinematic compensations, thus influencing the muscle recruitment pattern and the predicted required muscle forces and therefore determining changes in the resulting HCFs. In order to achieve this, personalized musculoskeletal models were created based on three-dimensional (3D) gait analysis data and morphological data extracted from low-dosage biplanar radiographic imaging. The effect of modeling subject-specific femoral torsion was additionally investigated by qualitatively analyzing changes in muscle lever arms for a broad range of hip motions and by comparing, in the examined cohort, HCFs predicted with personalized and generic models during gait.

MATERIALS AND METHODS

Participants

Thirty-seven healthy volunteers (27.7 ± 4.6 years old, 15 females, mean BMI = 23.0 ± 2.6) were recruited for this study. Subjects between 18 and 50 years of age were considered eligible for the study if they did not present back or lower-extremity pain at the time of the study; any surgery or significant injury on the back or lower extremities in the last 12 months; a history of open or arthroscopic hip surgery; known conditions affecting gait, balance, or physical activities; a BMI over 35 kg/m^2; or pregnancy.

Radiographic Data

A full-length radiograph of the lower limbs was acquired for each subject using a low-dosage biplanar EOS system (EOS Imaging Inc., France) (Folinais et al., 2013). An effective radiation dose lower than 0.63 mSv guaranteed minimal risks to the participants (Mettler et al., 2008; Buck et al., 2012; Rosskopf et al., 2016). Femoral torsion was assessed on 3D reconstructions of the femur, utilizing the biplanar EOS radiographs (sterEOS software, EOS Imaging Inc., France) (Buck et al., 2012). It was calculated as the angle between a line through the femoral neck and a line adapted to the posterior contour of the femoral condyles (Hernandez et al., 1981). The line through the femoral neck was defined as the midline between the cortices of the femoral neck through the caudally projected center of the femoral head. Antetorsion was defined as the clockwise rotation of the proximal relative to the distal femur.

Data from a randomly chosen leg for each subject were included in the analysis. Measured torsional values ranged from −7° of retrotorsion to + 38° of antetorsion, with a mean value of 16.2° ± 10.0°. The average difference between the two limbs of each subject was 4.2° (range: 0.1°–14.5°).

Motion-Capture Data

Lower-limb kinematics and kinetics were collected during gait using a 13-camera motion-capture system (Vicon Motion Systems Ltd., Oxford, United Kingdom) capturing at 200 Hz, synchronized with three force plates (Kistler Instrumentation, Winterthur, Switzerland) sampling at 1,000 Hz.

The lower extremities were equipped with 47 skin-mounted markers according to the IfB markers set (List et al., 2013) and extended with three markers on the trunk.

After the acquisition of a standing trial in an anatomic upright position, each subject completed five successful stride cycles for each leg. Walking speed was self-selected but controlled to be within ± 10% of the first assessed trial (cohort mean = 5.21 km/h, SD = 0.58 km/h).

All markers were labeled and gap-filled in Vicon Nexus (versions 2.8, 2.9, 2.10, Vicon, Oxford, United Kingdom). Kinematic data were filtered using a low-pass (10 Hz, fourth order) Butterworth filter. Ground reaction force (GRF) data were filtered using a low-pass Butterworth filter (20 Hz, fourth order), and heel strike and toe-off were determined from the GRF measurements using force thresholds (> 20 N for heel strike and < 20 N for toe-off).

Musculoskeletal Modeling

Musculoskeletal modeling was performed with a commercially available software (AnyBody Modeling System, version 7.3, Aalborg, Denmark) (Damsgaard et al., 2006), using motion-capture data as input.

Personalized models were created from a detailed musculoskeletal model of the lower limb (De Pieri et al., 2018), based on a cadaveric dataset (Carbone et al., 2015), which was scaled to match the anthropometrics of each patient and the marker data collected during a standing reference trial (Lund et al., 2015; **Figure 1A**). The hip joint is modeled as a 3-degrees of freedom (DOF) ball-and-socket joint, while knee, talocrural, and subtalar joints are modeled as 1-DOF hinges. Additionally, the position of the patella is defined as a function of the knee flexion angle. The distance between hip joint centers (HJCs) measured in the radiographic images was used as a reference for scaling the pelvic width to improve the models' accuracy (Fischer et al., 2018). In each subject-specific model, both femurs were morphed to include a transversal rotation between the proximal and distal sections, matching the subject's femoral torsion measured from the radiographic data (**Figure 1A**). The femoral morphing was based on radial basis function 3D transformation.

A kinematic analysis based on the marker trajectories was conducted to compute joint kinematics (Andersen et al., 2009; Lund et al., 2015; **Figure 1B**). Secondly, an inverse dynamics analysis, based on a third-order-polynomial muscle recruitment criterion, was performed to calculate required muscle activations and forces, as well as resulting joint moments and contact forces (Andersen, 2021).

As the spatial orientation of the femoral segment in the global reference frame is determined by the positions of the bony-landmark-based markers, the inclusion of a morphed femoral geometry did not affect the calculation of joint kinematics, rather just the position of muscles' origin and insertion points along the femur and their lines of action relative to the adjacent joints.

Femoral Torsion and Muscle Lever Arms

The morphed femurs present different orientations of the muscles' line of actions relative to the joints' positions, as illustrated in **Figure 2** for three different torsional configurations.

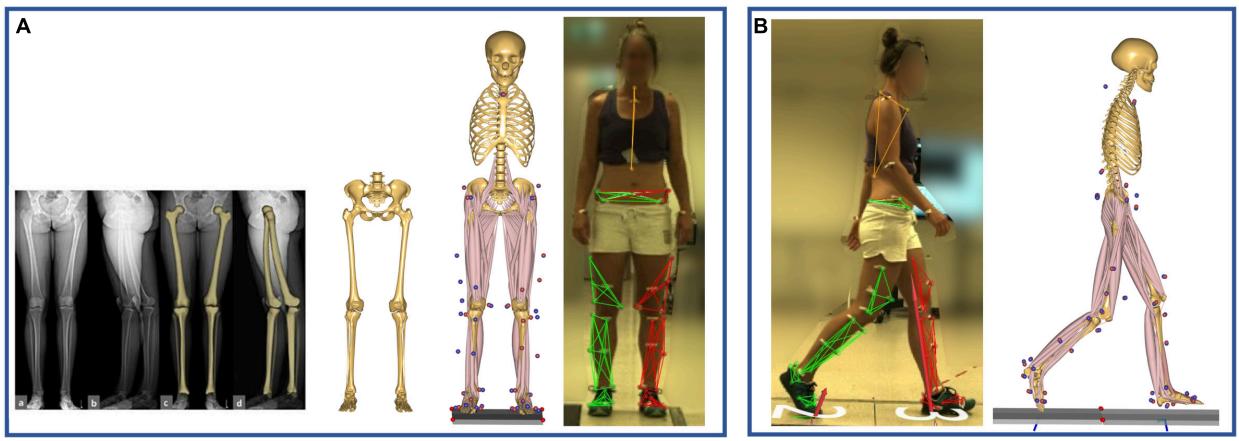

FIGURE 1 | (A) Model scaling and personalization based on subject-specific radiographic measurements, obtained through a low-dosage biplanar EOS system (EOS Imaging Inc., France). The distance between the hip joint centers, measured in the frontal plane, was used to scale the pelvic width, while the femoral torsion was calculated through 3D reconstructions of the femurs (sterEOS software, EOS Imaging Inc., France). The model was scaled to match the subject's anthropometrics based on marker data collected during a standing reference trial. **(B)** Kinematic and kinetic analyses during gait were based on the tracking of the measured marker trajectories.

The lever arms of the femur-spanning muscles were also qualitatively evaluated for four arbitrary modeled femoral morphologies: The baseline unmorphed model, characterized by a femoral antetorsion of 5.5°, as well as morphed femurs with retrotorsion of −15° and antetorsion of + 25° and + 45°. These femoral morphologies were implemented in a generic model corresponding to the 50th percentile male anthropometrics. Lever arms were calculated for each individual muscle fascicle across artificial ranges of hip sagittal motion (20° extension, 90° flexion), hip frontal motion (30° adduction, 50° abduction), and hip transversal motion (40° internal, 40° external rotation). Average lever arms were calculated for the fascicles constituting each muscle over the different joint ranges of motion (De Pieri et al., 2018). Additionally, muscle lever arms were also calculated for the morphed femur with + 45° of antetorsion and a fixed hip internal rotation angle of 20°, in order to mimic a compensatory kinematic strategy suspected to restore abduction capacity in pathological patients with torsional deformities (Arnold et al., 1997).

Gait Analysis

Gait trials were processed and analyzed through the toolkit AnyPyTools[1] (Lund et al., 2019), in the Python programming language (Python Software Foundation). 3D hip kinematics were calculated in the anatomical coordinate systems described by Klein Horsman et al. (2007) and based on the International Society for Biomechanics' (ISB) recommendations (Wu et al., 2002). The foot progression angle relative to the direction of gait was also calculated. The orientation of the foot was identified through an axis connecting the heel and the second-metatarsal markers, while the direction of gait was defined as the line connecting the positions of the heel marker in two consecutive ipsilateral heel strikes. 3D hip internal net moments (or torques) were reported in the proximal coordinate system (pelvis) according to ISB recommendations (Wu et al., 2002; Derrick et al., 2020). Joint moments were normalized by body mass.

All the data were time-normalized from heel strike (0%) to heel strike (100%) and interpolated to 1% steps (101 points). An average per patient was then calculated based on the five gait trials collected.

Muscle Forces and HCFs

The optimal configuration of muscle forces necessary for the generation of the overall lower-limb joint torques were computed based on the muscle recruitment criterion. The reported muscle forces are defined as the sum of the forces generated by all fascicles constituting each muscle.

Resulting HCFs were also calculated in a proximal (pelvis-based) coordinate system according to ISB recommendations (Wu et al., 2002; Derrick et al., 2020; **Figure 3**).

Muscle forces and HCFs were normalized by body weight, time-normalized from heel strike to heel strike, and averaged per patient.

Additionally, to estimate the orientation of the HCF on the acetabulum, the HCF vector was intersected with an idealized hemisphere representing the acetabulum, and the contact force pathways were plotted (Weber et al., 2012; De Pieri et al., 2020). The components of the HCF vector were decomposed in a reference frame with its origin in the HJC and aligned with the acetabular opening plane, standardized to 45° of inclination and 20° of anteversion for all subjects, as shown in **Figure 3**. Positive x components indicate anteriorly oriented forces, while positive z components indicate superolateral oriented forces. The diameter of the hemisphere was also standardized to 54 mm (Krebs et al., 2009). Average force contact pathways were calculated for each subject and for the mean HCF vector across the whole cohort.

[1]https://github.com/AnyBody-Research-Group/AnyPyTools

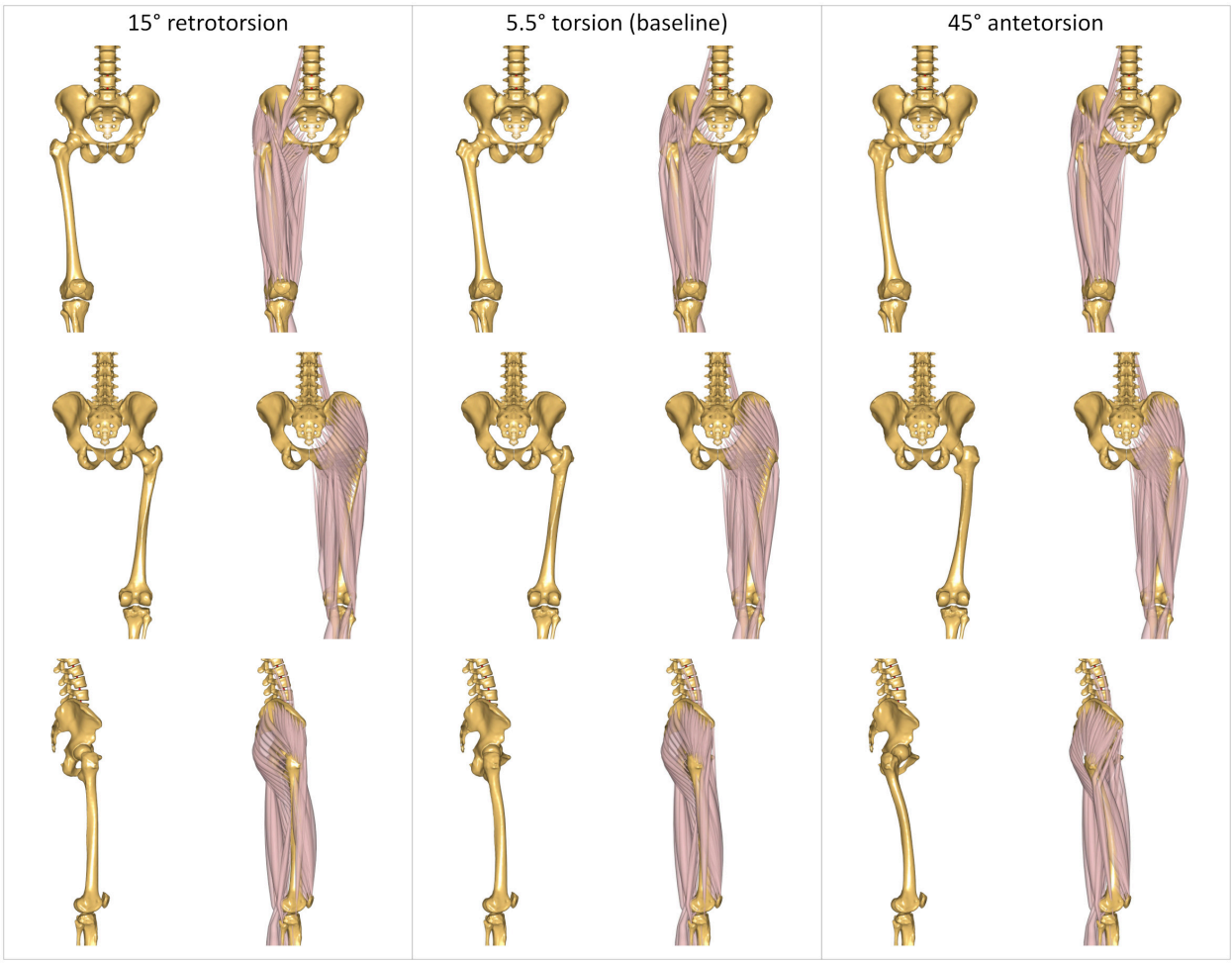

FIGURE 2 | Three representative modeled torsional configurations implemented in the AnyBody Modeling System. The femurs are characterized by 15° of retrotorsion (left); 5.5° of antetorsion (center), corresponding to the baseline unmorphed model; and 45° of antetorsion (right). Illustrations report anterior (top), posterior (middle), and lateral (bottom) views. Each view is reported without and with muscles, to better visualize the effect of the morphing on the bone geometry, and the resulting changes in the muscles' lines of action.

Statistical Parametric Mapping Analysis

The relationships between femoral torsion and lower-limb kinematics, hip internal net moments, HCFs, and muscle forces were analyzed by means of statistical parametric mapping (SPM) (Friston et al., 1994; SPM1d[2], v0.4.3; Pataky, 2012).

The three kinematic components of the hip joint were regarded as a vector field, describing the 3D variation over time of the kinematic vector trajectory (Pataky et al., 2013), while the foot progression angle was considered as separate one-dimensional, time-dependent scalar. Canonical correlation analyses (CCAs), the vectorial equivalent of a linear regression, were carried out to evaluate the effect of femoral torsion on hip kinematics in the examined cohort. The use of vector field analysis takes into consideration covariance between spatial components, thus reducing errors due to covariation bias (Pataky et al., 2013). Statistically significant correlation between femoral torsion and foot progression angle was instead analyzed through a scalar linear regression analysis.

CCAs were also conducted to identify statistically significant correlations between femoral torsion and hip internal net moments and HCFs, both described as 3D vectorial fields. Additionally, muscles were grouped according to their main function in hip extensors, hip flexors, hip abductors, and hip adductors. The forces generated by the muscles in each functional group were also considered as multidimensional vectorial field, similar to Pataky et al. (2013). CCA was also used to analyze the relationships between femoral torsion and the forces generated in each functional muscle compartment.

The relevant output test statistic—SPM{X2} for CCA and SPM{t} for linear regression—was evaluated at each point of the gait cycle (GC). The significance level was set at $\alpha = 0.05$, and the corresponding critical thresholds—X2* or t*—were calculated based on the temporal smoothness of the input data through random field theory. Finally, the probability

[2]www.spm1d.org

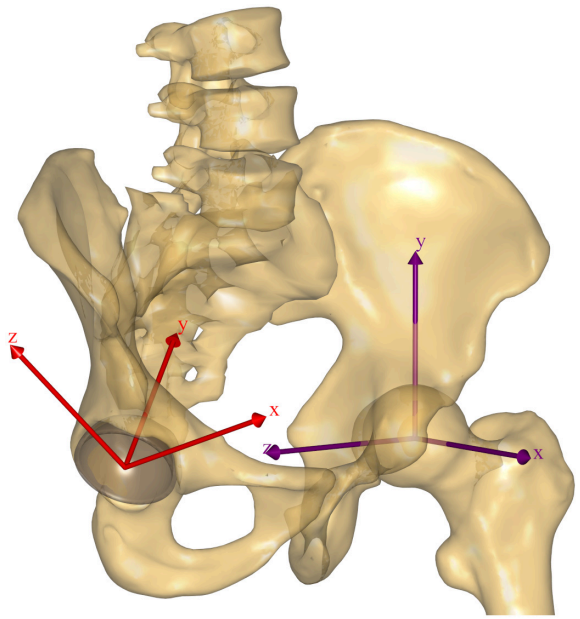

FIGURE 3 | The pelvis-based reference frame according to ISB recommendations is reported in purple for the left hip, while the acetabular reference frame is reported in red for the right hip. The latter is aligned with the acetabular opening plane for the decomposition of the HCF vector; its origin is coincident with the HJC, the *y* axis is perpendicular to the acetabular opening plane, and the *x* axis is oriented to the anterior (+)/posterior (–) direction, while the *z* axis is oriented to the superolateral direction (+) and passes through the mid-acetabular notch (–). The idealized hemisphere used to calculate the intersection of the HCF vector on the acetabulum is illustrated for the right hip in light gray.

that similar suprathreshold regions would have occurred from equally smooth random waveforms was calculated. In case of vectorial CCA, *post hoc* scalar field linear regressions were also conducted separately on each component of the vectorial field, with Bonferroni-corrected significance threshold levels, adjusted at $\alpha = 0.05/n$, with n indicating the number of components of the specific vectorial field.

In the interest of clarity, only differences which were statistically significant for more than 2% of GC are discussed.

Effect of Modeling Femoral Torsion

Finally, the effect of including subject-specific femoral torsion in the models was evaluated by comparing the predictions of the models with generic or personalized femoral morphologies. Specifically, an SPM vectorial paired Hotelling T^2 test was conducted to investigate differences in 3D HCFs, with a significance level of $\alpha = 0.05$. *Post hoc* scalar field linear paired *t*-tests were also conducted separately on each force component. The root mean square deviation (RMSD) between HCF components predicted with the generic or personalized models was also calculated for each subject and reported against subject-specific femoral torsion values.

RESULTS

Muscle Lever Arms

The qualitative analysis of muscle lever arms indicates a reduction of iliacus and rectus femoris hip flexing lever arm with increased antetorsion values, particularly when the hip is in an extended position, as well as changes in iliacus, psoas major, and rectus hip external/internal rotation lever arms.

The superior compartment of the gluteus maximus presents reduced lever arms for hip extension with a retrotorted femur, while both its extensive and abductive lever arms are increased for antetorted morphologies.

The abductor muscles see a decrease in their abductive lever arms with antetorted morphologies; however, the convenience of their lever arms is restored when an additional, fixed, 20° internal rotation of the hip is modeled (**Figure 4**). Gluteus medius and minimus also acquire a more convenient extensive lever arm for increased antetorsion values, while their internal/external rotation lever arms are affected in both retrotorted and antetorted configurations.

The lever arms around the hip of the adductor muscles are relatively unaffected by the modeling of different femoral morphologies.

A complete overview of the changes in muscle lever arms for different modeled femoral morphologies is reported as **Supplementary Figure 1**.

Gait Kinematics and Kinetics

Within the investigated cohort, statistically significant correlations between femoral torsion angles and the subjects' kinematics during gait were observed for the 3D hip joint angles during pre-swing to initial swing (57–63% GC). The *post hoc* linear regression analysis of the three individual kinematic components indicates a negative correlation between femoral torsion and hip external rotation. The foot progression angle presents a positive correlation with femoral torsion during terminal stance (39–56% GC) (**Figure 5**).

No statistically significant correlation was observed for the 3D hip internal joint moments in the investigated cohort (**Figure 6**).

Muscle Forces and HCFs

In terms of predicted muscle forces required during gait, correlations were found for hip flexors, extensors, abductors, and adductors muscle groups (**Figure 7**). The forces generated by the hip flexors correlated with femoral torsion during mid-stance and terminal stance (15–28% and 38–58% GC, respectively). The *post hoc* analysis revealed a positive correlation for the rectus femoris during mid-stance and for both rectus femoris and sartorius during terminal stance. The forces generated by the hip extensors correlated with femoral torsion from loading response to mid-stance and during terminal stance (7–33% and 39–46% GC). The *post hoc* analysis revealed a positive correlation for the gluteus maximus during terminal stance and a negative correlation for biceps femoris, semimembranosus, and semitendinosus during mid-stance. The forces generated by the hip abductors correlated with femoral torsion during

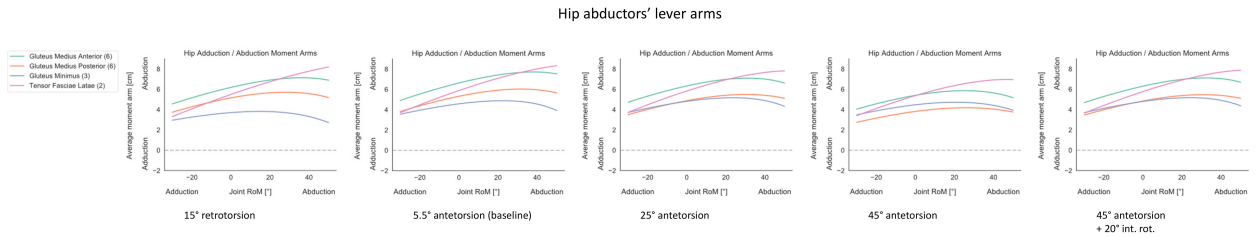

FIGURE 4 | Hip abductors' lever arms were calculated for each individual muscle fascicle across a range of hip frontal motion (30° adduction, 50° abduction). Average lever arms were calculated for the fascicles constituting each muscle and the specific number of fascicles is reported in brackets next to the muscle's name. Four different modelled femoral morphologies were compared: the baseline unmorphed model, characterized by a femoral antetorsion of 5.5°, as well as morphed femurs with retrotorsion of −15° and antetorsion of +25° and +45°, reported as columns. Additionally, muscle lever arms were also calculated for the morphed femur with +45° of ante-torsion and a fixed hip internal rotation angle of 20° (rightmost column), in order to mimic a compensatory kinematic strategy suspected to restore abduction capacity in pathological patients with torsional deformities. A complete overview of the changes in muscle lever arms is reported in **Supplementary Figure 1**.

terminal stance, initial swing, and terminal swing (35–55%, 61–75%, and 87–96% GC, respectively). The *post hoc* analysis revealed a negative correlation for the gluteus minimus during initial and terminal swing phases. The forces generated by the hip adductors correlated with femoral torsion during the initial swing phase (59–70% GC). The *post hoc* analysis did not reveal any prominent trend for the individual adductor muscles.

A statistically significant correlation was found between 3D HCFs and femoral torsion in the investigated cohort during terminal stance and mid-swing (48–52% and 65–79% GC). From the *post hoc* analysis, it emerged that subjects with higher antetorsion have more medially oriented HCFs in mid-stance and more anteriorly oriented HCFs during the swing phase (**Figure 8**).

A more extensive analysis of all SPM output test statistics is reported in **Supplementary Figure 2**.

The qualitative analysis of the mean HCF pathway reveals that the loads during gait are transmitted from the femur mostly to the anterior superolateral quadrant of the acetabulum (**Figure 9**). During the initial loading response (0–10% GC), the HCF vector is slightly posteriorly oriented in the upper half of the acetabulum, while during mid-stance and terminal stance (10–50% GC), corresponding to single-limb support, the HCF vector shifts more anteriorly and is characterized by higher values in terms of magnitude. During pre-swing (50–60% GC), the HCF vector starts translating inferomedially while maintaining an overall anterior orientation. During the swing phase, the intra-articular loads transmitted through the hip are smaller, and the HCF vector produces a longer contact path on the acetabulum, starting from the anterior/superolateral quarter, spanning through the anterior/inferomedial one, and ending in the center of the superolateral half.

Effect of Modeling Femoral Torsion

The inclusion of a morphed, personalized femoral torsional morphology in the models led to statistically significant differences in HCFs through the entire GC when compared to models with a generic (baseline) femoral morphology (**Figure 10**). In particular, the models with morphed femoral geometry predicted less proximally and medially oriented forces during mid-stance to terminal stance and more anteriorly oriented forces throughout the GC. The RMSD between HCF components predicted with generic or personalized models increased with a qualitative linear trend for larger deviations between subject-specific femoral torsion and the torsion of the baseline generic model (5.5°), for both antetorted and retrotorted configurations.

DISCUSSION

This study investigated the effect of femoral torsion on hip kinematics, kinetics, muscle forces, and contact forces during gait in a group of asymptomatic adults presenting a heterogeneous range of femoral torsion. For this purpose, personalized musculoskeletal models were created based on individual morphological data obtained with low-dosage radiography and driven with matching individual kinematic data acquired during motion-capture gait analysis. HCFs predicted through musculoskeletal models were compared against the predictions obtained with a generic model, and the changes in muscle lever arms associated with different degrees of femoral torsion were also qualitatively analyzed.

Within the investigated cohort, higher femoral antetorsion led to significantly higher anteromedial HCFs during gait (medial during loaded stance phase and anterior during swing phase). Additionally, statistically significant correlations with femoral torsion were observed for foot and hip kinematics. In particular, subjects with higher antetorsion walked with a more internally rotated foot during terminal stance and with a more internally rotated hip in the transition from stance to swing. This could indicate that specific kinematic patterns or compensatory mechanisms could be adopted also in the asymptomatic population. This result indicates that a complete evaluation of a condition must include a functional assessment of a subject/patient and specifically take into account his/her specific joint kinematics.

The analysis of the muscles' lever arms in different modeled femoral morphologies indicates that femoral antetorsion has an

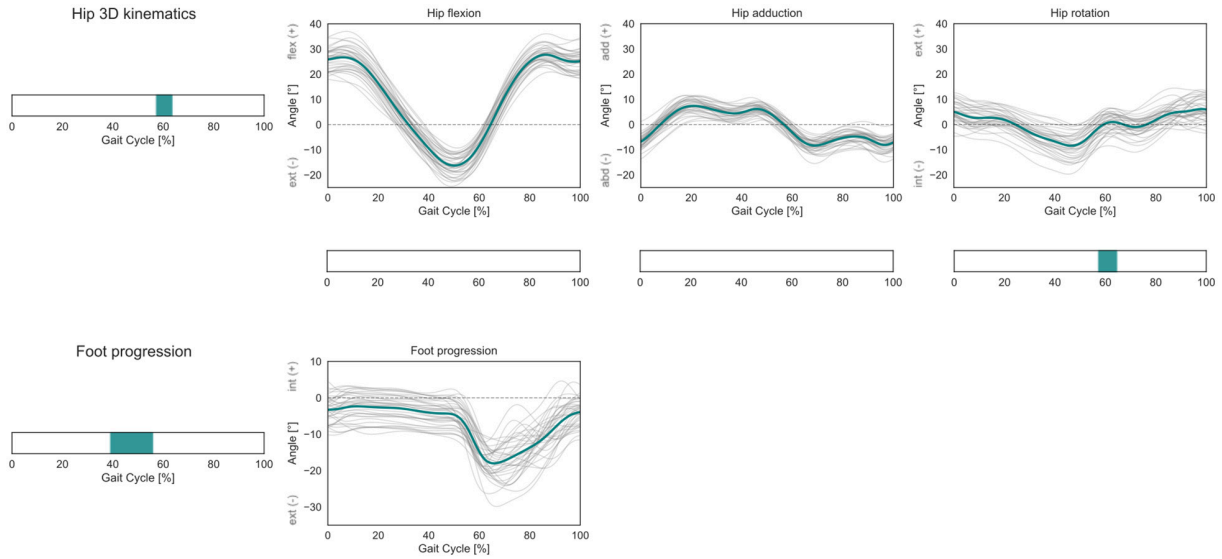

FIGURE 5 | Hip 3D kinematics and foot progression angle over the GC. Average profiles for each subject are reported in gray, while the cohort's mean is reported in turquoise. For the hip joint 3D kinematics, phases of GC in which a statistically significant correlation was observed in the SPM vector-field CCA are indicated in the leftmost panel. Below each kinematic component, the results of the *post hoc* scalar-field linear regression analyses are reported. For the foot progression angle, the phases of GC in which a statistically significant correlation was observed in the SPM scalar-field linear regression analysis are indicated in the leftmost panel.

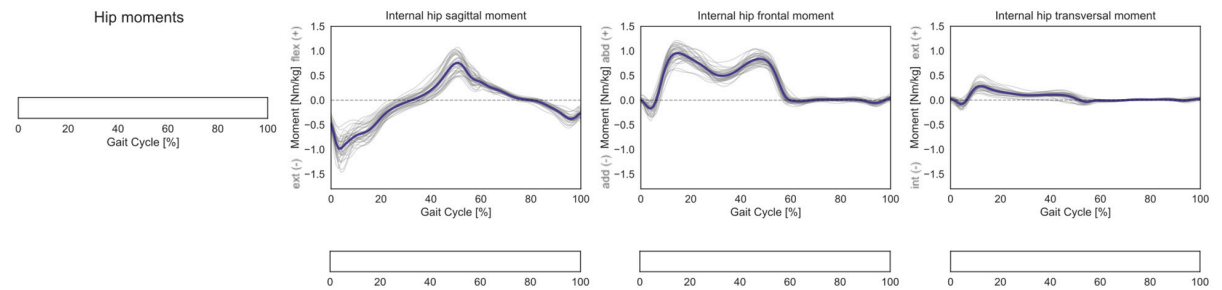

FIGURE 6 | Hip 3D internal net joint moments over the GC. Moments are normalized by body mass. Average profiles for each subject are reported in gray, while the cohort's mean is reported in dark blue. No statistically significant correlation was observed in the SPM vector-field CCA (leftmost panel), nor in the *post hoc* scalar-field linear regression analyses (below each kinematic component).

important effect on the lever arm length of several muscles and particularly on the abductive capacity of gluteus medius and gluteus minimus. Similar to that of Arnold et al. (1997), this study confirmed that internally rotating the hip can restore the hip abductor lever arms in the presence of excessive femoral antetorsion. Hip abductors have an important functional role in the stability of the hip and pelvis (Retchford et al., 2013), particularly during gait (van der Krogt et al., 2012). Muscle weakness of the hip abductors may result in compensatory activation of other muscles (van der Krogt et al., 2012) and lead to more anterior HCFs (Lewis et al., 2007). Moreover, muscle weaknesses in the presence of altered femoral morphology can further impair gait performance (Vandekerckhove et al., 2021). In the examined cohort, statistically significant correlations between femoral torsion and the muscle forces generated during gait by hip flexor, extensor, abductor, and adductor muscle groups were also observed. Femoral antetorsion, through altered kinematic strategies and/or different muscle activations and forces, may therefore lead to altered HCFs and pose a risk for articular damage.

The personalization of the musculoskeletal models based on subject-specific torsional values led to statistically significant differences in the predicted HCFs throughout the GC in comparison to the generic baseline model, based on a cadaveric template. This finding is in agreement with previous studies (Passmore et al., 2018; Kainz et al., 2020). Higher RMSD values were found for subjects with high femoral antetorsion or high femoral retrotorsion, indicating that the more a subject's morphology differs from the generic model, the more important it is to account for these differences. While a fully subject-specific modeling approach would require the inclusion of bone geometries and muscle lines of actions from CT scans or

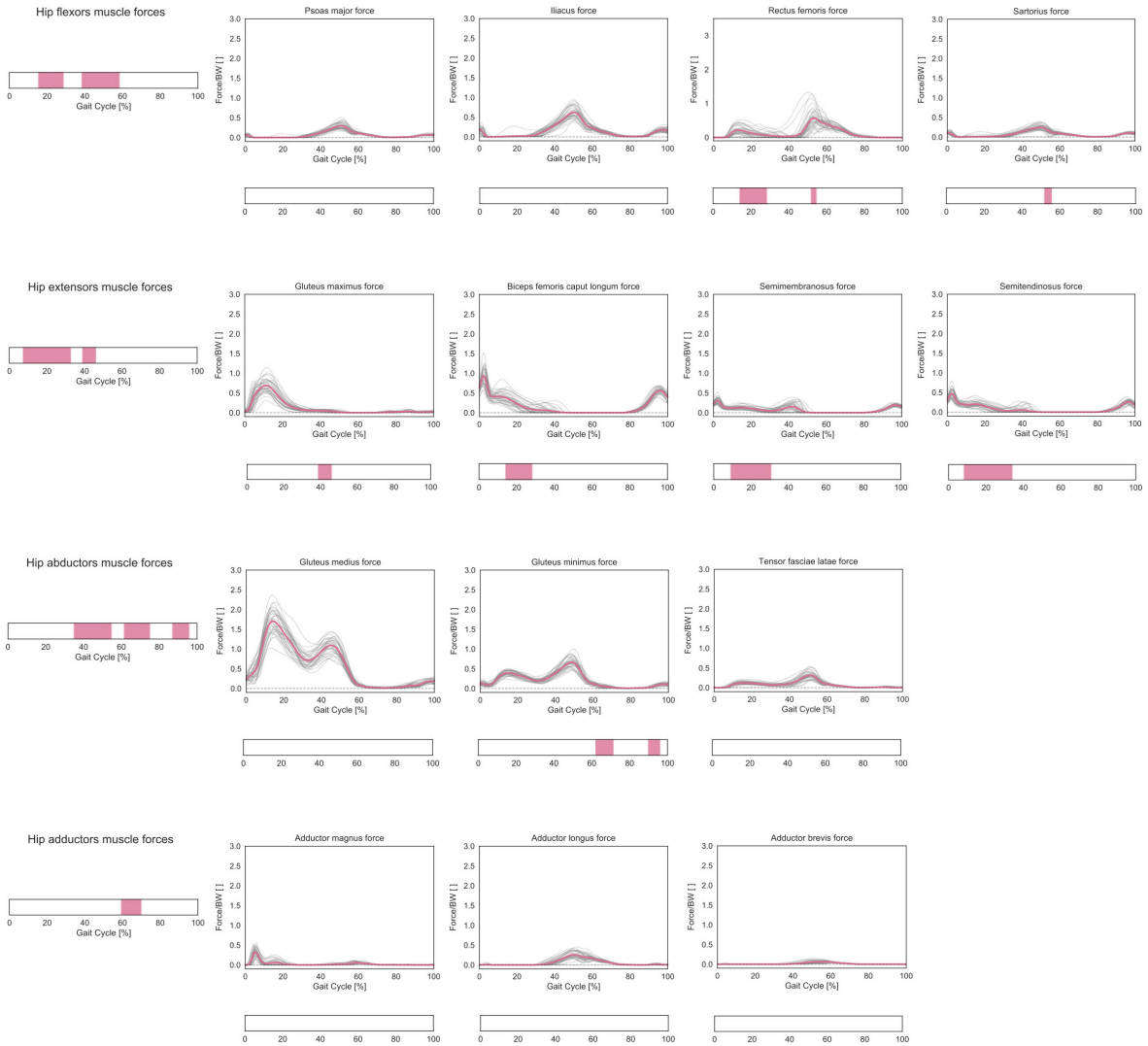

FIGURE 7 | Predicted lower-limb muscle forces during the GC. Forces are normalized by body weight (BW). Average profiles for each subject are reported in gray, while the cohort's mean is reported in pink. Muscles were grouped according to their main function in hip extensors, hip flexors, hip abductors, and hip adductors, and the predicted muscle forces in each functional group were considered as a multidimensional vectorial field. For each muscle compartment, phases of GC in which a statistically significant correlation was observed in the SPM vector-field CCA are indicated in the leftmost panel. Below each muscle, the results of the *post hoc* scalar-field linear regression analyses are reported.

MRI (Dejtiar et al., 2020; Modenese and Kohout, 2020), it is also a rather time-consuming approach (Andersen, 2021), and it could introduce additional uncertainties and errors in the identification of muscle insertion and origins (Carbone et al., 2012; Valente et al., 2014).

Morphing the femoral geometry of a generic model to match the torsional angle of a specific subject represents a rapid and effective alternative to personalized models, which could therefore be more applicable in a clinical setting. Using nominal torsional values as input, musculoskeletal models could also be personalized when the acquisition of imaging data is not possible and only clinical assessments of the torsional angles are available (Scorcelletti et al., 2020), even if these measurements are characterized by a larger uncertainty (Günther et al., 1996).

The mean HCF pathway revealed that loads during gait are transmitted from the femur mostly to the anterior superolateral quadrant of the acetabulum. While the qualitative analysis of the HCF pathway in this study was based on a generic acetabular orientation, including subject-specific information on acetabular inclination and anteversion might help to accurately identify whether certain subjects present high loads applied onto specific peripheral regions of the acetabulum. The clinical relevance of analyzing intra-articular load distributions in patients with hip pathologies remains to be further verified and would certainly require a more comprehensive analysis of all other anatomical factors that could predispose to hip pathologies. For instance, in patients with FAI syndrome, cartilage degeneration occurs mainly in the

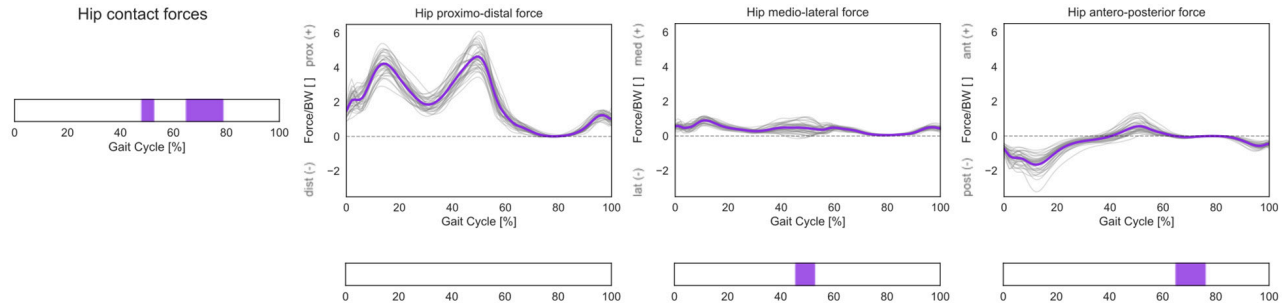

FIGURE 8 | 3D HCFs over the GC. HCFs were calculated in a proximal (pelvis-based) coordinate system according to ISB recommendations and are normalized by body weight (BW). Average profiles for each subject are reported in gray, while the cohort's mean is reported in violet. Phases of GC in which a statistically significant correlation was observed in the SPM vector-field CCA are indicated in the leftmost panel. Below each force component, the results of the *post hoc* scalar-field linear regression analyses are reported.

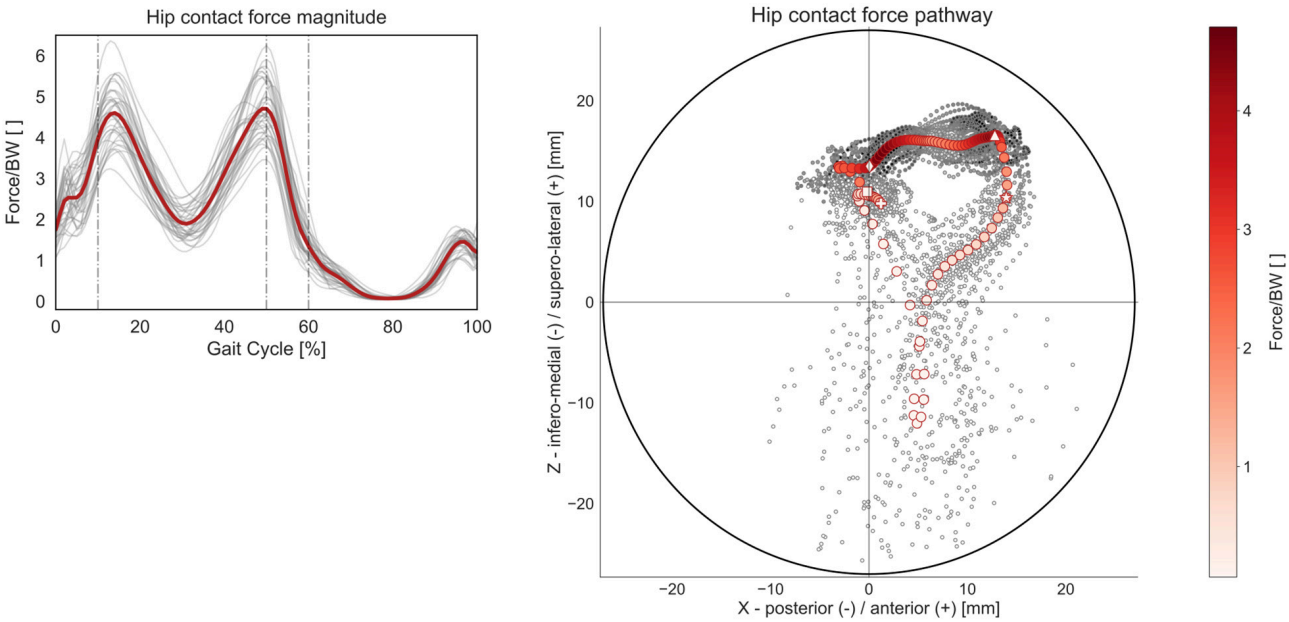

FIGURE 9 | HCF magnitude and acetabular pathway over the GC. Average profiles for each subject are reported in gray, while the cohort's mean is reported in red. Forces are reported normalized by body weight (BW). The HCF pathway was calculated as the intersection of the HCF vector with a hemisphere fitting the acetabulum, standardized to a diameter of 54 mm. Each circular marker represents one of the 101 time points in which the GC was discretized. The initial heel strike (0% GC) is highlighted with a squared marker, the transition from initial loading response to mid-stance (10% GC) with a diamond marker, the transition from terminal stance to pre-swing (50% GC) with a triangular marker, the transition from stance to swing phase (60% GC) with a star marker, and the final heel strike (100% GC) with a cross marker.

anterosuperior portion of the acetabulum (Beck et al., 2005). This was confirmed through a large multicenter observational study (Pascual-Garrido et al., 2019), which reported a high incidence of both anterior and superolateral peripheral cartilage lesions. A more anterior or more superolaterally oriented HCF may induce higher stresses in the more peripheral regions, thus accelerating cartilage degeneration. Finite elements analyses accounting for pathological hip anatomies, altered contact mechanics, and patient-specific loads might represent a more accurate tool to investigate the localized stresses that occur within the joint in the presence of FAI syndrome (Ng et al., 2016, 2017, 2018).

This study investigated the effect of a single alignment parameter such as femoral torsion on lower-limb function and specifically on hip loads. However, several other anatomical and morphological parameters could affect the mechanics of the hip. Anatomical variations in neck-shaft angle could similarly alter the relative alignment of the muscles around the joint and therefore affect the resulting HCFs (Kainz et al., 2020). Other parameters such as acetabular coverage, acetabular retroversion, and presence of cam/pincer deformities would not have a direct effect on hip mechanics in our models, given the assumption of a perfect ball-and-socket hip joint. Nevertheless, these factors, especially when pathological, could influence the overall

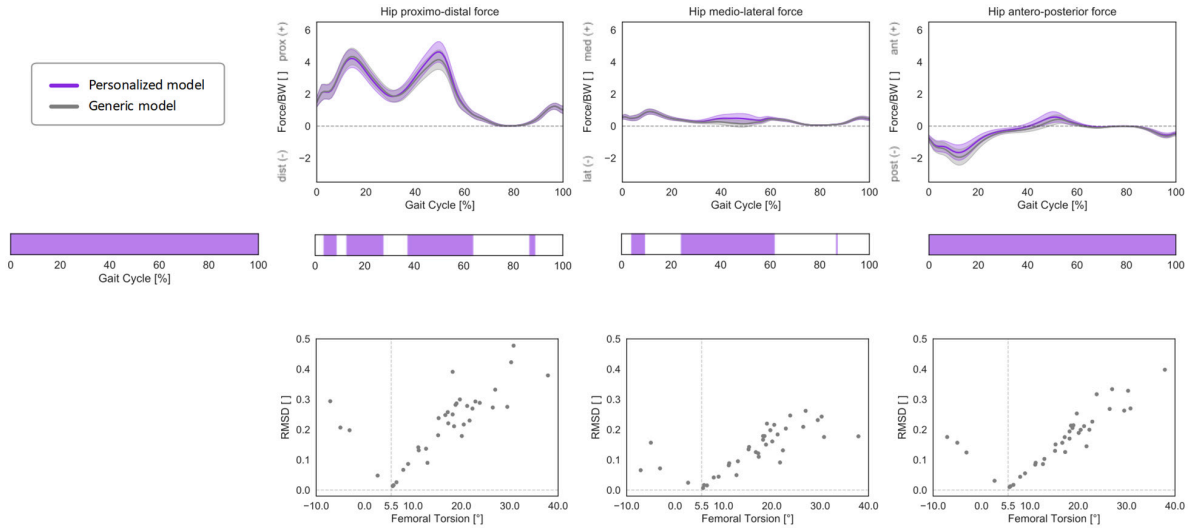

FIGURE 10 | 3D HCFs (mean ± standard deviation) over the GC computed with a generic, baseline musculoskeletal model (in gray) or with a personalized model accounting for subject-specific femoral torsion (in violet). HCFs were calculated in a proximal (pelvis-based) coordinate system according to ISB recommendations and are normalized by body weight (BW). Phases of GC in which a statistically significant correlation was observed in the SPM vectorial paired Hotelling T^2 are indicated in the leftmost panel. Below each force component, the results of the *post hoc* scalar-field paired *t*-tests are reported. Root mean standard deviation between the HCFs predicted with the two different models was calculated for each subject and plotted against subject-specific femoral torsion values. The torsional value of the baseline model geometry (5.5°) is reported as a dashed vertical line. Positive values indicate antetorsion, negative retrotorsion.

kinematics and kinetics of the affected subjects, for instance, through pain-avoiding strategies, and this could also influence the models' outcome.

The study was limited to 37 healthy individuals. The analysis of asymptomatic adults is not affected by symptoms and impairments that patients could experience, thus potentially providing an insight on the contribution of femoral torsion alone to the loading of the hip joint. No other anatomical parameter related to femoral or acetabular morphology was analyzed for the investigated subjects; therefore, it cannot be excluded that any of them presented an unknown pathological anatomy, which could have biased the results of this study. However, participants presenting pain in the lower back or in the lower extremities were excluded from the study, thus potentially excluding other severe (and symptomatic) pathoanatomies. Moreover, the recruited participants were all rather young, fit, and active and therefore do not represent the general population. Subject demographics, such as age, BMI, and sex, have been previously shown to relate to HCFs (De Pieri et al., 2019; Lunn et al., 2020). We did not find any statistically significant correlation between femoral torsion values and age or BMI in our investigated cohort, nor did we find a statistically significant difference between torsional values of males and females. While this does not indicate any clear bias in the selection of our cohort, a multivariate analysis based on a larger sample size would be required to exclude the effect of any other confounding factor, in terms of both demographics and anatomical variability. Additionally, one randomly chosen leg for each subject was included in the study. While other selection strategies, such as the more antetorted or dominant leg, could have led to different results, a left/right randomization was considered the most conservative option to avoid introducing any unknown bias, for instance, associated with other morphological factors that were not considered in this study.

Future work should aim at including symptomatic patients with excessive femoral antetorsion, which might present more pronounced kinematic compensatory mechanisms, such as in-toeing, as well as protective strategies to avoid pain (Ng et al., 2018). The qualitative evaluation of the muscle lever arms suggested that the effect of these torsional deformities might be more pronounced for pathological ranges of femoral torsion, when the moment-generating capacity of the abductor muscles is substantially reduced. This study was also limited to an analysis of gait, which represents the most commonly performed daily activity (Morlock et al., 2001); however, musculoskeletal modeling can be used to accurately assess HCFs during various activities of daily living (De Pieri et al., 2019; Lunn et al., 2020), in which patients with hip pathologies could present more physical impairments (Diamond et al., 2015; Kierkegaard et al., 2017).

Excessive femoral torsion can affect both hip and knee mechanics (Passmore et al., 2018) and is associated with functional impairments and motor limitations (Bruderer-Hofstetter et al., 2015). Torsional deformities of the femur and tibia (Bruce and Stevens, 2004; Alexander et al., 2020) have also been associated with knee and patellar complications (Eckhoff et al., 1997; Powers, 2003; Stevens et al., 2014; Bretin et al., 2011). However, a better understanding of the femorotibial and femoropatellar joint mechanics, specifically of their response to torsional forces, would require a more complex multi-DOF modeling approach of the knee complex, accounting for specific morphological variations of the tibia and femur, specifically of their articulating surfaces, as well as passive soft-tissue structures

which constrain knee rotations (Marra et al., 2014; Lenhart et al., 2015; Dejtiar et al., 2020).

CONCLUSION

The method proposed in this study, which accounts for both morphological and kinematic characteristics, can serve as a blueprint for a structured investigation of alterations in hip intra-articular loads as a result of altered femoral torsional alignment.

The use of low-dosage imaging techniques combined with gait analysis and musculoskeletal modeling might help in identifying in a clinical setting patients who could be at a higher risk for cartilage damage and early onset of hip OA due to femoral torsion alone. Additionally, it could help in identifying among patients with excessive femoral torsion those who present more severe functional impairments as a consequence of altered joint mechanics. Long-term monitoring of pediatric and adolescent patients might also provide a better understanding of the long-term effects of torsional abnormalities on joint intra-articular loads and cartilage health.

While this study investigated the effect of femoral torsion alone, the proposed method should be extended to account for all femoral and acetabular morphological variations that could lead to altered and pathological hip mechanics. A better understanding of the forces produced within the acetabulum and of the mechanical consequences of the overall limb alignment is necessary to improve individual diagnoses and to optimally plan targeted bone corrective surgeries of the lower extremities, which could reduce the long-term risk of (over-)loading-induced joint degeneration.

DATA AVAILABILITY STATEMENT

The datasets presented in this article are not readily available because of privacy restrictions. Requests to access the datasets should be directed to SF.

ETHICS STATEMENT

The studies involving human participants were reviewed and approved by Ethikkommission Zürich (BASEC-Nr. 2019-00688). The patients/participants provided their written informed consent to participate in this study. Written informed consent was obtained from the individual(s) for the publication of any potentially identifiable images or data included in this article.

AUTHOR CONTRIBUTIONS

ED contributed to study conceptualization, study design, method development, software, data curation, data visualization, data analysis, data interpretation, and writing. BF contributed to study conceptualization, study design, ethics, method development, data acquisition, data interpretation, and writing. RL contributed to study design, method development, data acquisition, data interpretation, and writing. SM contributed to method development, data acquisition, data curation, and writing. NC contributed to study design, method development, data interpretation, and writing. ML and SF contributed to study conceptualization, study design, ethics, data interpretation, and writing. All authors contributed to the article and approved the submitted version.

FUNDING

This research was partially funded by the Mäxi Foundation, Switzerland.

ACKNOWLEDGMENTS

We would like to thank Morten E. Lund for his important contribution in developing the morphing of the femoral geometries within the AnyBody Modeling System. We would also like to thank Simon Comtesse and Casimir Schwank for their help in the initial phases of establishing the study protocol, as well as Sarah Hermann and Louis Leuthard for their assistance with the acquisition of motion-capture data.

SUPPLEMENTARY MATERIAL

The Supplementary Material for this article can be found online at: https://www.frontiersin.org/articles/10.3389/fbioe.2021.679360/full#supplementary-material

REFERENCES

Alexander, N., Studer, K., Lengnick, H., Payne, E., Klima, H., and Wegener, R. (2019). The impact of increased femoral antetorsion on gait deviations in healthy adolescents. *J. Biomech.* 86, 167–174. doi: 10.1016/j.jbiomech.2019.02.005

Alexander, N., Wegener, R., Lengnick, H., Payne, E., Klima, H., Cip, J., et al. (2020). Compensatory gait deviations in patients with increased outward tibial torsion pre and post tibial derotation osteotomy. *Gait Posture* 77, 43–51. doi: 10.1016/j.gaitpost.2020.01.011

Andersen, M. S. (2021). "Introduction to musculoskeletal modelling," in *Computational Modelling of Biomechanics and Biotribology in the Musculoskeletal System*, eds Z. Jin, J. Li and Z. Chen (Amsterdam: Elsevier), 41–80. doi: 10.1016/b978-0-12-819531-4.00004-3

Andersen, M. S., Damsgaard, M., and Rasmussen, J. (2009). Kinematic analysis of over-determinate biomechanical systems. *Comp. Methods Biomech. Biomed. Eng.* 12, 371–384. doi: 10.1080/10255840802459412

Arnold, A. S., Komallu, A. V., and Delp, S. L. (1997). Internal rotation gait: a compensatory mechanism to restore abduction capacity decreased by bone deformity. *Dev. Med. Child Neurol.* 39, 40–44. doi: 10.1111/j.1469-8749.1997.tb08202.x

Beck, M., Kalhor, M., Leunig, M., and Ganz, R. (2005). Hip morphology influences the pattern of damage to the acetabular cartilage. Femoroacetabular impingement as a cause of early osteoarthritis of the hip. *J. Bone Joint Surg. Br.* 87, 1012–1018. doi: 10.1302/0301-620X.87B7.15203

Bosmans, L., Wesseling, M., Desloovere, K., Molenaers, G., Scheys, L., and Jonkers, I. (2014). Hip contact force in presence of aberrant bone geometry during normal and pathological gait. *J. Orthop. Res.* 32, 1406–1415. doi: 10.1002/jor.22698

Boyer, E., Novacheck, T. F., Rozumalski, A., and Schwartz, M. H. (2016). Long-term changes in femoral anteversion and hip rotation following femoral derotational osteotomy in children with cerebral palsy. *Gait Posture* 50, 223–228. doi: 10.1016/j.gaitpost.2016.09.004

Bretin, P., O'Loughlin, P. F., Suero, E. M., Kendoff, D., Ostermeier, S., Hüfner, T., et al. (2011). Influence of femoral malrotation on knee joint alignment and intra-articular contract pressures. *Arch. Orthop. Trauma Surg.* 131, 1115–1120. doi: 10.1007/s00402-010-1210-4

Bruce, W. D., and Stevens, P. M. (2004). Surgical correction of miserable malalignment syndrome. *J. Pediatr. Orthop.* 24, 392–396. doi: 10.1097/01241398-200407000-00009

Bruderer-Hofstetter, M., Fenner, V., Payne, E., Zdenek, K., Klima, H., and Wegener, R. (2015). Gait deviations and compensations in pediatric patients with increased femoral torsion. *J. Orthop. Res.* 33, 155–162. doi: 10.1002/jor.22746

Buck, F. M., Guggenberger, R., Koch, P. P., and Pfirrmann, C. W. A. (2012). Femoral and tibial torsion measurements with 3D models based on low-dose biplanar radiographs in comparison with standard CT measurements. *Am. J. Roentgenol.* 199, W607–W612. doi: 10.2214/AJR.11.8295

Carbone, V., Fluit, R., Pellikaan, P., van der Krogt, M. M., Janssen, D., Damsgaard, M., et al. (2015). TLEM 2.0 – a comprehensive musculoskeletal geometry dataset for subject-specific modeling of lower extremity. *J. Biomech.* 48, 734–741. doi: 10.1016/j.jbiomech.2014.12.034

Carbone, V., van der Krogt, M. M., Koopman, H. F. J. M., and Verdonschot, N. (2012). Sensitivity of subject-specific models to errors in musculo-skeletal geometry. *J. Biomech.* 45, 2476–2480. doi: 10.1016/j.jbiomech.2012.06.026

Cordier, W., and Katthagen, B. D. (2000). Femorale torsionsfehler. *Orthopade* 29, 795–801. doi: 10.1007/s001320050528

Damsgaard, M., Rasmussen, J., Christensen, S. T., Surma, E., and de Zee, M. (2006). Analysis of musculoskeletal systems in the anybody modeling system. *Simul. Model. Pract. Theory* 14, 1100–1111. doi: 10.1016/j.simpat.2006.09.001

De Pieri, E., Atzori, F., Ferguson, S. J., Dendorfer, S., Leunig, M., and Aepli, M. (2020). Contact force path in total hip arthroplasty: effect of cup medialisation in a whole-body simulation. *HIP Int.* doi: 10.1177/1120700020917321 [Epub ahead of print]

De Pieri, E., Lund, M. E., Gopalakrishnan, A., Rasmussen, K. P., Lunn, D. E., and Ferguson, S. J. (2018). Refining muscle geometry and wrapping in the TLEM 2 model for improved hip contact force prediction. *PLoS One* 13:e0204109. doi: 10.1371/journal.pone.0204109

De Pieri, E., Lunn, D. E., Chapman, G. J., Rasmussen, K. P., Ferguson, S. J., and Redmond, A. C. (2019). Patient characteristics affect hip contact forces during gait. *Osteoarthr. Cartil.* 27, 895–905. doi: 10.1016/j.joca.2019.01.016

Dejtiar, D. L., Dzialo, C. M., Pedersen, P. H., Jensen, K. K., Fleron, M. K., and Andersen, M. S. (2020). Development and evaluation of a subject-specific lower limb model with an eleven-degrees-of-freedom natural knee model using magnetic resonance and biplanar x-ray imaging during a quasi-static lunge. *J. Biomech. Eng.* 142:061001. doi: 10.1115/1.4044245

Derrick, T. R., van den Bogert, A. J., Cereatti, A., Dumas, R., Fantozzi, S., and Leardini, A. (2020). ISB recommendations on the reporting of intersegmental forces and moments during human motion analysis. *J. Biomech.* 99:109533. doi: 10.1016/j.jbiomech.2019.109533

Diamond, L. E., Dobson, F. L., Bennell, K. L., Wrigley, T. V., Hodges, P. W., and Hinman, R. S. (2015). Physical impairments and activity limitations in people with femoroacetabular impingement: a systematic review. *Br. J. Sports Med.* 49, 230–242. doi: 10.1136/bjsports-2013-093340

Eckhoff, D. G. (1994). Effect of limb malrotation on malalignment and osteoarthritis. *Orthop. Clin. North Am.* 25, 405–414. doi: 10.1016/s0030-5898(20)31925-8

Eckhoff, D. G., Brown, A. W., Kilcoyne, R. F., and Stamm, E. R. (1997). Knee version associated with anterior knee pain. *Clin. Orthop. Relat. Res.* 339, 152–155. doi: 10.1097/00003086-199706000-00020

Ejnisman, L., Philippon, M. J., Lertwanich, P., Pennock, A. T., Herzog, M. M., Briggs, K. K., et al. (2013). Relationship between femoral anteversion and findings in hips with femoroacetabular impingement. *Orthopedics* 36, e293–e300. doi: 10.3928/01477447-20130222-17

Erdemir, A., McLean, S., Herzog, W., and van den Bogert, A. J. (2007). Model-based estimation of muscle forces exerted during movements. *Clin. Biomech.* 22, 131–154. doi: 10.1016/j.clinbiomech.2006.09.005

Fabry, G. (2010). Clinical practice: static, axial, and rotational deformities of the lower extremities in children. *Eur. J. Pediatr.* 169, 529–534. doi: 10.1007/s00431-009-1122-x

Fabry, G., MacEwen, G. D., and Shands, A. R. (1973). Torsion of the femur. A follow up study in normal and abnormal conditions. *J. Bone Joint Surg. Am.* 55, 1726–1738. doi: 10.2106/00004623-197355080-00017

Felson, D. T. (2013). Osteoarthritis as a disease of mechanics. *Osteoarthr. Cartil.* 21, 10–15. doi: 10.1016/j.joca.2012.09.012

Fischer, M. C. M., Eschweiler, J., Schick, F., Asseln, M., Damm, P., and Radermacher, K. (2018). Patient-specific musculoskeletal modeling of the hip joint for preoperative planning of total hip arthroplasty: a validation study based on in vivo measurements. *PLoS One* 13:e0195376. doi: 10.1371/journal.pone.0195376

Folinais, D., Thelen, P., Delin, C., Radier, C., Catonne, Y., and Lazennec, J. Y. (2013). Measuring femoral and rotational alignment: EOS system versus computed tomography. *Orthop. Traumatol. Surg. Res.* 99, 509–516. doi: 10.1016/j.otsr.2012.12.023

Friston, K. J., Holmes, A. P., Worsley, K. J., Poline, J.-P., Frith, C. D., and Frackowiak, R. S. J. (1994). Statistical parametric maps in functional imaging: a general linear approach. *Hum. Brain Mapp.* 2, 189–210. doi: 10.1002/hbm.460020402

Ganz, R., Leunig, M., Leunig-Ganz, K., and Harris, W. H. (2008). The etiology of osteoarthritis of the hip: an integrated mechanical concept. *Clin. Orthop. Relat. Res.* 466, 264–272. doi: 10.1007/s11999-007-0060-z

Günther, K. P., Kessler, S., Tomczak, R., Pfeifer, P., and Puhl, W. (1996). Femoral anteversion – Reliability and clinical significance of different investigation techniques in children and adolescents. *Z. Orthop. Ihre Grenzgeb.* 134, 295–301. doi: 10.1055/s-2008-1039764

Hefti, F. (2000). Achsenfehler an den unteren extremitaten. *Orthopade* 29, 814–820. doi: 10.1007/s001320050531

Heller, M. O., Bergmann, G., Deuretzbacher, G., Claes, L., Haas, N. P., and Duda, G. N. (2001). Influence of femoral anteversion on proximal femoral loading: measurement and simulation in four patients. *Clin. Biomech.* 16, 644–649. doi: 10.1016/S0268-0033(01)00053-5

Hernandez, R. J., Tachdjian, M. O., Poznansk, A. K., and Dias, L. S. (1981). CT determination of femoral torsion. *Am. J. Roentgenol.* 137, 97–101. doi: 10.2214/ajr.137.1.97

Hetsroni, I., Dela Torre, K., Duke, G., Lyman, S., and Kelly, B. T. (2013). Sex differences of hip morphology in young adults with hip pain and labral tears. *Arthroscopy* 29, 54–63. doi: 10.1016/j.arthro.2012.07.008

Hogervorst, T., Bouma, H., de Boer, S. F., and de Vos, J. (2011). Human hip impingement morphology. *J. Bone Joint Surg. Br.* 93, 769–776. doi: 10.1302/0301-620X.93B6.25149

Hogervorst, T., Eilander, W., Fikkers, J. T., and Meulenbelt, I. (2012). Hip ontogenesis: how evolution, genes, and load history shape hip morphotype and cartilotype. *Clin. Orthop. Relat. Res.* 470, 3284–3296. doi: 10.1007/s11999-012-2511-4

Jani, L., Schwarzenbach, U., Afifi, K., Scholder, P., and Gisler, P. (1979). [Progression of idiopathic coxa antetorta. a) Spontaneous progression of idiopathic coxa antetorta (controlled clinical study of 148 patients at the end of adolescence)]. *Orthopade* 8, 5–11.

Kainz, H., Killen, B. A., Wesseling, M., Perez-Boerema, F., Pitto, L., Aznar, J. M. G., et al. (2020). A multi-scale modelling framework combining musculoskeletal rigid-body simulations with adaptive finite element analyses, to evaluate the impact of femoral geometry on hip joint contact forces and femoral bone growth. *PLoS One* 15:e0235966. doi: 10.1371/journal.pone.0235966

Keshmiri, A., Maderbacher, G., Baier, C., Zeman, F., Grifka, J., and Springorum, H. R. (2016). Significant influence of rotational limb alignment parameters on patellar kinematics: an in vitro study. *Knee Surg. Sports Traumatol. Arthrosc.* 24, 2407–2414. doi: 10.1007/s00167-014-3434-2

Kierkegaard, S., Langeskov-Christensen, M., Lund, B., Naal, F. D., Mechlenburg, I., Dalgas, U., et al. (2017). Pain, activities of daily living and sport function at different time points after hip arthroscopy in patients with femoroacetabular impingement: a systematic review with meta-analysis. *Br. J. Sports Med.* 51, 572–579. doi: 10.1136/bjsports-2016-096618

Klaue, K., Durnin, C. W., and Ganz, R. (1991). The acetabular rim syndrome. A clinical presentation of dysplasia of the hip. *J. Bone Joint Surg. Br.* 73, 423–429. doi: 10.1302/0301-620x.73b3.1670443

Klein Horsman, M. D., Koopman, H. F. J. M., van der Helm, F. C. T., Prosé, L. P., and Veeger, H. E. J. (2007). Morphological muscle and joint parameters for musculoskeletal modelling of the lower extremity. *Clin. Biomech.* 22, 239–247. doi: 10.1016/j.clinbiomech.2006.10.003

Krebs, V., Incavo, S. J., and Shields, W. H. (2009). The anatomy of the acetabulum: what is normal? *Clin. Orthop. Relat. Res.* 467, 868–875. doi: 10.1007/s11999-008-0317-1

Leigh, R. J., Osis, S. T., and Ferber, R. (2016). Kinematic gait patterns and their relationship to pain in mild-to-moderate hip osteoarthritis. *Clin. Biomech.* 34, 12–17. doi: 10.1016/j.clinbiomech.2015.12.010

Lenhart, R. L., Kaiser, J., Smith, C. R., and Thelen, D. G. (2015). Prediction and validation of load-dependent behavior of the tibiofemoral and patellofemoral joints during movement. *Ann. Biomed. Eng.* 43, 2675–2685. doi: 10.1007/s10439-015-1326-3

Lewis, C. L., Sahrmann, S. A., and Moran, D. W. (2007). Anterior hip joint force increases with hip extension, decreased gluteal force, or decreased iliopsoas force. *J. Biomech.* 40, 3725–3731. doi: 10.1016/j.jbiomech.2007.06.024

List, R., Gülay, T., Stoop, M., and Lorenzetti, S. (2013). Kinematics of the trunk and the lower extremities during restricted and unrestricted squats. *J. Strength Cond. Res.* 27, 1529–1538. doi: 10.1519/JSC.0b013e3182736034

Lund, M. E., Andersen, M. S., de Zee, M., and Rasmussen, J. (2015). Scaling of musculoskeletal models from static and dynamic trials. *Int. Biomech.* 2, 1–11. doi: 10.1080/23335432.2014.993706

Lund, M. E., Rasmussen, J., and Andersen, M. S. (2019). AnyPyTools: a python package for reproducible research with the anybody modeling system. *J. Open Source Softw.* 4:1108. doi: 10.21105/joss.01108

Lunn, D. E., De Pieri, E., Chapman, G. J., Lund, M. E., Redmond, A. C., and Ferguson, S. J. (2020). Current preclinical testing of new hip arthroplasty technologies does not reflect real-world loadings: capturing patient-specific and activity-related variation in hip contact forces. *J. Arthroplasty* 35, 877–885. doi: 10.1016/j.arth.2019.10.006

Marra, M. A., Vanheule, V., Rasmussen, J., Verdonschot, N. J. J., Andersen, M. S., Fluit, R., et al. (2014). A subject-specific musculoskeletal modeling framework to predict in vivo mechanics of total knee arthroplasty. *J. Biomech. Eng.* 137:020904. doi: 10.1115/1.4029258

Mettler, F. A., Huda, W., Yoshizumi, T. T., and Mahesh, M. (2008). Effective doses in radiology and diagnostic nuclear medicine: a catalog. *Radiology*, 248, 254–263. doi: 10.1148/radiol.2481071451

Modenese, L., and Kohout, J. (2020). Automated generation of three-dimensional complex muscle geometries for use in personalised musculoskeletal models. *Ann. Biomed. Eng.* 48, 1793–1804. doi: 10.1007/s10439-020-02490-4

Morlock, M., Schneider, E., Bluhm, A., Vollmer, M., Bergmann, G., Müller, V., et al. (2001). Duration and frequency of every day activities in total hip patients. *J. Biomech.* 34, 873–881. doi: 10.1016/S0021-9290(01)00035-5

Ng, K. C. G., Lamontagne, M., Labrosse, M. R., and Beaulé, P. E. (2016). Hip joint stresses due to cam-type femoroacetabular impingement: a systematic review of finite element simulations. *PLoS One* 11:e0147813. doi: 10.1371/journal.pone.0147813

Ng, K. C. G., Mantovani, G., Lamontagne, M., Labrosse, M. R., and Beaulé, P. E. (2017). Increased hip stresses resulting from a cam deformity and decreased femoral neck-shaft angle during level walking. *Clin. Orthop. Relat. Res.* 475, 998–1008. doi: 10.1007/s11999-016-5038-2

Ng, K. C. G., Mantovani, G., Modenese, L., Beaulé, P. E., and Lamontagne, M. (2018). Altered walking and muscle patterns reduce hip contact forces in individuals with symptomatic cam femoroacetabular impingement. *Am. J. Sports Med.* 46, 2615–2623. doi: 10.1177/0363546518787518

Novais, E. N., Ferrer, M. G., Williams, K. A., and Bixby, S. D. (2019). Acetabular retroversion and decreased posterior coverage are associated with sports-related posterior hip dislocation in adolescents. *Clin. Orthop. Relat. Res.* 477, 1101–1108. doi: 10.1097/CORR.0000000000000514

Pascual-Garrido, C., Li, D. J., Grammatopoulos, G., Yanik, E. L., and Clohisy, J. C. (2019). The pattern of acetabular cartilage wear is hip morphology-dependent and patient demographic-dependent. *Clin. Orthop. Relat. Res.* 477, 1021–1033. doi: 10.1097/CORR.0000000000000649

Passmore, E., Graham, H. K., Pandy, M. G., and Sangeux, M. (2018). Hip- and patellofemoral-joint loading during gait are increased in children with idiopathic torsional deformities. *Gait Posture* 63, 228–235. doi: 10.1016/j.gaitpost.2018.05.003

Pataky, T. C. (2012). One-dimensional statistical parametric mapping in Python. *Comput. Methods Biomech. Biomed. Eng.* 15, 295–301. doi: 10.1080/10255842.2010.527837

Pataky, T. C., Robinson, M. A., and Vanrenterghem, J. (2013). Vector field statistical analysis of kinematic and force trajectories. *J. Biomech.* 46, 2394–2401. doi: 10.1016/j.jbiomech.2013.07.031

Popovic, T., Samaan, M. A., Link, T. M., Majumdar, S., and Souza, R. B. (2020). Patients with symptomatic hip osteoarthritis have altered kinematics during stair ambulation. *PM R* 13, 128–136. doi: 10.1002/pmrj.12398

Powers, C. M. (2003). The influence of altered lower-extremity kinematics on patellofemoral joint dysfunction: a theoretical perspective. *J. Orthop. Sports Phys. Ther.* 33, 639–646. doi: 10.2519/jospt.2003.33.11.639

Retchford, T. H., Crossley, K. M., Grimaldi, A., Kemp, J. L., and Cowan, S. M. (2013). Can local muscles augment stability in the hip? A narrative literature review. *J. Musculoskelet. Neuronal Interact.* 13, 1–12.

Rosskopf, A. B., Pfirrmann, C. W. A., and Buck, F. M. (2016). Assessment of two-dimensional (2D) and three-dimensional (3D) lower limb measurements in adults: comparison of micro-dose and low-dose biplanar radiographs. *Eur. Radiol.* 26, 3054–3062. doi: 10.1007/s00330-015-4166-5

Schmaranzer, F., Lerch, T. D., Siebenrock, K. A., Tannast, M., and Steppacher, S. D. (2019). Differences in femoral torsion among various measurement methods increase in hips with excessive femoral torsion. *Clin. Orthop. Relat. Res.* 477, 1073–1083. doi: 10.1097/CORR.0000000000000610

Scorcelletti, M., Reeves, N. D., Rittweger, J., and Ireland, A. (2020). Femoral anteversion: significance and measurement. *J. Anat.* 237, 811–826. doi: 10.1111/joa.13249

Solomon, L. (1976). Patterns of osteoarthritis of the hip. *J. Bone Joint Surg. Br.* 58, 176–183.

Stevens, P. M., Gililland, J. M., Anderson, L. A., Mickelson, J. B., Nielson, J., and Klatt, J. W. (2014). Success of torsional correction surgery after failed surgeries for patellofemoral pain and instability. *Strategies Trauma Limb Reconstr.* 9, 5–12. doi: 10.1007/s11751-013-0181-8

Tanzer, M., and Noiseux, N. (2004). Osseous abnormalities and early osteoarthritis. *Clin. Orthop. Relat. Res.* 429, 170–177. doi: 10.1097/01.blo.0000150119.49983.ef

Thomas, G. E., Kiran, A., Batra, R. N., Hart, D., Spector, T., Taylor, A., et al. (2012). The association between hip morphology and end-stage osteoarthritis at 12-year follow up. *Osteoarthr. Cartil.* 20:S204. doi: 10.1016/j.joca.2012.02.331

Tönnis, D., and Heinecke, A. (1999). Acetabular and femoral anteversion: relationship with osteoarthritis of the hip. *J. Bone Joint Surg. Am.* 81, 1747–1770. doi: 10.2106/00004623-199912000-00014

Upadhyay, S. S., Moulton, A., and Burwell, R. G. (1985). Biological factors predisposing to traumatic posterior dislocation of the hip. A selection process in the mechanism of injury. *J. Bone Joint Surg. Br.* 67, 232–236. doi: 10.1302/0301-620x.67b2.3884614

Valente, G., Pitto, L., Testi, D., Seth, A., Delp, S. L., Stagni, R., et al. (2014). Are subject-specific musculoskeletal models robust to the uncertainties in parameter identification? *PLoS One* 9:e112625. doi: 10.1371/journal.pone.0112625

van der Krogt, M. M., Delp, S. L., and Schwartz, M. H. (2012). How robust is human gait to muscle weakness? *Gait Posture* 36, 113–119. doi: 10.1016/j.gaitpost.2012.01.017

Vandekerckhove, I., Wesseling, M., Kainz, H., Desloovere, K., and Jonkers, I. (2021). The effect of hip muscle weakness and femoral bony deformities on gait performance. *Gait Posture* 83, 280–286. doi: 10.1016/j.gaitpost.2020.10.022

Weber, T., Dendorfer, S., Dullien, S., Grifka, J., Verkerke, G. J., and Renkawitz, T. (2012). Measuring functional outcome after total hip replacement with subject-specific hip joint loading. *Proc. Inst. Mech. Eng. H* 226, 939–946. doi: 10.1177/0954411912447728

Wenger, D. E., Kendell, K. R., Miner, M. R., and Trousdale, R. T. (2004). Acetabular labral tears rarely occur in the absence of bony abnormalities. *Clin. Orthop. Relat. Res.* 426, 145–150. doi: 10.1097/01.blo.0000136903.01368.20

Wu, G., Siegler, S., Allard, P., Kirtley, C., Leardini, A., Rosenbaum, D., et al. (2002). ISB recommendation on definitions of joint coordinate system of various joints for the reporting of human joint motion—part I: ankle, hip, and spine. *J. Biomech.* 35, 543–548. doi: 10.1016/S0021-9290(01)00222-6

Zeng, W. N., Wang, F. Y., Chen, C., Zhang, Y., Gong, X. Y., Zhou, K., et al. (2016). Investigation of association between hip morphology and prevalence of osteoarthritis. *Sci. Rep.* 6:23477. doi: 10.1038/srep23477

Conflict of Interest: The authors declare that the research was conducted in the absence of any commercial or financial relationships that could be construed as a potential conflict of interest.

frontiers in Bioengineering and Biotechnology

MINI REVIEW
published: 27 July 2021
doi: 10.3389/fbioe.2021.668699

Approach to Posture and Gait in Huntington's Disease

Lauren S. Talman[1] and Amie L. Hiller[1,2]*

[1] Department of Neurology, Oregon Health & Science University, Portland, OR, United States, [2] Portland VA Healthcare System, Portland, OR, United States

Disturbances of gait occur in all stages of Huntington's disease (HD) including the premanifest and prodromal stages. Individuals with HD demonstrate the slower speed of gait, shorter stride length, and increased variability of gait parameters as compared to controls; cognitive disturbances in HD often compound these differences. Abnormalities of gait and recurrent falls lead to decreased quality of life for individuals with HD throughout the disease. This scoping review aims to outline the cross-disciplinary approach to gait evaluation in HD and will highlight the utility of objective measures in defining gait abnormalities in this patient population.

Keywords: Huntington's disease, posture, wearable sensors, gait, multi-disciplinary approach

OPEN ACCESS

Edited by:
Egon Perilli,
Flinders University, Australia

Reviewed by:
Fu-Lien Wu,
University of Illinois at Urbana-Champaign, United States
Jan Roth,
Charles University, Czechia

****Correspondence:***
Lauren S. Talman
talman@ohsu.edu

Specialty section:
This article was submitted to Biomechanics, a section of the journal Frontiers in Bioengineering and Biotechnology

Received: *17 February 2021*
Accepted: *28 June 2021*
Published: *27 July 2021*

Citation:
Talman LS and Hiller AL (2021) Approach to Posture and Gait in Huntington's Disease. Front. Bioeng. Biotechnol. 9:668699. doi: 10.3389/fbioe.2021.668699

INTRODUCTION

Huntington's disease (HD) is a genetic neurodegenerative disorder caused by autosomal dominant inheritance of an expanded CAG repeat portion in the huntingtin gene on chromosome 4. HD is characterized by progressive motor, cognitive and behavioral changes with "manifest" disease defined by the motor syndrome. "Premanifest" HD describes the entire period prior to the motor onset of disease and "prodromal" HD describes a phase of the premanifest disease when subtle motor symptoms may arise. While striatal degeneration is a pathologic hallmark of HD, longitudinal imaging studies have demonstrated progressive atrophy of the cortex and white matter tracts as well (Tabrizi et al., 2012). There is additional evidence to suggest that degeneration of the cerebellum occurs (Rüb et al., 2013). These pathologic changes help to explain the motor heterogeneity observed clinically in patients with HD. Though adult-onset HD is often recognized by the presence of hyperkinetic movements, namely chorea, individuals with HD also experience impairment involuntary control of movement including bradykinesia, motor impersistence, loss of postural reflexes, and ataxia. This loss of voluntary motor control is often more functionally disabling than the presence of chorea (Hart et al., 2013). Dystonia is common, though the specific effects of dystonia on gait dysfunction are not well established (Vuong et al., 2018). Head-to-head comparisons of gait performance in HD vs. other neurologic diseases are limited, though some studies do suggest that a higher degree of variability in gait measures distinguishes HD from Parkinson's disease (PD), cerebellar ataxias, and others (Moon et al., 2016). Individuals with HD are at relatively high risk for falls with fallers demonstrating a higher degree of chorea, truncal sway, and bradykinesia as compared to non-fallers (Grimbergen et al., 2008). Abnormalities of posture and gait may arise even in the premanifest stage (Rao et al., 2008). As the disease advances, gait dysfunction can become a significant source of disability and influences overall quality of life (Vuong et al., 2018).

Juvenile HD (JHD), defined as the onset of manifest disease prior to age 20, deserves mention but will not be the focus of this review. Whereas chorea is the most common motor feature of adult-onset HD, JHD typically manifests as an akinetic-rigid syndrome, and large database studies have suggested that gait dysfunction is a more common presenting sign in JHD (Fusilli et al., 2018).

Though there are myriad clinical descriptions of gait in adult-onset HD, quantitative measures of gait dysfunction may provide a more sensitive marker of disease progression. A biomarker is currently lacking in HD, and thus, a noninvasive method of tracking disease and monitoring the effects of intervention is attractive. In this review, wearable sensors will be highlighted as these have significant momentum in the field and have the potential to capture changes in function at home. Due to the complex nature of HD, the focus of this review on gait dysfunction will be presented in the context of a multi-disciplinary model of research and care.

Using a PubMed search with terms including "Huntington's disease, sensors, gait, posture, multi-disciplinary," articles presented in this review were selected based on publication date with those published in the prior 10 years prioritized. The purpose of this scoping review is not to present a comprehensive discussion of all available literature but rather to synthesize existing knowledge and highlight the need for future research (Colquhoun et al., 2014).

DEFINING GAIT DYSFUNCTION IN HD THROUGH USE OF WEARABLE SENSORS

Clinical evaluation of posture and gait is subjective by nature and rating scales may not reflect motor behavior at home or small changes over time. This includes the Unified Huntington Disease Rating Scale (UHDRS), a tool used to track changes in HD symptoms, with higher scores reflecting greater severity of disease (Huntington Study Group, 1996). The motor portion [total motor score (TMS)] of the UHDRS devotes 12 of 124 points to the examination of gait and balance and, therefore, may be more limited in capturing small changes in these domains over time. In addition to the UHDRS, other clinical scales may correlate with disease severity including Timed Up and Go (TUG), and Berg Balance scale (Rao et al., 2009); however, the Berg Balance Scale may be less sensitive to changes in the premanifest and early manifest stages (Rumpf et al., 2010). Due to possible time and space requirements for the aforementioned scales, researchers have explored several simple clinical tests of balance and found that stance with feet close together and tandem gait tests were sensitive for detecting postural instability (Brožová et al., 2011).

Objective measures of balance and gait using technology have emerged as a more sensitive way to distinguish disease states. Though wearable sensors will be highlighted in this review, there are certainly other objective measures that can be used to assess gait and balance in HD. Studies of posturography have detected impairments in both static and dynamic balance in both premanifest and manifest HD subjects with modest association to disease severity (Reyes et al., 2018). Gait performance using the GAITRite mat may distinguish individuals with HD from controls though may be less sensitive than posturography when these tools are compared head-to-head (Beckmann et al., 2018). Three-dimensional motion capture systems may also be employed as an effective tool to measure the effects of intervention (Mirek et al., 2018).

Wearable inertial sensors such as those utilizing a tri-axial gyroscope, accelerometer, and magnetometer, also objectively measure components of gait and posture. Sensors provide an increased volume of data over longer periods and can be applied in either the laboratory or home setting, the latter of which provides a more accurate reflection of function in daily life. Numerous studies outline the utility of wearable sensors in older adults and individuals with other neurologic disorders such as PD (Rovini et al., 2017). Sensor-based technology in HD is not as well established; however, the use of sensors to objectively define gait parameters in HD could have implications for monitoring disease progression and efficacy of therapeutic interventions.

Several studies have demonstrated that data obtained from sensors may distinguish HD subjects from controls and various stages of HD may be associated with measurable differences in motor activity. Using self-adhesive accelerometer-based sensors in the home setting, one study exploring activity state showed that patients with HD, in general, spend significantly more time lying down as compared to controls (Adams et al., 2017).

There is also evidence to suggest that the severity of motor symptoms may correlate with sensor-based gait measures. In a study of 15 individuals with HD and five controls, accelerometer-based sensors detected between-group differences in deviation step time. Gait parameters differed significantly between those with higher vs. lower TMS (Andrzejewski et al., 2016). In another study that used a single triaxial accelerometer, individuals with HD demonstrated a significant reduction in stride length and gait velocity while stride time and stance time were significantly increased. Measures of gait variability correlated with disease severity as measured by the UHDRS-TMS and total functional capacity (TFC), the latter of which is a surrogate for disease stage (Dalton et al., 2013).

Further exploration into whether wearable sensors may differentiate different disease states supports these earlier findings. In a dual center study, 43 patients with manifest HD and 43 controls completed four 10-m walk tests while wearing accelerometer gyroscope sensors on each shoe. Patients with HD and controls had significantly different stride length, gait velocity, stride time, and stance time. Patients with HD had significantly greater variability in all parameters of gait, with the greatest variability noted in stride time, stance time, and swing time. Disease severity correlated with measures of gait variability with the strongest correlation between these clinical measures and stride time coefficient of variance (CV), swing time CV, and stance time CV. Subgroup analysis of individuals with early, moderate, or advanced disease demonstrated significant between-group differences in stride length, gait velocity, stride time, and stance time with stride time as the sole parameter distinguishing moderate from advanced disease (Gaßner et al., 2020).

The effect of sensory input on postural stability has also been explored using sensors. One observational study of 39 participants including healthy controls, individuals with premanifest and manifest HD demonstrated that those with manifest HD had increased postural sway both in sitting and standing positions (Porciuncula et al., 2020). Postural sway increases for individuals with premanifest HD with the removal

of *both* visual sensory input and proprioceptive input while individuals with manifest HD had increased sway with loss of proprioceptive input alone. Gaze fixation appeared to improve sway in the premanifest cohort while it did not affect postural sway in manifest HD. Though further studies are required to confirm this observation, these findings could suggest that early intervention with gaze fixation training in premanifest or early HD may have a beneficial effect on postural sway and balance.

THE EFFECTS OF COGNITION ON GAIT IN HD

Though disease onset is defined by the emergence of motor symptoms, it is not uncommon for individuals with HD to develop cognitive dysfunction years prior. Cognitive impairment in HD is comprised of a decline in executive function, concentration, and memory (Paulsen, 2011; Teixeira et al., 2016). Furthermore, individuals with HD are known to have difficulty with task shifting and dividing attention (Aron et al., 2003; Vaportzis et al., 2015; Maurage et al., 2017). Formal cognitive testing through neuropsychological evaluation often helps to better define the specific cognitive deficits of an individual.

A link between the decline in cognition and gait dysfunction has been noted in other patient populations (Amboni et al., 2012). Several studies have explored this relationship in HD. A retrospective longitudinal study supports a relationship between mobility as measured by the Tinetti Mobility Test (TMT), measures of cognition, and motor severity as defined by the UHDRS (Kloos et al., 2017). Among the cognitive measures tested, the Symbol Digit Modality Test (SDMT) and Stroop interference correlated more closely than others with measures of mobility, though the strength of this correlation was modest based on applied criteria. The Pearson correlation coefficient was 0.48 and 0.40 for TMT with SDMT and Stroop interference, respectively.

In HD, as in other neurologic disorders, there is decreased automaticity of movement and, thus, attention-requiring tasks often worsen performance. Individuals with HD have difficulty multitasking, and this is highlighted when cognitive interference is imposed during gait evaluation, an approach termed dual-tasking. The decline in the ability to dual-task (DT) has been linked with falls in other populations including older adults, individuals with multiple sclerosis, and those with PD (Toulotte et al., 2006; Hamilton et al., 2009; Jacobs et al., 2014).

Several studies have examined the effect of dual-task conditions on gait performance in HD. One such study used a video motion system to define gait variables in a group of 15 participants with HD and 15 controls. Gait measurements were obtained under motor dual-task conditions (walking while carrying a tray) and cognitive dual-task conditions (walking while counting backward). While gait speed was unchanged with motor DT, this, in addition to cadence and strength, decreased in the setting of cognitive DT in the HD cohort. Decreased gait speed in the cognitive DT condition was associated with an increased TMS on the UHDRS and poorer performance on verbal fluency, Stroop, and the SDMT (Delval et al., 2008).

Another group of researchers aimed to further examine the link between cognition and ability to dual-task and the effect of dual-task performance on fall risk in a group of individuals with manifest HD. Using the walking while talking task (WWTT), both "simple" and "complex" dual-task conditions were explored (Fritz et al., 2016). The dual-task cost (DTC) was defined as the change in performance between dual-task conditions and single-task conditions. The result shows that the time required to complete the simple dual-task WWTT correlated with the TMS, while the complex dual-task time correlated significantly with TFC. Using a patient-reported number of falls over 3 months, the risk of falls did appear to correlate with time for both the simple and complex WWTT tasks; this relationship was particularly strong in the subgroup of individuals with TMS $>$ 35 (more advanced disease).

Additional support for the link between cognitive impairment and the ability to dual-task during measures of balance was brought to light in a 2019 study. A group of 17 individuals with HD and 17 control subjects completed a cognitive battery, motor evaluation, and self-evaluation of balance. Variables of postural sway were measured using the inertial sensor instrumented SWAY (i-SWAY). These variables were measured in multiple conditions: feet together vs. apart, eyes open vs. closed, firm vs. soft surface, with vs. without dual-task (The Controlled Oral Word Association Test). Individuals with HD had higher measures of postural sway (all variables) in all conditions as compared to controls. Narrow base, decreased visual input, and dual-task conditions worsened performance. Impaired visuospatial processing on cognitive measures correlated with increased total sway and jerk. Though postural sway did not correlate with prospective falls, these results may have been limited by self-report (Purcell et al., 2019).

A more recent study from the same group of researchers further explored the effect of dual-task conditions on mobility by comparing gait measures during three 2-min walk tests under single task, fast as possible, and dual-task conditions using the Mobility Lab software and Opal wearable sensors (Opal^{TM}, APDM, Inc., Portland, OR, United States). Gait speed, stride length, lateral step variability, and stride length variability differed significantly between HD and control groups under all conditions. Under DT conditions, individuals with HD took a greater number of steps and time to complete a turn (Purcell et al., 2020).

Dual-task training as a strategy to reduce the risk of falls has been noted in older adults and other patient populations (Mirelman et al., 2011; Dorfman et al., 2014; Fritz et al., 2015). Further studies with perhaps less reliance on self-report of falls will be required to determine whether this approach may be applicable and effective for the HD population.

EXERCISE AND REHABILITATION

Exercise is thought to be a neuroprotective tool in other degenerative disorders (Frazzitta et al., 2015; Paillard et al., 2015); however, the effects of exercise and rehabilitation on the course of HD are still under review. Furthermore, the response

of balance and gait to exercise/rehabilitation interventions in HD has not been systematically studied with available studies exploring this topic employing varying interventions and recruiting small sample sizes.

A recent mixed-methods systematic review aimed to provide recommendations based on studies exploring the effects of physical therapy and exercise interventions on overall function in HD (Quinn et al., 2020). While there was only weak evidence for balance training and postural control training, there was strong evidence for gait training in HD, stemming from a review of six randomized control trials (RCTs), six pre/posttest control group studies, and two studies without control groups. Though one of the RCTs did provide accelerometers to record daily activity (Busse et al., 2013), others relied on observation or exercise diaries to track adherence to and effect of the intervention. The challenge of generalizing effects of exercise/therapy is highlighted by the variability of interventions employed in the RCTs included in this review: a combined in-gym bicycling program and home walking program (Busse et al., 2013), a home exercise program guided by an exercise DVD (Khalil et al., 2013), home use of a danced-focused video game (Kloos et al., 2013), one-on-one task-specific therapy at home (Quinn et al., 2014), gym aerobic and resistance training (Quinn et al., 2016), and a multidisciplinary intervention consisting of physical therapy and cognitive therapy along with a home exercise program (Cruickshank et al., 2018). Gait speed and balance (as measured by the Berg Balance Score) improved primarily with the exercise DVD/home walking program. One-on-one physical therapy improved gait and mobility measures including gait speed and TUG (Quinn et al., 2020).

The effects of exercise on cognition in HD are unknown and data are limited. While one aforementioned multimodal exercise intervention did lead to improvement in verbal learning and memory, others have shown no change in cognitive measures pre and post-intervention (Busse et al., 2013; Quinn et al., 2016; Frese et al., 2017; Cruickshank et al., 2018). Larger studies with reproducible protocols will be needed to address this question further.

Several studies have emphasized the utility of more intensive multidisciplinary inpatient rehabilitation programs (Zinzi et al., 2009; Ciancarelli et al., 2013; Thompson et al., 2013). One such Norwegian program demonstrated improved gait function, balance, physical quality of life, and mood when patients with early to mid-stage HD were admitted to an inpatient rehabilitation center for three 3-week sessions per year (Piira et al., 2013, 2014). Though this approach is not feasible in many communities, these studies suggest that more intensive rehabilitation programs incorporating a multidisciplinary approach through physical therapy, occupational therapy, and speech therapy may be the most effective model to improve overall function in HD.

DISCUSSION

Gait dysfunction in HD is multifactorial, relating not only to the effects of motor manifestations of the disease but also cognitive limitations. Clinical evaluation of gait dysfunction relies on subjective descriptions, while the use of sensor-based technology provides more objective measures. Sensor technology has evolved, with the current focus on wearable devices which provide real-time data in both the laboratory and home settings. Sensors appear to be sensitive in distinguishing between individuals with HD and controls, and sensor-based gait parameters may correlate with disease stage and motor severity. Individuals with HD have decreased reserve to adapt to cognitive dual tasking with worsened performance on measures of both postural sway and gait. The correlation between performance on cognitive dual tasks and risk of falls is yet to be determined due to reliance on self-report. Early identification of individuals with executive dysfunction through formal neuropsychiatric cognitive testing may help clinicians to target particular patients for dual-task training or exercise interventions. Furthermore, particular attention to individuals with premanifest HD may allow for earlier intervention.

There are clear limitations to the existing data regarding gait dysfunction in HD. Many of the studies presented have recruited small sample sizes, and results are difficult to compare due to the employment of varying technologies and protocols. In addition, though there is evidence for gait dysfunction arising even in the premanifest stage of HD, longitudinal data are lacking. Ongoing longitudinal studies, such as ENROLL-HD, may provide an ideal context to further expand on the existing knowledge. In addition to its potential as a marker of disease progression and possible endpoint in intervention studies, gait dysfunction in HD impacts overall function and quality of life. Addressing this important symptom utilizing a multidisciplinary team approach would have a significant impact on this patient population.

AUTHOR CONTRIBUTIONS

LT and AH contributed to the conception of the manuscript. LT wrote the first draft of the manuscript. Both authors contributed to manuscript revision, read, and approved the submitted version.

REFERENCES

Adams, J. L., Dinesh, K., Xiong, M., Tarolli, C. G., Sharma, S., Sheth, N., et al. (2017). Multiple wearable sensors in Parkinson and Huntington disease individuals: a pilot study in clinic and at home. *Digit. Biomark.* 1, 52–63. doi: 10.1159/000479018

Amboni, M., Barone, P., Iuppariello, L., Lista, I., Tranfaglia, R., Fasano, A., et al. (2012). Gait patterns in Parkinsonian patients with or without mild cognitive impairment. *Mov. Disord.* 27, 1536–1543. doi: 10.1002/mds.25165

Andrzejewski, K. L., Dowling, A. V., Stamler, D., Felong, T. J., Harris, D. A., Wong, C., et al. (2016). Wearable sensors in Huntington disease: a pilot study. *J. Huntingtons Dis.* 5, 199–206. doi: 10.3233/JHD-160197

Aron, A. R., Watkins, L., Sahakian, B. J., Monsell, S., Barker, R. A., and Robbins, T. W. (2003). Task-set switching deficits in early-stage Huntington's disease: implications for basal ganglia function. *J. Cogn. Neurosci.* 15, 629–642.

Beckmann, H., Bohlen, S., Saft, C., Hoffmann, R., Gerss, J., Muratori, L., et al. (2018). Objective assessment of gait and posture in premanifest and manifest Huntington disease–a multi-center study. *Gait Posture* 62, 451–457. doi: 10.1016/j.gaitpost.2018.03.039

Brožová, H., Stochl, J., Klempíř, J., Kucharík, M., Růžička, E., and Roth, J. (2011). A sensitivity comparison of clinical tests for postural instability in patients with Huntington's disease. *Gait Posture* 34, 245–247. doi: 10.1016/j.gaitpost.2011.05.006

Busse, M., Quinn, L., Debono, K., Jones, K., Collett, J., Playle, R., et al. (2013). A randomized feasibility study of a 12-week community-based exercise program for people with Huntington's disease. *J. Neurol. Phys. Ther.* 37, 149–158. doi: 10.1097/NPT.0000000000000016

Ciancarelli, I., Tozzi Ciancarelli, M. G., and Carolei, A. (2013). Effectiveness of intensive neurorehabilitation in patients with Huntington's disease. *Eur. J. Phys. Rehabil. Med.* 49, 189–195.

Colquhoun, H. L., Levac, D., O'Brien, K. K., Straus, S., Tricco, A. C., Perrier, L., et al. (2014). Scoping reviews: time for clarity in definition, methods, and reporting. *J. Clin. Epidemiol.* 67, 1291–1294. doi: 10.1016/j.jclinepi.2014.03.013

Cruickshank, T. M., Reyes, A. P., Penailillo, L. E., Pulverenti, T., Bartlett, D. M., Zaenker, P., et al. (2018). Effects of multidisciplinary therapy on physical function in Huntington's disease. *Acta Neurol. Scand.* 138, 500–507. doi: 10.1111/ane.13002

Dalton, A., Khalil, H., Busse, M., Rosser, A., van Deursen, R., and Ólaighin, G. (2013). Analysis of gait and balance through a single triaxial accelerometer in presymptomatic and symptomatic Huntington's disease. *Gait Posture* 37, 49–54. doi: 10.1016/j.gaitpost.2012.05.028

Delval, A., Krystkowiak, P., Delliaux, M., Dujardin, K., Blatt, J. L., Destée, A., et al. (2008). Role of attentional resources on gait performance in Huntington's disease. *Mov. Disord.* 23, 684–689. doi: 10.1002/mds.21896

Dorfman, M., Herman, T., Brozgol, M., Shema, S., Weiss, A., Hausdorff, J. M., et al. (2014). Dual-task training on a treadmill to improve gait and cognitive function in elderly idiopathic fallers. *J. Neurol. Phys. Ther.* 38, 246–253. doi: 10.1097/NPT.0000000000000057

Frazzitta, G., Maestri, R., Bertotti, G., Riboldazzi, G., Boveri, N., Perini, M., et al. (2015). Intensive rehabilitation treatment in early Parkinson's disease: a randomized pilot study with a 2-year follow-up. *Neurorehabil. Neural Repair* 29, 123–131. doi: 10.1177/1545968314542981

Frese, S., Petersen, J. A., Ligon-Auer, M., Mueller, S. M., Mihaylova, V., Gehrig, S. M., et al. (2017). Exercise effects in Huntington disease. *J. Neurol.* 264, 32–39. doi: 10.1007/s00415-016-8310-1

Fritz, N. E., Cheek, F. M., and Nichols-Larsen, D. S. (2015). Motor-cognitive dual-task training in persons with neurologic disorders: a systematic review. *J. Neurol. Phys. Ther.* 39, 142–153. doi: 10.1097/NPT.0000000000000090

Fritz, N. E., Hamana, K., Kelson, M., Rosser, A., Busse, M., and Quinn, L. (2016). Motor-cognitive dual-task deficits in individuals with early-mid stage Huntington disease. *Gait Posture* 49, 283–289. doi: 10.1016/j.gaitpost.2016.07.014

Fusilli, C., Migliore, S., Mazza, T., Consoli, F., De Luca, A., Barbagallo, G., et al. (2018). Biological and clinical manifestations of juvenile Huntington's disease: a retrospective analysis. *Lancet Neurol.* 17, 986–993. doi: 10.1016/S1474-4422(18)30294-1

Gaßner, H., Jensen, D., Marxreiter, F., Kletsch, A., Bohlen, S., Schubert, R., et al. (2020). Gait variability as digital biomarker of disease severity in Huntington's disease. *J. Neurol.* 267, 1594–1601. doi: 10.1007/s00415-020-09725-3

Grimbergen, Y. A. M., Knol, M. J., Bloem, B. R., Kremer, B. P. H., Roos, R. A. C., and Munneke, M. (2008). Falls and gait disturbances in Huntington's disease. *Mov. Disord.* 23, 970–976. doi: 10.1002/mds.22003

Hamilton, F., Rochester, L., Paul, L., Rafferty, D., O'Leary, C. P., and Evans, J. J. (2009). Walking and talking: an investigation of cognitive-motor dual tasking in multiple sclerosis. *Mult. Scler.* 15, 1215–1227. doi: 10.1177/1352458509106712

Hart, E. P., Marinus, J., Burgunder, J. M., Bentivoglio, A. R., Craufurd, D., Reilmann, R., et al. (2013). Better global and cognitive functioning in choreatic versus hypokinetic-rigid Huntington's disease. *Mov. Disord.* 28, 1142–1145. doi: 10.1002/mds.25422

Huntington Study Group (1996). Unified Huntington's disease rating scale: reliability and consistency. *Mov. Disord.* 11, 136–142. doi: 10.1002/mds.870110204

Jacobs, J. V., Nutt, J. G., Carlson-Kuhta, P., Allen, R., and Horak, F. B. (2014). Dual tasking during postural stepping responses increases falls but not freezing in people with Parkinson's disease. *Parkinsonism Relat. Disord.* 20, 779–781. doi: 10.1016/j.parkreldis.2014.04.001

Khalil, H., Quinn, L., van Deursen, R., Dawes, H., Playle, R., Rosser, A., et al. (2013). What effect does a structured home-based exercise programme have on people with Huntington's disease? A randomized, controlled pilot study. *Clin. Rehabil.* 27, 646–658. doi: 10.1177/0269215512473762

Kloos, A. D., Fritz, N. E., Kostyk, S. K., Young, G. S., and Kegelmeyer, D. A. (2013). Video game play (Dance Dance Revolution) as a potential exercise therapy in Huntington's disease: a controlled clinical trial. *Clin. Rehabil.* 27, 972–982. doi: 10.1177/0269215513487235

Kloos, A. D., Kegelmeyer, D. A., Fritz, N. E., Daley, A. M., Young, G. S., and Kostyk, S. K. (2017). Cognitive dysfunction contributes to mobility impairments in Huntington's disease. *J. Huntingtons Dis.* 6, 363–370. doi: 10.3233/JHD-170279

Maurage, P., Heeren, A., Lahaye, M., Jeanjean, A., Guettat, L., Verellen-Dumoulin, C., et al. (2017). Attentional impairments in Huntington's disease: a specific deficit for the executive conflict. *Neuropsychology* 31, 424–436. doi: 10.1037/neu0000321

Mirek, E., Filip, M., Chwała, W., Szymura, J., Pasiut, S., Banaszkiewicz, K., et al. (2018). The influence of motor ability rehabilitation on temporal-spatial parameters of gait in Huntington's disease patients on the basis of a three-dimensional motion analysis system: an experimental trial. *Neurol. Neurochir. Pol.* 52, 575–580. doi: 10.1016/j.pjnns.2018.02.001

Mirelman, A., Maidan, I., Herman, T., Deutsch, J. E., Giladi, N., and Hausdorff, J. M. (2011). Virtual reality for gait training: can it induce motor learning to enhance complex walking and reduce fall risk in patients with Parkinson's disease? *J. Gerontol. A Biol. Sci. Med. Sci.* 66, 234–240. doi: 10.1093/gerona/glq201

Moon, Y., Sung, J., An, R., Hernandez, M. E., and Sosnoff, J. J. (2016). Gait variability in people with neurological disorders: a systematic review and meta-analysis. *Hum. Mov. Sci.* 47, 197–208. doi: 10.1016/j.humov.2016.03.010

Paillard, T., Rolland, Y., and de Souto Barreto, P. (2015). Protective effects of physical exercise in Alzheimer's disease and Parkinson's disease: a narrative review. *J. Clin. Neurol.* 11, 212–219. doi: 10.3988/jcn.2015.11.3.212

Paulsen, J. S. (2011). Cognitive impairment in Huntington disease: diagnosis and treatment. *Curr. Neurol. Neurosci. Rep.* 11, 474–483. doi: 10.1007/s11910-011-0215-x

Piira, A., van Walsem, M. R., Mikalsen, G., Nilsen, K. H., Knutsen, S., and Frich, J. C. (2013). Effects of a one year intensive multidisciplinary rehabilitation program for patients with Huntington's disease: a prospective intervention study. *PLoS Curr.* 5:ecurrents.hd.9504af71e0d1f87830c25c394be47027. doi: 10.1371/currents.hd.9504af71e0d1f87830c25c394be47027

Piira, A., van Walsem, M. R., Mikalsen, G., Øie, L., Frich, J. C., and Knutsen, S. (2014). Effects of a two-year intensive multidisciplinary rehabilitation program for patients with Huntington's disease: a prospective intervention study. *PLoS Curr.* 6:ecurrents.hd.2c56ceef7f9f8e239a59ecf2d94cddac. doi: 10.1371/currents.hd.2c56ceef7f9f8e239a59ecf2d94cddac

Porciuncula, F., Wasserman, P., Marder, K. S., and Rao, A. K. (2020). Quantifying postural control in premanifest and manifest huntington disease using wearable sensors. *Neurorehabil. Neural. Repair.* 34, 771–783. doi: 10.1177/1545968320939560

Purcell, N. L., Goldman, J. G., Ouyang, B., Bernard, B., and O'Keefe, J. A. (2019). The effects of dual-task cognitive interference and environmental challenges on balance in Huntington's disease. *Mov. Disord. Clin. Pract.* 6, 202–212. doi: 10.1002/mdc3.12720

Purcell, N. L., Goldman, J. G., Ouyang, B., Liu, Y., Bernard, B., and O'Keefe, J. A. (2020). The effects of dual-task cognitive interference on gait and turning in Huntington's disease. *PLoS One* 15:e0226827. doi: 10.1371/journal.pone.0226827

Quinn, L., Debono, K., Dawes, H., Rosser, A. E., Nemeth, A. H., Rickards, H., et al. (2014). Task-specific training in Huntington disease: a randomized controlled feasibility trial. *Phys. Ther.* 94, 1555–1568. doi: 10.2522/ptj.20140123

Quinn, L., Hamana, K., Kelson, M., Dawes, H., Collett, J., Townson, J., et al. (2016). A randomized, controlled trial of a multi-modal exercise intervention in Huntington's disease. *Parkinsonism Relat. Disord.* 31, 46–52. doi: 10.1016/j.parkreldis.2016.06.023

Quinn, L., Kegelmeyer, D., Kloos, A., Rao, A. K., Busse, M., and Fritz, N. E. (2020). Clinical recommendations to guide physical therapy practice for Huntington disease. *Neurology* 94, 217–228. doi: 10.1212/WNL.0000000000008887

Rao, A. K., Muratori, L., Louis, E. D., Moskowitz, C. B., and Marder, K. S. (2008). Spectrum of gait impairments in presymptomatic and symptomatic Huntington's disease. *Mov. Disord.* 23, 1100–1107. doi: 10.1002/mds.21987

Rao, A. K., Muratori, L., Louis, E. D., Moskowitz, C. B., and Marder, K. S. (2009). Clinical measurement of mobility and balance impairments in Huntington's disease: validity and responsiveness. *Gait Posture* 29, 433–436.

Reyes, A., Salomonczyk, D., Teo, W. P., Medina, L. D., Bartlett, D., Pirogovsky-Turk, E., et al. (2018). Computerised dynamic posturography in premanifest and manifest individuals with Huntington's disease. *Sci. Rep.* 8:14615. doi: 10.1038/s41598-018-32924-y

Rovini, E., Maremmani, C., and Cavallo, F. (2017). How wearable sensors can support Parkinson's disease diagnosis and treatment: a systematic review. *Front. Neurosci.* 11:555. doi: 10.3389/fnins.2017.00555

Rüb, U., Hoche, F., Brunt, E. R., Heinsen, H., Seidel, K., Del Turco, D., et al. (2013). Degeneration of the cerebellum in Huntington's disease (HD): possible relevance for the clinical picture and potential gateway to pathological mechanisms of the disease process. *Brain Pathol.* 23, 165–177. doi: 10.1111/j.1750-3639.2012.00629.x

Rumpf, S., Bohlen, S., Bechtel, N., Koch, R., Lange, H., and Reilmann, R. (2010). F15 Balance control in Huntington's disease: is the berg balance scale a useful test for clinical and quantitative motor assessment? *J. Neurol. Neurosurg. Psychiatry* 81:A27. doi: 10.1136/jnnp.2010.222620.15

Tabrizi, S. J., Reilmann, R., Roos, R. A., Durr, A., Leavitt, B., Owen, G., et al. (2012). Potential endpoints for clinical trials in premanifest and early Huntington's disease in the TRACK-HD study: analysis of 24 month observational data. *Lancet Neurol.* 11, 42–53. doi: 10.1016/S1474-4422(11)70263-0

Teixeira, A. L., de Souza, L. C., Rocha, N. P., Furr-Stimming, E., and Lauterbach, E. C. (2016). Revisiting the neuropsychiatry of Huntington's disease. *Dement Neuropsychol.* 10, 261–266. doi: 10.1590/s1980-5764-2016dn1004002

Thompson, J. A., Cruickshank, T. M., Penailillo, L. E., Lee, J. W., Newton, R. U., Barker, R. A., et al. (2013). The effects of multidisciplinary rehabilitation in patients with early-to-middle-stage Huntington's disease: a pilot study. *Eur. J. Neurol.* 20, 1325–1329. doi: 10.1111/ene.12053

Toulotte, C., Thevenon, A., Watelain, E., and Fabre, C. (2006). Identification of healthy elderly fallers and non-fallers by gait analysis under dual-task conditions. *Clin. Rehabil.* 20, 269–276. doi: 10.1191/0269215506cr929oa

Vaportzis, E., Georgiou-Karistianis, N., Churchyard, A., and Stout, J. C. (2015). Dual task performance may be a better measure of cognitive processing in Huntington's disease than traditional attention tests. *J. Huntingtons Dis.* 4, 119–130. doi: 10.3233/JHD-140131

Vuong, K., Canning, C. G., Menant, J. C., and Loy, C. T. (2018). Gait, balance, and falls in Huntington disease. *Handb. Clin. Neurol.* 159, 251–260. doi: 10.1016/B978-0-444-63916-5.00016-1

Zinzi, P., Salmaso, D., Frontali, M., and Jacopini, G. (2009). Patients' and caregivers' perspectives: assessing an intensive rehabilitation programme and outcomes in Huntington's disease. *J. Public Health* 17, 331–338. doi: 10.1007/s10389-009-0252-y

Conflict of Interest: The authors declare that the research was conducted in the absence of any commercial or financial relationships that could be construed as a potential conflict of interest.

Publisher's Note: All claims expressed in this article are solely those of the authors and do not necessarily represent those of their affiliated organizations, or those of the publisher, the editors and the reviewers. Any product that may be evaluated in this article, or claim that may be made by its manufacturer, is not guaranteed or endorsed by the publisher.

frontiers in Bioengineering and Biotechnology

ORIGINAL RESEARCH
published: 28 July 2021
doi: 10.3389/fbioe.2021.703508

Using Musculoskeletal Models to Estimate *in vivo* Total Knee Replacement Kinematics and Loads: Effect of Differences Between Models

Cristina Curreli[1,2]*, *Francesca Di Puccio*[3], *Giorgio Davico*[1,2], *Luca Modenese*[4] and *Marco Viceconti*[1,2]

[1] Department of Industrial Engineering, Alma Mater Studiorum - University of Bologna, Bologna, Italy, [2] Medical Technology Lab, IRCCS Istituto Ortopedico Rizzoli, Bologna, Italy, [3] Dipartimento di Ingegneria Civile e Industriale, Università di Pisa, Pisa, Italy, [4] Department of Civil and Environmental Engineering, Imperial College London, London, United Kingdom

OPEN ACCESS

Edited by:
Simone Tassani,
Pompeu Fabra University, Spain

Reviewed by:
Olga Barrera,
Oxford Brookes University,
United Kingdom
Oliver Röhrle,
University of Stuttgart, Germany

***Correspondence:**
Cristina Curreli
cristina.curreli@unibo.it

Specialty section:
This article was submitted to Biomechanics, a section of the journal Frontiers in Bioengineering and Biotechnology

Received: 30 April 2021
Accepted: 23 June 2021
Published: 28 July 2021

Citation:
Curreli C, Di Puccio F, Davico G, Modenese L and Viceconti M (2021) Using Musculoskeletal Models to Estimate in vivo Total Knee Replacement Kinematics and Loads: Effect of Differences Between Models. Front. Bioeng. Biotechnol. 9:703508. doi: 10.3389/fbioe.2021.703508

Total knee replacement (TKR) is one of the most performed orthopedic surgeries to treat knee joint diseases in the elderly population. Although the survivorship of knee implants may extend beyond two decades, the poor outcome rate remains considerable. A recent computational approach used to better understand failure modes and improve TKR outcomes is based on the combination of musculoskeletal (MSK) and finite element models. This combined multiscale modeling approach is a promising strategy in the field of computational biomechanics; however, some critical aspects need to be investigated. In particular, the identification and quantification of the uncertainties related to the boundary conditions used as inputs to the finite element model due to a different definition of the MSK model are crucial. Therefore, the aim of this study is to investigate this problem, which is relevant for the model credibility assessment process. Three different generic MSK models available in the OpenSim platform were used to simulate gait, based on the experimental data from the fifth edition of the "Grand Challenge Competitions to Predict *in vivo* Knee Loads." The outputs of the MSK analyses were compared in terms of relative kinematics of the knee implant components and joint reaction (JR) forces and moments acting on the tibial insert. Additionally, the estimated knee JRs were compared with those measured by the instrumented knee implant so that the "global goodness of fit" was quantified for each model. Our results indicated that the different kinematic definitions of the knee joint and the muscle model implemented in the different MSK models influenced both the motion and the load history of the artificial joint. This study demonstrates the importance of examining the influence of the model assumptions on the output results and represents the first step for future studies that will investigate how the uncertainties in the MSK models propagate on disease-specific finite element model results.

Keywords: musculoskeletal modeling, joint contact forces, knee implant kinematics, total knee replacement, model credibility assessment

INTRODUCTION

Total knee replacement (TKR) surgeries are commonly performed to alleviate severe pain at the knee joint resulting from musculoskeletal (MSK) disorders/conditions (e.g., inflammatory arthritis) that mostly affect elderly patients. In recent times, this is considered an effective procedure in orthopedics with a failure rate at 10 years postoperatively lower than 5% (Khan et al., 2016). But because of the popularity of this surgical procedure in the aging population, even 5% of failures produce some 10,000 revision surgeries every year in Europe. In contrast, patient-reported outcome measures suggest that 20–30% of the patients are not happy with the functional outcome of the surgery (Nakano et al., 2020). This calls for the development of new better-performing designs, whose safety and efficacy could be conveniently evaluated at the very early phases of the design taking advantage of the growing use of numerical modeling techniques.

A promising modeling strategy in the field of computational biomechanics that can be used to accelerate implant design innovation and improve subject-specific TKR outcomes is based on the combination of MSK multibody-dynamics analysis and finite element analysis (FEA) (Zhang et al., 2017; Shu et al., 2020b). The MSK modeling technique uses the classic multibody approach to estimate rigid body mechanics (i.e., joint kinematics and dynamics with ideal joint actuators) combined with muscle models to estimate muscle forces (i.e., replacing actuators with muscles) and joint reactions (JRs) by means of numerical optimization techniques. Additionally, FEA is a powerful tool to predict tissue-level mechanics such as contact pressure and surface damage of the implant surfaces. The main idea is that, by using the outputs of the MSK simulations in terms of load history and motion of the artificial joint as input conditions for the finite element model, it is possible to obtain a more realistic prediction of the joint biomechanics for each patient. This approach has been recently used in the literature to address specific research questions. Zhang et al. (2017) developed a combined MSK–FEA patient-specific computational wear prediction framework that estimates the damaging process in the tibial insert (TI) during gait in a patient implanted with an instrumented prosthesis. An *in silico* wear simulator was also developed by Shu et al. (2020a) using finite element models and loading conditions of different daily activities obtained by MSK modeling. Recently, a multiscale forward-dynamic framework of the lower extremity that combined muscle modeling and deformable FEA was presented in the study by Hume et al. (2019). This approach was used to predict healthy joint mechanics during different physical activities, and it is considered a promising strategy for the preclinical evaluation and design of TKR.

One of the most crucial aspects of this combined modeling approach is the definition of the MSK model that best describes both the anatomy and the physiology of the specific patient. Subject-specific MSK models that use medical images to create individualized geometries and properties of the patient under investigation are, in recent times, an attractive solution for the problem (Marra et al., 2015; Valente et al., 2017; Modenese et al., 2018). However, they require complex modeling workflows and *ad hoc* data collection even when applying well-documented approaches (Modenese et al., 2018), so the use of generic MSK models is in most cases the preferred solution due to its feasibility, at least until fully automated approaches become available (Modenese and Kohout, 2020; Modenese and Renault, 2021). Generic models are based on cadaveric data and mainly differ from each other in the MSK anatomy, kinematic of the joints and coordinate system definition, degrees of freedom, number, and properties of the muscles, and other biological structures such as ligaments. Numerous generic MSK models with varying levels of complexity have been presented in the literature over the last years (Delp et al., 1990; Anderson and Pandy, 1999; Arnold et al., 2010; Modenese et al., 2011; Marra et al., 2015; Rajagopal et al., 2016; Lai et al., 2017), giving a wide range of possible choices for this study. Thus, selecting the most suitable model for a specific study is challenging and requires a detailed understanding of the effect of different model parameters on the simulation results. Recent studies tried to address this problem by investigating the sensitivity of the estimated joint kinematic, muscle forces, joint torques, and JRs on the MSK modeling choices (Martelli et al., 2015; Myers et al., 2015; Roelker et al., 2017; Zuk et al., 2018). Zuk et al. (2018) used the generic gait2392 (Delp et al., 1990) and gait2354 (Anderson and Pandy, 1999) models, both available in OpenSim (Delp et al., 2007), to investigate the effect of the model input perturbation on the magnitude and profile of the muscle forces. They analyzed factors such as the maximum isometric force, segment masses, location of the hip joint center, number of muscles, and use of different dynamic simulation methods. Myers et al. (2015) developed an open-source probabilistic MSK modeling framework to assess how measurement error and parameter uncertainty such as marker placement, movement artifacts, body segment parameters, and muscle parameters propagate through a gait simulation. They used the gait2392 OpenSim model (Delp et al., 1990) and concluded that the effect of the parameter changes, resulting in mean bounds that ranged from 2.7 to 8.1 Nm in joint moments, 2.7°-6.4° in joint kinematics, and 35.8 to 130.8 N in muscle forces. The effect of the different joint axis definitions has been studied by Martelli et al. (2015) that found an average variation of 2.38° and 0.33 of body weight (BW) for the joint angles and joint forces, respectively. Roelker et al. (2017) made a global comparison of joint kinematics, muscle activation and force during gait between four different OpenSim models (Delp et al., 1990; Arnold et al., 2010; Hamner et al., 2010; Caruthers et al., 2016). Their study showed that differences in coordinate system definition and muscle parameters may significantly impact the simulation results. In addition, they found that among all factors, muscle parameters, skeletal anatomy, coordinate system definition, virtual marker location, and scale factors influence kinematics and kinetics outputs the most.

To the knowledge of the authors, there are no studies in the literature that identify and quantify the uncertainties related to the boundary conditions, due to differences in the definition of generic MSK models, which are used as inputs to coupled finite element models. This study aims to investigate this aspect by comparing predicted TKR kinematics and knee joint forces during level walking obtained from three different generic MSK

TABLE 1 | Main differences among the three models, i.e., Arnold, Rajagopal, and Lai.

Model	Arnold	Rajagopal	Lai
Muscle model	Schutte (Schutte et al., 1993) + Thelen (Thelen, 2003)	Millard (Millard et al., 2013)	Millard (Millard et al., 2013)
Muscle parameters	Ward (Ward et al., 2009)	Ward (Ward et al., 2009) + Handsfield (Handsfield et al., 2014)[a]	Ward (Ward et al., 2009) + Handsfield (Handsfield et al., 2014)[b]
Kinematic of the TFJ	Walker (Walker et al., 1988)	Walker (Walker et al., 1988)	Modified Walker (Walker et al., 1988)
Range of motion for FE rotation	[0–100°]	[0–120°]	[0–140°]
Coordinates implemented in the TFJ[c]	FE, IE, AA rotations PD, AP translations	FE, IE, AA rotations PD, AP translations	FE, IE, AA rotations ML, PD, AP translations

[a] *Lower extremity muscle architecture was improved by combining the cadever-based estimates of optimal muscle fiber lengths and pennation angles derived by Ward et al. (2009) with magnetic resonance imaging (MRI) muscle volume data of 24 young healthy subjects reported in Handsfield et al. (2014).*
[b] *The muscle tendon parameters and paths defined in the Rajagopal model were updated for 22 muscle tendon units (11 per leg). They did not change the muscle maximum isometric forces.*
[c] *The FE is the only indipendent coordinate implemented in the TFJ for all the three models.*

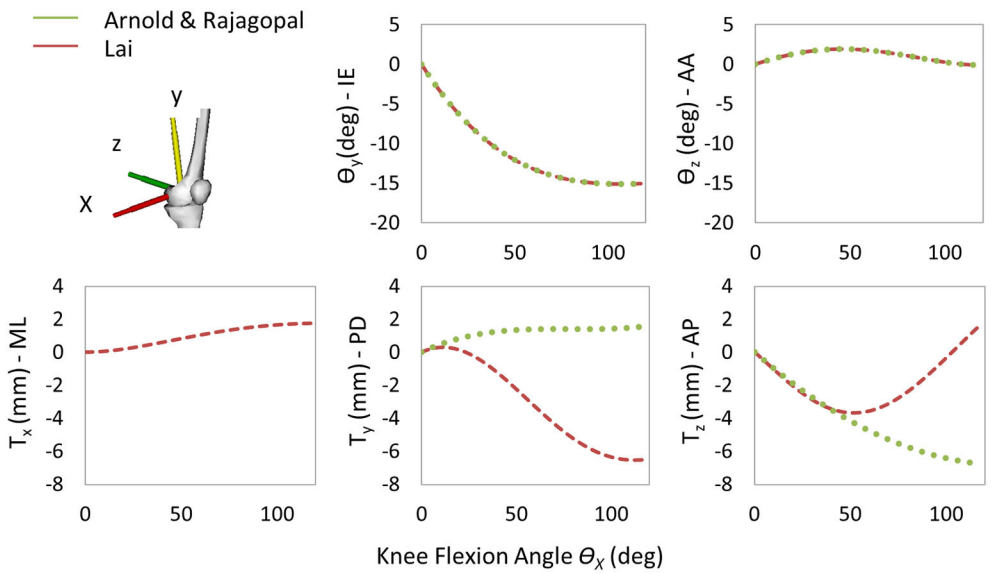

FIGURE 1 | Trends of the coupled translations and rotations of the tibia with respect to the femur as a function of the knee flexion angle for the three models. Only one curve is reported for Arnold and Rajagopal since the same knee spline functions are implemented in the models.

models, each scaled to fit the patient of the Fifth Knee Grand Challenge (KGC) (Fregly et al., 2012).

MATERIALS AND METHODS

Experimental Data

Experimental data obtained from the fifth edition of the KGC Competitions (Fregly et al., 2012; Kinney et al., 2013) of a specific patient labeled PS (age: 86, height: 180 cm, and mass: 75 kg) were used in this study. In particular, a standing reference trial (*PS_staticfor2*) and four overground gait trials at the self-selected speed of the subject (*PS_ngait_og,* trials *1*, *7*, *8*, and *11*) were used for the model scaling and walking simulations, respectively. The *in vivo* forces and moments acting on the left knee joint were available from six load cell sensors embedded in the tibial implant (eTibia). Motion capture data were synchronized and preprocessed using an *ad hoc* MATLAB® script in order to select the time interval for the gait cycle (i.e., between two consecutive heel strikes of the left foot) and to obtain OpenSim input files. The ground reaction force data, computed about the center of pressure, were filtered with a zero-lag fourth-order low-pass Butterworth filter with a cut-off frequency of 30 Hz.

Musculoskeletal Models

The following three generic MSK models were selected for this study: Lower Limb Model 2010 (Arnold et al., 2010), Rajagopal2016 Full-Body Model (Rajagopal et al., 2016), and Lai2017 Full Upper and Lower Body Model (Lai et al., 2017). The three models, called hereinafter Arnold, Rajagopal, and Lai, respectively, are available on the OpenSim's website and shared the same body segment geometries, inertial properties, and body coordinate reference systems (CRS). The inertial properties come from a cohesive set of 21 cadaveric specimens (height: 168.4 ± 9.3 cm and mass: 82.7 ± 15.2 kg) (Ward et al., 2009), and

the bone geometries were created by digitalizing a set of bones from a 170-cm tall male subject. While anatomically similar, these three models implement different tibiofemoral joint (TFJ) kinematics and muscle models. Arnold is based on the gait2392 lower limb model (Delp et al., 1990) and uses the equations reported in the study by Walker et al. (1988) for the knee joint kinematic definition. Compared with gait2392, the Arnold model more accurately describes the muscle geometries and physiology. Rajagopal tries to overcome some of the major limitations of the Arnold model (i.e., extensive use of ellipsoidal wrapping surfaces and muscle parameters suited for elderly individuals). Finally, the Lai model is an improved version of the Rajagopal model capable of simulating pedaling and fast running in addition to walking. The TFJ kinematics is slightly modified in Lai compared with the Arnold and the Rajagopal model where the same equations are used to define anterior–posterior (AP) and proximal–distal translation, internal–external (IE), and abduction–adduction (AA) rotation as function of the flexion–extension (FE) degree of freedom. It is important to notice that in the Lai model, the medial–lateral (ML) translation was also included in the TFJ kinematics, and an offset of 3.6, −1.7, and 1 mm in the X-, Y-, and Z-direction, respectively, was introduced to reposition the tibia with respect to the femur. Main differences among the three models are reported in **Table 1**. A comparison of the trends of the coupled translations and rotations of the tibia with respect to the femur as a function of FE angle is shown in **Figure 1**.

The generic models were scaled to approximate the anthropometry of the subject under this study. Then, the femoral component (FC) and the TI geometries were added to the kinematic chain to enable the study of the implant kinematics, relevant for any FEA application. In particular, the FC was rigidly connected to the left femur and the left tibia to TI using two welding joints (**Figure 2A**). The geometry. *stl* files of the implant were converted in. *vtp* format files by using the nmsBuilder software[1] (Valente et al., 2017). To find the relative position and orientation between the implant components and the corresponding bones, the provided *Full Leg.wrp* geometry file was used as a reference. This file includes bone geometries of the left leg of the subject with properly positioned and oriented implant components. The realistic alignment was thus reproduced by identifying bony landmark positions (i.e., hip joint center and medial and lateral epicondyles) in the femur of the generic model and one of the subject PS as shown in **Figure 2B**. The same virtual marker set (47 markers) defined by looking at the experimental marker positions was assigned to all the three models.

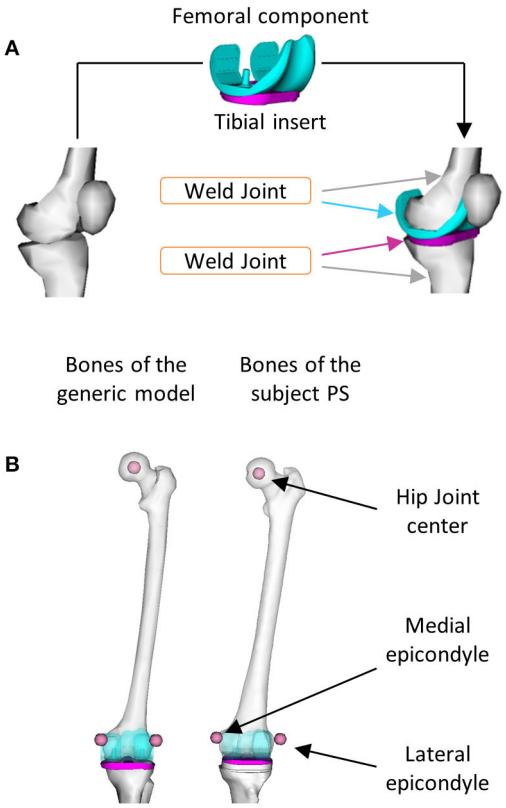

FIGURE 2 | Procedures used to include the implant components in the model: **(A)** Two welding joints were defined to connect the femoral component to the left femur and the tibial insert to the left tibia and **(B)** Bony landmarks were identified in the left femur of the generic model and in the one of the subject PS.

Simulation Workflow

The simulations were performed using OpenSim 3.3 and MATLAB®. As shown in **Figure 3**, two main analyses were conducted as follows: a kinematics analysis to estimate the relative pose of the TI with respect to the FC (kinematic output) and a dynamic analysis to compute the loads acting between the two implant components (dynamic output). For all three models, the same setup files used as inputs to the simulations were employed.

Kinematic Analysis

Joint coordinates were first computed using the inverse kinematic (IK) OpenSim tool that solves a weighted least square problem to best reproduce the experimental kinematic data by minimizing the distance between corresponding pairs of virtual and experimental markers (Lu and O'Connor, 1999). The body kinematic (BK) tool was then used to obtain information about the pose of the TI and the FC during the simulated gait task (**Figure 3**). BK records the orientation and the position of the reference system of each body (located at the center of mass) with respect to the ground CRS.

Dynamic Analysis

Muscle forces were first estimated using the static optimization (SO) approach. SO solves the muscle redundancy problem by minimizing the sum of muscle activations squared (Anderson and Pandy, 2001). Ideal force generators (i.e., reserve actuators) to ensure dynamic consistency were added about each joint. A unitary maximum force was assigned to prevent them from altering the muscle recruitment by taking too much of the joint

[1]http://www.nmsbuilder.org/

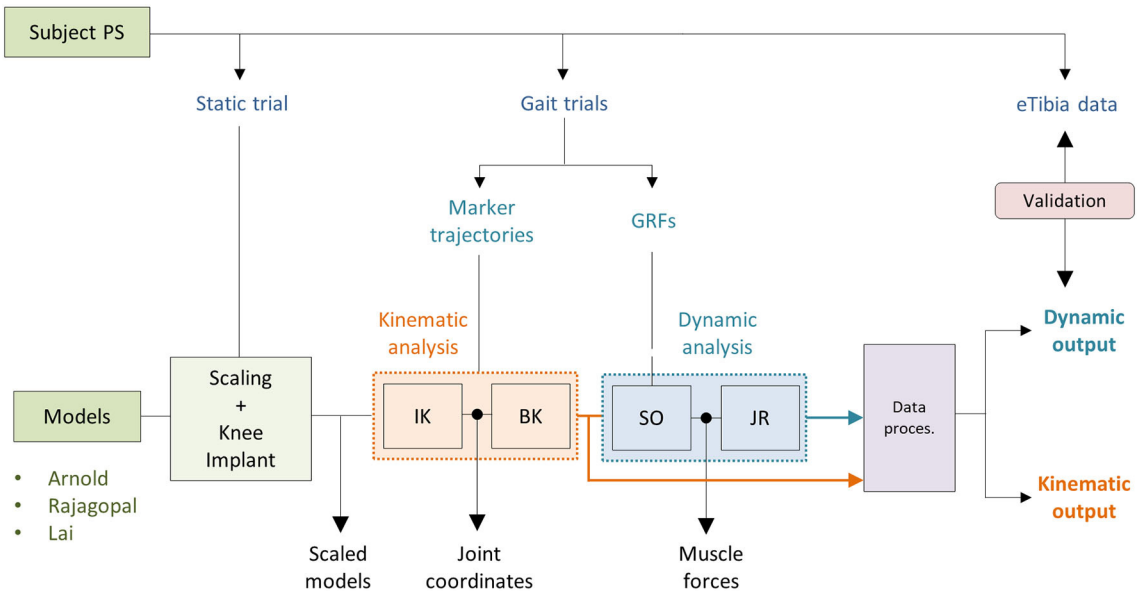

FIGURE 3 | Simulation workflow performed using OpenSim 3.3 and Matlab®.

torque. Residual actuators with a maximum generalized force of 100 N were applied to the pelvis joint. Also, the maximum isometric force of all the muscles involved in the FE of the left knee was reduced by 35%. A reduced strength of the flexor/extensor muscles has been reported for patients who undergo TKR (Marra et al., 2015). The JR analysis (Steele et al., 2012) was then performed to compute the knee JR forces and moments acting on the tibia (**Figure 3**).

Comparison of Results and Model Validation

The data obtained from the kinematic and dynamic analyses were processed with an *ad hoc* Matlab® script (**Figure 3**). In this step, the pose of the TI relative to the FC during the simulated gait task was computed. The forces and moments acting on the tibia, estimated using the JR analysis, were first referred to the TI coordinate reference system and then transformed in order to compare them with the measured loads of the instrumented eTibia device. The coordinate system of the eTibia load measurements was, in fact, not consistent with the body CRS of the TI. Medial and lateral contact forces (F_{MED} and F_{LAT}) were computed using the regression equations provided by the KGC competition dataset that consider the terms related to the superior–inferior force (Fz_T) and varus–valgus moment (My_T):

$$F_{MED} = 0.510\,Fz_T + 0.0213\,My_T \quad (1)$$

$$F_{LAT} = 0.49\,Fz_T - 0.0213\,My_T \quad (2)$$

where the force is expressed in N and the moment in N mm. The total compressive contact force (F_{TOT}) is then computed as the $F_{LAT} + F_{MED}$.

Based on the four gait trials, mean and SD were computed for both predicted and measured quantities in each time interval of the gait cycle. Also, maximum SD and maximum variation range (VR) metrics were calculated to quantify within and between model prediction variability, respectively. The first index is a measure of dispersion defined as the maximum value of the SD computed at each time interval and considering the simulation results of all the four trials obtained with the same model. The maximum VR is a measure of variability between model predictions obtained considering the maximum difference between the minimum and maximum mean value calculated at each time interval with the three models. In order to validate the simulation results and quantify the difference between model prediction and experimental measurements obtained from the instrumented implant, root mean squared errors (RMSE) and the coefficient of determination (R^2) were computed individually for each trial and hereby reported as mean across the four trials.

RESULTS

Kinematic Results

The Euler angle (θ_x, θ_y, and θ_z) trajectories and the position vector components (FT_x, FT_y, and FT_z) that defined the pose of the TI with respect to the FC during the simulated gait trial are shown in **Figure 4**. The curves had similar trends but non-negligible differences in magnitude were observed especially in the AP and SI translations. The VR was lower than 0.9° for the three Euler angles and 1 mm for the ML translation, while maximum VR values equal to 4.65 mm and 7.72 mm were observed during the stance phase in the AP translation and during the swing phase for the SI translation, respectively (**Table 2**). Within and between model variability in terms of maximum SD values and VR are reported in **Table 2** for all the six quantities that define the kinematic output.

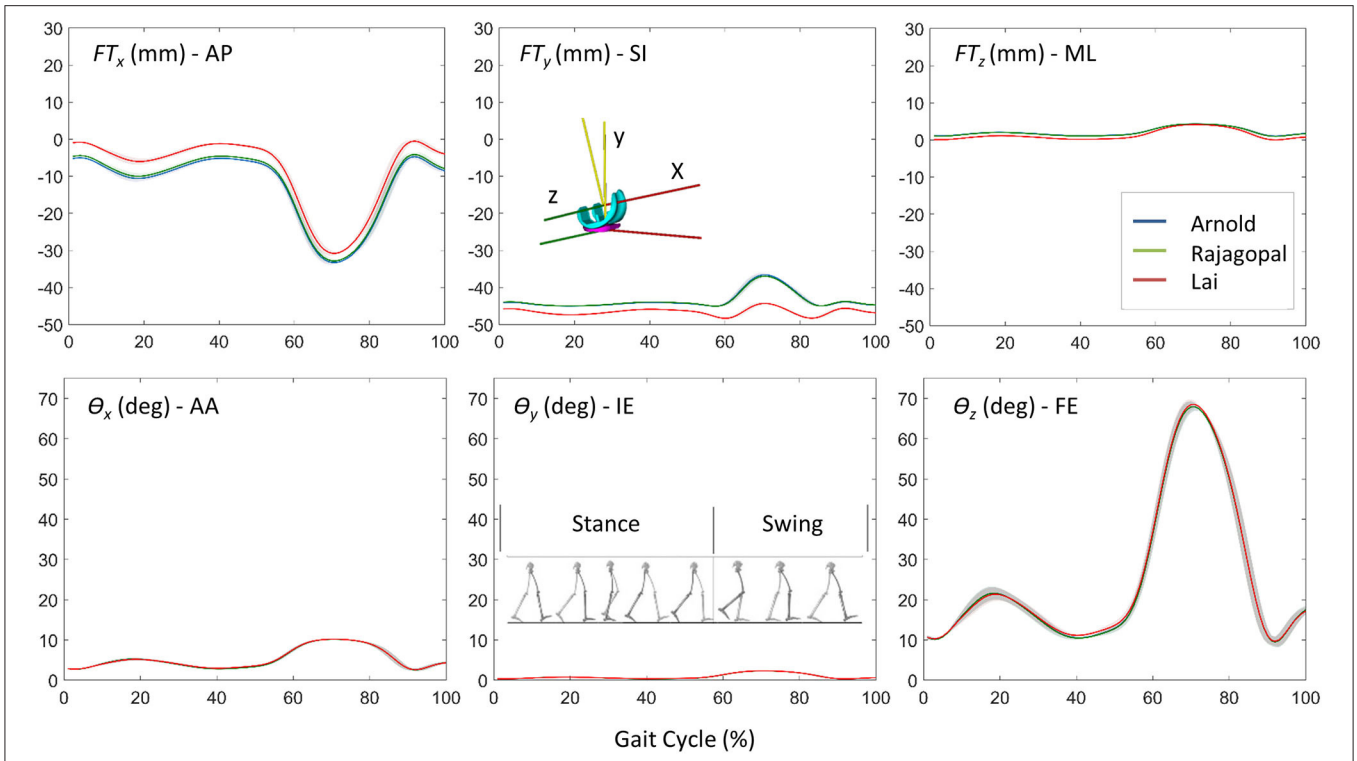

FIGURE 4 | The comparison of kinematic results for the three models: position vector components (FT_x, FT_y, and FT_z) and Euler angles (θx, θy, and θz) that defined the pose of the TI with respect to the FC during the simulated gait trial.

TABLE 2 | Within and between model variability in terms of maximum SD values and variation range for all the quantities that define the kinematic and dynamic musculoskeletal simulation output.

		Kinematic output						Dynamic output					
		FTx (mm)	FTy (mm)	FTz (mm)	θx (deg)	θy (deg)	θz (deg)	Fx (N)	Fy (N)	Fz (N)	Mx (Nm)	My (Nm)	Mz (Nm)
Max SD	Arnold	2.87	1.18	0.39	0.22	0.97	5.57	124.3	293.7	15.54	6.87	3.29	13.5
	Rajagopal	2.88	1.15	0.41	0.22	0.98	5.59	93.37	228.61	20.04	5.07	3.09	3.14
	Lai	2.92	0.72	0.48	0.22	0.98	5.62	97.33	235.8	17.67	4.94	2.82	3.57
Max VR		4.65	7.72	1.03	0.032	0.194	0.84	222	933.61	112.53	7.76	2.91	40.85

Dynamic Results and Model Validation

Figure 5 shows the JR forces and moments acting on the TI and expressed in the CRS of the TI component, as predicted by the dynamic MSK simulations. Maximum SD and VR values were found large for the normal force and the moment about the FE axis (**Table 2**). Maximum VR values of about 930 N and 40 Nm were observed for *Fy* and *Mz*, respectively, in correspondence of the first characteristic peak (i.e., ∼20% gait cycle, during heel strike). Medial, lateral, and total knee joint contact forces acting on the TI as predicted by the three MSK models and measured *in vivo* via the instrumented implant are shown in **Figure 6**. Two typical force peaks at approximately the time of the toe-off and heel strike can be observed in the medial, lateral, and total contact forces. Experimental data from the instrumented knee implant reported maximum values of the total knee contact force of about 2.2 BW and 1.9 BW for the first and second peak, respectively, while predicted values ranged from about 1 BW to 2.3 BW and from 2.4 BW to 2.9 BW. Lateral forces were in general underestimated by all the three models while the medial forces were slightly overpredicted. Results in terms of RMSE and R^2 for the total contact force are reported in **Table 3** together with the maximum SD for the measured and predicted medial, lateral, and total contact forces. The mean RMSE of total contact force across the models range from 0.38 and 0.62 BW and R^2 values range from 0.22 to 0.80.

DISCUSSION

The aim of this study was to compare the simulation results obtained from three different generic MSK models, scaled to fit the patient of the Fifth KGC, in terms of TKR kinematics

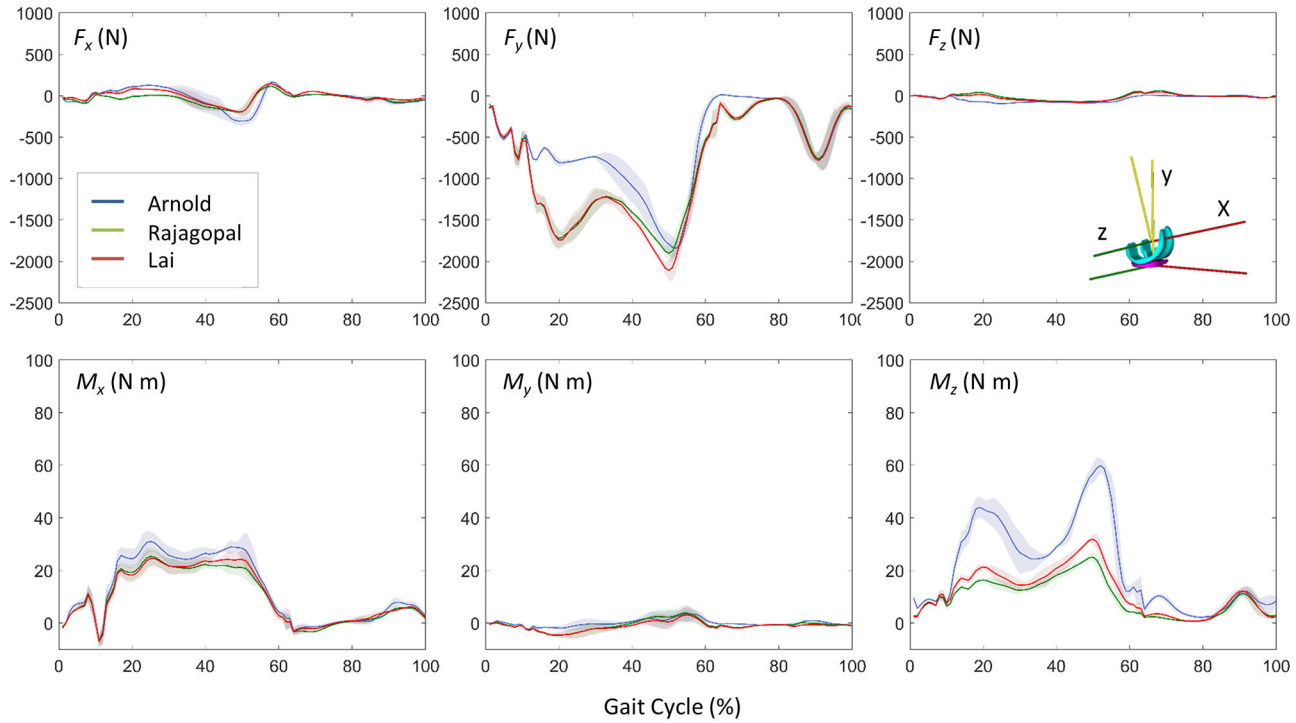

FIGURE 5 | Dynamic results comparison for the three models: three force and moment components acting on the TI predicted by the musculoskeletal models (mean ± SD).

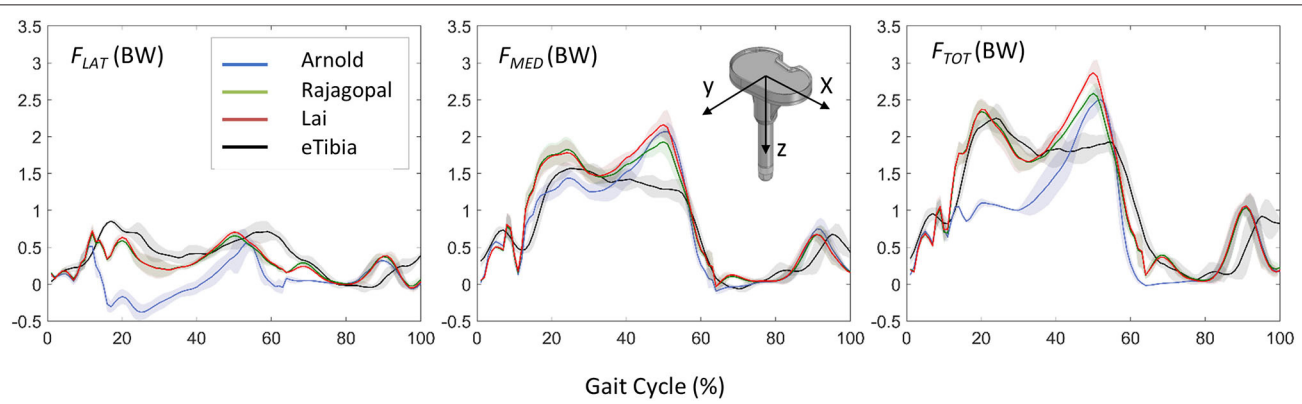

FIGURE 6 | Comparison between the predicted loads and the *in vivo* measurements in terms of lateral, medial, and total forces acting on the TI component and expressed in the coordinate reference systems of the instrumented eTibia device.

and knee joint force during level walking which can be used as boundary conditions in a coupled finite element model when scaled to fit the patient of the Fifth KGC (Fregly et al., 2012). The estimated knee JRs were also compared with those measured by the instrumented knee implant to quantify the "global goodness of fit" for each model. As we did not have a true value for the knee kinematics (typically provided by fluoroscopy, not available in the Fifth KGC for the gait trials analyzed in this study), we could only compare these in terms of relative differences between the three models. In the predicted relative pose of the two implant components, for example, a slight shift in the AP and SI translation curves was found for the Lai model. This can be justified by the different tibia positions with respect to the femoral body as described in the "Musculoskeletal Models" section and by the different kinematic definitions of the knee joint as explained in **Figure 1**. The most recent Lai model was developed to better predict the activation pattern of muscles during walking, pedaling, and fast running. It considers an increased range for the flexion angle and a different knee spline function definition for the custom joint. Small differences can

TABLE 3 | Maximum SD for the predicted and measured F_{TOT}, F_{LAT}, and F_{MED}.

	Max SD			RMSE F_{TOT} (BW)	R^2 F_{TOT}
	F_{LAT} (BW)	F_{MED} (BW)	F_{TOT} (BW)		
Arnold	0.28	0.23	0.4	0.62	0.22
Rajagopal	0.14	0.22	0.31	0.38	0.80
Lai	0.16	0.25	0.32	0.43	0.77
eTibia	0.18	0.25	0.37	–	–

Root mean squared error (RMSE) and coefficient of determination (R^2) are computed for the results of three models considering the total contact force acting at the tibial insert component.

be observed by looking at the kinematic results suggested by the Rajagopal and Arnold models (<12.6% maximum percentage difference for AP, SI, and ML translations and <1% for AA, IE, and FE rotations). This is probably due to a non-identical definition of the whole kinematic chain which might result in a non-identical solution of the scaling and IK problem. Rajagopal and Arnold used the same spline functions for the TFJ, but differences can be observed, for example, in the knee FE range or the patellofemoral joint definition.

A comparison of the results obtained in terms of knee implant kinematics with respect to the literature is complicated by the following two facts: on the one hand, only few studies are focused on the use of MSK models to predict the relative pose of the knee implant components during gait, and on the other hand, in these studies, different coordinate systems are used to monitor the relative pose of the two implant components. For instance, in the study proposed by Zhang et al. (2017), which used the same experimental data obtained from the KGC, the FE, IE rotations, and AP translations estimated by the MSK simulations were considered as inputs to the finite element model. The trend of the FE angle is very similar to the one obtained in this study; however, the differences observed by comparing the results related to the other two movements might be due to a different initial location of the origins of the FC and TI CRS.

The accuracy of the three models in predicting the force transmitted at the knee joint was found comparable with that reported in previous studies (Marra et al., 2015; Chen et al., 2016; Andersen, 2018). The correlation between the prediction and measured values of the model is pretty low for the Arnold's model ($R^2 = 0.22$), better for the Lai's model ($R^2 = 0.77$), and even better for the Rajagopal's model ($R^2 = 0.80$). The average error, expressed in terms of RMSE was 0.62, 0.38, and 0.43 BW for the Arnold, Rajagopal, and Lai models, respectively. An overestimation of the total contact force can be observed by looking at the results obtained with all the models in correspondence of the second peak; this might be due to compensatory patterns adopted by the patient. It is not unusual in knee replacement patients to see as compensatory pattern a shift of the load to the other leg during the bipodal phase.

The important differences in terms of predicted joint forces between the three models can be justified by the adoption of a different musculotendinous dynamics model and muscle architectural parameters. Arnold uses the old Schutte1993Muscle model (Schutte et al., 1993) with exceptions on the back muscles that were adapted from the gait_2393 OpenSim model and remain as Thelen2003Muscle format (Thelen, 2003). These muscle models have been updated with the Millard2012EquilibriumMuscle used in Rajagopal and Lai which seems to better describe the specific patient physiology. The characteristic curves defining musculotendon behavior (i.e., tendon force-length, fiber force-length, and force-velocity curves) were improved and more force-generating properties of realistic muscles (e.g., maximum isometric force, optimal fiber length, fiber pennation angles, and tendon slack length) based on magnetic resonance images of healthy subjects were considered (Handsfield et al., 2014). Lai implements further improvements aimed to decrease co-activation of antagonist muscles due to excessing passive force generated by knee and hip extensors.

The adjustments implemented in Lai's model (briefly described in "Musculoskeletal Models" section), which proved to be useful to better predict fast walking and running with respect to Rajagopal's model (Lai et al., 2017), did not produce an improvement in predicting joint forces for a TKR subject. This points out a critical aspect in the use of generic MSK models, also discussed in a previous study (Silva et al., 2021): the need of adapting modeling features in the context of their intended use, for example, exploring and describing common pathology-specific patterns. This overlaps with the theme of personalized models.

Some limitations of this study are important to be mentioned. First, only three generic MSK models were used in the comparative analyses. However, as also mentioned in the "Introduction" section, they were selected because they use the same body geometries, inertial properties, and body coordinate systems. This allows the authors to evaluate the only effect of the different joint kinematic definitions and the different muscle model implementations on the simulation results. Among the factors that mostly affect model predictions are in fact discrepancies in coordinate system definitions, virtual marker sets, and body geometries (Roelker et al., 2017). Another important limitation that is worth mentioning is related to the fact that only gait trials performed by one subject are simulated. Additional analyses that also evaluate inter-subject variability and movement tasks other than level walking should be considered in future studies.

CONCLUSION

This comparative study demonstrated that selecting a generic MSK model is an important step. Modelers should be aware of the effect of the MSK modeling assumptions and their influence on the kinematic and dynamic results that depending on the context of use might or might not be critical. This is obviously a delicate point if the results of the MSK simulations are the main outcomes of the analysis but also if they are used as inputs for finite element models in a combined MSK-FEA approach. This study represents a good starting point for future investigations that will evaluate how uncertainties related to MSK models propagate in the FEA results. Detailed studies on uncertainty quantification analyses

in the combined MSK-FEA approach will undoubtedly provide important insight in the context of model credibility assessment for the biomechanics community.

DATA AVAILABILITY STATEMENT

The raw data supporting the conclusions of this article will be made available by the authors, without undue reservation.

AUTHOR CONTRIBUTIONS

CC, FDP, and LM: conceptualization and methodology. CC, GD, and LM: simulations and data processing. CC and GD: data curation. CC: writing—original draft preparation and visualization. CC, GD, LM, FDP, and MV: writing—review and editing. FDP and LM: supervision. MV: funding acquisition. All authors contributed to the article and approved the submitted version.

FUNDING

This study was supported by the Mobilise-D project (H2020-EU.3.1.7-IMI22017-13-7; Grant Agreement No. 820820).

ACKNOWLEDGMENTS

CC would like to thank Prof. Andrew Philips for kindly hosting her at the Structural Biomechanics group at Imperial College London during part of this study. LM was supported by an Imperial College Research Fellowship granted by Imperial College London.

REFERENCES

Andersen, M. S. (2018). How sensitive are predicted muscle and knee contact forces to normalization factors and polynomial order in the muscle recruitment criterion formulation? *Int. Biomech.* 5, 88–103. doi: 10.1080/23335432.2018.1514278

Anderson, F. C., and Pandy, M. G. (1999). A dynamic optimization solution for vertical jumping in three dimensions. *Computer Methods Biomech. Biomed. Eng.* 2, 201–231. doi: 10.1080/10255849908907988

Anderson, F. C., and Pandy, M. G. (2001). Static and dynamic optimization solutions for gait are practically equivalent. *J. Biomech.* 34, 153–161. doi: 10.1016/S0021-9290(00)00155-X

Arnold, E. M., Ward, S. R., Lieber, R. L., and Delp, S. L. (2010). A model of the lower limb for analysis of human movement. *Ann. Biomed. Eng.* 38, 269–279. doi: 10.1007/s10439-009-9852-5

Caruthers, E. J., Thompson, J. A., Chaudhari, A. M. W., Schmitt, L. C., Best, T. M., Saul, K. R., et al. (2016). Muscle forces and their contributions to vertical and horizontal acceleration of the Center of mass during sit-to-stand transfer in young, healthy adults. *J. Appl. Biomech.* 32, 487–503 doi: 10.1123/jab.2015-0291

Chen, Z., Zhang, Z., Wang, L., Li, D., Zhang, Y., and Jin, Z. (2016). Evaluation of a subject-specific musculoskeletal modelling framework for load prediction in total knee arthroplasty. *Med. Eng. Phys.* 38, 708–716. doi: 10.1016/j.medengphy.2016.04.010

Delp, S. L., Anderson, F. C., Arnold, A. S., Loan, P., Habib, A., John, C. T., et al. (2007). OpenSim: open-source software to create and analyze dynamic simulations of movement. *IEEE Trans. Biomed. Eng.* 54, 1940–1950. doi: 10.1109/TBME.2007.901024

Delp, S. L., Loan, J. P., Hoy, M. G., Zajac, F. E., Topp, E. L., and Rosen, J. M. (1990). An interactive graphics-based model of the lower extremity to study orthopaedic surgical procedures. *IEEE Trans. Biomed. Eng.* 37, 757–767. doi: 10.1109/10.102791

Fregly, B. J., Besier, T. F., Lloyd, D. G., Delp, S. L., Banks, S. A., Pandy, M. G., et al. (2012). Grand challenge competition to predict in vivo knee loads. *J. Orthopaedic Res.* 30, 503–513. doi: 10.1002/jor.22023

Hamner, S. R., Seth, A., and Delp, S. L. (2010). Muscle contributions to propulsion and support during running. *J. Biomech.* 43, 2709–2716. doi: 10.1016/j.jbiomech.2010.06.025

Handsfield, G. G., Meyer, C. H., Hart, J. M., Abel, M. F., and Blemker, S. S. (2014). Relationships of 35 lower limb muscles to height and body mass quantified using MRI. *J. Biomech.* 47, 631–638. doi: 10.1016/j.jbiomech.2013.12.002

Hume, D. R., Navacchia, A., Rullkoetter, P. J., and Shelburne, K. B. (2019). A lower extremity model for muscle-driven simulation of activity using explicit finite element modeling. *J. Biomech.* 84, 153–160. doi: 10.1016/j.jbiomech.2018.12.040

Khan, M., Osman, K., Green, G., and Haddad, F. S. (2016). The epidemiology of failure in total knee arthroplasty. *Bone Joint J.* 98-B, 105–112. doi: 10.1302/0301-620X.98B1.36293

Kinney, A. L., Besier, T. F., D'Lima, D. D., and Fregly, B. J. (2013). Update on grand challenge competition to predict in vivo knee loads. *J. Biomech. Eng.* 135:021012. doi: 10.1115/1.4023255

Lai, A. K. M., Arnold, A. S., and Wakeling, J. M. (2017). Why are antagonist muscles co-activated in my simulation? A musculoskeletal model for analysing human locomotor tasks. *Ann. Biomed. Eng.* 45, 2762–2774. doi: 10.1007/s10439-017-1920-7

Lu, T. W., and O'Connor, J. J. (1999). Bone position estimation from skin marker co-ordinates using global optimisation with joint constraints. *J. Biomech.* 32, 129–134. doi: 10.1016/S0021-9290(98)00158-4

Marra, M. A., Vanheule, V., Fluit, R., Koopman, B. H. F. J. M., Rasmussen, J., Verdonschot, N., et al. (2015). A subject-specific musculoskeletal modeling framework to predict *in vivo* mechanics of total knee arthroplasty. *J. Biomech. Eng.* doi: 10.1115/1.4029258

Martelli, S., Valente, G., Viceconti, M., and Taddei, F. (2015). Sensitivity of a subject-specific musculoskeletal model to the uncertainties on the joint axes location. *Comput. Methods Biomech. Biomed. Eng.* 18, 1555–1563. doi: 10.1080/10255842.2014.930134

Millard, M., Uchida, T., Seth, A., and Delp, S. L. (2013). Flexing computational muscle: modeling and simulation of musculotendon dynamics. *ASME J. Biomech. Eng.* 135:021005. doi: 10.1115/1.4023390

Modenese, L., and Kohout, J. (2020). Automated generation of three-dimensional complex muscle geometries for use in personalised musculoskeletal models. *Ann. Biomed. Eng.* 48, 1793–1804. doi: 10.1007/s10439-020-02490-4

Modenese, L., Montefiori, E., Wang, A., Wesarg, S., Viceconti, M., and Mazzà, C. (2018). Investigation of the dependence of joint contact forces on musculotendon parameters using a codified workflow for image-based modelling. *J. Biomech.* 73, 108–118. doi: 10.1016/j.jbiomech.2018.03.039

Modenese, L., Phillips, A. T. M., and Bull, A. M. J. (2011). An open source lower limb model: hip joint validation. *J. Biomech.* 44, 2185–2193. doi: 10.1016/j.jbiomech.2011.06.019

Modenese, L., and Renault, J.-B. (2021). Automatic generation of personalised skeletal models of the lower limb from three-dimensional bone geometries. *J. Biomech.* 116:110186. doi: 10.1016/j.jbiomech.2020.110186

Myers, C. A., Laz, P. J., Shelburne, K. B., and Davidson, B. S. (2015). A probabilistic approach to quantify the impact of uncertainty propagation in musculoskeletal simulations. *Ann. Biomed. Eng.* 43, 1098–1111. doi: 10.1007/s10439-014-1181-7

Nakano, N., Shoman, H., Olavarria, F., Matsumoto, T., Kuroda, R., and Khanduja, V. (2020). Why are patients dissatisfied following a total knee

replacement? A systematic review. *Int. Orthopaedics (SICOT)* 44, 1971–2007. doi: 10.1007/s00264-020-04607-9

Rajagopal, A., Dembia, C., DeMers, M., Delp, D., Hicks, J., and Delp, S. (2016). Full body musculoskeletal model for muscle- driven simulation of human gait. *IEEE Trans. Biomed. Eng.* 63, hbox2068–2079. doi: 10.1109/TBME.2016.2586891

Roelker, S. A., Caruthers, E. J., Baker, R. K., Pelz, N. C., Chaudhari, A. M. W., and Siston, R. A. (2017). Interpreting musculoskeletal models and dynamic simulations: causes and effects of differences between models. *Ann. Biomed. Eng.* 45, 2635–2647. doi: 10.1007/s10439-017-1894-5

Schutte, L. M., Rodgers, M. M., Zajac, F. E., and Glaser, R. M. (1993). Improving the efficacy of electrical stimulation-induced leg cycle ergometry: an analysis based on a dynamic musculoskeletal model. *IEEE Trans. Rehabil. Eng.* 1, 109–125. doi: 10.1109/86.242425

Shu, L., Hashimoto, S., and Sugita, N. (2020a). Enhanced *in-silico* polyethylene wear simulation of total knee replacements during daily activities. *Ann. Biomed. Eng.* 49, 323–333. doi: 10.1007/s10439-020-02555-4

Shu, L., Li, S., and Sugita, N. (2020b). Systematic review of computational modelling for biomechanics analysis of total knee replacement. *Biosurface Biotribol.* 6, 3–11. doi: 10.1049/bsbt.2019.0012

Silva, M., Freitas, B., Andrade, R., Carvalho, Ó., Renjewski, D., Flores, P., et al. (2021). Current perspectives on the biomechanical modelling of the human lower limb: a systematic review. *Arch. Computat. Methods Eng.* 28, 601–636. doi: 10.1007/s11831-019-09393-1

Steele, K. M., DeMers, M. S., Schwartz, M. H., and Delp, S. L. (2012). Compressive tibiofemoral force during crouch gait. *Gait Posture* 35, 556–560. doi: 10.1016/j.gaitpost.2011.11.023

Thelen, D. G. (2003). Adjustment of muscle mechanics model parameters to simulate dynamic contractions in older adults. *J. Biomech. Eng.* 125, 70–77. doi: 10.1115/1.1531112

Valente, G., Crimi, G., Vanella, N., Schileo, E., and Taddei, F. (2017). NMSBUILDER: freeware to create subject-specific musculoskeletal models for OpenSim. *Comput. Methods Programs Biomed.* 152, 85–92. doi: 10.1016/j.cmpb.2017.09.012

Walker, P. S., Rovick, J. S., and Robertson, D. D. (1988). The effects of knee brace hinge design and placement on joint mechanics. *J. Biomech.* 21, 965–974. doi: 10.1016/0021-9290(88)90135-2

Ward, S. R., Eng, C. M., Smallwood, L. H., and Lieber, R. L. (2009). Are current measurements of lower extremity muscle architecture accurate? *Clin. Orthop. Relat. Res.* 467, 1074–1082. doi: 10.1007/s11999-008-0594-8

Zhang, J., Chen, Z., Wang, L., Li, D., and Jin, Z. (2017). A patient-specific wear prediction framework for an artificial knee joint with coupled musculoskeletal multibody-dynamics and finite element analysis. *Tribol. Int.* 109, 382–389. doi: 10.1016/j.triboint.2016.10.050

Zuk, M., Syczewska, M., and Pezowicz, C. (2018). Sensitivity analysis of the estimated muscle forces during gait with respect to the musculoskeletal model parameters and dynamic simulation techniques. *J. Biomech. Eng.* doi: 10.1115/1.4040943. [Epub ahead of print].

Conflict of Interest: The authors declare that the research was conducted in the absence of any commercial or financial relationships that could be construed as a potential conflict of interest.

Publisher's Note: All claims expressed in this article are solely those of the authors and do not necessarily represent those of their affiliated organizations, or those of the publisher, the editors and the reviewers. Any product that may be evaluated in this article, or claim that may be made by its manufacturer, is not guaranteed or endorsed by the publisher.

frontiers in Bioengineering and Biotechnology

ORIGINAL RESEARCH
published: 05 November 2021
doi: 10.3389/fbioe.2021.701712

Saccade and Fixation Eye Movements During Walking in People With Mild Traumatic Brain Injury

Ellen Lirani-Silva [1], Samuel Stuart [2,3], Lucy Parrington [1,4], Kody Campbell [1,4] and Laurie King [1,4]*

[1]Balance Disorders Laboratory, Department of Neurology, Oregon Health and Science University, Portland, OR, United States, [2]Department of Sport, Exercise and Rehabilitation, Northumbria University, Newcastle Upon Tyne, United Kingdom, [3]Northumbria Healthcare NHS Foundation Trust, North Shields, United Kingdom, [4]Veterans Affairs Portland Oregon Health Care System, Portland, OR, United States

Background: Clinical and laboratory assessment of people with mild traumatic brain injury (mTBI) indicate impairments in eye movements. These tests are typically done in a static, seated position. Recently, the use of mobile eye-tracking systems has been proposed to quantify subtle deficits in eye movements and visual sampling during different tasks. However, the impact of mTBI on eye movements during functional tasks such as walking remains unknown.

Objective: Evaluate differences in eye-tracking measures collected during gait between healthy controls (HC) and patients in the sub-acute stages of mTBI recovery and to determine if there are associations between eye-tracking measures and gait speed.

Methods: Thirty-seven HC participants and 67individuals with mTBI were instructed to walk back and forth over 10-m, at a comfortable self-selected speed. A single 1-min trial was performed. Eye-tracking measures were recorded using a mobile eye-tracking system (head-mounted infra-red Tobbii Pro Glasses 2, 100 Hz, Tobii Technology Inc. VA, United States). Eye-tracking measures included saccadic (frequency, mean and peak velocity, duration and distance) and fixation measurements (frequency and duration). Gait was assessed using six inertial sensors (both feet, sternum, right wrist, lumbar vertebrae and the forehead) and gait velocity was selected as the primary outcome. General linear model was used to compare the groups and association between gait and eye-tracking outcomes were explored using partial correlations.

Results: Individuals with mTBI showed significantly reduced saccade frequency (p = 0.016), duration (p = 0.028) and peak velocity (p = 0.032) compared to the HC group. No significant differences between groups were observed for the saccade distance, fixation measures and gait velocity (p > 0.05). A positive correlation was observed between saccade duration and gait velocity only for participants with mTBI (p = 0.025).

Conclusion: Findings suggest impaired saccadic eye movement, but not fixations, during walking in individuals with mTBI. These findings have implications in real-world function including return to sport for athletes and return to duty for military service members. Future research should investigate whether or not saccade outcomes are influenced by the time after the trauma and rehabilitation.

OPEN ACCESS

Edited by:
Simone Tassani,
Pompeu Fabra University, Spain

Reviewed by:
Mark Ettenhofer,
University of California, United States
Michelle LaPlaca,
Georgia Institute of Technology, United States

****Correspondence:***
Ellen Lirani-Silva
ellenlirani@gmail.com

Specialty section:
This article was submitted to Biomechanics, a section of the journal Frontiers in Bioengineering and Biotechnology

Received: *28 April 2021*
Accepted: *15 October 2021*
Published: *05 November 2021*

Citation:
Lirani-Silva E, Stuart S, Parrington L, Campbell K and King L (2021) Saccade and Fixation Eye Movements During Walking in People With Mild Traumatic Brain Injury. Front. Bioeng. Biotechnol. 9:701712. doi: 10.3389/fbioe.2021.701712

Keywords: saccades, traumatic brain injury, gait, eye tracking, vision

INTRODUCTION

Evidence suggests that visual impairments may occur with mild traumatic brain injury (mTBI) (Ciuffreda et al., 2007; Capó-Aponte et al., 2012; Ventura et al., 2016). These impairments have the potential to affect functional capabilities in everyday life. For example, the visual system allows us to collect vital information about the environment required for safe navigation; it also plays a critical role in coordinating locomotion (Srivastava et al., 2018). In general, potential visual dysfunction of mTBI patients has been assessed using self-report and symptom-based outcomes (e.g. vestibular/ocular-motor screening, VOMS) (Mucha et al., 2014; Kontos et al., 2017; Whitney and Sparto, 2019). Although symptom-based outcomes of ocular motor performance are intended for aiding in concussion diagnosis, they may have limited ability to detect subtle deficits (Meier et al., 2015; Hunt et al., 2016; Snegireva et al., 2018). Comparatively, eye-tracking systems may detect and quantify subtle deficits in visual processes, especially with newer non-invasive technologies capable of sampling at the high frequency needed for capturing quick eye movements (i.e. 100 Hz) (Snegireva et al., 2018). While limited studies exist, this area of research has received increased attention over the last 2 decades (Pearson et al., 2007; Maruta et al., 2010b; Johnson et al., 2015; Snegireva et al., 2018), with impairment of eye-movement outcome measures in mTBI reported.

Most studies using eye-tracking systems with mTBI patients have been restricted to static/seated tests and with this testing paradigm, many differences in eye-movement between healthy controls and people with mTBI have been reported (Stuart et al., 2020a). For example, individuals with diagnosis of acute or post-acute (<12 weeks) mTBI have been found to have: 1) an increased pro-saccade error rate, and an increased saccadic reaction time latency during anti-saccade tasks (Balaban et al., 2016) in a battery of seated oculomotor, vestibular and reaction time tests.; 2) poor saccadic accuracy and longer response latency during horizontal and vertical saccade tasks on the performance of a vestibulo-ocular, visuo-ocular and reaction time battery of tests (I-Portal Neuro Otologic Test Center chair system) (Cochrane et al., 2019); 3) fewer saccades and more blinks compared with their baseline during a seated rapid number-naming task (King-Devick test) (Hecimovich et al., 2019); 4) greater gaze resultant distance, pro-saccadic errors and horizontal velocity in mTBI during a sport-like antisaccade postural control task (Wii Fit Soccer Heading Game) (Murray et al., 2017); 5) shorter time to first saccade, and greater intra-individual variability during a computer-based test performed seated (Suh et al., 2006); 6) longer anti-saccade reaction time at initial assessment (Webb et al., 2018), and greater anti-saccadic directional errors and lower gains in mTBI at initial assessment and follow-up in a visual stimulus test performed seated (Webb et al., 2018). Also, compared with healthy controls, mTBI patients have been found to have greater initial fixation error and greater accuracy error during the performance of a computer-based task (tracking of a circular target) (DiCesare et al., 2017). Although important, it is unclear how much these findings in static/seated tests relate to the demands involved in normal daily activity (Pelz and Canosa, 2001; Maruta et al., 2010a), including dynamic gait.

It is generally considered that gait impairments exist in mTBI populations, albeit some have found otherwise (Fino et al., 2018). For example, reduced gait speed was observed in patients in the acute stage, while stride length had mixed results across acute to subacute recovery stages. The most commonly reported deficit is gait speed, with mTBI groups walking slower in both single and dual task conditions (Fino et al., 2018). Gait requires integration of sensory systems information to be paired with the complex control and coordination of body segments for motor planning. Here, the visual system plays a critical role in the control of gait when all sensory information is available, and in cases of unreliable sensory information (Kennedy et al., 2003). Efficient locomotion is dependent on visual information gathered, specially, by saccades and fixation movements (Srivastava et al., 2018). It is plausible therefore, that deficits in eye movement may influence gait in a negative way. In such cases, we may expect to see an association between eye-tracking and gait metrics. To our knowledge this area has received little attention and is critical to understanding whether visual deficits impact real-world function in people with mTBI. Therefore, the aims of this study were twofold: 1) to evaluate differences in eye-tracking measures collected during gait between healthy controls and patients in the sub-acute stages (<12 weeks post injury) of mTBI recovery; and 2) to determine if there are associations between eye-tracking measures and gait speed in mTBI.

MATERIALS AND METHODS

Participants

Data for this study were collected at two independent research sites: Oregon Health and Science University (OHSU) and Northumbria University (NU). Individuals with mTBI and healthy controls (HC) were recruited as part of an ongoing study at OHSU (ClinicalTrials.gov identifier: NCT03479541), while only HC participants were recruited at NU. For OHSU, approval of the study was granted through a joint Institutional Review Board from OHSU and Veterans Affairs Portland Health Care System (IRB # 17,370). At NU, the study was approved by the University Research Ethics Committee (REF: 23,365). Written informed consent was obtained prior to participation in the study from all participants. Sixty-seven individuals with mTBI and 37 age-matched HCs were enrolled in this study. For individuals with mTBI to be included, they had to: 1) be between 18 and 60 years old; 2) have a physician confirmed diagnosis of acute or post-acute mTBI (up to 12 weeks post-mTBI) based on VA/DoD clinical practice guidelines (Injury and Group, 2016). The medical diagnosis of all mTBI participants were double checked and confirmed based on their medical

TABLE 1 | Demographic participant information.

Variables	Controls (n = 37)	mTBI (n = 67)	*p*- values
Age (Years)	32.40 (18.42)	32.85 (11.64)	0.012
Sex (M/F)	25/12	13/53	<0.001
Height (m)	1.76 (0.11)	1.69 (0.09)	0.001
Weight (kg)	85.98 (19.49)	73.55 (13.89)	<0.001
BMI	27.60 (4.84)	25.78 (5.15)	0.004
Days since mTBI (days)	—	43.23 (20.08)	—
Gait speed (m/s)	1.27 (0.16)	1.23 (0.17)	0.342

TABLE 2 | Injury Mechanism of participants of mTBI group.

Injury mechanisms	Number of participants (n)	Distribution of cause of injury (%)
Sport-related	17	25.4
Motor Vehicle Accident	21	31.3
Fall	15	22.4
Bike	1	1.5
Other	13	19.4
Total	67	100

history or by our research team physician; 3) have no cognitive impairments that could interfere with task execution. People were excluded from the study if they: 1) had any other neurological or musculoskeletal condition that could explain motor dysfunction; 2) had moderate to severe substance-use disorder within the past month (Association, 2013); 3) had significant pain during the evaluation (7/10 by patient subjective report); 4) were currently pregnant; 5) had a past history of peripheral vestibular pathology or ocular motor deficits; 6) were unable to maintain 24 h without medications that may interfere with balance. Participants in the HC group must have had no cognitive impairments that could interfere with task execution, no diagnosis of concussion or any other condition that could influence variables assessed by this study. All participants had normal or corrected to normal vision (prescription lenses were worn during testing if required). Age, sex, height and mass were recorded for all participants. Days since injury and injury mechanism were also recorded for mTBI participants (**Tables 1**, **2**).

Equipment and Experimental Procedures

Participants wore a mobile eye tracking system (head-mounted infra-red Tobii Pro Glasses 2, Tobii Technology Inc. VA, United States) and six inertial sensors (Opal v2, APDM Inc.) while performing a walking task. This protocol was based on previous studies investigating mTBI and other populations (Foulsham et al., 2011; Stuart et al., 2019b; Durant and Zanker, 2020; Stuart et al., 2020b). The Tobii system acquired the participant's gaze coordinates through binocularly recording the participants pupils at a 100 Hz sampling frequency by means of infrared illumination. The inertial sensors consisted of tri-axial accelerometers, gyroscopes, and magnetometers, that measured segment accelerations, rotational rate and relative position at a 128 Hz sampling frequency. Inertial sensors were worn on both feet, sternum, right wrist, lumbar vertebrae and the forehead. Previous studies have shown that these sensors are valid and reliable for quantifying gait (Morris et al., 2019).

Participants walked back and forth over 10-m, at a comfortable self-selected speed. Each participant performed a single 1-min trial, which has been shown as an appropriate length of time to collect and conclusively interpret steady state gait measurements (Lord et al., 2013; Kribus-Shmiel et al., 2018; Kroneberg et al., 2018). Additionally, this length of test was shown to be logistically advantageous for pathological populations which may not be able to walk for extended periods of time (Nunes et al., 2017). The eye-tracker was calibrated prior to the walking task using the manufacturer's single point calibration method. After the calibration and the walking trial started, participants were free to look wherever they wanted and begin walking. No instructions were giving to participants about where to look while walking as we aimed to look at real-world visual exploration (no structured visual requirements). Previous works have used the same task strategy (Stuart et al., 2015; Hunt et al., 2018; Drewes et al., 2021). When the walking trial finished, eye tracking data were stored within the Tobii system, and inertial sensor data were transmitted wirelessly to a nearby laptop for processing and storage. Participants at both sites (OHSU and NU) performed the same protocol, and both sites had similar laboratory spaces and setups when participants performed the 1-mintue walk.

Data and Statistical Analysis

Raw eye tracking data (gaze coordinates–x,y) were extracted from the Tobii Pro Glasses 2 software and processed in Matlab using a custom-made validated velocity-based saccade detection algorithm (Stuart et al., 2014; Stuart et al., 2019b). Eye tracking outcomes included saccadic (frequency, peak velocity, duration and distance) and fixation measurements (frequency and duration). Gait velocity was calculated from the inertial sensors using the Mobility Lab software, V2 (APDM, Portland, OR, United States) (Morris et al., 2019). Gait velocity was selected as the primary gait outcome, because of its sensitivity in detecting gait differences between controls and individuals with mTBI (Fino, 2016; Howell et al., 2018).

Data were initially inspected for normality. Normality tests and inspection indicated a normal distribution for saccade frequency, saccade duration, saccade peak velocity and gait speed. Non-normal distribution was detected for age, height, weight, saccade distance, fixation frequency and fixation duration. Independent samples t-tests were used to compare differences between groups on demographic data with normal distribution, while Mann-Whitney U tests were used for non-normally distributed demographic variables. A Chi-Squared test was used to assess sex differences between the groups.

To test whether gait velocity and eye tracking outcomes differed between people with mTBI and HC, we fit a general linear model for each outcome. Demographic characteristics identified as significantly different between groups were used as co-variates in the models. Each model was adjusted for group (mTBI vs HC) and any co-variates. Initial models included group x co-variate interactions. If no group x co-variate effect was found

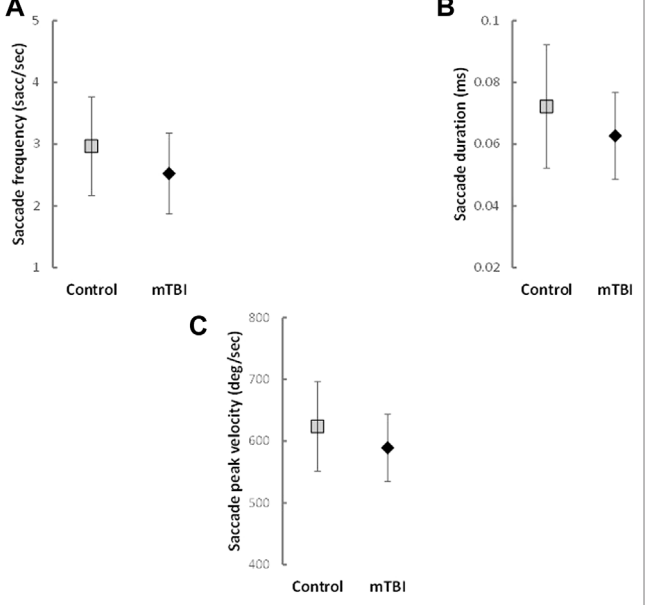

FIGURE 1 | Means and Standard Deviations of saccade outcomes with significant differences between groups.

at a 0.05 significance level, the interaction was removed from the final models.

The association between gait and eye-tracking outcomes within the mTBI group was explored using partial correlations controlling for demographic characteristics that were significantly different between groups. Only eye tracking measures that were significantly different between groups were used for correlation analysis. Statistical analyses were conducted using SAS 9.4 (SAS Institute Inc. Cary, NC, United States) and statistical significance was set at $p < 0.05$.

RESULTS

Demographic Characteristics and Injury Mechanisms

Demographic characteristics are presented in **Table 1**. Injury mechanisms are presented in **Table 2**. The injury mechanisms included: sport-related (25.4%), motor vehicle accident (31.3%), injury caused by a fall (22.4%), bike accident (1.5%) and other general causes (19.4%).

There was no difference between groups for age ($U = 1{,}005.500$, z = −1.591, $p = 0.112$). There were significantly more males in the HC group than in the mTBI group ($x^2_{(2,\ N=104)} = 23.994$, $p < 0.001$). Participants from the HC group were significantly taller and heavier than the HC group ($U = 621.00$, $z = -4.213$, $p = 0.001$ and $U = 722.00$, $z = -3.516$, $p < 0.001$, respectively). As a result, we calculated body mass index (BMI) for participants and used it with sex as co-variates for the general linear models. Partial correlations were completed while controlling for sex and BMI. BMI was significantly lower for the mTBI group compared to the HC group ($U = 810.00$, z = −2.916, $p = 0.004$).

None of the models had significant group x sex, group x BMI, or group x sex x BMI effects. Therefore, results for the models for gait velocity and eye tracking outcomes focused on main effects for group, adjusting for sex, and BMI. There was no significant difference in gait velocity between mTBI and HC groups ($F_{(1,100)} = 0.91$, $p = 0.342$, partial $\eta^2 = 0.009$) after controlling for sex and BMI (**Table 1** and **Supplementary Table S1**).

Differences Between Groups for Eye Tracking Outcomes

Analysis controlling for sex and BMI indicated that participants with mTBI had reduced saccade frequency ($F_{(1,100)} = 6.05$, $p = 0.016$, partial $\eta^2 = 0.057$; **Figure 1A**), saccade durations ($F_{(1,100)} = 4.98$, $p = 0.028$, partial $\eta^2 = 0.048$; **Figure 1B**) and saccade peak velocities ($F_{(1,100)} = 4.71$, $p = 0.032$, partial $\eta^2 = 0.045$; **Figure 1C**) compared to the HC group. No significant differences existed between groups for saccade distance ($F_{(1,100)} = 0.12$, $p = 0.726$, partial $\eta^2 = 0.001$), fixation frequency ($F_{(1,100)} = 0.39$, $p = 0.531$, partial $\eta^2 = 0.004$) or fixation duration ($F_{(1,100)} = 1.64$, $p = 0.204$, partial $\eta^2 = 0.018$). Parameter estimates for each general linear model can be found in **Supplementary Table S1** and means and standard deviations in **Supplementary Table S2**.

Correlations Between Eye Tracking Outcomes and Gait Velocity

A positive correlation was observed between saccade duration and gait velocity only for participants with mTBI. Specifically, participants with mTBI that had reduced saccade duration also had slower gait velocity (r = 0.287, $p = 0.025$; **Figure 2**). No other correlations between eye tracking outcomes and gait velocity were observed for either group (**Supplementary Table S3**).

DISCUSSION

This study compared saccadic and fixation eye movements during walking between people with mTBI and HC, and

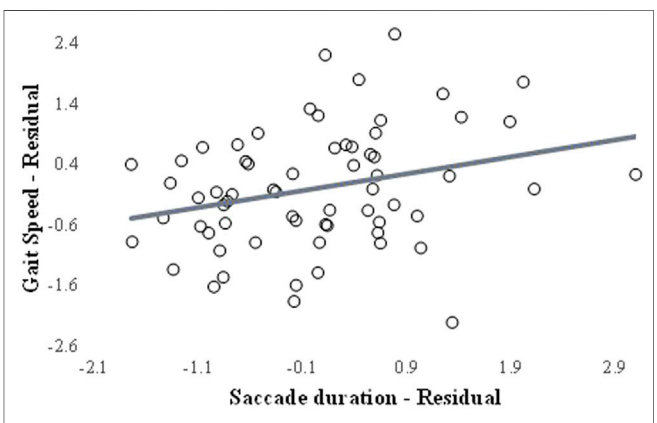

FIGURE 2 | Scatter plot between the residuals of saccade duration and gait velocity.

evaluated whether associations existed between eye-tracking measures and gait speed. Our main findings were: 1) participants with mTBI showed reduced saccade frequency, duration and peak velocity compared with an HC group; 2) reduced saccade duration positively correlated with slower gait velocity within the mTBI group. These findings suggest that mTBI affects eye movements while walking and highlight the importance of objective eye-tracking measures to better quantify mTBI impairments during tasks representative of daily life/function.

We observed deficits only for saccade outcomes, not fixations, in individuals with mTBI. Similar deficits in saccadic eye movements have been reported in older adults and other neurological populations while executing dynamic tasks such as walking (Dowiasch et al., 2015; Stuart et al., 2017). For example, reduced saccade frequency has been associated with deficits in cognition (Nelson et al., 2004) and slower saccade peak velocity has been found to be a predictor of attention decline in patients with Parkinson's disease (Stuart et al., 2019a).The deficits we observed in saccadic function (i.e. reduced saccade frequency, duration and peak velocity) are outcomes that have been linked to attentional processes (Stuart et al., 2017). Attention has an important role on both walking (Morris et al., 2016) and saccadic control (Stuart et al., 2016; Ventura et al., 2016). Thus, we speculate that our findings indicate that mTBI participants may present reduced visuospatial attention while walking. Attentional deficits are commonly observed in people with persistent post-concussion symptoms and, although most of the cases resolve in 1 or 2 weeks, some cognitive impairments can last for up to 3 months–a timeline cohesive with our sample of mTBI participants (i.e. within 12 weeks of acute mTBI) (Rabinowitz et al., 2014; Wang and Li, 2016). Future studies should investigate the correlates between saccadic eye movements and cognition in tasks with greater visual demand such as obstacle avoidance, precision stepping, athletic and military tasks.

Saccade frequency is the basis of visual exploration (Kimmig et al., 2001), and the reduced saccade movements found herein may also indicate that patients with mTBI use a restricted exploration of the environment while walking. Dowiasch et al. (Dowiasch et al., 2015) suggested that changes in saccadic eye movements, such as diminished frequency and velocities, might be related to a narrow viewing strategy. This strategy could be explained by a greater effort being required for walking (Di Fabio et al., 2003) or less confidence in exploring the environment (Hadley et al., 1985), which could result from mTBI symptoms. The mTBI participants may have used a more restricted strategy of environment exploration to avoid exacerbation of mTBI-related symptoms, which can be provoked during ocular motor tasks. Considering that self-initiated eye movements can cause symptoms related to the mTBI (Mucha et al., 2014) it is possible that following an mTBI people voluntarily reduce saccadic eye movements in order to minimize symptoms, like dizziness and headache. However, to confirm that, future explorations of the relationship of saccade movements during walking and clinical symptoms of mTBI individuals are needed.

Although previous studies indicate an overlapping of saccade and gait control pathways (Srivastava et al., 2018), only saccade outcomes differentiated the two groups in this study, and we did not find differences between groups for gait velocity. These results are contradictory with some findings within the literature that indicate slower gait velocity in individuals with mTBI (Martini et al., 2011; Buckley et al., 2016; Fino, 2016; Fino et al., 2018). However, methodological aspects could explain the differences between studies including small sample size (Fino, 2016). Additionally, given saccades and locomotion are mediated by the integration of multiple brain areas and overlapping neural circuits (Srivastava et al., 2018), it is possible that participants with mTBI were allocating more attentional resources to walking instead of visual processing their environment. However, we were surprised that the only association between eye-tracking variables and gait velocity in the mTBI group were between saccade duration and gait velocity.

There is evidence of impaired sensorimotor integration in people with mTBI and balance deficits which may explain the impaired saccadic function. However, a recent study demonstrated that measures of sensorimotor integration, measured with the sensory organization (SOT) test, did not significantly relate to measures of saccadic accuracy, latency, and velocities measured during a seated target capture directed task (Campbell et al., 2021). Therefore, future studies would be needed to quantify relationships between sensorimotor integration for balance with context-free saccadic function during gait. It is important to highlight that our results are encouraging and suggest that eye tracking measures during walking, especially saccade outcomes, have potential for clinical application. These findings have implications for real world function, and measurements of saccades could be used as part of a diagnostic assessment for distinguishing mTBI from HC, as follow-up measures of intervention effects, as well as determination for return to sport for athletes and return to duty for military service members.

There is conflicting evidence on the utility of seated/static eye tracking measures in the assessment of deficits following mTBI (Balaban et al., 2016; Cochrane et al., 2019; Kelly et al., 2019; Stuart et al., 2020a). Seated or static eye-tracking evaluations allow for rigorous experimental control on evaluating the ocular motor system (Stuart et al., 2020a). However, the static evaluation position may allow for additional attentional resources to compensate for any deficits in ocular motor tasks following mTBI. In contrast, when people are navigating an environment while walking, deficits in ocular motor function may be more easily detected because of attentional demands required for not only visual processing but also motor coordination and cognitive processing tasks (Stuart et al., 2017; Stuart et al., 2020a). Therefore, eye tracking evaluation during gait may reveal more subtle impairments to gaze behavior not present during a static/seated evaluation. Further, there are some differences that may occur in dynamic laboratory testing compared to real world walking in the community (Foulsham et al., 2011). Future, studies should incorporate both static and dynamic evaluations, laboratory and real world, of ocular motor function to better understand the deficits caused by mTBI. For now, our work provides preliminary evidence of reduced saccadic function during walking after mTBI which is consistent with other work in a PD population (Stuart et al., 2017).

Although our results are promising, more studies are needed to identify different aspects that may contribute to changes in saccades during walking in mTBI individuals, including time since injury. For example, in a pilot study, Mullen et al. (Mullen et al., 2014) showed that individuals with mTBI presented changes in saccade movement, during a seated reaction time test 1 week after the injury, but not after 3 weeks. Our study included participants in post-acute mTBI stages (between 2 and 12 weeks) and so, results may have been impacted by the range of time after the initial concussion. It is plausible that those in the acute mTBI stage have more accentuated deficits in saccadic function while walking than those in post-acute stage. Future studies in this field should also investigate eye movements in a more complex environment including real world environments and dual task functions. The comparison between tasks that involve a higher motor control demand and static/sitting task should also be performed to verify if changes on eye movement control is task-related. Also, the inclusion of gait speed as the only gait characteristic measure may have limited some of our findings. Gait speed is a measure that essentially consists of an accumulation of more subtle gait characteristics (Morris et al., 2016) and may not detect subtle deficits in gait, and also may not correlate with eye movement deficits. Future studies should examine a comprehensive range of eye movement and gait characteristics (which will require greater numbers of participants) to explore subtle relationships that may exist as a result of underlying deficits. We limited gait metric comparisons between groups to gait velocity because of the variable's ability to differentiate between groups from previous studies (Fino, 2016; Howell et al., 2018). However, other components of gait, specifically percent of time spent in double support, have also been shown to be different in those with chronic symptoms of mTBI (Cao et al., 2020). This variable is of particular interest because saccade frequency increases during the double support phase of gait. In our study, we are not able to identify the relationship between eye movement measures with specific gait phases as we did not have both eye-tracking and sensors, synchronized. Future studies should investigate not only a more comprehensive range of gait and eye movements characteristics, but also how specific phases of gait are related to eye movement control. Also, our findings do not allow us to indicate how specific neuronal circuits (or brain areas) are correlated with deficits in eye movement control in mTBI. Neural circuits that control eye movement include both cortical and subcortical regions of the brain and these circuits are widely distributed throughout the brain (Bigler, 2018). Many of these brain circuits are vulnerable to a concussive injury. Thus, future studies should propose protocols that include the data collection of eye tracking and neural activity/neuroimage, simultaneously, during real world tasks like walking. Data of this nature would allow a better understanding of how specific brain areas affected by the mTBI can be related with deficits in eye movement control.

CONCLUSION

The current study demonstrated impaired gaze function in individuals with mTBI compared to HC by evaluating saccades and fixations during gait. Specifically, we found saccadic outcomes were impaired in mTBI during walking, with no changes between groups for fixation outcomes or gait velocity. Saccadic outcomes during walking have the potential to contribute to a better impairment characterization or diagnosis of individuals with mTBI, and perhaps aid in determining when a person can optimally return to complex activities such as sport or military service.

DATA AVAILABILITY STATEMENT

The raw data supporting the conclusions of this article will be made available by the authors, without undue reservation.

ETHICS STATEMENT

The studies involving human participants were reviewed and approved by a joint Institutional Review Board from OHSU and Veterans Affairs Portland Health Care System (IRB # 17370) and the University Research Ethics Committee of Northumbria University (REF: 23365). The patients/participants provided their written informed consent to participate in this study.

AUTHOR CONTRIBUTIONS

ES, LK, SS, LP and KC contributed to the conception and design of this study. ES, SS, LP and KC collected the data for this study. ES, LP and KC performed the statistical analysis. ELS and LP wrote the first draft of the manuscript. All authors contributed to the manuscript revision and read and approved the submitted version.

FUNDING

Funding was provided by the US Department of Defense (#W81XWH-17-1-0424).

SUPPLEMENTARY MATERIAL

The Supplementary Material for this article can be found online at: https://www.frontiersin.org/articles/10.3389/fbioe.2021.701712/full#supplementary-material.

REFERENCES

Association, A. P. (2013). *American Psychiatric Association: Diagnostic and Statistical Manual of Mental Disorders*. American Psychiatric Association.

Balaban, C., Hoffer, M. E., Szczupak, M., Snapp, H., Crawford, J., Murphy, S., et al. (2016). Oculomotor, Vestibular, and Reaction Time Tests in Mild Traumatic Brain Injury. *PLoS One* 11 (9), e0162168. doi:10.1371/journal.pone.0162168

Bigler, E. D. (2018). Structural Neuroimaging in Sport-Related Concussion. *Int. J. Psychophysiology* 132 (Pt A), 105–123. doi:10.1016/j.ijpsycho.2017.09.006

Buckley, T. A., Vallabhajosula, S., Oldham, J. R., Munkasy, B. A., Evans, K. M., Krazeise, D. A., et al. (2016). Evidence of a Conservative Gait Strategy in Athletes with a History of Concussions. *J. Sport Health Sci.* 5 (4), 417–423. doi:10.1016/j.jshs.2015.03.010

Campbell, K. R., Parrington, L., Peterka, R. J., Martini, D. N., Hullar, T. E., Horak, F. B., et al. (2021). Exploring Persistent Complaints of Imbalance after mTBI: Oculomotor, Peripheral Vestibular and central Sensory Integration Function. *Ves*, 1–12. doi:10.3233/ves-201590

Cao, L., Chen, X., and Haendel, B. F. (2020). Overground Walking Decreases Alpha Activity and Entrains Eye Movements in Humans. *Front. Hum. Neurosci.* 14, 561755. doi:10.3389/fnhum.2020.561755

Capó-Aponte, J. E., Urosevich, T. G., Temme, L. A., Tarbett, A. K., and Sanghera, N. K. (2012). Visual Dysfunctions and Symptoms during the Subacute Stage of Blast-Induced Mild Traumatic Brain Injury. *Mil. Med.* 177 (7), 804–813. doi:10.7205/milmed-d-12-00061

Ciuffreda, K. J., Kapoor, N., Rutner, D., Suchoff, I. B., Han, M. E., and Craig, S. (2007). Occurrence of Oculomotor Dysfunctions in Acquired Brain Injury: a Retrospective Analysis. *Optom. - J. Am. Optometric Assoc.* 78 (4), 155–161. doi:10.1016/j.optm.2006.11.011

Cochrane, G. D., Christy, J. B., Almutairi, A., Busettini, C., Swanson, M. W., and Weise, K. K. (2019). Visuo-oculomotor Function and Reaction Times in Athletes with and without Concussion. *Optom. Vis. Sci.* 96 (4), 256–265. doi:10.1097/OPX.0000000000001364

Di Fabio, R. P., Greany, J. F., and Zampieri, C. (2003). Saccade-stepping Interactions Revise the Motor Plan for Obstacle Avoidance. *J. Mot. Behav.* 35 (4), 383–397. doi:10.1080/00222890309603158

DiCesare, C. A., Kiefer, A. W., Nalepka, P., and Myer, G. D. (2017). Quantification and Analysis of Saccadic and Smooth Pursuit Eye Movements and Fixations to Detect Oculomotor Deficits. *Behav. Res.* 49 (1), 258–266. doi:10.3758/s13428-015-0693-x

Dowiasch, S., Marx, S., EinhÃ¤user, W., and Bremmer, F. (2015). Effects of Aging on Eye Movements in the Real World. *Front. Hum. Neurosci.* 9, 46. doi:10.3389/fnhum.2015.00046

Drewes, J., Feder, S., and Einhäuser, W. (2021). Gaze during Locomotion in Virtual Reality and the Real World. *Front. Neurosci.* 15, 656913. doi:10.3389/fnins.2021.656913

Durant, S., and Zanker, J. M. (2020). The Combined Effect of Eye Movements Improve Head Centred Local Motion Information during Walking. *PLoS One* 15 (1), e0228345. doi:10.1371/journal.pone.0228345

Fino, P. C. (2016). A Preliminary Study of Longitudinal Differences in Local Dynamic Stability between Recently Concussed and Healthy Athletes during Single and Dual-Task Gait. *J. Biomech.* 49 (9), 1983–1988. doi:10.1016/j.jbiomech.2016.05.004

Fino, P. C., Parrington, L., Pitt, W., Martini, D. N., Chesnutt, J. C., Chou, L.-S., et al. (2018). Detecting Gait Abnormalities after Concussion or Mild Traumatic Brain Injury: A Systematic Review of Single-Task, Dual-Task, and Complex Gait. *Gait & Posture* 62, 157–166. doi:10.1016/j.gaitpost.2018.03.021

Foulsham, T., Walker, E., and Kingstone, A. (2011). The where, what and when of Gaze Allocation in the Lab and the Natural Environment. *Vis. Res.* 51 (17), 1920–1931. doi:10.1016/j.visres.2011.07.002

Hadley, E., Radebaugh, T. S., and Suzman, R. (1985). Falls and Gait Disorders Among the Elderly. *Clin. Geriatr. Med.* 1 (3), 497–500. doi:10.1016/s0749-0690(18)30919-4

Hecimovich, M., King, D., Dempsey, A., Gittins, M., and Murphy, M. (2019). *In Situ* use of the King-Devick Eye Tracking Test and Changes Seen with Sport-Related Concussion: Saccadic and Blinks Counts. *The Physician and Sportsmedicine* 47 (1), 78–84. doi:10.1080/00913847.2018.1525261

Howell, D. R., Kirkwood, M. W., Provance, A., Iverson, G. L., and Meehan, W. P., 3rd (2018). Using Concurrent Gait and Cognitive Assessments to Identify Impairments after Concussion: a Narrative Review. *Concussion* 3 (1), Cnc54. doi:10.2217/cnc-2017-0014

Hunt, A. W., Mah, K., Reed, N., Engel, L., and Keightley, M. (2016). Oculomotor-Based Vision Assessment in Mild Traumatic Brain Injury: A Systematic Review. *J. Head Trauma Rehabil.* 31 (4), 252–261. doi:10.1097/HTR.0000000000000174

Hunt, D., Stuart, S., Nell, J., Hausdorff, J. M., Galna, B., Rochester, L., et al. (2018). Do people with Parkinson's Disease Look at Task Relevant Stimuli when Walking? an Exploration of Eye Movements. *Behav. Brain Res.* 348, 82–89. doi:10.1016/j.bbr.2018.03.003

Injury, T. M. o. C.-m. T. B., and Group, W. (20162021). *VA/DoD Clinical Practice Guidelines for the Management of Concussion-Mild Traumatic Brain Injury*. [OnlineAvailable at: https://www.healthquality.va.gov/guidelines/Rehab/mtbi/.

Johnson, B., Hallett, M., and Slobounov, S. (2015). Follow-up Evaluation of Oculomotor Performance with fMRI in the Subacute Phase of Concussion. *Neurology* 85 (13), 1163–1166. doi:10.1212/wnl.0000000000001968

Kelly, K. M., Kiderman, A., Akhavan, S., Quigley, M. R., Snell, E. D., Happ, E., et al. (2019). Oculomotor, Vestibular, and Reaction Time Effects of Sports-Related Concussion: Video-Oculography in Assessing Sports-Related Concussion. *J. Head Trauma Rehabil.* 34 (3), 176–188. doi:10.1097/htr.0000000000000437

Kennedy, P. M., Carlsen, A. N., Inglis, J. T., Chow, R., Franks, I. M., and Chua, R. (2003). Relative Contributions of Visual and Vestibular Information on the Trajectory of Human Gait. *Exp. Brain Res.* 153 (1), 113–117. doi:10.1007/s00221-003-1633-z

Kimmig, H., Greenlee, M., Gondan, M., Schira, M., Kassubek, J., and Mergner, T. (2001). Relationship between Saccadic Eye Movements and Cortical Activity as Measured by fMRI: Quantitative and Qualitative Aspects. *Exp. Brain Res.* 141 (2), 184–194. doi:10.1007/s002210100844

Kontos, A. P., Deitrick, J. M., Collins, M. W., and Mucha, A. (2017). Review of Vestibular and Oculomotor Screening and Concussion Rehabilitation. *J. Athl Train.* 52 (3), 256–261. doi:10.4085/1062-6050-51.11.05

Kribus-Shmiel, L., Zeilig, G., Sokolovski, B., and Plotnik, M. (2018). How many Strides Are Required for a Reliable Estimation of Temporal Gait Parameters? Implementation of a New Algorithm on the Phase Coordination index. *PLoS One* 13 (2), e0192049. doi:10.1371/journal.pone.0192049

Kroneberg, D., Elshehabi, M., Meyer, A.-C., Otte, K., Doss, S., Paul, F., et al. (2018). Less Is More - Estimation of the Number of Strides Required to Assess Gait Variability in Spatially Confined Settings. *Front. Aging Neurosci.* 10, 435. doi:10.3389/fnagi.2018.00435

Lord, S., Galna, B., and Rochester, L. (2013). Moving Forward on Gait Measurement: toward a More Refined Approach. *Mov Disord.* 28 (11), 1534–1543. doi:10.1002/mds.25545

Martini, D. N., Sabin, M. J., DePesa, S. A., Leal, E. W., Negrete, T. N., Sosnoff, J. J., et al. (2011). The Chronic Effects of Concussion on Gait. *Arch. Phys. Med. Rehabil.* 92 (4), 585–589. doi:10.1016/j.apmr.2010.11.029

Maruta, J., Lee, S. W., Jacobs, E. F., and Ghajar, J. (2010a). A Unified Science of Concussion. *Ann. N Y Acad. Sci.* 1208 (1), 58–66. doi:10.1111/j.1749-6632.2010.05695.x

Maruta, J., Suh, M., Niogi, S. N., Mukherjee, P., and Ghajar, J. (2010b). Visual Tracking Synchronization as a Metric for Concussion Screening. *J. Head Trauma Rehabil.* 25 (4), 293–305. doi:10.1097/HTR.0b013e3181e67936

Meier, T. B., Brummel, B. J., Singh, R., Nerio, C. J., Polanski, D. W., and Bellgowan, P. S. F. (2015). The Underreporting of Self-Reported Symptoms Following Sports-Related Concussion. *J. Sci. Med. Sport* 18 (5), 507–511. doi:10.1016/j.jsams.2014.07.008

Morris, R., Lord, S., Bunce, J., Burn, D., and Rochester, L. (2016). Gait and Cognition: Mapping the Global and Discrete Relationships in Ageing and Neurodegenerative Disease. *Neurosci. Biobehavioral Rev.* 64, 326–345. doi:10.1016/j.neubiorev.2016.02.012

Morris, R., Stuart, S., McBarron, G., Fino, P. C., Mancini, M., and Curtze, C. (2019). Validity of Mobility Lab (Version 2) for Gait Assessment in Young Adults, Older Adults and Parkinson's Disease. *Physiol. Meas.* 40 (9), 095003. doi:10.1088/1361-6579/ab4023

Mucha, A., Collins, M. W., Elbin, R. J., Furman, J. M., Troutman-Enseki, C., DeWolf, R. M., et al. (2014). A Brief Vestibular/Ocular Motor Screening (VOMS) Assessment to Evaluate Concussions. *Am. J. Sports Med.* 42 (10), 2479–2486. doi:10.1177/0363546514543775

Mullen, S. J., Yücel, Y. H., Cusimano, M., Schweizer, T. A., Oentoro, A., and Gupta, N. (2014). Saccadic Eye Movements in Mild Traumatic Brain Injury: A Pilot

Study OPEN ACCESS. *Can. J. Neurol. Sci.* 41 (1), 58–65. doi:10.1017/s0317167100016279

Murray, N. G., D'Amico, N. R., Powell, D., Mormile, M. E., Grimes, K. E., Munkasy, B. A., et al. (2017). ASB Clinical Biomechanics Award winner 2016: Assessment of Gaze Stability within 24-48 Hours post-concussion. *Clin. Biomech.* 44, 21–27. doi:10.1016/j.clinbiomech.2017.03.002

Nelson, J. D., Cottrell, G. W., Movellan, J. R., and Sereno, M. I. (2004). Yarbus Lives: a Foveated Exploration of How Task Influences Saccadic Eye Movement. *J. Vis.* 4 (8), 741. doi:10.1167/4.8.741

Nunes, F., Alhalabi, L., Brown, W., King, C., Shlobin, O., and Nathan, S. (2017). Does 1-Minute Walk Test Predict Results of 6-Minute Walk Test in Patients with Idiopathic Pulmonary Fibrosis? *CHEST* 152 (4), A486. doi:10.1016/j.chest.2017.08.513

Pearson, B. C., Armitage, K. R., Horner, C. W. M., and Carpenter, R. H. S. (2007). Saccadometry: the Possible Application of Latency Distribution Measurement for Monitoring Concussion. *Br. J. Sports Med.* 41 (9), 610–612. doi:10.1136/bjsm.2007.036731

Pelz, J. B., and Canosa, R. (2001). Oculomotor Behavior and Perceptual Strategies in Complex Tasks. *Vis. Res* 41 (25-26), 3587–3596. doi:10.1016/s0042-6989(01)00245-0

Rabinowitz, A. R., Li, X., and Levin, H. S. (2014). Sport and Nonsport Etiologies of Mild Traumatic Brain Injury: Similarities and Differences. *Annu. Rev. Psychol.* 65, 301–331. doi:10.1146/annurev-psych-010213-115103

Snegireva, N., Derman, W., Patricios, J., and Welman, K. E. (2018). Eye Tracking Technology in Sports-Related Concussion: a Systematic Review and Meta-Analysis. *Physiol. Meas.* 39 (12), 12TR01. doi:10.1088/1361-6579/aaef44

Srivastava, A., Ahmad, O. F., Pacia, C. P., Hallett, M., and Lungu, C. (2018). The Relationship between Saccades and Locomotion. *Jmd* 11 (3), 93–106. doi:10.14802/jmd.18018

Stuart, S., Galna, B., Delicato, L. S., Lord, S., and Rochester, L. (2017). Direct and Indirect Effects of Attention and Visual Function on Gait Impairment in Parkinson's Disease: Influence of Task and Turning. *Eur. J. Neurosci.* 46 (1), 1703–1716. doi:10.1111/ejn.13589

Stuart, S., Galna, B., Lord, S., and Rochester, L. (2015). A Protocol to Examine Vision and Gait in Parkinson's Disease: Impact of Cognition and Response to Visual Cues. *F1000Res* 4, 1379. doi:10.12688/f1000research.7320.210.12688/f1000research.7320.1

Stuart, S., Galna, B., Lord, S., Rochester, L., and Godfrey, A. (20142014). Quantifying Saccades while Walking: Validity of a Novel Velocity-Based Algorithm for mobile Eye Tracking. *Conf. Proc. IEEE Eng. Med. Biol. Soc.*, 5739–5742. doi:10.1109/EMBC.2014.6944931

Stuart, S., Lawson, R. A., Yarnall, A. J., Nell, J., Alcock, L., Duncan, G. W., et al. (2019a). Pro Saccades Predict Cognitive Decline in Parkinson's Disease: ICICLE-PD. *Mov Disord.* 34 (11), 1690–1698. doi:10.1002/mds.27813

Stuart, S., Lord, S., Hill, E., and Rochester, L. (2016). Gait in Parkinson's Disease: A Visuo-Cognitive challenge. *Neurosci. Biobehavioral Rev.* 62, 76–88. doi:10.1016/j.neubiorev.2016.01.002

Stuart, S., Parrington, L., Martini, D., Peterka, R., Chesnutt, J., and King, L. (2020a). The Measurement of Eye Movements in Mild Traumatic Brain Injury: A Structured Review of an Emerging Area. *Front. Sports Act. Living* 2, 5. doi:10.3389/fspor.2020.00005

Stuart, S., Parrington, L., Martini, D., Popa, B., Fino, P. C., and King, L. A. (2019b). Validation of a Velocity-Based Algorithm to Quantify Saccades during Walking and Turning in Mild Traumatic Brain Injury and Healthy Controls. *Physiol. Meas.* 40 (4), 044006. doi:10.1088/1361-6579/ab159d

Stuart, S., Parrington, L., Morris, R., Martini, D. N., Fino, P. C., and King, L. A. (2020b). Gait Measurement in Chronic Mild Traumatic Brain Injury: A Model Approach. *Hum. Mov. Sci.* 69, 102557. doi:10.1016/j.humov.2019.102557

Suh, M., Basu, S., Kolster, R., Sarkar, R., McCandliss, B., and Ghajar, J. (2006). Increased Oculomotor Deficits during Target Blanking as an Indicator of Mild Traumatic Brain Injury. *Neurosci. Lett.* 410 (3), 203–207. doi:10.1016/j.neulet.2006.10.001

Ventura, R. E., Balcer, L. J., Galetta, S. L., and Rucker, J. C. (2016). Ocular Motor Assessment in Concussion: Current Status and Future Directions. *J. Neurol. Sci.* 361, 79–86. doi:10.1016/j.jns.2015.12.010

Wang, M.-L., and Li, W.-B. (2016). Cognitive Impairment after Traumatic Brain Injury: The Role of MRI and Possible Pathological Basis. *J. Neurol. Sci.* 370, 244–250. doi:10.1016/j.jns.2016.09.049

Webb, B., Humphreys, D., and Heath, M. (2018). Oculomotor Executive Dysfunction during the Early and Later Stages of Sport-Related Concussion Recovery. *J. Neurotrauma* 35 (16), 1874–1881. doi:10.1089/neu.2018.5673

Whitney, S. L., and Sparto, P. J. (2019). Eye Movements, Dizziness, and Mild Traumatic Brain Injury (mTBI): A Topical Review of Emerging Evidence and Screening Measures. *J. Neurol. Phys. Ther.* 43 (Suppl. 2), S31–s36. doi:10.1097/npt.0000000000000272

Conflict of Interest: The authors declare that the research was conducted in the absence of any commercial or financial relationships that could be construed as a potential conflict of interest.

Publisher's Note: All claims expressed in this article are solely those of the authors and do not necessarily represent those of their affiliated organizations, or those of the publisher, the editors and the reviewers. Any product that may be evaluated in this article, or claim that may be made by its manufacturer, is not guaranteed or endorsed by the publisher.

frontiers in Bioengineering and Biotechnology

ORIGINAL RESEARCH
published: 11 March 2022
doi: 10.3389/fbioe.2022.820186

Relationship Between the Choice of Clinical Treatment, Gait Functionality and Kinetics in Patients With Comparable Knee Osteoarthritis

Simone Tassani[1], Laura Tio[2], Francisco Castro-Domínguez[2,3], Jordi Monfort[2,3], Juan Carlos Monllau[2,4], Miguel Angel González Ballester[1,5] and Jérôme Noailly[1]*

[1]BCN MedTech, DTIC, Universitat Pompeu Fabra, Barcelona, Spain, [2]IMIM, Barcelona, Spain, [3]Rheumatology Department, Hospital del Mar, Barcelona, Spain, [4]Orthopedic Surgery and Traumatology Department, Hospital del Mar, Barcelona, Spain, [5]ICREA, Barcelona, Spain

Objective: The objective of this study was to investigate the relationship between the choice of clinical treatment, gait functionality, and kinetics in patients with comparable knee osteoarthritis.

Design: This was an observational case-control study.

Setting: The study was conducted in a university biomechanics laboratory.

Participants: Knee osteoarthritis patients were stratified into the following groups: clinical treatment (conservative/total knee replacement (TKR) planned), sex (male/female), age (60–67/68–75), and body mass index (BMI) (<30/≥30). All patients had a Kellgren–Lawrence score of 2 or 3 (N = 87).

Main Outcome Measures: All patients underwent gait analysis, and two groups of dependent variables were extracted:

- Spatiotemporal gait variables: gait velocity, stride time, and double-support time, which are associated with patient functionality.
- Kinetic gait variables: vertical, anterior–posterior, and mediolateral ground reaction forces, vertical free moment, joint forces, and moments at the ankle, knee, and hip. Multifactorial and multivariate analyses of variance were performed.

Results: Functionality relates to treatment decisions, with patients in the conservative group walking 25% faster and spending 24% less time in the double-support phase. However, these differences vary with age and are reduced in older subjects. Patients who planned to undergo TKR did not present higher knee forces, and different joint moments between clinical treatments depended on the age and BMI of the subjects.

Conclusions: Knee osteoarthritis is a multifactorial disease, with age and BMI being confounding factors. The differences in gait between the two groups were mitigated by

Abbreviations: BMI, Body mass Index; KL, Kellgren–Lawrence; KOA, Knee osteoarthritis; MANOVA, Multivariate Analysis of Variance; OA, Osteoarthritis; SYSADOAs, Symptomatic slow action drugs for osteoarthritis; TKR, Total knee replacement.

OPEN ACCESS

Edited by:
Andrea Malandrino, Universitat Politecnica de Catalunya, Spain

Reviewed by:
João Abrantes, Universidade Lusófona, Portugal
Björn Rath, Klinikum Wels-Grieskirchen, Austria

****Correspondence:***
Simone Tassani
simone.tassani@upf.edu

Specialty section:
This article was submitted to Biomechanics, a section of the journal Frontiers in Bioengineering and Biotechnology

Received: *22 November 2021*
Accepted: *31 January 2022*
Published: *11 March 2022*

Citation:
Tassani S, Tio L, Castro-Domínguez F, Monfort J, Monllau JC, González Ballester MA and Noailly J (2022) Relationship Between the Choice of Clinical Treatment, Gait Functionality and Kinetics in Patients With Comparable Knee Osteoarthritis. Front. Bioeng. Biotechnol. 10:820186. doi: 10.3389/fbioe.2022.820186

confounding factors and risk factors, such as being a woman, elderly, and obese, reducing the variability of the gait compression loads. These factors should always be considered in gait studies of patients with knee osteoarthritis to control for confounding effects.

Keywords: Knee osteoarthritis (KOA), gait, confounding adjustment, multifactorial analysis, functionality

INTRODUCTION

The definition of objective criteria for total knee replacement (TKR) remains a matter of debate, leading to different rates of surgery in different countries (Ghomrawi et al., 2014). The clinician–patient relationship (O'Neill et al., 2007) and their expectations and beliefs about conservative therapy and surgery (O'Brien et al., 2019) are likely to influence the final treatment; therefore, it is difficult to find objective criteria to help the decision.

Osteoarthritis (OA) is more prevalent in women (4.8%) than in men (2.8%) and increases with age and obesity (Cross et al., 2014). Therefore, sex, body mass index (BMI), and age play a direct role in the progression of the disease and are possible sources of confounding (Kyriacou and Lewis, 2016). The variation of the Kellgren–Lawrence (KL) grade is often used to define the radiological progression of knee osteoarthritis (KOA) (Braun and Gold, 2012). However, the pain experienced by patients is not directly related to KL grade (Schiphof et al., 2013). Therefore, it is still unclear whether the KL grade or the functionality of the patients, in terms of pain, discomfort, or capability to perform daily activities, should guide the treatment decision of KOA in terms of TKR or conservative management.

KOA core treatment is nonpharmacological (e.g., exercise and weight loss). If it is necessary, pharmacological treatment must be chosen carefully considering the patient profile, e.g., nonsteroidal anti-inflammatory agents, symptomatic slow-acting drugs for osteoarthritis (SYSADOAs), or hyaluronic acid infiltrations (Author Anonymous, 2000).

Beyond a certain point of OA progression, these treatments are ineffective, and clinical decisions switch to TKR. Nonetheless, different rates of TKR have been described in different countries (Gómez-Barrena et al., 2014; Gunsche et al., 2020). These data highlight the importance of identifying homogeneous indication criteria for TKR. Objective treatment decisions should be an index of KOA progression (Astephen et al., 2008) and might be reflected by specific gait functionality and kinetics that are unavoidably altered along the course of the disease. However, translating such a mental exercise into practical recommendations may not be straightforward.

The literature pointed out that macro factors, such as obesity, can directly affect the microlevel development of the pathology (Felson et al., 1988; Coggon et al., 2002; Berenbaum et al., 2013; Wluka et al., 2013). If sex, age, and weight have any effect on OA, they should be studied simultaneously in a multifactorial analysis to detect possible nonlinearities in the assessment of KOA. This analysis should be performed taking into consideration the fact that the same factors also affect gait. In fact, sex (McKean et al., 2007), age (Paterson et al., 2009; Park et al., 2016) BMI (Messier et al., 1996; De Souza et al., 2005; Dufek et al., 2012) and the stage of OA (Wang et al., 2010; De Pieri et al., 2019) influence gait, and it is difficult to understand which factors are dependent and independent. As a result, there are no defined objective criteria for selecting TKR (Gómez-Barrena et al., 2014).

Accordingly, an attempt was made to investigate whether any relation exists between the treatment decision and gait functionality and kinetics. The study was performed in a prospective clinical cohort of KOA patients with similar KL grades. Sex, age, and BMI were considered to verify possible interactions and confounding effects (Kyriacou and Lewis, 2016) in the treatment selection through a multifactorial and multivariate analysis. It was hypothesized that patients undergoing TKR have less gait functionality, higher loads, and higher moments at the joints.

MATERIALS AND METHODS

The present work presents a case control study in which patients with similar KL levels are stratified based on the clinical decision whether to undergo TKR and on other clinically relevant factors as possible sources of confounding. The analysis was performed prior to intervention.

Patient Recruitment

The clinical histories of all patients diagnosed with KOA at the Rheumatology/Orthopaedic Surgery Department of Hospital del Mar, Barcelona, Spain, were revised prospectively to build a

TABLE 1 | Patient eligibility criteria.

Inclusion criteria
Male and Females aged between 60 and 75 years (both included)
Fulfilment of the American College of Rheumatology (ACR) classification criteria for clinical Knee OA
Presence of radiographic OA in the knee joint, scored as 2 or 3 according to Kellgren and Lawrence (KL) definition
Presence of symptomatology (pain, dysfunction and/or effusion) in the last 3 months
Ability to provide written informed consent
Exclusion Criteria
Need for assistance or support to walk (crutch, walker)
Present OA either in the lateral femorotibial compartment or in the patellofemoral compartment exclusively
Secondary OA
Partial or total meniscectomy
Inflammatory or connective tissue diseases
Overuse of the joint from work or sporting activities
Pathological varus or valgus deformity
Underlying health condition
Uncompensated diseases
Fibromyalgia
Presence of microcrystals in the articular space
MRI contraindications
Abuse substances use in the 6 months prior to the study

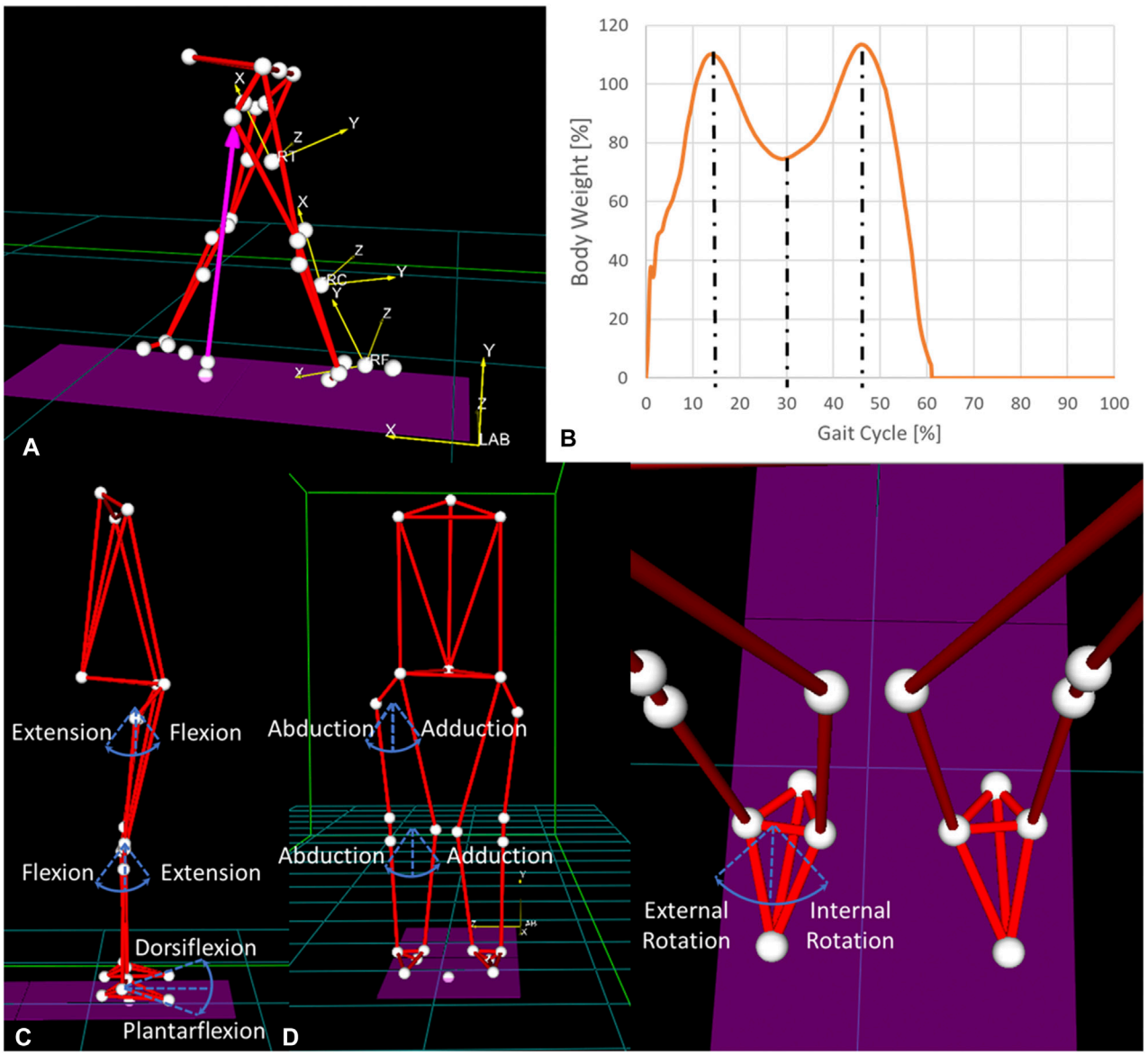

FIGURE 1 | (A) Reference systems of the laboratory and of the right thigh, calf, and foot and **(B)** vertical ground reaction force during a gait cycle. The three dashed lines identify the three points of analysis. **(C)** Articular rotations in the sagittal plane, **(D)** articular rotations in the coronal plane, and **(E)** articular rotations in the transverse plane.

proper cohort (eligibility criteria in **Table 1**). Selected patients were asked to follow a wash-up treatment for a period of 3 months for intra-articular hyaluronic acid infiltrations, 2 months for any SYSADOA, 1 month for oral or intra-articular corticoids, and 1 week for nonsteroidal anti-inflammatory drugs or opioid drugs. The study followed the Good Clinical Practice guidelines and the Declaration of Helsinki, and the Clinical Research Ethical Committee approved the protocol (2016/6747/I). All participants signed an approved informed consent.

The recruitment was performed according to the clinical treatment as follows: a conservative group, that included patients with a diagnosis of KOA attending to follow-up clinical visits at any of the two Departments and following namely any nonsurgical procedure, such as pharmacological treatment or healthier lifestyle modifications (exercise, weight loss, etc.) or a TKR-planned group, that involved patients enrolled in the waiting list for a TKR surgery. To avoid confusion by secondary relevant factors, sex, age (categorized as 60–67 and 68–75 years old), and BMI (categorized as nonobese, BMI <30, and obese, BMI 30 or higher) were also considered in the recruitment. This approach enables the identification of the effect of each factor on gait, as well as their interactions.

All patients had a KL score of 2 or 3 where grade 2 (minimal) presents definite osteophytes and possible joint space narrowing

TABLE 2 | Definition of the directions of each force and moment used in the study.

Force	Component of the reference system
Hip Medio-Lateral shear (HPML)	Component Z of the reference of the pelvis
Hip Compression (HPCP)	Component X of the reference of the thigh
Hip Anterior-Posterior (HPAP)	Vector product of the HPML and HPCP
Knee Medio-Lateral shear (KML)	Component Z of the reference of the thigh
Knee Compression (KCP)	Component X of the reference of the calf
Knee Anterior-Posterior (KAP)	Vector product of KML and KCP
Ankle Medio-Lateral (AML)	Component Z of the reference of the calf
Moment	**Component of the reference system**
Hip Flex-Extension (HPFE)	Component Z of the reference of the pelvis
Hip Intra-Extra (HPIE)	Component X of the reference of the thigh
Hip Abduction-Adduction (HPAA)	Vector product of the HPFE and HPIE
Knee Flex-Extension (KFE)	Component Z of the reference of the thigh
Knee Intra-extra (KIE)	Component X of the reference of the calf
Knee Abduction-Adduction (KAA)	Vector product of KFE and KIE
Ankle Dorsi-Plantar Flexion (ADPF)	Component Z of the reference of the calf

while grade 3 (moderate) presents moderate multiple osteophytes, definite narrowing of joint space and some sclerosis and possible deformity of bone ends. KL was controlled and matched as a possible source of confounding by indication (Kyriacou and Lewis, 2016).

Gait Analysis

Gait analysis was performed using eight cameras (1.5 Mpixel, 250 fps; BTS Smart-DX 700, BTS Engineering, Milan, Italy) and two force plates (500-Hz sampling; BTS P-6000, BTS Engineering, Milan, Italy). The Helen Hayes marker protocol with medial markers was used (Davis et al., 1991). Briefly, the protocol consists of 22 reflective markers (**Figures 1C,D**), three markers for trunk (one marker in correspondence to the 7th cervical vertebra, one by the right acromion and one by the left acromion), pelvis (one marker on each ASIS and one marker in the second sacral vertebra), thighs (one marker on the lateral femoral condyle, and one on the medial femoral condyle and the last one placed on the lateral portion of the thigh in the great trochanter area), shank (one marker on the lateral malleolus one on the medial malleolus and one placed directly on the lateral portion of the shank in the region of the fibula's head) and two markers for each foot (one marker in the space between the heads of the second and third metatarsals and one on the heel). At first a static acquisition was performed, and medial markers were removed prior to perform the gait sequences. Each subject was asked to perform a minimum of five valid gait sequences over a 10-m catwalk at a self-selected speed. The volunteer had a free walk of at least 3 m before stepping over two force plates. Human gait has intrinsic variability; however, sometimes single gait trials can be visually very different from the average. For this reason, a visual consistency evaluation was performed over valid walking trials. Only gaits trials that showed no discrepancies were included in the analysis (see **Supplementary Materials**). At the end of this process, the parameters computed in each trial were normalized over one gait cycle. Kinetics variables were also normalized over the body weight. Finally, the 5 gait trials of each subject were arithmetically averaged, and a second-level analysis was carried out throughout the study.

TABLE 3 | Distribution of the recruited subjects over the 16 groups.

Sex	Clinical treatment	Age	BMI	N
Male	Conservative	60–67	Nonobese	5
Male	Conservative	60–67	Obese	6
Male	Conservative	68–75	Nonobese	6
Male	Conservative	68–75	Obese	6
Male	TKR-planned	60–67	Nonobese	2
Male	TKR-planned	60–67	Obese	1
Male	TKR-planned	68–75	Nonobese	3
Male	TKR-planned	68–75	Obese	7
Female	Conservative	60–67	Nonobese	7
Female	Conservative	60–67	Obese	6
Female	Conservative	68–75	Nonobese	6
Female	Conservative	68–75	Obese	6
Female	TKR-planned	60–67	Nonobese	6
Female	TKR-planned	60–67	Obese	7
Female	TKR-planned	68–75	Nonobese	6
Female	TKR-planned	68–75	Obese	7

Gait analysis allowed the extraction of two groups of dependent variables.

Spatiotemporal gait variables

The velocity of gait was computed as the ratio of the distance between the two heel strikes to the time needed to perform a gait cycle. The first heel strike of each leg was identified using the ground reaction force registration while the second one was identified using the 3D visualization of the markers of the foot during gait. Video recording and force plate recording were already synchronized during capture, avoiding discrepancies in the measurement. The time of a stride and the percentage of time spent in double support were also recorded as indices of functionality.

Kinetic gait variables

Vertical, anterior–posterior, and mediolateral ground reaction forces were extracted from the force plates. The vertical free moment was also extracted. An inverse dynamic analysis was performed, and the results were projected onto joint coordinate systems (**Figure 1A**; **Table 2**). Joint contact forces and internal moments were computed using Smart Analyzer (BTS Engineering, Milan, Italy) at the ankle, knee, and hip of the osteoarthritic leg. They included compression, mediolateral and anterior–posterior shear forces, and flexion–extension, abduction–adduction, and internal-external rotation moments at hip and knee. Ankle dorsi–plantar flexion moments and medio-lateral forces were also computed (**Figures 1C–E**).

For each patient, force and moment values were normalized to body weight and analyzed at the percentage of the gait cycle where the derivative of the vertical ground reaction force was zero, thereby identifying three time points (**Figure 1B**).

Design of Experiment

Recruited patients were grouped based on clinical treatment, age, BMI, and sex, as previously described. Each factor had two levels;

TABLE 4 | Functional Averages and standard deviation for functional parameters. Yellow color indicates significant multivariate effect. Green color indicates significant univariate effect. $p < 0.018$.

		Stride time [s]		Double support time [s]		Mean velocity [m/s]	
		Average	SD	Average	SD	Average	SD
Sex	Male	1.139	0.108	0.138	0.031	1.037	0.206
	Female	1.207	0.124	0.172	0.053	0.855	0.190
BMI	Nonobese	1.159	0.120	0.145	0.038	0.976	0.235
	Obese	1.195	0.122	0.168	0.053	0.892	0.192
Age	60–67	1.167	0.126	0.154	0.055	0.992	0.229
	68–75	1.188	0.119	0.161	0.041	0.878	0.191
Clinical Treatment	Conservative	1.136	0.101	0.138	0.028	1.021	0.200
	TKR-planned	1.232	0.126	0.182	0.056	0.818	0.180
Clinical Treatment * Age	Conservative/60–67	1.102	0.084	0.132	0.025	1.097	0.195
	Conservative/68–75	1.169	0.106	0.144	0.030	0.946	0.178
	TKR-planned/60–67	1.251	0.098	0.169	0.039	0.854	0.173
	TKR-planned/68–75	1.208	0.131	0.179	0.044	0.805	0.180
Clinical Treatment * Sex * BMI	Conservative/Female/<30	1.157	0.123	0.148	0.026	0.940	0.132
	Conservative/Female/>30	1.168	0.057	0.152	0.015	0.907	0.094
	Conservative/Male/<30	1.101	0.090	0.114	0.023	1.169	0.200
	Conservative/Male/>30	1.117	0.085	0.137	0.022	1.079	0.149
	TKR/Female/<30	1.231	0.102	0.168	0.040	0.860	0.188
	TKR/Female/>30	1.274	0.148	0.215	0.071	0.709	0.137
	TKR/Male/<30	1.168	0.069	0.163	0.034	0.875	0.238
	TKR/Male/>30	1.275	0.109	0.150	0.032	0.918	0.167

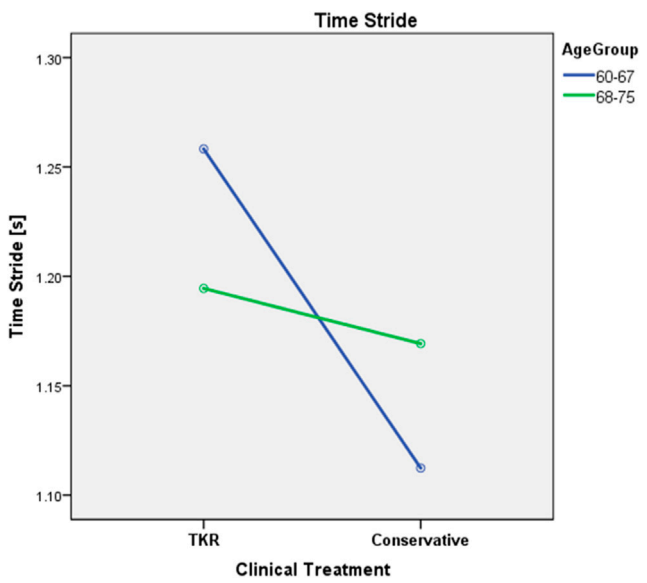

FIGURE 2 | Effect of the interaction between clinical treatment and age over mean stride time ($p = 0.006$).

therefore, the entire analysis comprised 16 groups. Three multivariate and multifactorial analyses of variance (MANOVA) were performed: one for the spatiotemporal parameters and two for the kinetic parameters (Bonferroni correction $p < 0.018$). The power analysis for the principal effects, assuming an average effect size of 0.15, suggests sample sizes of 96, 64, and 64 participants to obtain actual powers of 0.84, 0.90, and 0.95, respectively, for spatiotemporal and kinetic analyses.

To explore possible confounding effects further, different covariates were included in the analysis: height for the spatiotemporal analysis, and stride time and velocity for the force and moment analyses. The analysis at three different time points led to include time as a "within factor" comparing the variations of force and moment along the analyzed gait (repeated measure analysis).

Whenever one of the factors was found to be significant, a univariate ANOVA was performed to identify the significant variables. Significance was adjusted over the number of dependent variables tested through Bonferroni correction (spatiotemporal $p < 0.018$, forces $p < 0.005$, moments $p < 0.006$). Analyses were performed using SPSS (version 23.0; IBM Corp., Armonk, NY, United States) for the osteoarthritic leg.

RESULTS

Descriptive Results

Eighty-seven subjects were recruited (global powers 0.78, 0.99, and 0.99) and stratified into 16 groups derived based on the combination of the four factors of the analysis (**Table 3**). Seventy-two subjects presented with bilateral KOA. The remaining 15 were split into conservative (8) and TKR (7) to maintain a balanced analysis. Male patients belonging to the TKR-planned group were particularly difficult to recruit.

Spatiotemporal Functionality

All residuals showed a normal distribution. The averages and standard deviations for the four main factors are reported in **Table 4**, together with the significance of the main factors and the list of significant

TABLE 5 | Forces means and standard deviation. Yellow color indicates significant multivariate effect ($p < 0.018$). Green color indicates significant univariate effect. ($p < 0.005$). Vertical (VE), Anterior-Posterior (AP) and Medio-Lateral (ML) ground reaction (GR) forces, respectively GRVE, GRAP and GRML. Joints forces were computed at the Ankle (A), Knees (K) and Hips (HP) of osteoarthritic leg and were referred as compression (CP), Medio-Lateral (ML) and Anterior-Posterior (AP) shear, respectively AML, KCP, KML, KAP, HPCM, HPML, HPAP.

			GRVE	GRAP	GRML	AML	KML	KAP	KCP	HPML	HPAP	HPCP
Sex	Female	Mean	96.411	-0.401	4.722	0.931	1.063	1.308	8.748	0.423	0.393	7.459
		SD	4.914	2.694	1.872	0.367	0.532	0.515	0.464	0.399	0.734	0.435
	Male	Mean	95.286	-0.652	4.780	0.781	0.531	1.439	8.600	0.364	0.149	7.301
		SD	7.589	3.162	1.618	0.508	0.553	0.604	0.734	0.377	0.846	0.646
Clinical Treatment	TKR	Mean	96.116	-0.080	5.297	0.963	0.777	1.328	8.703	0.528	0.388	7.447
		SD	4.958	2.443	1.846	0.476	0.656	0.597	0.491	0.418	0.786	0.437
	Conservative	Mean	95.800	-0.844	4.310	0.793	0.890	1.390	8.673	0.295	0.214	7.351
		SD	6.752	2.957	1.584	0.391	0.550	0.507	0.646	0.339	0.757	0.578
Age	60–67	Mean	96.080	-0.603	4.273	0.808	0.911	1.390	8.709	0.287	0.379	7.388
		SD	7.232	3.079	1.663	0.400	0.502	0.486	0.685	0.367	0.803	0.611
	68–75	Mean	95.818	-0.422	5.157	0.920	0.778	1.339	8.666	0.494	0.215	7.398
		SD	5.092	2.610	1.761	0.464	0.672	0.614	0.498	0.389	0.785	0.452
BMI	Obese	Mean	95.346	-0.328	5.203	0.838	0.897	1.429	8.636	0.491	0.189	7.357
		SD	5.102	2.547	1.686	0.341	0.581	0.498	0.482	0.387	0.788	0.440
	Nonobese	Mean	96.624	-0.712	4.221	0.902	0.774	1.286	8.743	0.291	0.408	7.435
		SD	6.933	3.242	1.728	0.526	0.620	0.603	0.680	0.373	0.793	0.600
Time												
Time*Sex												
Time*BMI												

interactions. Height was a significant covariate ($p = 0.007$, **Supplementary Material**), suggesting the influence of subject height on stride, double-support times, and velocity. Functionality appears to be related to age and clinical treatment. TKR-planned patients needed more time to take a step (8.52% increase), spent more time in the double-stand position (31.94%), and walked more slowly (19.92%). Age was also a significant factor with a multivariate effect. However, its dependence seemed to vary with treatment, as shown by the interaction between clinical treatment and age. In particular, the time required to make a stride varied depending on the interaction between the two factors. **Figure 2** suggests that subjects from the conservative group needed less time for a stride, but younger subjects had greater variability than older subjects.

Kinetics

Analysis of Forces

Clinical treatment was not related to the forces experienced during gait. Sex was the only factor that affected the forces (**Table 5**). Females showed slightly higher compression forces at the hip, as averaged over the three time points, even if forces were normalized by body weight, and inertial factors were considered as covariate. However, the test for repeated measures over the three time points confirmed a significant influence of time, but only for some of the analyzed forces (**Table 5**). This dependence was further influenced by sex and BMI. **Figure 3** shows the different variations in the load profile over time in men and women. In particular, **Figure 3A** shows that, whereas peak loads are similar between males and females in the hip, the minimum load is higher in women, resulting in reduced load variations from heel strike to toe off. As for the interaction between time and BMI, the knee compression force showed higher peak loads and larger variations along gait in nonobese versus obese subjects (**Figure 4A**). The results were repeated at ground level (**Figure 4B**).

Complete descriptions of the averages and standard deviations for the four main factors over the three time points are reported in the **Supplementary Material**.

Analysis of Joint Moments

The clinical treatment chosen by the patients was not related directly to the joint moments experienced during gait (**Table 6**). However, joint moments are correlated with age. Younger patients showed, on average, approximately half of the values of the older subjects (**Figure 5**; **Table 6**). A significant interaction between age and BMI has also been reported. In obese subjects, age did not affect the moment profile along gait (**Figures 6A**), while significant differences between ages were reported for nonobese subjects (**Figures 6B**). Interactions among clinical treatment, age, and BMI were reported, as illustrated by the ankle dorsiflexion moment profiles in the different combinations of subjects (**Figure 7**). Conservative subjects showed a higher peak of ankle moment in the presence of obesity and an age range of 60–67 (**Figures 7A**) and in nonobese subjects aged 68–75 (**Figures 7D**) but not in the other combinations. Higher-level interactions among the four factors were also observed.

Complete descriptions of averages and standard deviations for the four main factors over the three time points are reported in the **Supplementary Material**.

DISCUSSION

TKR is the "gold-standard" treatment for patients with severe symptomatic KOA who have failed nonsurgical management and suffer significant impairment in their quality of life. Nevertheless, the proportion of people with unfavorable long-term outcomes ranges from 10 to 34% (Beswick et al., 2012). TKR decisions are

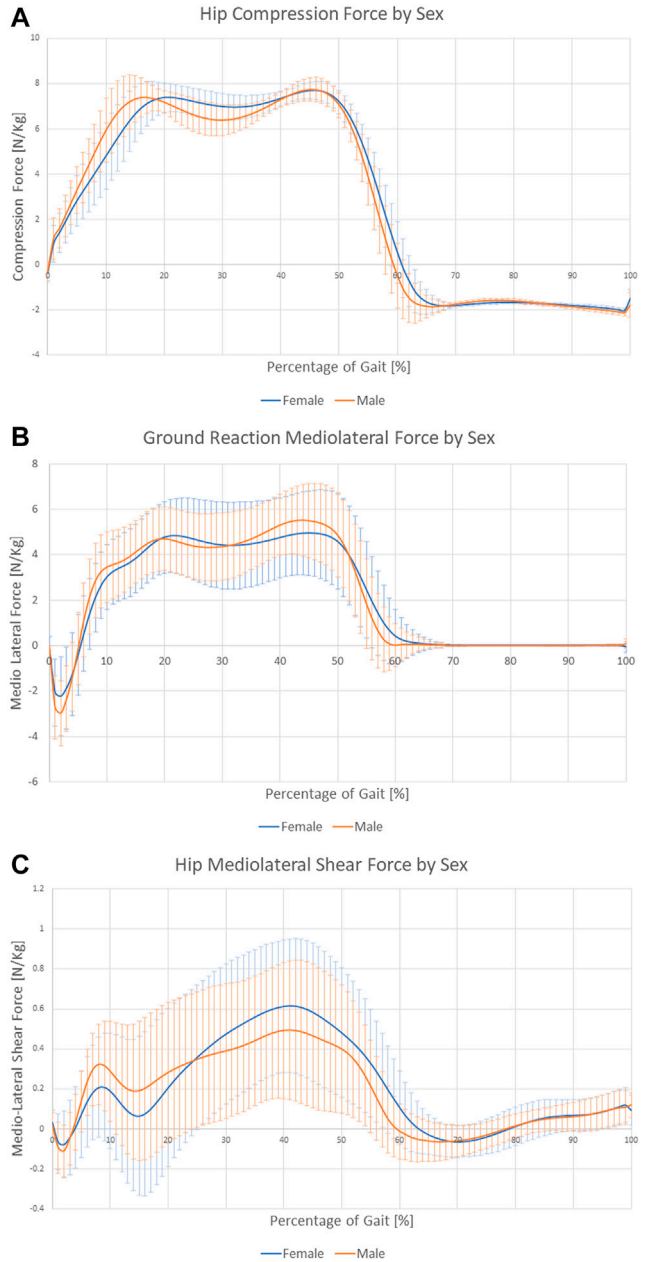

FIGURE 3 | Forces compared between the two sexes: **(A)** hip compression force profile, **(B)** ground reaction mediolateral force, and **(C)** hip mediolateral shear force.

still conditioned by a high degree of susceptibility related to patient's and doctor's thoughts and beliefs. Although the analysis of gait measurements in OA might provide valuable objective biomarkers, previous studies have failed to achieve consensus (Mills et al., 2013). Such difficulty can be partially explained by the presence of confounding effects (Kyriacou and Lewis, 2016) and the lack of multifactorial analyses designed to understand such effects. In the present study, an attempt was made to achieve a better integrated vision of KOA patients and their gait by considering four different factors and three covariates in a cohort of 87 subjects. The final aim of this study was to identify objective criteria for TKR decisions.

Recruitment

Subject recruitment to achieve balanced groups was challenging, showing the commonly reported higher prevalence of KOA in women (Buckwalter and Lappin, 2000). The men who were difficult to recruit belonged to three groups of TKR treatment. The total number of candidates examined at the Hospital del Mar, Barcelona, Spain, for the TKR-planned group exceeded 500 per year, so the outcome of the recruitment suggests that epidemiologically, within the inclusion criteria of this study, the combination of TKR-planned/male/obese/elderly is the only one with a prevalence similar to that of women.

Multifactorial Manova

Multifactorial ANOVA and MANOVA are powerful statistical tools which have many potentialities but also some limitations. Researchers must be aware of both in order to perform a good analysis of the results.

Multifactorial analysis allows to perform statistical evaluation of several factors using a single test. Moreover, the stratification of patients in several subgroups allows to analyze also the interactions among more factors permitting the evaluation of non-linearities. However, the power of the test is not constant among all the factors and interaction analyzed. In the present study four main factors are presented i.e., clinical treatment, sex, BMI and age. These four factors are tested at the maximum power allowed by the test since for each of them all the patients are divided only in two groups (39 TKR-planned against 48 Conservative, 36 male against 51 female, 40 subjects with age 60–67 against 47 with age 68–75, 46 obese and 41 non obese). This approach allows to verify effects of the analyzed factor, independently by the presence of other factors. In the present study the power obtained for the two analyses of kinetic data testify a high power of the test related to the main factors. The computed power of the spatiotemporal MANOVA was 0.78, which is slightly less than the standard value of 0.8. This might reflect in 2% higher probability of type II error. Multifactorial analysis allows also to evaluate the effect of interaction among factors; however, researchers must consider that the dimension of the groups is decreased as the level of the interaction increase. This means that, while first level interactions can still be considered robust results since performed over four groups of about 20 subjects each, higher level interactions must be considered as preliminary results to be confirmed in future works. In particular, the limited number of TKR-planned men in three of the studied groups is expected to introduce imbalance in the study when high-level interactions, including sex, are analyzed. Hence, results limited to the interactions of clinical treatment–sex–age and clinical treatment–sex–age–BMI should be considered as preliminary.

Finally, when multifactorial MANOVA results are presented, standard deviations can be very high because they include all the analyzed subjects. However, the analyses considered the effect of each separated factor, therefore significant factors can be trusted to be significant despite the showed high standard deviation.

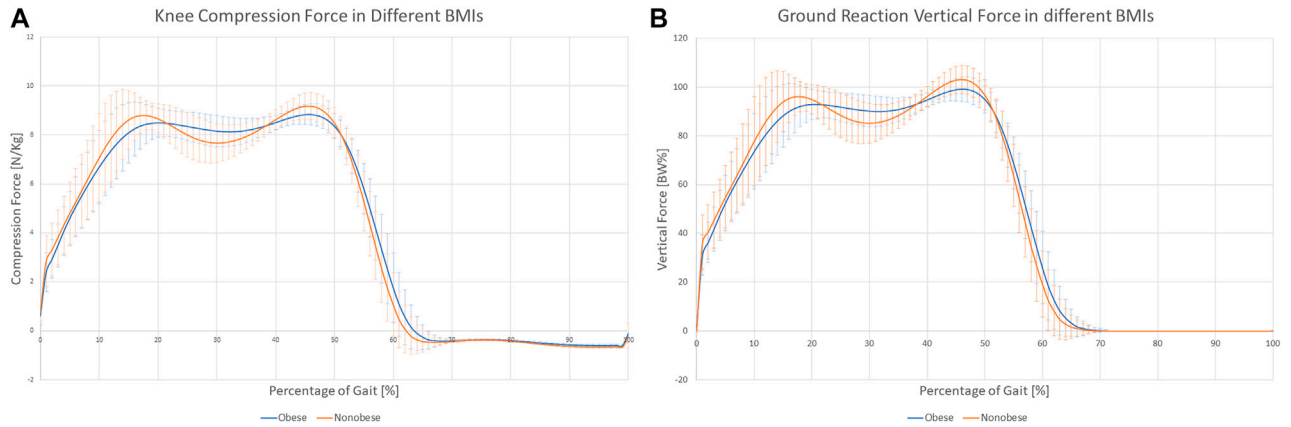

FIGURE 4 | Knee compression **(A)** and ground reaction **(B)** force profiles for Obese and Nonobese subjects.

TABLE 6 | Moments means and standard deviation. Yellow color indicates significant multivariate effect ($p < 0.018$). Green color indicates significant univariate effect. ($p < 0.006$). Ground reaction free moment (GRFM), Flexion-Extension (FE), Abduction-Adduction (AA) and Internal-External rotation (IE) moments are reported at knee and hip of osteoarthritic leg, respectively KFE, KAA, KIE and HPFE, HPAA, HPIE. Dorsi-Plantar Flexion moment of the ankle is also reported (ADPF).

			GRFM	AFE	KFE	KAA	KIE	HPFE	HPAA	HPIE
Sex	Female	Mean	0.042	0.562	0.043	0.328	0.039	0.093	0.676	0.023
		SD	0.218	0.170	0.213	0.126	0.043	0.216	0.125	0.055
	Male	Mean	0.044	0.599	0.011	0.334	0.031	0.060	0.546	0.004
		SD	0.223	0.196	0.218	0.142	0.049	0.231	0.137	0.057
Clinical Treatment	TKR	Mean	0.006	0.566	0.036	0.380	0.030	0.097	0.647	0.018
		SD	0.212	0.197	0.219	0.130	0.046	0.211	0.137	0.060
	Conservative	Mean	0.072	0.586	0.008	0.291	0.040	0.065	0.601	0.013
		SD	0.216	0.156	0.213	0.122	0.045	0.225	0.149	0.053
Age	60–67	Mean	0.031	0.594	0.028	0.298	0.024	0.115	0.617	0.015
		SD	0.214	0.176	0.211	0.107	0.043	0.218	0.137	0.056
	68–75	Mean	0.052	0.563	0.014	0.359	0.046	0.049	0.625	0.015
		SD	0.222	0.187	0.221	0.146	0.046	0.231	0.152	0.057
BMI	Obese	Mean	0.030	0.572	0.011	0.326	0.033	0.067	0.626	0.006
		SD	0.188	0.180	0.193	0.105	0.043	0.236	0.146	0.051
	Nonobese	Mean	0.057	0.584	0.057	0.336	0.039	0.094	0.616	0.025
		SD	0.250	0.182	0.235	0.158	0.049	0.215	0.146	0.061
Age*BMI										
Clinical Treatment * Age* BMI										
Sex * Clinical Treatment * Age * BMI										

Gait

The evaluation of gait results must be performed taking into consideration that statistical tests cannot identify causation but only relation among factors. The common nomenclature of dependent and independent variables is used only to discriminate between fixed factors and measured variables.

Identifiers of functionality were found to depend on the clinical treatment. Subjects selected for TKR presented a less functional joint because they required more time for a stride, walked more slowly, and spent more time in double support than subjects selected for conservative treatment.

The correlation between time for a stride and severity of OA is one of the few strong evidences in the literature (Chen et al., 2003; Astephen et al., 2008; Zeni and Higginson, 2009). The results related to the correlation between the variation in gait velocity and the severity of OA are not so clear (Heiden et al., 2009; Butler et al., 2011). According to the results, these apparent contradictions might be related to the lack of inclusion of height as a covariate or to the absence of age as a factor of analysis. In fact, older subjects seemed to be less affected by velocity variations. Finally, TKR-planned subjects spent a higher percentage of time in double support, showing a gait characterized by different proportions of single- and double-support phases. This can be related to pain or fear of pain, as subjects perceive the double-support phase as a secure position (Haddas et al., 2018). However, the reported differences were not constant over the years.

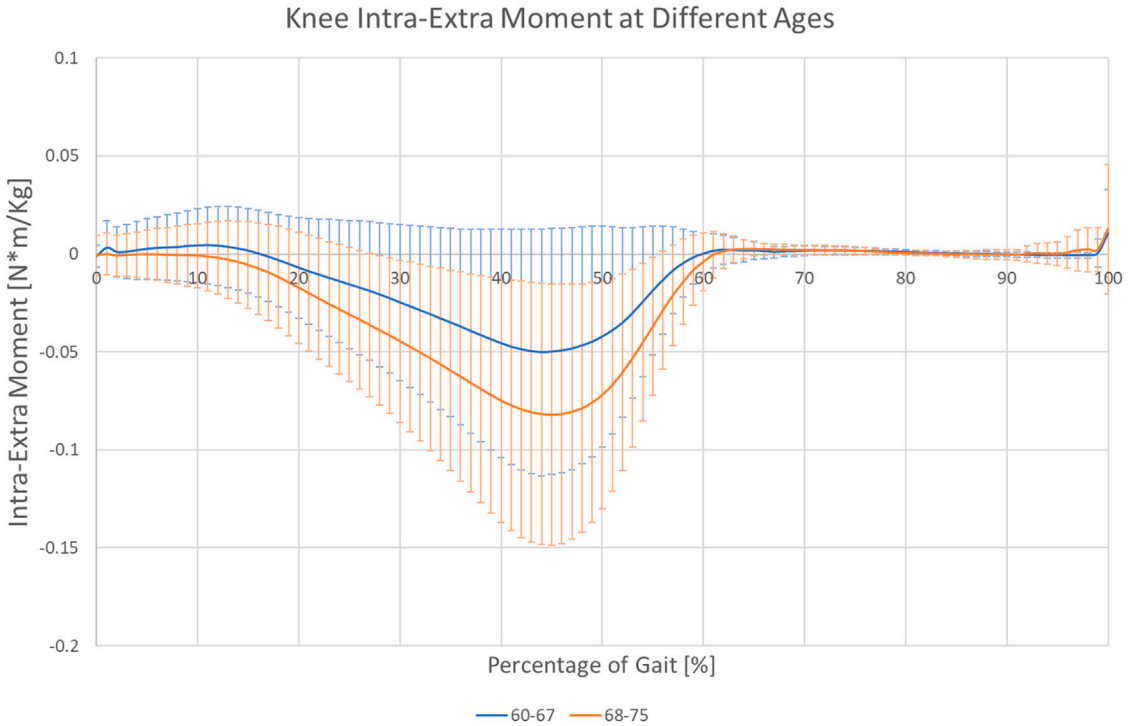

FIGURE 5 | Knee internal-external rotation moment profile for 60–67- and 68–75-year-old subjects.

FIGURE 6 | Variation of the ground reaction free moment for the two age groups while considering Obese **(A)** or Nonobese **(B)**.

In fact, while younger subjects require less time for stride than elders in the conservative group, this relation might be inverted in TKR-planned subjects (**Figure 2**; **Table 4**, $p = 0.006$). Due to the unquestionable interactions between gait and clinical data (such as pain, function or emotional variables), the future study of their association may allow to link clinical situations directly to the gait characteristics of the subject.

Subjects waiting for TKR do not apply a higher mechanical load on their joints or higher joint moments, thus rejecting the original hypothesis. Sex was the only main factor showing a relationship with the analyzed forces. Moreover, the effect is related to time and presents different patterns. Men seemed to have larger variations in hip compression and mediolateral ground reaction forces (**Figures 3A,B**), and women showed higher variability of mediolateral shear forces at the hip (**Figure 3C**). Finally, analysis of BMI confirmed the importance of inertial effects, showing greater variation in nonobese subjects. This variation was consistent at the ground, knee, and hip levels (**Figure 4** and **Supplementary Results**). Joint moments apparently correlated with the clinical treatment, but its impact depended on BMI, age (**Figure 7**), and sex (**Supplementary Material**). Therefore,

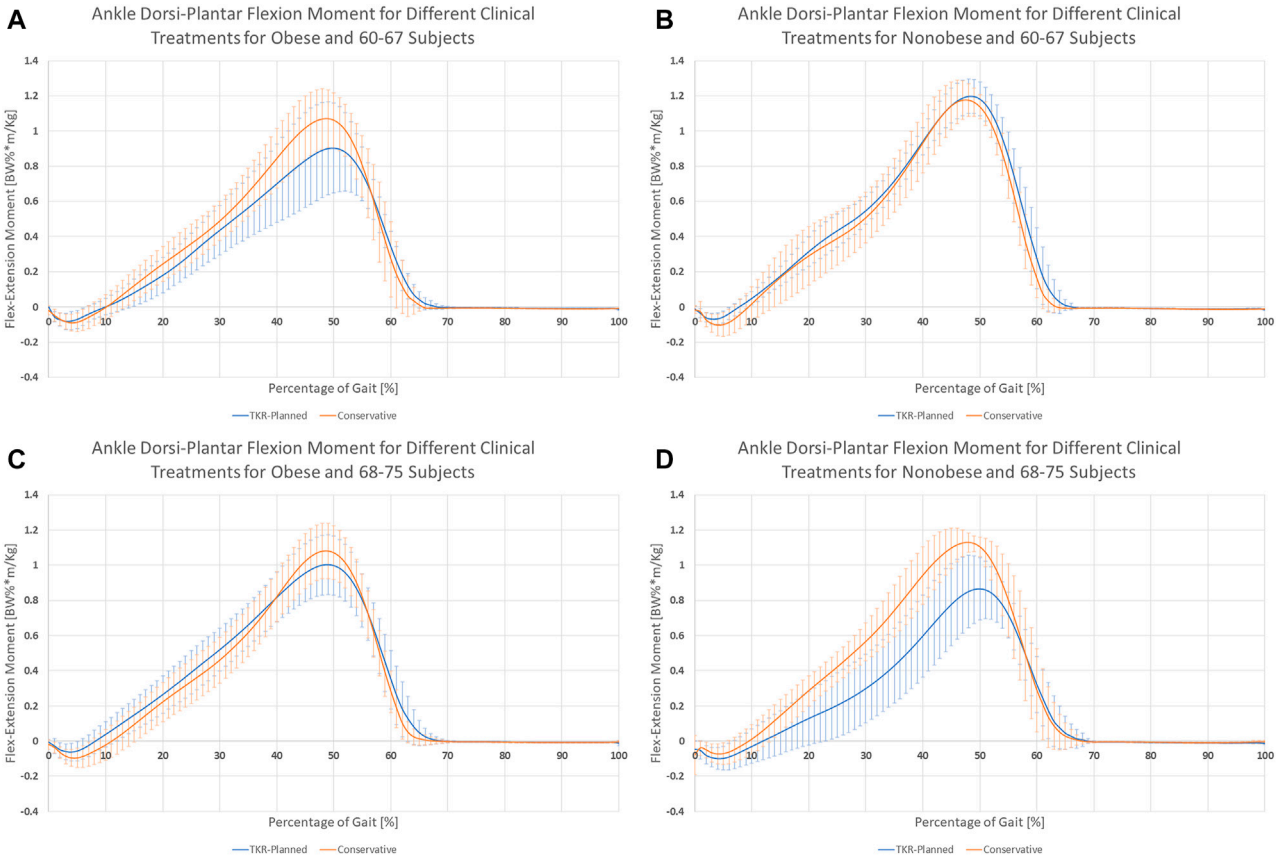

FIGURE 7 | Interaction between clinical treatment, BMI, and age over ankle dorsi-plantar flexion. Behavior differences between the two clinical treatment are visible in **(A)** obese subjects with age range 60–67 and **(D)** nonobese subjects with age range 68–75. In **(B)** nonobese subjects age 60–67 and **(C)** obese subjects age 68–75, no significant differences are noticeable between the two clinical treatments.

differences between groups were visible only under specific combinations of factors.

Age also had a direct effect on moments during gait. Elderly patients had higher absolute moment values (**Table 6**), suggesting an effect of the change in posture during aging. Age also showed a significant interaction with BMI in the MANOVA (p = 0.011). **Figure 6** shows that differences in the ground reaction free moment are minimal between the two age groups for obese subjects but become relevant in nonobese patients (p = 0.018), suggesting an increased variability related to low BMI.

The three points analysis over the time of gait also allowed to perform a screening of variables variability along gait. Time was supposed to be a significant variable since the values in analyses were selected in three representative points of the gait. However, only four forces presented a significant relation with time and no moments showed significant time dependency. This was not expected and make the analysis of the variability an interesting point to explore.

Variations in gait patterns presented in this study might be related to pain or stiffness, but a longitudinal study would be required to identify specific causal relationships.

Limitations

The presented study has some limitations.

The grouping of subjects by clinical treatment is assumed to be correct. This can sometimes be misleading, and a minority of subjects might be incorrectly selected, thereby increasing the noise in the analysis.

Spatiotemporal analysis did not consider swing and stance because they always sum up to 100% of the gait cycle and lead to the cancelation of variability in the multivariate analysis, moreover the used variables can present some relation among them, which is not suggested for MANOVA analysis, however this would not affect the subsequent univariate analysis which can therefore confirm the results of the MANOVA.

Contact forces computed as a result of inverse dynamics are considered to be the minimum necessary to maintain dynamic equilibrium in the system. Muscle co-contraction is a known issue in OA subjects (Thoma et al., 2016) that can introduce relevant variations in the compression forces, but it was not addressed in this study.

Finally, a longitudinal study considering the long-term treatment outcome is recommended to investigate the quality of treatment decision making. Nonetheless, the fact that several

parameters can interact with treatment decisions is an important issue that must be considered.

CONCLUSION

This study shows that the medical management pathway for demographic, anthropometric, and radiographically comparable patients is mainly related to the reduced functionality of subjects selected to undergo TKR. This result can easily be assessed in clinics, helping medical doctors standardize the decision-making process in different hospitals. However, results suggest that age, BMI, and sex are confounding factors in treatment decisions, preventing the description of a fixed threshold that allow to discriminate between the kind of therapy.

Mechanical factors are limited to joint moments and interact with age and BMI. Different moments might be related to the different positions of the joints, and therefore different contact points at the cartilage level. These data should be evaluated in future studies, together with the kinematics of the subjects, to verify the stiffness of these patients (Zeni and Higginson, 2009) and the relation to the perceived pain.

The effects on gait are complex, and comprehensive analysis must consider all the factors together; otherwise, a study might result in nonreproducible or not comparable results. For instance (Astephen et al., 2008) presented a list of significant parameters that were not significant in this study. They show how the variability of the gait profile decrease with the increasing severity of OA. This is something that in our study was related to age and BMI. Variation of the selected parameters along the gait cycle might be related to several factors that might or not be related to severity of OA. This makes the study of variability through tools like time series analysis of particular interest to understand the pathology.

In summary, the message of the study is that the relation among the studied factors is not linear. Therefore, to describe the final treatment decision, objective gait descriptors should be combined with the aforementioned factors, because the clinical situation of the subject might require different evaluation threshold.

DATA AVAILABILITY STATEMENT

The original contributions presented in the study are included in the article/**Supplementary Material**, further inquiries can be directed to the corresponding author.

ETHICS STATEMENT

The studies involving human participants were reviewed and approved by Clinical Research Ethical Committee of Parc de Salut Mar. The patients/participants provided their written informed consent to participate in this study.

AUTHOR CONTRIBUTIONS

ST and LT designed the study, analysed, and interpreted the results and drafted the article. ST, LT, and FC-D collected the data. ST, LT, FC-D, and JN revised critically the manuscript. All the authors gave the final approval of the version to be submitted.

FUNDING

Funds from the Spanish Government (HOLOA-DPI2016-80283-C2-1/2-R, RYC-2015-18888, MDM-2015-0502) and from DTIC-UPF are acknowledged.

ACKNOWLEDGMENTS

A special thanks to all the volunteers who participated in the study.

SUPPLEMENTARY MATERIAL

The Supplementary Material for this article can be found online at: https://www.frontiersin.org/articles/10.3389/fbioe.2022.820186/full#supplementary-material

REFERENCES

Astephen, J. L., Deluzio, K. J., Caldwell, G. E., and Dunbar, M. J. (2008). Biomechanical Changes at the Hip, Knee, and Ankle Joints during Gait Are Associated with Knee Osteoarthritis Severity. *J. Orthop. Res.* 26, 332–341. doi:10.1002/jor.20496

Author Anonymous (2000). Recommendations for the Medical Management of Osteoarthritis of the Hip and Knee: 2000 Update. American College of Rheumatology Subcommittee on Osteoarthritis Guidelines. *Arthritis Rheum.* 43, 1905–1915. doi:10.1002/1529-0131(200009)43:9<1905::AID-ANR1>3.0.CO;2-P

Berenbaum, F., Eymard, F., and Houard, X. (2013). Osteoarthritis, Inflammation and Obesity. *Curr. Opin. Rheumatol.* 25, 114–118. doi:10.1097/BOR.0b013e32835a9414

Beswick, A. D., Wylde, V., Gooberman-Hill, R., Blom, A., and Dieppe, P. (2012). What Proportion of Patients Report Long-Term Pain after Total Hip or Knee Replacement for Osteoarthritis? A Systematic Review of Prospective Studies in Unselected Patients. *BMJ Open* 2, e000435. doi:10.1136/bmjopen-2011-000435

Braun, H. J., and Gold, G. E. (2012). Diagnosis of Osteoarthritis: Imaging. *Bone* 51, 278–288. doi:10.1016/j.bone.2011.11.019

Buckwalter, J. A., and Lappin, D. R. (2000). The Disproportionate Impact of Chronic Arthralgia and Arthritis Among Women. *Clin. Orthopaedics Relat. Res.* 372, 159–168. doi:10.1097/00003086-200003000-00018

Butler, R. J., Barrios, J. A., Royer, T., and Davis, I. S. (2011). Frontal-Plane Gait Mechanics in People with Medial Knee Osteoarthritis Are Different from Those in People with Lateral Knee Osteoarthritis. *Phys. Ther.* 91, 1235–1243. doi:10.2522/ptj.20100324

Chen, C. P. C., Chen, M. J. L., Pei, Y.-C., Lew, H. L., Wong, P.-Y., and Tang, S. F. T. (2003). Sagittal Plane Loading Response during Gait in Different Age Groups and in People with Knee Osteoarthritis. *Am. J. Phys. Med. Rehabil.* 82, 307–312. doi:10.1097/01.phm.0000056987.33630.56

Coggon, D., Reading, I., Croft, P., McLaren, M., Barrett, D., and Cooper, C. (2001). Knee Osteoarthritis and Obesity. *Int. J. Obes.* 25, 622–627. doi:10.1038/sj.ijo.0801585

Creaby, M. W., Wang, Y., Bennell, K. L., Hinman, R. S., Metcalf, B. R., Bowles, K.-A., et al. (2010). Dynamic Knee Loading Is Related to Cartilage Defects and

Tibial Plateau Bone Area in Medial Knee Osteoarthritis. *Osteoarthritis and Cartilage* 18, 1380–1385. doi:10.1016/j.joca.2010.08.013

Cross, M., Smith, E., Hoy, D., Nolte, S., Ackerman, I., Fransen, M., et al. (2014). The Global burden of Hip and Knee Osteoarthritis: Estimates from the Global Burden of Disease 2010 Study. *Ann. Rheum. Dis.* 73, 1323–1330. doi:10.1136/annrheumdis-2013-204763

Davis, R. B., Õunpuu, S., Tyburski, D., and Gage, J. R. (1991). A Gait Analysis Data Collection and Reduction Technique. *Hum. Move. Sci.* 10, 575–587. doi:10.1016/0167-9457(91)90046-Z

De Pieri, E., Lunn, D. E., Chapman, G. J., Rasmussen, K. P., Ferguson, S. J., and Redmond, A. C. (2019). Patient Characteristics Affect Hip Contact Forces during Gait. *Osteoarthritis and Cartilage* 27, 895–905. doi:10.1016/j.joca.2019.01.016

De Souza, S. A. F., Faintuch, J., Valezi, A. C., Sant' Anna, A. F., Gama-Rodrigues, J. J., De Batista Fonseca, I. C., et al. (2005). Gait Cinematic Analysis in Morbidly Obese Patients. *Obes. Surg.* 15, 1238–1242. doi:10.1381/096089205774512627

Dufek, J. S., Currie, R. L., Gouws, P.-L., Candela, L., Gutierrez, A. P., Mercer, J. a., et al. (2012). Effects of Overweight and Obesity on Walking Characteristics in Adolescents. *Hum. Move. Sci.* 31, 897–906. doi:10.1016/j.humov.2011.10.003

Felson, D. T., Anderson, J. J., Naimark, A., Walker, A. M., and Meenan, R. F. (1988). Obesity and Knee Osteoarthritis. *Ann. Intern. Med.* 109, 18–24. doi:10.7326/0003-4819-109-1-18

Ghomrawi, H. M. K., Alexiades, M., Pavlov, H., Nam, D., Endo, Y., Mandl, L. A., et al. (2014). Evaluation of Two Appropriateness Criteria for Total Knee Replacement. *Arthritis Care Res.* 66, 1749–1753. doi:10.1002/acr.22390

Gómez-Barrena, E., Padilla-Eguiluz, N. G., García-Rey, E., Cordero-Ampuero, J., and García-Cimbrelo, E. (2014). Factors Influencing Regional Variability in the Rate of Total Knee Arthroplasty. *The Knee* 21, 236–241. doi:10.1016/j.knee.2013.01.003

Günsche, J. L., Pilz, V., Hanstein, T., and Skripitz, R. (2020). The Variation of Arthroplasty Procedures in the Oecd Countries: Analysis of Possible Influencing Factors by Linear Regression. *Orthop. Rev. (Pavia)* 12. doi:10.4081/or.2020.8526

Haddas, R., Lieberman, I. H., and Block, A. (2018). The Relationship between Fear-Avoidance and Objective Biomechanical Measures of Function in Patients with Adult Degenerative Scoliosis. *Spine (Phila Pa 1976)* 43, 647–653. doi:10.1097/BRS.0000000000002381

Heiden, T. L., Lloyd, D. G., and Ackland, T. R. (2009). Knee Joint Kinematics, Kinetics and Muscle Co-contraction in Knee Osteoarthritis Patient Gait. *Clin. Biomech.* 24, 833–841. doi:10.1016/j.clinbiomech.2009.08.005

Kyriacou, D. N., and Lewis, R. J. (2016). Confounding by Indication in Clinical Research. *JAMA* 316, 1818. doi:10.1001/jama.2016.16435

McKean, K. A., Landry, S. C., Hubley-Kozey, C. L., Dunbar, M. J., Stanish, W. D., and Deluzio, K. J. (2007). Gender Differences Exist in Osteoarthritic Gait. *Clin. Biomech.* 22, 400–409. doi:10.1016/j.clinbiomech.2006.11.006

Messier, S. P., Ettinger, W. H., Doyle, T. E., Morgan, T., James, M. K., O'Toole, M. L., et al. (1996). Obesity: Effects on Gait in an Osteoarthritic Population. *J. Appl. Biomech.* 12, 161–172. doi:10.1123/jab.12.2.161

Mills, K., Hunt, M. A., and Ferber, R. (2013). Biomechanical Deviations during Level Walking Associated with Knee Osteoarthritis: A Systematic Review and Meta-Analysis. *Arthritis Care Res.* 65, a–n. doi:10.1002/acr.22015

O'Brien, P., Bunzli, S., Ayton, D., Dowsey, M. M., Gunn, J., and Manski-Nankervis, J.-A. (2019). What Are the Patient Factors that Impact on Decisions to Progress to Total Knee Replacement? A Qualitative Study Involving Patients with Knee Osteoarthritis. *BMJ Open* 9, e031310. doi:10.1136/bmjopen-2019-031310

O'Neill, T., Jinks, C., and Ong, B. N. (2007). Decision-making Regarding Total Knee Replacement Surgery: A Qualitative Meta-Synthesis. *BMC Health Serv. Res.* 7, 1–9. doi:10.1186/1472-6963-7-52

Park, J.-H., Mancini, M., Carlson-Kuhta, P., Nutt, J. G., and Horak, F. B. (2016). Quantifying Effects of Age on Balance and Gait with Inertial Sensors in Community-Dwelling Healthy Adults. *Exp. Gerontol.* 85, 48–58. doi:10.1016/j.exger.2016.09.018

Paterson, K. L., Lythgo, N. D., and Hill, K. D. (2009). Gait Variability in Younger and Older Adult Women Is Altered by Overground Walking Protocol. *Age and Ageing* 38, 745–748. doi:10.1093/ageing/afp159

Schiphof, D., Kerkhof, H. J. M., Damen, J., De Klerk, B. M., Hofman, A., Koes, B. W., et al. (2013). Factors for Pain in Patients with Different Grades of Knee Osteoarthritis. *Arthritis Care Res.* 65, 695–702. doi:10.1002/acr.21886

Thoma, L. M., McNally, M. P., Chaudhari, A. M., Flanigan, D. C., Best, T. M., Siston, R. A., et al. (2016). Muscle Co-contraction during Gait in Individuals with Articular Cartilage Defects in the Knee. *Gait & Posture* 48, 68–73. doi:10.1016/j.gaitpost.2016.04.021

Wluka, A. E., Lombard, C. B., and Cicuttini, F. M. (2013). Tackling Obesity in Knee Osteoarthritis. *Nat. Rev. Rheumatol.* 9, 225–235. doi:10.1038/nrrheum.2012.224

Zeni, J. A., and Higginson, J. S. (2009). Dynamic Knee Joint Stiffness in Subjects with a Progressive Increase in Severity of Knee Osteoarthritis. *Clin. Biomech.* 24, 366–371. doi:10.1016/j.clinbiomech.2009.01.005

Conflict of Interest: The authors declare that the research was conducted in the absence of any commercial or financial relationships that could be construed as a potential conflict of interest.

Publisher's Note: All claims expressed in this article are solely those of the authors and do not necessarily represent those of their affiliated organizations, or those of the publisher, the editors and the reviewers. Any product that may be evaluated in this article, or claim that may be made by its manufacturer, is not guaranteed or endorsed by the publisher.

Advantages of publishing in Frontiers

OPEN ACCESS
Articles are free to read for greatest visibility and readership

FAST PUBLICATION
Around 90 days from submission to decision

HIGH QUALITY PEER-REVIEW
Rigorous, collaborative, and constructive peer-review

TRANSPARENT PEER-REVIEW
Editors and reviewers acknowledged by name on published articles

Frontiers
Avenue du Tribunal-Fédéral 34
1005 Lausanne | Switzerland

Visit us: www.frontiersin.org
Contact us: frontiersin.org/about/contact

REPRODUCIBILITY OF RESEARCH
Support open data and methods to enhance research reproducibility

DIGITAL PUBLISHING
Articles designed for optimal readership across devices

FOLLOW US
@frontiersin

IMPACT METRICS
Advanced article metrics track visibility across digital media

EXTENSIVE PROMOTION
Marketing and promotion of impactful research

LOOP RESEARCH NETWORK
Our network increases your article's readership